Toxicokinetic Studies on

(New) Synthetic Opioids

Dissertation

zur Erlangung des Grades

des Doktors der Naturwissenschaften

der Naturwissenschaftlich-Technischen Fakultät

der Universität des Saarlandes

von

Frederike Nordmeier

Saarbrücken

2021

Tag des Kolloquiums:	15.12.2021
Dekan:	Univ.-Prof. Dr. rer. nat. Jörn Walter
Berichterstatter:	Univ.-Prof. Dr. rer. nat. Markus R. Meyer Univ.-Prof. Dr. rer. nat. Thorsten Lehr
Vorsitz:	Univ.-Prof. Dr. rer. nat. Veit Flockerzi
Akad. Mitarbeiter:	PD Dr. rer. nat. Martin Frotscher

Vorwort

Die nachfolgende Arbeit entstand unter der Anleitung von Herrn Univ.-Prof. Dr. rer. nat. Markus R. Meyer und Herrn Univ.-Prof. Dr. med. Peter H. Schmidt in der Abteilung Experimentelle und Klinische Toxikologie der Fachrichtung 2.4 Experimentelle und Klinische Pharmakologie und Toxikologie der Universität des Saarlandes in Homburg und im Institut für Rechtsmedizin der Universität des Saarlandes in Homburg von Mai 2018 bis August 2021.

Danksagung

Mein besonderer Dank gilt:

meinem Doktorvater Herrn Professor Dr. Markus R. Meyer sowie Herrn Professor Dr. Peter H. Schmidt für die herzliche Aufnahme in ihre Arbeitskreise, die Überlassung des interessanten Dissertationsthemas, die Möglichkeit, selbstständig und wissenschaftlich zu arbeiten und aktiv an nationalen und internationalen Fachkongressen teilzunehmen, die ausgezeichnete fachliche Betreuung sowie die stete Unterstützung und Offenheit bei Problemen,

Herrn Professor Thorsten Lehr für die Übernahme des Koreferats und die Möglichkeit der Durchführung der pharmakokinetischen Modellierung,

Frau Dr. Nadine Schäfer für ihre fachliche Expertise, die Begleitung und Anleitung der Arbeit, die fachliche Diskussionsbereitschaft (auch am Wochenende), die ganzen Freiräume, die ich bei meiner Arbeit bekommen habe, und den steten Einsatz bei Problemen,

Herrn Professor Dr. Michael Menger und Herrn Professor Dr. Matthias W. Laschke sowie dem gesamten Team des Instituts für Klinische und Experimentelle Chirurgie in Homburg für das Know-how bei der Durchführung der Tierversuche und für die Überlassung von experimenteller und personeller Unterstützung, ohne die die Durchführung der Studie nicht möglich gewesen wäre,

meinen Kolleginnen und Kollegen, insbesondere Adrian Dörr, Benjamin Peters und Nadja Walle, für die Unterstützung bei den Tierversuchen und allen für das angenehme Arbeitsklima, die gute Zusammenarbeit, die fachliche Expertise, ein stets offenes Ohr auch in anstrengenden Zeiten (auch für das Auffangen von Frust) und das „Aushalten“ meiner Arbeitswut und meines Ordnungswahns,

meinen (ehemaligen) Kollegen aus der Abteilung der Experimentellen und Klinischen Toxikologie, allen voran Tanja Gampfer, aber auch Selina Hemmer und Cathy Jacobs, für die Diskussionsbereitschaft und anregenden Denkanstöße während der Seminare, die anfängliche experimentelle Unterstützung, die

freundliche Aufnahme in deren Arbeitskreis, die Freundschaften, die daraus entstanden sind und die grenzenlose Unterstützung in schwierigen Zeiten,

Iryna Sihinevich für die Durchführung der pharmakokinetischen Modellierung, das Bereitstehen bei sämtlichen Fragen und das Kümmern um viele Probleme,

Frau Gabriele Ulrich für die gewissenhafte Ausführung der Rattenversuche,

Herrn Dr. Stefan Potente für die tatkräftige Unterstützung bei der Durchführung der Tierexperimente,

Esther Bubel-Weichel und Roland Klotz für die Unterstützung und Hilfsbereitschaft im Sektionssaal sowie Bereitstellung sämtlicher Utensilien,

meinen Freunden (vor allem Björn, Tanja und Insa: ohne euch wäre ich sicher das ein oder andere Mal untergegangen) für die grenzenlose Unterstützung, das stets offene Ohr, die Möglichkeit Frust abzubauen, das Mitfiebern, Miterleben und Aushalten aller Höhen und Tiefen einer Promotion, das Wiederaufbauen nach Niederschlägen und das füreinander da sein trotz teilweise sehr großer Entfernungen,

meinen Eltern, die mich immer bedingungslos unterstützt und hinter mir gestanden haben, die es mir ermöglicht haben und mich darin bekräftig haben, diesen Weg zu gehen, ohne die vieles nicht möglich gewesen wäre und die meinen Kummer immer ausgehalten und mitgetragen haben. Ich weiß, ihr seht es als Selbstverständlichkeit an, aber das, was ihr leistet, geht definitiv darüber hinaus. Ich liebe euch von ganzem Herzen und bin euch unendlich dankbar für alles.

„All our dreams can come true
if we have the courage to pursue them.”

Walt Disney (1901-1966)

ZUSAMMENFASSUNG

Für die Erhebung toxikokinetischer (TK) Daten wurde in dieser Arbeit der Metabolismus ausgewählter neuer synthetischer Opioide (NSO) (U-47931E, U-51754 und Methoxyacetylfentanyl) in verschiedenen in vitro/in vivo Modellen untersucht. Hierbei zeigte sich eine gute Übereinstimmung der verschiedenen angewandten Modelle. Zusätzlich wurde eine Schweinestudie mit dem populären NSO U-47700 nach intravenöser Verabreichung durchgeführt. Tramadol diente dabei als Referenzsubstanz, um die Kompatibilität des Schweinemodells mit humanen Daten zu überprüfen. Alle untersuchten U-Substanzen wurden hauptsächlich durch *N*-Demethylierung, Hydroxylierung und Kombinationen beider Wege verstoffwechselt und Methoxyacetylfentanyl durch Dealkylierung und Hydroxylierung. Phase II Metabolite wurden nur in geringem Ausmaß gebildet. Das Schweinemodell zeigte eine gute Übereinstimmung mit dem humanen Metabolismus. Eine populationskinetische Modellierung ergab, dass ein Drei-Kompartiment-Modell die TK Parameter beider Substanzen am besten beschrieben hat. Das Modell konnte in Zusammenhang mit einer allometrischen Einzelspezies-Skalierung erfolgreich für die Vorhersage humaner Tramadol-Expositionen genutzt werden. Die Ermittlung der Gewebeverteilung der Substanzen zeigte, dass Lunge, Leber, Niere, Duodenalinhalt und Gallenflüssigkeit geeignete Matrizes für qualitative postmortale Analysen sind. Die Substanzen zeigten zudem in den meisten Organen nur geringe Tendenzen für postmortale Umverteilungsprozesse.

SUMMARY

Toxicokinetic (TK) data are essential for an enhanced interpretation of clinical and forensic cases. In the presented work, the metabolic fate of three different model new synthetic opioids (NSO), namely U-47931E, U-51754, and methoxyacetylfentanyl, was investigated using different in vitro and in vivo approaches. The results revealed a good agreement between the various applied models. Furthermore, the TK of one of the most popular NSO, U-47700, was elucidated in a pig model following intravenous administration. Tramadol was assessed as reference for the examination of the comparability of porcine and human TK. Main metabolites of all U-substances were formed by *N*-demethylation, hydroxylation and combinations thereof. Methoxyacetylfentanyl was metabolized by dealkylation and hydroxylation. Phase II metabolites were formed to a limited extent. The major urinary metabolic pathways for U-47700 in pigs were comparable to those of humans. A three-compartment model best described the TK properties as modeled in a single species population TK approach. By usage of this TK model, published human data could successfully be predicted in terms of tramadol. Investigations of perimortem and postmortem (PM) distribution patterns of the drugs revealed that lung, liver, kidney, duodenum content, and bile are suitable matrices for qualitative PM analysis. Moreover, U-47700, tramadol and their metabolites show only low to moderate tendency for PM redistribution in most of the studied organs.

TABLE OF CONTENTS

1. INTRODUCTION

1.1 (Synthetic) Opioids

As highly potent and effective analgesics, opioids are currently widespread used for the treatment of moderate to severe pain (1). This large class of pharmaceuticals is structurally related to the natural plant alkaloids (e.g., morphine), also called opiates. In addition, semisynthetic derivates (e.g. oxycodone), synthetic derivates (e.g. fentanyl, tramadol), and endogenous opioids such as enkephalins and endorphins exist (2). Opioids are acting by binding as agonists or antagonists at the cell surface opioid receptor (OR) appearing mainly as μ-, κ-, or δ-subtype (3). The predominantly localization of these receptors is the central nervous system (brain, spinal column), but they are also found throughout the peripheral tissue such as on vascular, cardiac, lung, gut, and peripheral blood cells (2). The activation of the G-protein-coupled OR leads to a series of intracellular signals resulting in reduction of cell excitability and neurotransmission (2). Subsequently, the activation of the μ-OR (MOR) generates analgesic effects. In general, OR binding causes different side effects. Typical side effects are respiratory depression, unconsciousness, and miosis also known as classical opioid toxidrome. Furthermore, sedation, a decreased gastrointestinal motility, nausea, constipation, and intestinal bloating are often observed after the intake of opioids (2). Other effects linked to OR engagement are changes in mood, while euphoria is mediated by the MOR and dysphoria by the κ-OR (KOR) (4). Despite their profound pain relieving effects, opioids are known to have a high potential for dependency and abuse as well as for tolerance development (3).

MOR agonists are effective against acute pain, but have a lower response to the treatment of chronic pain and may present an unsatisfactory therapeutic window (1). To improve the opioid therapeutic range, synthetic opioids including the combination of MOR agonism and monoamine reuptake inhibition were developed. Tramadol is one of the first compounds developed in this field (5). This prodrug is responsible for a complex pharmacokinetic profile. There, the opioid agonist activity is predominantly provided by its metabolite *O*-desmethyltramadol and to a minor extent by the parent compound, both shown in Fig. 1 (1).

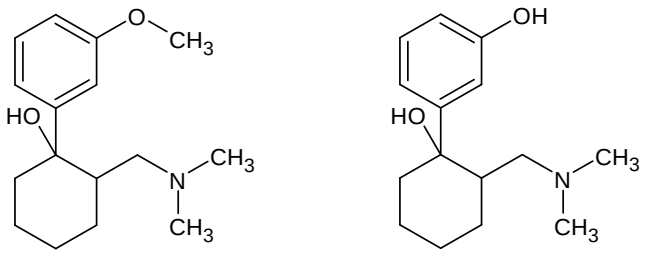

Fig. 1: Structure of tramadol and its main metabolite *O*-desmethyltramadol

1.1.1 New Synthetic Opioids

In the recent years, the drugs of abuse (DOA) market with its psychoactive substances significantly expanded. Next to “traditional” illicit drugs such as cannabis, amphetamine, cocaine, or heroin, the continuous emergence of progressively more so-called new psychoactive substances (NPS) could be observed every single year (6). Since classical psychoactive substances are scheduled these days in most countries (7), NPS are dealing with the advantage of initially circumventing legislation in most cases. Nevertheless, NPS still have the same or even more pronounced psychoactive effects due to the fact that they are structurally related to classical DOA (8, 9). NPS are mostly supplied via specialized internet shops as ‘research chemicals’, ‘legal highs’, or ‘bath salts’ (9). Amongst others, they include synthetic cannabinoids, phenethylamines, cathinones, benzodiazepines, or opioids (10). In the end of 2019, the European (EU) Monitoring Center for Drugs and Drug Addiction (EMCDDA) and the EU Early Warning System (EWS) monitored around 790 NPS of which 53 were reported in Europe for the first time (Fig. 2) (11).

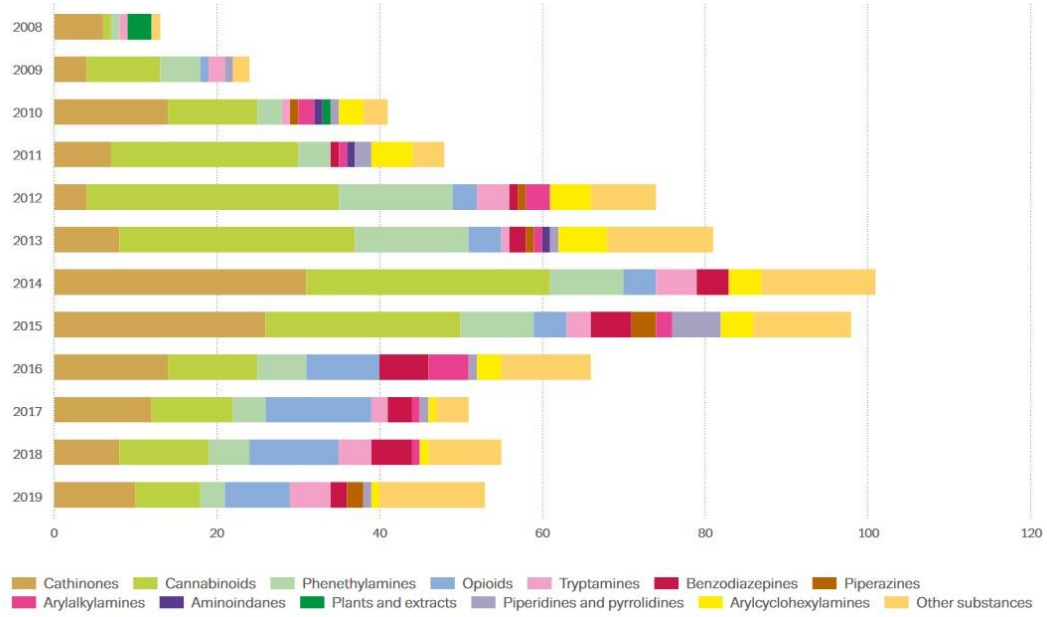

Fig. 2: Number and categories of NPS reported by the EU early warning system for the first time from 2008 until 2019. Figure taken from the EMCDDA European Drug Report 2020 (11).

During the last years, a decrease in new appearances of NPS was recorded and may reflect the results of continued efforts and newly developed laws to control NPS in Europe as well as in the source countries. To avoid these laws, newly developed or discovered compounds continuously floated into the DOA market and others disappeared illustrating the dynamic nature of this part of drug market (11). Nevertheless, NPS still pose a great risk in public health due to unpredictable toxic effects. Thereby, one problem is the high variability of the active agent content of these products resulting in possible accidental overdoses (6, 12). In addition, NPS usually arise at the illicit market without previous

collected safety data or clinical trials and thus with the lack of toxicokinetic (TK) data making consumers the first test persons (13). Because of an increasing consumption and the associated possible influence on drivers, NPS became a relevant topic in forensic toxicology, e.g. in driving under the influence of drugs (DUID) cases (14). Unfortunately, they are often not covered by routine analytical approaches. Together with the hazardous risk potential and the lack of TK data, NPS are gaining more and more importance in clinical and forensic toxicology. On this occasion, TK data are necessary and helpful when interpreting clinical or forensic cases in which the question of e.g., the time of consumption or the concentration of a substance at a certain time point has to be clarified. Thus, these data are inalienable to draw up a profound expert opinion especially in DUID cases or in intoxication cases of poisoned persons.

Although new appearances of some substance classes decreased during the last years, new appearances of new synthetic opioids (NSO) still increased until 2017/2018 (11). Due to their high potency, NSO depict a elevated risk of poisoning to their consumers and thus resulted in many fatal overdoses in the last years (15–17). Additionally, many intoxications with life-threating conditions characterized by the classical opioid toxidrome were reported (18–20). In comparison to classical opioids such as morphine or fentanyl, NSO often display a higher affinity to MOR and an enhanced penetration of the blood-brain barrier owning higher lipophilicity (21). NSO could be divided into fentanyl analogs and non-fentanyl derived compounds acting as strong OR agonists (19). NSO are often not “new” chemical appearances (22). Most NSO derive from older patent literature of pharmaceutical companies and were initially developed as new analgesic agents, but discarded due to their side-effects and never advanced in clinical trials (23, 24).

Fentanyl analogs as well as fentanyl itself own a nanomolar affinity to MOR and thus a much higher affinity as compared to morphine or heroin (10). Various fentanyl analogs have been designed over the last decade. They are usually developed by a modification or a replacement of the propionyl chain or the ethylphenyl part as shown in Fig 3. Furthermore, different substituents were intercalaried resulting in a very variable potency (25).

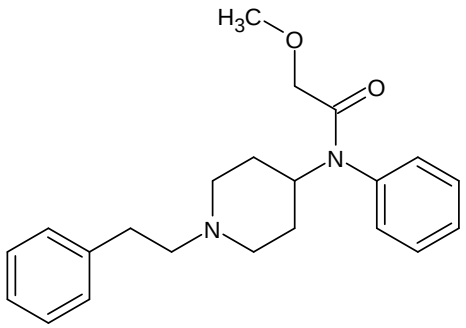

Fig. 3: Structure of the fentanyl analog methoxyacetylfentanyl generated by the modification of the propionyl chain.

One of the largest groups of non-fentanyl derived NSO consists of so-called ‘U-compounds’ investigated by the Upjohn Company in the 1970s and 1980s and sharing a *N*-(2-ethylamino) amide core structure (23). These substances own the peculiarity not being related to classical opioids (26). Based on substantial modifications, they display a higher affinity to MOR (e.g. U-47700), or a higher affinity to KOR (e.g. U-51754) as shown in Fig. 4 (23, 27).

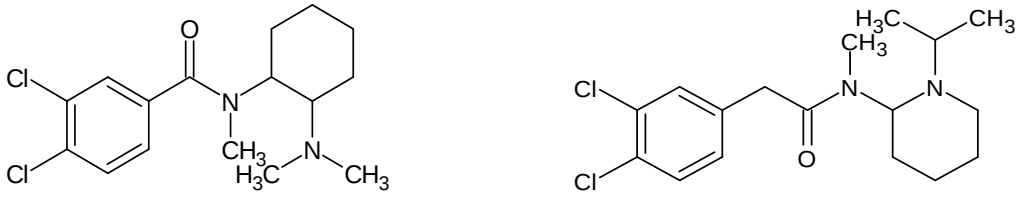

Fig. 4: Examples for U-compounds with affinity to MOR referred to U-47700 (left) and with affinity to KOR referred to U-51754 (right).

U-47700 was one of the first U-compounds identified during the pharmaceutical development processes and was one of the most popular substances of this NSO subclass (21). Many poisoning and fatal cases are related to this substance (28–32) making a more in-depth understanding explicitly in TK indispensable in clinical and forensic toxicology cases. Hence, systematic and controlled studies are essential, but due to ethical reasons and the absence of pre-clinical trials, human studies are a challenging task. Therefore, a comparable animal model already established for synthetic cannabinoids (33–37) has to be used and verified for NSO. Yet, one important step is the comparison of the assessed TK data to those obtained from the already studied synthetic opioid tramadol, being most closely structurally related to U-47700 (see chapter 3.3).

1.2 Drug detection in biological matrices

Monitoring intoxications and the comprehension of the TK of a drug need the assessment of concentrations in different matrices, particularly in serum and blood. Due to their high potency, especially NSO are active in very low doses. Thus, the parent drugs and their metabolites usually appear at very low concentrations in biological matrices. A consequence is the need of high sensitive and specific analytical methods (38). There are several qualitative multi target screening approaches for the determination of NSO in different matrices published in the literature (39–43) as well as numerous methods for the quantification in conventional and non-conventional matrices (31, 44–47). Predominantly, liquid chromatography-tandem mass spectrometry (LC-MS/MS) was used for the detection mostly after solid-phase extraction or liquid-liquid extraction (23, 38). Unfortunately, none of them covered U-47700, tramadol and their main metabolites. Therefore, a new quantification method using LC-MS/MS allowing for the simultaneous determination of U-47700, tramadol and their main metabolites in serum and whole blood was developed and fully validated according to national and

international guidelines (see Chapter 3.3). In terms of the determination of postmortem (PM) concentrations in tissues, a standard addition approach was used for quantification (see Chapter 3.4 and 3.5).

A common and very important tool in analytical toxicology is LC-MS/MS. Many different approaches using low or high resolution (HR) MS/MS techniques are described in the literature (48). One commonly used ionization technique for NSO is electrospray ionization (ESI) (29, 41, 45). Triple-quadrupole MS e.g., facilitates the simultaneous identification and quantification of multiple analytes. The selected system used in this work offers the opportunity of using a multiple-reaction monitoring (MRM) simultaneously monitoring quantitative and qualitative transition ions. Hence, a LC-MS/MS assay using MRM in positive mode following ESI was a suitable detection method for the NSO in this work (see Chapter 3.3). The advanced resolution and high accuracy of HRMS systems allows a distinction of mass-to-charge (m/z) ratios with a very small mass error (49). Over a wide m/z range, HRMS instruments can collect full scan data with this high detection sensitivity and thus allow the computation of empirical molecular formulas of precursor ions based on the formed fragment ions. Consequently, these instruments are helpful tools for metabolite identification and structure elucidation (48, 50–52). An already developed Orbitrap-based LC-HR-MS/MS screening approach (53–58), which has been extensively used for several drug metabolism studies, was applied in this work for the identification of the metabolic patterns of the investigated NSO (See Chapter 3.1 and 3.2).

1.3 Toxicokinetics

1.3.1 Basic Pharmacokinetic (Toxicokinetic) Concepts

The aim of pharmacokinetics (PK) is the description of the relationship of drug concentrations and administered doses in a living organism (59). Thus, PK describes the entirety of all processes that a drug is subjected to in the body (60). Regarding DOA, the term “pharmacokinetic” should be replaced by the term “toxicokinetic” due to the toxic effects evoked by the consumption of these substances instead of a pharmaceutical use. The field of PK or TK consists of the liberation of a drug from its administered form, the absorption, distribution, metabolism, and finally the excretion (59). In terms of pharmaceuticals, PK data are collected during extensive pre-clinical studies before admission for human use. As already mentioned, concerning NPS, these data are usually not available or rather do not exist. Hence, TK studies have to be performed after the appearance on the illicit drug market and moreover after first consumptions (13). Several TK parameters are considered in more detail in the following section.

1.3.2 Metabolism and metabolic investigations

One important part in a TK study and commonly one of the first investigations is the estimation of metabolic patterns of the drugs of investigation (61). Various substances are extensively metabolized and form many biomarkers. In some cases, parent compounds are not detectable anymore (56, 62). These circumstances make metabolism studies of NPS and thus the knowledge of analytical targets, that is to say the main urinary metabolites, essential for the understanding and monitoring of intoxications. They are of major interest since urine is the preferred matrix in abstinence monitoring programs, doping analysis, workspace drug testing, and in case of supposed intoxications (63–66).

In general, a metabolic biotransformation converts lipophilic compounds into hydrophilic and mostly detoxified forms, which could be more readily excreted (mostly via urine or bile) (67). Drug metabolism mainly occurs in the liver and can be separated into two reaction phases. In phase I reactions, the drugs are modified by the introduction of reactive or polar groups. These reactions such as oxidation, reduction, hydrolysis, epoxidation, dealkylation, or (de-)cyclization are mostly catalyzed by cytochrome P450 monooxygenases (CYP) (68). In the following, these modified and activated compounds are further conjugated to polar compounds such as glutathione, sulfate, acetate, glycine, or glucuronic acid in a phase II reaction. These reactions are catalyzed by a broad range of specified transferases like glucuronosyltransferases, sulfotransferases, or glutathione S-transferases (69).

Regarding NSO, several in vitro and in vivo studies were published presenting an overview of urinary metabolic patterns (25, 56, 70, 71). The main phase I reaction of fentanyl analogs are variable and depend on the modification or replacement of the propionyl chain. However, they are mostly metabolized by *N*-dealkylation, hydroxylation/oxidation of the phenethyl substructure/piperidine ring, cleaving off the phenethyl moiety, or amide hydrolysis. Phase II metabolites are mostly formed by glucuronidation or sulfation (25, 72, 73). Predominant phase I biotransformations of the non-fentanyl NSO U-compounds are *N*-demethylation, hydroxylation and their combinations (7,8). Metabolic studies showed only limited amounts of phase II metabolites (glucuronides, sulfates, or methylated forms) (56).

For the identification of phase I and II metabolites, various approaches exist differentiating between in vitro and in vivo models. Frequently used human in vitro models are pooled human liver microsomes (pHLM) or pooled human liver S9 fractions (phS9) (74, 75). Liver microsomes of other species e.g., pigs represent an alternative, if their metabolism should be analyzed. However, the possibility of losing the formation of specific metabolites when not all needed co-substrates of the metabolizing enzymes were added limits these studies (74). Additionally, the output of observed metabolic reactions depend on the subcellular fraction, which is used. For example, pHLM only contain membrane-bound enzymes and thus cover the reactions catalyzed by CYP enzymes, uridine 5'-diphospho-glucuronyltransferases, or flavin containing monooxygenases. On the contrary, phS9 fractions also contain cytosolic enzymes like sulfotransferases and thus cover more phase II metabolic reactions. As alternative to these cheap, time-saving, and easy performing approaches, primary human hepatocytes or human hepatocyte cell

lines are widely used even though these approaches are dealing with some difficulties such as high costs, elaborate handling, or inconsistency in the expression of metabolic enzymes (74). In general, in vitro systems offer the drawback of a static closed system resulting in the lack of some metabolites, because they are formed by multiple reaction stages and interactions such as under recirculation in the body. Furthermore, through a possible low formation of the basis phase I metabolites, a minor formation of phase II metabolites might occur (54). The output of in vitro assays generally never reflects the quantitative human urinary pattern, since not all built metabolites are inevitably excreted into urine. Therefore, human urinary samples are best suitable for the elucidation of the metabolic pattern. To circumvent the lacking opportunity of the implementation of controlled human studies, human urine samples from clinical or forensic cases can be utilized (76). Nonetheless, these studies are fraught for instance by mostly unknown type and dosage of the consumed drugs. A second common tool for the assessment of urinary excretion profiles are in vivo approaches with controlled studies in animal models (76), even though interspecies differences in the enzymatic pattern could lead to differences regarding the metabolism rate or forms of built metabolites (77, 78). One benefit of animal models over in vitro approaches is the reflection of the complexity of a metabolizing organism and the coverage of a certain time period with urinary excretion patterns. Rats represent a well-established and commonly used animal model (54, 56, 78–80), but limitations such as restricted routes of administration and limited amounts of body fluids pose difficulties with further TK studies in this model. To overcome these disadvantages, pigs can suit as an additional animal model (33, 35, 36, 81). Pigs not only bear benefits with respect to the quantity of sampled specimens. They are also strongly related to the human species in respect of CYP enzymes (82), anatomical structure, and physiological properties (83) resulting in a quite similar metabolism. Therefore, in the first TK study conducted in this work, the metabolic pattern determined in an in vitro metabolism approach was compared to the urinary metabolic pattern of rats regarding different NSO (see Chapter 3.1). In the further comprehensive TK study, it was examined whether the pig reflects the human excretion profile of the NSO U-47700 and the results were compared with alternative in vitro and in vivo approaches (see Chapter 3.2).

1.3.3 TK parameters resulting from blood and tissue distribution and TK modeling approaches

The distribution of a substance in the body is strongly related to the route of administration and thus to the bioavailability. Hence, the route of administration has to be well-considered when planning a TK study. The bioavailability measures the percentage amount of the active ingredient that is available unchanged in the systematic circulation (84). NSO are consumed through different routes, amongst others nasal, oral, rectal, and intravenous (i.v.) (19). Within oral, nasal, and rectal ingestion, the absorbed substance amount can be reduced by passages through bio membranes or by first-pass metabolism and thus results in less than 100% bioavailability. However, concerning NSO, i.v. administration also

reflects common user habits. This form of administration ensures that the whole extent of unaffected substance reaches the systemic circulation (100% bioavailability). (19). Hence, an exact quantification while verifying a TK model and assessing TK data could be guaranteed.

TK refers to the rate and extent of distribution of a substance into the blood circulation and to different tissues as well as to the rate of elimination (85) and can be reduced to mathematical equations describing such processes. To describe the concentration-time profile of a substance during a TK study, contemplating the body as a system of kinetic compartments has proven helpful. A compartmental analysis is an intricated mathematical model, which could be applied for the description of concentration-time profiles based on the calculation of different parameters such as the area under the curve (AUC), the elimination half-life time ($t_{1/2}$), the volume of distribution (V_d), or the clearance (Cl) (84). The AUC describes the integral of the concentration-time profile of a substance and is proportional to the bioavailable amount. The $t_{1/2}$ refers to the time period in which a concentration of a drug drops to the half of its origin. V_d is a fictive volume in which the whole amount of a drug must be distributed to reach the measured concentration in a homogenous solution of the analyzed body fluid. Cl is the virtual volume of body fluid cleared of the substance in a defined time unit and therefore a measuring unit of the elimination rate (85). In such an analysis, compartments not necessarily have a physiological basis, but a compartment is an element of an exchange system being homogeneous in itself and owning uniform kinetic parameters (86, 87). During compartmental analysis, one has to decide between a one-compartment model and multi-compartment models. In a one-compartment model, all body fluids are in a steady-state status and the whole body could be regarded as one systematic compartment (central compartment as blood and tissues with instantaneous equilibration) into which a substance is delivered (88). Multi-compartment models describe the distribution of a substance into one or few additional peripheral compartments (tissues with slower equilibration) and consider the redistribution between those compartments as well. Thus, these models regard the decrease of the concentration of a substance in a central compartment and simultaneously the increase in one or more peripheral compartments (distribution phase). If a certain state of equilibration is reached, both concentrations decrease in the same rate (elimination phase) (84). One commonly used model for drugs following i.v. administration is the three-compartment model consisting of a central compartment and two peripheral compartments (highly and scarcely perfused tissues). The concentration-time-profile of such a model depends on an additional tissue release phase next to the distribution and elimination phase.

Furthermore, one has to decide between individual and population (pop) TK modeling. Individual TK approaches characteristically employ noncompartmental models and are best to define individual TK profiles or if fast processing TK parameters are needed (89). In contrast, popTK modeling approaches rely on concentration-time data from multiple individuals and data from all individuals are evaluated simultaneously (90). PopTK models are mainly based on complex mathematical and compartmental methods and thus the model development is a time-consuming process. In popTK approaches covariate information such as age, sex, weight, and renal/hepatic function are incorporated enabling the possibility

to explain sources of interindividual TK variability within a population (89). This approach is based on a nonlinear mixed-effects model whereas "nonlinear" implies that dependent parameters such as the concentration are nonlinearly related to the model parameters. "Mixed-effects" corresponds to the parameterization including fixed effects (parameters not varying throughout the individuals) and random effects (parameters varying across individuals). In conclusion, the development of a popTK model consists of different aspects involving the experimental data, structural, statistical, and covariate models as well as a modeling software (90). One advantage of popTK models is the possibility of an allometric scaling (single and multiple species) and thus the extrapolation of TK parameters across different species. Due to ethical reasons, particularly concerning NPS or DOA, TK studies have to be conducted in non-human species, even though human TK are necessary to evaluate clinical or forensic toxicology data. Thus, allometric scaling techniques are an important tool in TK for the prediction of human TK data by the use of data collected from animal species. Amongst others, this empirical examination is based on the relationship between the metabolic rate, the size of the used animal model, and the species of interest (91).

Concerning tramadol, multiple pre-clinical studies of this pharmaceutical agent were performed in man. Nevertheless, most of those PK studies were performed following oral administration, whereas only few exist after i.v. administration (92). Indeed, several PK studies using different animal models were performed with this substance (93–95). After i.v. administration, tramadol concentrations rapidly decreased during the first hour and showed a slower decline afterwards. The maximum serum concentration of the active metabolite *O*-desmethyltramadol is reached about 4.5 h following i.v. administration in humans (96), whereas different animals show a faster biotransformation to this metabolite (93). In conclusion, all studies showed a high tissue affinity of this lipophilic substance, resulting in a $t_{1/2}$ of about 6 h in human which is independent of the route of administration (96).

Regarding NSO, a detailed knowledge of TK is mostly lacking, especially regarding U-47700. However, in comparison to the basic and lipophilic properties of U-47700 and tramadol, a similar TK behavior might be possible. Yet, one systematic animal study was performed using the rat as experimental model for investigations on blood distribution of U-47700 (80). Apart from this, the distribution in blood was described in one human case report (29) and the tissue distribution in several human fatal cases (30). These data showed a comparable $t_{1/2}$ of U-47700 to tramadol in human (29), whereas elimination might occur faster in rats (80). However, data on TK of NSO are restricted and should be accomplished using systematic and controlled TK studies. As already mentioned, pigs provide sufficient sample amounts and display comparable physiological and anatomical structures to human (82, 83). This animal model was found to be suitable as TK model for another NPS subclass, namely synthetic cannabinoids (33–37). Therefore, TK properties of the NSO U-47700 including blood as well as tissue distribution with tramadol as reference compound was elucidated using a pig animal model (see Chapter 3.3 and 3.4).

1.4 Postmortem Toxicology

The evaluation of results of toxicological analyses in postmortem (PM) cases is one of the most challenging tasks for forensic toxicologists. Several parameters such as dose and time of intake, time of death, and the PM interval (PMI) are mostly unknown. PM drug concentrations usually do not mirror the concentrations at time of death. Furthermore, the drug concentrations may vary dependent on the sampling site or the PMI (97). Changes that occur in the concentration of drugs during or after death are also referred to as PM redistribution (PMR) and the potential for PMR must be considered in many, but not in all drugs (59, 98). There are various and complex underlying mechanisms and factors resulting in PMR consisting of an interaction between the changes occurring in the body during or after death and the PK properties of a substance (59, 98). One key element of PMR is the release from several organs with high drug concentrations (drug reservoir) to surrounding organs and tissues with lower concentrations driven by diffusion processes (97). Next to diffusion processes, the cell death, and the decrease of intracellular pH have a big impact of drug accumulation and further redistribution into the extracellular space (97, 99). Thus, the basic and lipophilic properties as well as the V_d can be considered for the interpretation whether a substance is prone for PMR or not. In addition, processes as changes in blood fluidity, hemolysis (breakdown of red blood cells), hypostasis (sediment to lower parts of the body by gravity), or protein break down could have an impact on site dependent concentration changes in drug levels if drugs display an antemortem binding to red blood cells or proteins (59, 100). After death, putrefaction processes with body decomposition as well as neo-formation, artefactual formation, or degradation of drugs can also account for drug concentrations changes (100). In addition, substances may be further metabolized and excreted into urine in the agonal phase. Based on the duration of the agonal phase, markable changes of the PM drug level are the consequence (59). To assess the probability of a substance to undergo PMR, several parameters next to the already described physicochemical properties of a substance could be taken into consideration. First, a central-to-peripheral blood concentration ratio greater than 1 can indicate a predisposition for PMR (101). Next, substances with a liver-to-peripheral blood ratio greater than 5 might underlie a PMR potential (102). Another issue in PM toxicology is that routinely analyzed specimens such as blood are sometimes not available and alternative matrices have to be used. Thus, knowledge on the tissue distribution of a substance is essential. In the pig TK study, the PM tissue distribution of U-47700, tramadol and their main metabolites was assessed. Furthermore, it was examined whether these substances are prone to PMR or not during storage at room temperature over three different PMI and the PM distribution should be compared to the perimortem distribution (see Chapter 3.5).

2. AIMS AND SCOPES

New synthetic opioids display a public health concern and usually little or nothing is familiar about the TK data of these substances before they appear on the illicit drug market. As TK data are essential for a trustworthy interpretation of analytical results from clinical and forensic cases, the aim of this dissertation was a further knowledge acquisition about TK data of different NSO. First, the metabolic fate of methoxyacetylfentanyl, U-47931E, and U-51754 as representatives of fentanyl derived and non-fentanyl derived NSO should be investigated using in vitro and in vivo approaches with a following comparison of the models. For a comprehensive knowledge, a TK study of the NSO U-47700 should be performed in a systematic controlled pig study following i.v. administration. There, parameters such as metabolism, time-dependent distribution in serum and blood, kinetic properties, as well as perimortem and PM tissue distribution should be elucidated.

The following steps had to be conducted:

- Detection, identification, and comparison of phase I and II metabolites of U-47931E, U-51754, and methoxyacetylfentanyl studied in rat urine and phS9 fractions under the use of LC-HR-MS/MS
- Elucidation of the metabolic pattern of U-47700 in pig urine using LC-HR-MS/MS and comparison with the metabolic pattern studied in different in vitro and in vivo approaches as well as in human urine
- Development of an analytical LC-MS/MS method for the simultaneous detection and quantification of U-47700, tramadol, and their main metabolites in pig serum and whole blood
- Determination of concentration-time profiles of U-47700 following i.v. administration to pigs in comparison to tramadol
- Modeling of the concentration-time profiles and assessment whether this model can be used for the extrapolation to human data
- Investigations of the perimortem and postmortem distribution of U-47700, tramadol and their main metabolites in representative specimens, such as relevant organs, tissues, and body fluids, following i.v. administration to pigs
- Investigations of time-dependent postmortem concentration changes throughout three different time points in the studied organs, tissues, and body fluids in comparison to the perimortem findings

3. PUBLICATIONS OF THE RESULTS

The results of this dissertation were published in the following papers:

3.1 Studies on the in vitro and in vivo metabolism of the synthetic opioids U-51754, U-47931E, and methoxyacetylfentanyl using hyphenated high-resolution mass spectrometry (103)

(DOI: 10.1038/s41598-019-50196-y)

Authors Contributions Frederike Nordmeier conducted and evaluated the experiment as well as composed the manuscript; Lilian H. J. Richter developed the incubations using pooled human liver S9 fractions; Nadine Schaefer, Markus R. Meyer, and Peter H. Schmidt assisted with scientific discussions and the development of the experiments as well as supervised the research.

SCIENTIFIC REPORTS
nature research

OPEN

Studies on the in vitro and in vivo metabolism of the synthetic opioids U-51754, U-47931E, and methoxyacetylfentanyl using hyphenated high-resolution mass spectrometry

Received: 30 May 2019
Accepted: 9 September 2019
Published online: 24 September 2019

Frederike Nordmeier[1], Lilian H. J. Richter[2], Peter H. Schmidt[1], Nadine Schaefer[1] & Markus R. Meyer[2]

New Synthetic Opioids (NSOs) are one class of New Psychoactive Substances (NPS) enjoying increasing popularity in Europe. Data on their toxicological or metabolic properties have not yet been published for most of them. In this context, the metabolic fate of three NSOs, namely, trans-3,4-dichloro-*N*-[2-(dimethylamino)cyclohexyl]-*N*-methyl-benzenacetamide (U-51754), trans-4-bromo-*N*-[2-(dimethylamino)cyclohexyl]-*N*-methyl-benzamide (U-47931E), and 2-methoxy-*N*-phenyl-*N*-[1-(2-phenylethyl)piperidin-4-yl] acetamide (methoxyacetylfentanyl), was elucidated by liquid chromatography high-resolution mass spectrometry after pooled human S9 fraction (phS9) incubations and in rat urine after oral administration. The following major reactions were observed: demethylation of the amine moiety for U-51754 and U-47931E, *N*-hydroxylation of the hexyl ring, and combinations thereof. *N*-dealkylation, *O*-demethylation, and hydroxylation at the alkyl part for methoxyacetylfentanyl. Except for U-47931E, parent compounds could only be found in trace amounts in rat urine. Therefore, urinary markers should preferably be metabolites, namely, the *N*-demethyl-hydroxy and the hydroxy metabolite for U-51754, the *N*-demethylated metabolite for U-47931E, and the *N*-dealkylated metabolite as well as the *O*-demethylated one for methoxyacetylfentanyl. In general, metabolite formation was comparable *in vitro* and *in vivo*, but fewer metabolites, particularly those after multiple reaction steps and phase II conjugates, were found in phS9. These results were consistent with those of comparable compounds obtained from human liver microsomes, human hepatocytes, and/or human case studies.

There has been a rapid increase in New Psychoactive Substances (NPS) over the last decade. Many of them are not yet controlled and predominantly sold via the Internet as 'legal' replacements for drugs already subject to controls, such as heroin, cannabis or cocaine. New Synthetic Opioids (NSOs) are one class of NPS, mostly consisting of analogues of the highly potent analgesic fentanyl exploiting the fentanyl phenylpiperidine structure[1]. There are also other non-fentanyl synthetic opioids that share neither the fentanyl-like nor the classical morphine-like chemical structure. In Europe, their availability and popularity has grown continuously over recent years[2]. NSOs include compounds that were produced by pharmaceutical companies looking for new pharmaceutics, but were never registered for medical use due to strong side effects or insufficient action. Furthermore, NSOs are illegally synthesised in clandestine laboratories in China through modification of molecule residues[3–6]. Multiple cases of

[1]Institute of Legal Medicine, Saarland University, 66421, Homburg, Germany. [2]Department of Experimental and Clinical Toxicology, Institute of Experimental and Clinical Pharmacology and Toxicology, Center for Molecular Signaling (PZMS), Saarland University, 66421, Homburg, Germany. Correspondence and requests for materials should be addressed to M.R.M. (email: markus.meyer@uks.eu)

classical opioid toxidrome and several overdose deaths in Europe related to NSOs have been reported in recent years[3,7–10]. On the one hand, users are often not aware of consuming these compounds, because batches might be sold as heroin, other illicit opioids or even as counterfeit pain killers[3,11]. On the other, only little is known and published about the toxicology of these substances[12].

Two non-fentanyl-related compounds discussed in drug user forums and available for sale on the Internet are trans-3,4-dichloro-*N*-[2-(dimethylamino)cyclohexyl]-*N*-methyl-benzenacetamide (U-51754) and trans-4-bromo-*N*-[2-(dimethylamino)cyclohexyl]-*N*-methyl-benzamide (U-47931E, bromadoline). Both are structurally related to 3,4-dichloro-*N*-[(1 R,2 R)-2-(dimethylamino)cyclohexyl]-*N*-methylbenzamide, commonly known as U-47700, and were synthesised by the Upjohn Company in an attempt to produce non-addicting analgesics as potent as morphine. Oral doses for U-51754 range from 12 to 25 mg and for U-47931E from 25 to 50 mg[13–15]. Despite being discussed in drug user forums since U-47700 was subjected to controls, both compounds have not been detected in forensic or clinical samples so far[16], which may be due to the lack of information about suitable urine screening targets.

Another NSO, a fentanyl analogue, which has been associated with several fatal intoxications, is 2-methoxy-*N*-phenyl-*N*-[1-(2-phenylethyl)piperidin-4-yl] acetamide, commonly known as methoxyacetylfentanyl[17]. So far, fatalities in Sweden, Denmark, and the USA have been reported, together with numerous seizures throughout Europe[18]. According to drug user forums, the ingested dose of methoxyacetylfentanyl ranges from 0.5 to 5 mg depending on the route of administration[19,20]. However, no reports regarding potency are available yet[17,18].

To understand and monitor intoxications with NSOs, knowledge of analytical targets is necessary for toxicological analysis. As urine is the preferred matrix for comprehensive screening, e.g. in abstinence monitoring programmes, doping analysis, workspace drug testing, and in the case of suspected intoxications, metabolites should be known.

Owing to the lack of such data, the aim of the present work was to elucidate the metabolic patterns of the synthetic non-fentanyl opioids U-51754 and U-47931E and of methoxyacetylfentanyl by using liquid chromatography high-resolution tandem mass spectrometry (LC-HR-MS/MS). Metabolic identification was performed *in vitro* using pooled human S9 fractions (phS9) and *in vivo* analysing rat urine after oral administration. Finally, both models were compared.

Experimental

Chemicals and reagents. Methoxyacetylfentanyl hydrochloride (purity ≥ 98%), U-51754 hydrochloride (purity 98%), and U-47931E were purchased from LGC Standards (Wesel, Germany). Isocitrate, isocitrate dehydrogenase, superoxide dismutase, 3′-phosphoadenosine-5′-phosphosulfate (PAPS), S-(5′-adenosyl)-L-methionine (SAM), dithiothreitol (DTT), reduced glutathione (GSH), acetyl carnitine, and acetyl coenzyme A (AcCoA) were all purchased from Sigma (Taufkirchen, Germany), $NADP^+$ from Biomol (Hamburg, Germany), and acetonitrile (LC-MS grade), ammonium formate (analytical grade), formic acid (LC-MS grade), methanol (LC-MS grade), glucuronidase (EC No. 3.2.1.32)/arylsulfatase (EC No. 3.1.6.1) from Helix pomatia L, and all other chemicals and reagents (analytical grade) from VWR (Darmstadt, Germany). phS9 (20 mg protein/mL, from 30 individual donors), UGT reaction mix solution A (25 mM UDP-glucuronic acid), and UGT reaction mix solution B (250 mM Tris–HCl, 40 mM $MgCl_2$, and 0.125 mg/mL alamethicin) were obtained from Corning (Amsterdam, The Netherlands). After delivery, the enzyme preparations were thawed at 37 °C, aliquoted, snap-frozen in liquid nitrogen, and stored at −80 °C until use.

Incubation conditions for identification of phase I and II metabolites by LC-HR-MS/MS in phS9. The incubation conditions were in accordance to the experimental design developed by Richter *et al.*[21]. Incubations of phS9 (final protein concentration of 2 mg/mL) were performed after 10 min pre-incubation at 37 °C with 25 µg/mL alamethicin (UGT reaction mix solution B), 90 mM phosphate buffer (pH 7.4), 2.5 mM Mg^{2+}, 2.5 mM isocitrate, 0.6 mM $NADP^+$, 0.8 U/mL isocitrate dehydrogenase, 100 U/mL superoxide dismutase, 0.1 mM AcCoA, and 2.3 mM acetyl carnitine. Afterwards, to reach a final volume of incubation mixture of 150 µL, 2.5 mM UDP-glucuronic acid (UGT reaction mix solution A), 40 µM aqueous PAPS, 1.2 mM SAM, 1 mM DTT, 10 mM GSH, and 25 µM substrate in phosphate buffer were added. All given concentrations are final concentrations. By adding the substrate, the reaction was initiated and the mixture was incubated for 60 and 360 min respectively. After 60 min a 60 µL aliquot of the mixture was transferred into a reaction tube. Reactions were terminated by adding 20 µL of ice-cold acetonitrile. The remaining mixture was incubated for additional 5 h. Thereafter, the reactions were stopped by adding 30 µL of ice-cold acetonitrile. The solutions were cooled for 30 min at −18 °C and centrifuged for 2 min at 14,000 rpm. The supernatants were transferred into autosampler vials and 5 µL injected onto the Orbitrap-based LC-HR-MS/MS system as described below. To confirm the absence of interfering compounds and to identify non-metabolically originated compounds, additional blank incubations without substrate and control samples without phS9 were prepared.

Rat urine samples. According to an established study design[22–24], the investigations were performed using rat urine samples from male Wistar rats (Charles River, Sulzfeld, Germany) for toxicological diagnostic reasons according to German law. The experimental protocol was approved by an ethics committee (Landesamt für Verbraucherschutz, Saarbrücken, Germany). For metabolite identification, the compounds were administered in an aqueous suspension by gastric intubation of a single 0.6 mg/kg (U-47931E, U-51754) or 0.06 mg/kg (methoxyacetylfentanyl) body weight dose, calculated based on doses reported in trip reports and scaled by dose-by-factor approach from man to rat according to Sharma and McNeill[16]. The rats were housed in metabolism cages for 24 h, having water ad libitum. Urine was collected separately from faeces over a 24 h period using a grid plate. Blank urine samples were collected before drug administration to verify that the samples were free of interfering compounds. The samples were aliquoted and stored at −20 °C before analysis.

Sample preparation for identification of phase I and II metabolites by LC-HR-MS/MS in rat urine. In accordance to published procedures[25], 100 µL of urine was mixed with 500 µL of acetonitrile for precipitation. After shaking and centrifugation for 2 min at 14,000 rpm, the supernatant was transferred into new vials and gently evaporated to dryness under a stream of nitrogen. Afterwards, the extract was reconstituted in 50 µL of eluent A and eluent B (1:1, v/v) and transferred into autosampler vials.

According to previous studies[26], additionally, urine samples were treated with β-glucuronidase/arylsulfatase for conjugate cleavage prior to the extraction procedure. A volume of 200 µL urine was incubated with 20 µL β-glucuronidase/arylsulfatase and 180 µL 100 mM aqueous ammoniumacetate buffer (pH 5.2) for 2 h at 55 °C. The extract was precipitated by adding 1 mL of acetonitrile and stored for 5 min at −20 °C. After shaking and centrifugation, the supernatant was gently evaporated and reconstituted with 100 µL of mobile phase A and B (1:1, v/v) described below.

Furthermore, a basic solid phase extraction (SPE) was performed[23]. SPE was carried out using Biotage HCX columns (Isolute Confirm HXC cartridges, 130 mg, 3 mL from Biotage, Uppsala, Sweden). They were conditioned with 1 mL of methanol and 1 mL of water. An aliquot of 2.5 mL urine was mixed with 2 mL of water and 50 µL of internal standard (0.01 mg/mL trimipramine-d_3) and loaded onto the cartridges. Two washing steps with 1 mL water and 1 mL HCl (0.01 M) were performed. Maximum vacuum was applied for a short time. After adding 2 mL of methanol, the columns were dried for one min under maximum vacuum. Analyte elution was performed with 1 mL methanol/33% aqueous ammonia (98:2 v/v). The eluate was evaporated to dryness under a gentle stream of nitrogen at 70 °C and reconstituted with 50 µL of methanol. For conjugate cleavage, additional urine aliquots were treated with glucuronidase/arylsulfatase prior to the extraction procedure. An aliquot of 2.5 mL urine was adjusted to pH 5.2 with 1 M acetic acid. After incubation with 50 µL glucuronidase/arylsulfatase for 2 h at 55 °C following centrifugation, SPE was performed as described above. Five microlitres of the extracts were injected onto the LC-HR-MS/MS system with conditions described below.

LC-HR-MS/MS instrumentation for identification of phase I and II metabolites. As described previously[27], the extracts were analysed using a Thermo Fisher Scientific (TF, Dreieich, Germany) Dionex UltiMate 3000 RS pump consisting of a degaser, a quaternary pump, and an UltiMate autosampler, coupled to a TF Q-Exactive Plus system equipped with a heated electrospray ionization (HESI)-II source.

The LC conditions were as follows: Gradient elution was run on a TF Accucore PhenylHexyl column (100 mm × 2.1 mm, 2.6 µm) with column oven temperature of 60 °C. The mobile phase consisted of 2 mM aqueous ammonium formate containing 0.1% (v/v) formic acid and 1% (v/v) acetonitrile (pH 3, eluent A), and 2 mM ammonium formate solution with acetonitrile/methanol (50:50, v/v) containing 0.1% (v/v) formic acid and 1% (v/v) water (eluent B). The gradient and flow rate were programmed as follows: 0–1 min hold 99% A, 1–10 min 99% A to 1% A, both with flow rate 0.5 mL/min, 10–11.5 min hold, 11.5–13.5 min hold 99% A, both with flow rate 0.8 mL/min.

The HESI-II source conditions were as follows: sheath gas, 60 arbitrary units (AU); auxiliary gas, 10 AU; spray voltage, 3.00 kV; heater temperature, 320 °C; ion transfer capillary temperature, 320 °C; and S-lense RF level, 60.0.

The mass spectrometry was operated in positive ionisation mode using full scan (FS) and subsequent data dependent acquisition (DDA) mode with inclusion list containing the *m/z* values of expected metabolites. Mass calibration was done prior to analysis according to the manufacture's recommendations using external mass calibrators. The settings for FS data were as follows: resolution, 35,000; microscans, 1; automatic gain control (AGC) target, 1e6; maximum injection time (IT), 120 ms; scan range for U-compounds, *m/z* 100–600 and for methoxyacetylfentanyl, *m/z* 180–600. The settings for the DDA mode were as follows: option "do not pick others", enabled; dynamic exclusion, off; resolution, 17,500; microscans, 1; loop count, 5; AGC target, 2e5; maximum IT, 250 ms; isolation window, 1.0 *m/z*, high collision dissociation (HCD) with stepped normalised collision energy (NCE), 17.5, 35, and 52.5%; spectrum data type, profile; underfill ratio, 0.5%. For data handling Xcalibur Qual Browser software version 3.0.63 was used. The MS settings as well as the LC conditions were the same for analysing all samples.

Results

ESI^+ HR-MS/MS of the investigated compounds and tentative identification of their phase I metabolites based on MS/MS fragmentation. An overview of all tentatively identified phase I and II metabolites is given in Tables 1–3, including elemental compositions, exact masses, accurate masses, characteristic fragment ions, mass errors, and retention times. Selected ESI^+ MS^2 spectra of the most abundant metabolites are shown in Figs 1–3. Selected mass spectral data for additional metabolites are shown in the Electronic Supplementary Material (EMS). Owing to the high number of tentatively identified metabolites, not all are discussed in detail in the following. The numbering of given examples is in accordance with the respective tables.

As already described for U-47700 in previous metabolism studies[28], the HR-MS data indicated that U-51754 and U-47931E could be broken down into two parts at the amide nitrogen usually forming fragment ions that belong to the dichlorophenyl-*N*-methylacetamide part or the cyclohexyl part. The fragment ions of the unmodified or modified dichlorophenyl part or the cyclohexyl part were used (according to Figs 1 and 2 and Tables 1 and 2) for the spectra interpretation and identification of the expected metabolites based on the accurate precursor mass (PM) and calculated molecular formulas. Based on the procedure described, 14 phase I metabolites of U-51754 could be identified. In phS9 incubates, 10 metabolites were detected (A1–6, A9-11, A13). In these, *N*-demethyl-U-51754 formed the most abundant peak. In rat urine, seven metabolites were observed (A1, A6-8, A11-12, A14), with *N*-demethyl-hydroxy-U-51754 being the main metabolite. In urine samples, seven additional phase II metabolites were found (A15-21), five conjugated with glucuronic acid and two with sulphuric acid. Nine phase I metabolites of U-47931E could be identified. In this connection, *N*-demethyl-U-47931E was the most abundant peak in phS9 incubates and rat urine samples. *In vitro*, three metabolites were found (B1-3), and

ID	Analyte	Elemental composition	Monoisotopic exact masses	Monoisotopic accurate masses	Error (ppm)	Accurate fragment masses (*m/z*)								
						Product 1	Error (ppm)	Product 2	Error (ppm)	Product 3	Error (ppm)	Product 4	Error (ppm)	RT (min)
	U-51754	$C_{17}H_{25}ON_2Cl_2$	343.1338	343.1336	−0.585	298.0758	−0.556	218.0134	−0.062	158.9763	−0.105	112.1124	2.559	5.62
A1	*N*-demethyl I-	$C_{16}H_{23}ON_2Cl_2$	329.1181	329.1183	0.356	298.0757	−0.885	218.0133	−0.247	158.9760	−1.494	112.1118	−2.403	5.60
A2	*N*-demethyl II-	$C_{16}H_{23}ON_2Cl_2$	329.1181	329.1177	−1.485	284.0609	1.905	203.9982	2.037	158.9767	3.892	98.0969	4.349	5.47
A3	*N,N*-bisdemethyl-	$C_{15}H_{21}ON_2Cl_2$	315.1025	315.1020	−1.580	284.0602	−0.401	203.9977	−0.124	158.9765	1.649	98.0968	3.684	5.42
A4	*N,N,N*-tridemethyl-	$C_{14}H_{20}ON_2Cl_2$	301.0868	301.0872	0.964	284.0604	0.268	203.9980	1.076	158.9763	0.130	98.0970	5.803	5.22
A5	Hydroxy I-	$C_{17}H_{25}O_2N_2Cl_2$	359.1287	359.1287	−0.221	314.0711	0.538	218.0134	−0.135	158.9762	−0.412	110.0969	4.204	4.75
A6	Hydroxy II-	$C_{17}H_{25}O_2N_2Cl_2$	359.1287	359.1286	−0.489	314.0707	−0.559	234.0082	−0.469	174.9711	−0.644	112.1123	1.972	4.15
A7	Dihydroxy I-	$C_{17}H_{25}O_3N_2Cl_2$	375.1236	375.1214	−6.067	330.0651	−2.170	234.0079	−1.840	174.9709	−1.863	110.0968	3.145	3.32
A8	Dihydroxy II-	$C_{17}H_{25}O_3N_2Cl_2$	375.1236	375.1536	3.050	330.0927	1.001	250.0273	2.964	190.9890	3.223	112.1124	2.924	5.21
A9	*N*-oxide-	$C_{17}H_{25}O_2N_2Cl_2$	359.1287	359.1292	1.130	298.0947	−1.128	218.0132	−0.855	158.9766	2.265	112.1124	2.860	5.52
A10	*N*-oxide-hydroxy-	$C_{17}H_{25}O_3N_2Cl_2$	375.1236	375.1236	−0.316	314.0710	0.416	218.0134	−0.108	158.9762	−0.338	110.0969	4.204	4.90
A11	*N*-demethyl-hydroxy I-	$C_{16}H_{23}O_2N_2Cl_2$	345.1131	345.1130	−0.424	314.0707	−0.083	218.0133	−0.103	158.9761	−1.083	110.0966	1.236	4.86
A12	*N*-demethyl-hydroxy II-	$C_{16}H_{23}O_2N_2Cl_2$	345.1131	345.1128	−0.963	314.0709	−0.041	234.0083	−0.000	174.9711	−0.819	112.1123	2.158	4.49
A13	*N,N*-bisdemethyl-hydroxy I-	$C_{15}H_{21}O_2N_2Cl_2$	331.0974	331.0977	0.7805	314.0711	0.449	203.9978	0.145	158.9763	−0.074	79.055	9.865	4.77
A14	*N,N*-bisdemethyl-hydroxy II-	$C_{15}H_{21}O_2N_2Cl_2$	331.0974	331.0976	0.410	314.0708	−0.413	219.9925	−0.690	174.9711	−0.434	112.1123	2.191	4.48
A15	hydroxy-glucuronide	$C_{23}H_{33}O_8N_2Cl_2$	535.1608	535.1611	0.471	359.1273	−1.253	314.0707	0.736	234.0082	−0.546	112.1123	1.996	4.58
A16	dihydroxy-glucuronide	$C_{23}H_{33}O_9N_2Cl_2$	551.1557	551.1549	−1.536	375.1234	−0.705	330.0695	0.157	250.9661	−0.080	112.1123	2.087	3.76
A17	*N*-demethyl-hydroxy-glucuronide	$C_{22}H_{31}O_8N_2Cl_2$	521.1451	521.1451	−0.101	345.1129	−0.534	314.0706	0.631	234.0082	−0.673	112.1123	2.089	3.59
A18	*N*-demethyl-hydroxy-sulfate	$C_{16}H_{23}O_5N_2Cl_2S$	425.0699	425.0685	−3.257	394.0266	−2.983	345.1121	−2.736	314.0701	−2.398	112.1121	−0.114	4,23
A19	*N*-demethyl-dihydroxy-glucuronide	$C_{22}H_{30}O_9N_2Cl_2$	537.1401	537.1386	−2.828	361.1070	−3.280	330.0649	−2.773	250.0025	−3.260	112.1121	−0.054	3.82
A20	*N,N*-bisdemethyl-hydroxy-glucuronide	$C_{21}H_{28}O_8N_2Cl_2$	507.1295	507.1260	4.656	331.0975	0.028	300.0554	0.548	219.9925	−0.938	112.1124	2.466	3.59
A21	*N,N*-bisdemethyl-hydroxy-sulfate	$C_{15}H_{20}O_5N_2Cl_2S$	411.0542	411.0529	−5.071	331.0962	−4.097	300.0542	−2.954	219.9921	−1.624	112.1122	0.746	4.15

Table 1. Identification (ID), U-51754 and its metabolites as well as elemental composition, exact mass, accurate mass, characteristic product ions, mass errors, and retention time (RT) of the compounds detected in pS9 incubations and in rat urine after oral administration. Elemental composition and all given masses are protonated forms.

in vitro all nine (B1-9) metabolites were detected. In the urine samples, four additional glucuronides were identified (B10-13).

The HR-MS data of methoxyacetylfentanyl indicated that the molecule could be cleaved between the piperidine ring and the *N*-phenylacetamide moiety leading to the most abundant fragment ion of the phenylethylpiperidine. The phenethyl chain represented another characteristic fragment ion. The fragment ions of the unmodified or modified phenylethylpiperidine, phenethyl chain or methoxy-*N*-phenylacetamide were used (according to Fig. 3 and Table 3) for the spectra interpretation of methoxyacetylfentanyl metabolites. In total, 15 phase I metabolites could be tentatively identified for methoxyacetylfentanyl. In phS9 incubates, 14 metabolites were detected (C1-9, C11-15) with *O*-demethyl-methoxyacetylfentanyl forming the most abundant peak. In rat urine, 11 metabolites were observed (C1-2, C4, C6-8, C10-12, C14-15), with hydroxy-methoxyacetylfentanyl being the main metabolite. In urine samples, six additional glucuronides were found (C16-21). One of them could be identified in phS9 as well.

ESI$^+$ HR-MS/MS fragmentation of U-51754. U-51754 (PM at *m/z* 343.1336) was characterised by the most abundant fragment ion at *m/z* 298.0758 ($C_{15}H_{18}ONCl_2$), indicating loss of the dimethylamine moiety. The

ID	Analyte	Elemental composition	Monoisotopic exact masses	Monoisotopic accurate masses	Error (ppm)	Accurate fragment masses (*m/z*)								
						Product 1	Error (ppm)	Product 2	Error (ppm)	Product 3	Error (ppm)	Product 4	Error (ppm)	RT (min)
	U-47931E	$C_{15}H_{22}ON_2Br$	325.0909	325.0911	0.191	280.0332	0.069	199.9706	0.064	182.9440	0.230	126.1279	1.251	4.10
B1	*N*-demethyl-	$C_{14}H_{20}ON_2Br$	311.0753	311.0752	−0.392	280.0331	−0.095	199.9705	−0.061	182.9441	0.272	112.1124	3.325	3.98
B2	*N*,*N*-bisdemethyl-	$C_{13}H_{18}ON_2Br$	297.0596	297.0594	−0.919	280.0327	−1.551	199.9702	0.103	182.9437	−1.391	98.0969	4.346	3.89
B3	Hydroxy I-	$C_{15}H_{22}O_2N_2Br$	341.0859	341.0858	−0.313	296.0278	−0.973	278.0174	−0.434	182.9439	−0.433	142.1226	−0.373	3.45
B4	Hydroxy II-	$C_{15}H_{22}O_2N_2Br$	341.0859	341.0860	0.238	296.0280	−0.075	215.9654	−0.133	198.9388	−0.610	126.1226	0.737	4.38
B5	*N*-demethyl-hydroxy I-	$C_{14}H_{20}O_2N_2Br$	327.0702	327.0704	0.434	296.0278	−0.933	278.0174	−0.027	182.9440	−0.4257	128.1071	0.619	3.30
B6	*N*-demethyl-hydroxy II-	$C_{14}H_{20}O_2N_2Br$	327.0702	327.0706	1.061	296.0284	1.101	215.9655	0.092	198.9389	−0.024	112.1124	2.969	4.19
B7	*N*,*N*-bisdemethyl-hydroxy I-	$C_{13}H_{18}O_2N_2Br$	313.0546	313.0544	−0.690	296.0280	−0.380	278.0173	−0.813	182.9439	−0.301	114.0916	2.581	3.15
B8	*N*,*N*-bisdemethyl-hydroxy II-	$C_{13}H_{18}O_2N_2Br$	313.0546	313.0500	1.610	296.0283	0.718	215.9655	0.718	198.9388	−0.809	98.0970	5.462	4.14
B9	*N*-demethyl-dihydroxy-	$C_{14}H_{20}O_3N_2CBr$	343.0651	343.0646	−1.738	312.0227	−0.899	231.9600	−1.527	214.9336	−1.070	112.1124	2.745	4.34
B10	Hydroxy-glucuronide	$C_{21}H_{30}O_8N_2Br$	517.1179	517.1186	1.139	341.0863	1.022	296.0282	0.370	215.9655	0.049	126.1278	0.737	3.77
B11	Dihydroxy-glucuronide	$C_{21}H_{30}O_9N_2Br$	533.1129	533.1129	0.016	312.0227	−0.905	231.9604	0.216	214.9337	−0.803	112.1124	2.839	4.35
B12	*N*-demethyl-hydroxy-glucuronide	$C_{20}H_{28}O_8N_2Br$	503.1023	503.1029	1.103	327.0704	0.431	296.0282	0.498	198.9388	−0.683	112.1124	2.563	3.65
B13	*N*,*N*-bisdemethyl-hydroxy-glucuronide	$C_{19}H_{26}O_8N_2Br$	489.0866	489.0866	−0.165	313.0544	−0.642	296.0283	0.718	215.9654	−0.199	198.9388	−0.643	3.58

Table 2. Identification (ID), U-47931E and its metabolites as well as elemental composition, exact mass, accurate mass, characteristic product ions, mass errors, and retention time (RT) of the compounds detected in pS9 incubations and in rat urine after oral administration. Elemental composition and all given masses are protonated forms.

3,4-dichlorophenyl-*N*-methylacetamide (*m/z* at 218.0134, $C_9H_{10}ONCl_2$) and the *N*-methylcyclohexanamine (*m/z* at 112.1124, $C_7H_{14}N$) were other characteristic fragment ions. Low-abundant fragment ions at *m/z* 158.9763 and 81.0707 were related to the 3,4-dichloro-1-methylbenzene and the cyclohexyl ring respectively.

N-demethyl-U-51754. According to Fig. 1, the fragmentation pattern of the most abundant metabolite, *N*-demethyl-U-51754 (**A1**, PM at *m/z* 329.1183), showed, as expected, an initial loss of methanamine forming the most abundant fragment ion at *m/z* 298.0757 followed by the cleavage at the amide nitrogen producing the fragment ion at *m/z* 218.0133, which belongs to the dichlorophenyl-*N*-methylacetamide part. Furthermore, the metabolite was identified by a fragmentation pattern similar to that of the parent substance, indicating loss of methyl at the amine moiety. *N*-demethyl-U-51754 formed two isomers in phS9 incubations, which could be separated chromatographically. Thus, the position of *N*-demethylation must be different. The spectrum of **A2** (EMS) represented fragment shifts due to the loss of a methyl group (−14.0156 u) at the fragments related to the dichlorophenyl-*N*-methylacetamide and the cyclohexyl-dichlorophenyl-*N*-methylacetamide.

Hydroxy-U-51754. The hydroxy metabolite **A5** (PM at *m/z* 359.1287) was identified by the parent ion as well as the fragment ions at *m/z* 314.0711, representing the loss of dimethylamine at the cyclohexyl ring. The fragment ions at *m/z* 218.0134 and 158.9762 corresponded to an unaltered phenyl-*N*-methylacetamide. However, the presence of the fragment ions at *m/z* 79.0550 and 110.0969 indicated the loss of water after hydroxylation at the cyclohexyl ring. Taking these findings together, this spectrum might be the result of a monohydroxylation at the cyclohexyl ring. Regarding this PM and those of other hydroxylated metabolites, multiple peaks occurred in the chromatogram, which implicated sites of hydroxylation at the cyclohexyl ring. However, it was not possible to determine the exact position of hydroxylation and its relationship to different retention times. Regarding monohydroxylation, several metabolites could be identified. The first peak with the PM of *m/z* 359.1287 was related to a hydroxylation that occurred at the benzyl ring or the methylene linker (**A6**). **A6** was identified by the characteristic fragment ions at *m/z* 81.0706 and 112.1123, indicating an unaltered cyclohexyl ring and thus excluding this as the site of hydroxylation. Additionally, no loss of water was observed after cleavage of the hydroxy group. However, the ions at *m/z* 174.9711 and 234.0082 with a mass shift of +15.9946 u (O) indicated a hydroxylation at the dichloro-methylbenzene moiety. Thus, this spectrum might be the result of monohydroxylation at either

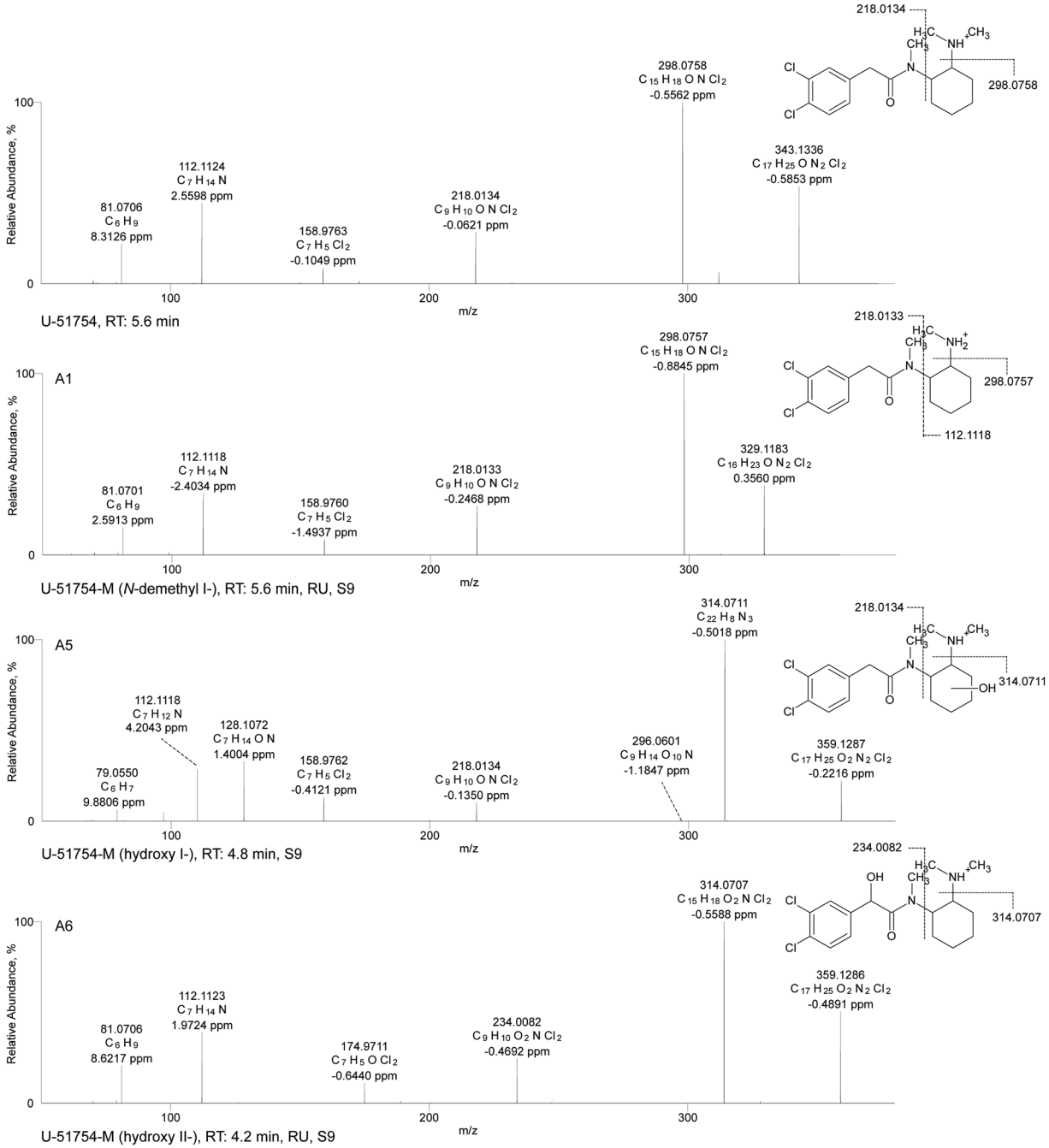

Figure 1. HR-MS/MS spectra of U-51754 and selected phase I metabolites. The spectra with proposed structures, retention times (RT), detected in rat urine (RU) and/or pooled human S9 fraction incubations (S9), and predominant fragmentation patterns of U-51754 and metabolites are arranged according to their presentation in the text.

the benzyl ring or the methylene linker. The exact position of the hydroxy group could not be elucidated by the methods applied.

ESI$^+$ HR-MS/MS fragmentation of U-47931E. U-47931E (PM of *m/z* 325.0911) showed a concise fragmentation pattern. The 4-bromobenzaldehyde moiety represented the most abundant fragment ion at *m/z* 182.9940 (C_7H_5OBr). Loss of dimethylamine and the 4-bromobenzamide led to other characteristic fragment ions at *m/z* 280.0322 ($C_{13}H_{18}ONBr$) and 199.9706 (C_7H_7ONBr). Low-abundant fragment ions at *m/z* 81.0705 (C_6H_9) and 126.1279 ($C_8H_{16}N$) were related to the cyclohexyl ring and the dimethyl cyclohexanamine respectively.

***N*-demethyl-hydroxy-U-47931E and *N,N*-bisdemethyl-hydroxy-U-47931E.** According to Fig. 2, the *N*-demethylated hydroxylated metabolite (**B5**, PM at *m/z* 327.0704) was identified by the fragment ion at *m/z*

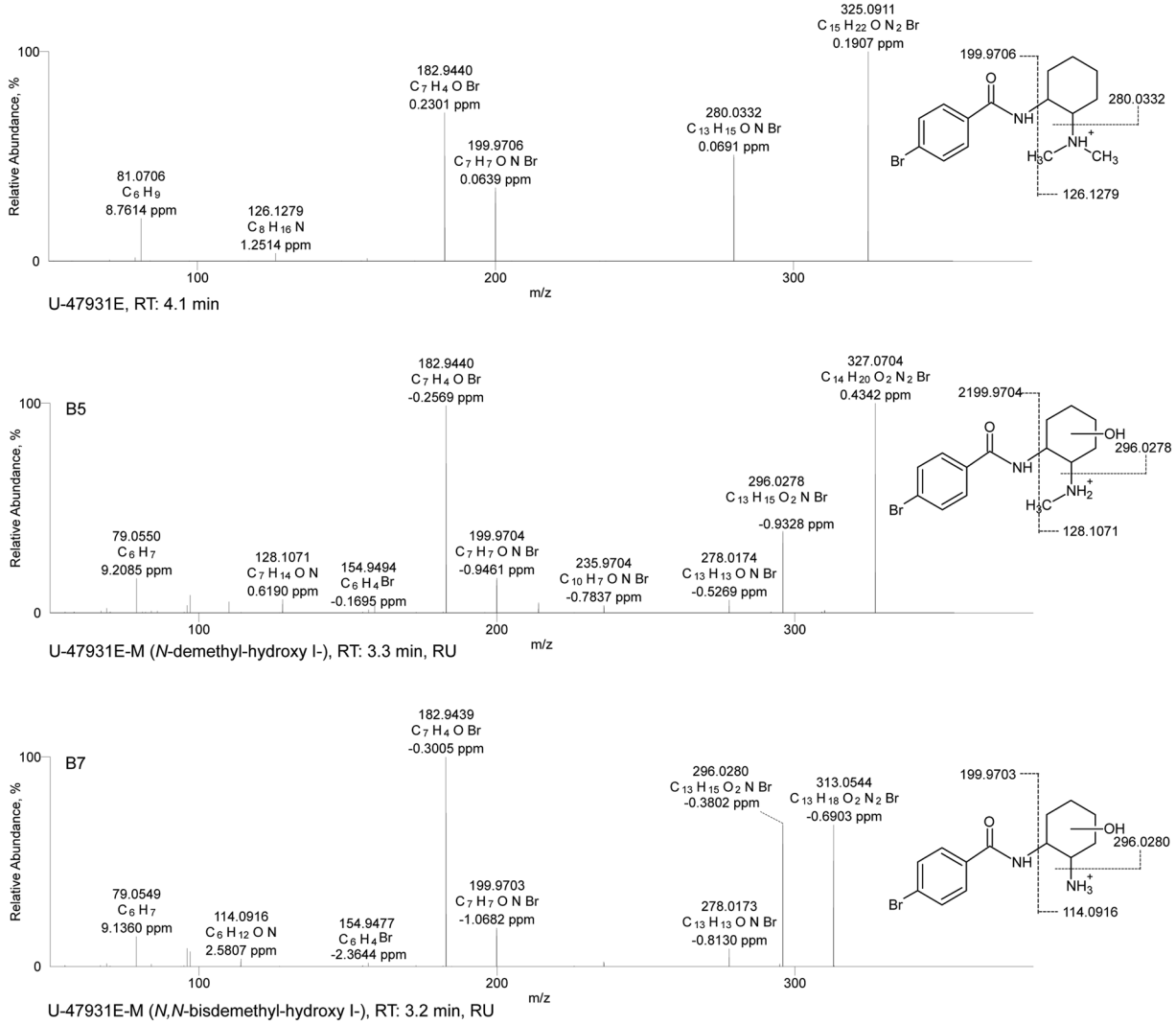

Figure 2. HR-MS/MS spectra of U-47931E and selected phase I metabolites. The spectra with proposed structures, retention times (RT), detected in rat urine (RU) and/or pooled human S9 fraction incubations (S9), and predominant fragmentation patterns of U-47931E and metabolites are arranged according to their presentation in the text.

296.0278, showing a loss of the methylamine and the characteristic mass shift of a hydroxy group (+15.9946 u, O). Furthermore, the concise fragment ions such as 182.9440 and 199.9704 were also present in the parent spectrum, indicating an unaltered bromobenzamide part. The fragment ions at *m/z* 79.0550 and 278.0174 resulted from loss of water at the cyclohexyl ring. Taking these findings together, this spectrum seemed to be related to an *N*-demethylated metabolite with further monohydroxylation at the cyclohexyl ring. The same characteristics were observed for the *N*,*N*-bisdemethylated hydroxylated metabolite (**B7**, PM at *m/z* 313.0544), which showed a similar fragmentation pattern to **B5** except for the precursor ion. Thus, hydroxylation must occur at the cyclohexyl ring, too. Regarding hydroxylated metabolites, multiple peaks occurred in the chromatogram, implicating multiple sites of hydroxylation at the cyclohexyl ring. Concerning the structure of the metabolite, it should be mentioned that the exact position of the hydroxy group in the cyclohexyl ring could not be deduced from the fragmentation pattern and with the analytical methods used here.

Additionally, after SPE, minor amounts of all hydroxylated metabolites could be detected, with hydroxylation occurring at the benzyl instead of the cyclohexyl ring (**B4**, **B6**, **B8**, EMS). All fragmentation patterns showed the characteristic mass shift due to the presence of a hydroxy group at fragments related to the bromobenzyl ring, indicating monohydroxylation at the aromatic system.

ESI$^+$ HR-MS/MS fragmentation of methoxyacetylfentanyl. The HR-MS data of methoxyacetylfentanyl (PM of *m/z* 353.2225) formed the most abundant fragment ion at *m/z* 188.1435 ($C_{13}H_{18}N$). The phenethyl chain represented another characteristic fragment at *m/z* 105.0704 (C_8H_9). More fragment ions in low abundance were observed in the spectrum The fragment ion at *m/z* 84.0811 represented the intact piperidine ring, whereas degradation of the piperidine ring led to the minor fragment ions at *m/z* 134.0966 ($C_9H_{12}N$), 146.0958 ($C_{10}H_{12}N$),

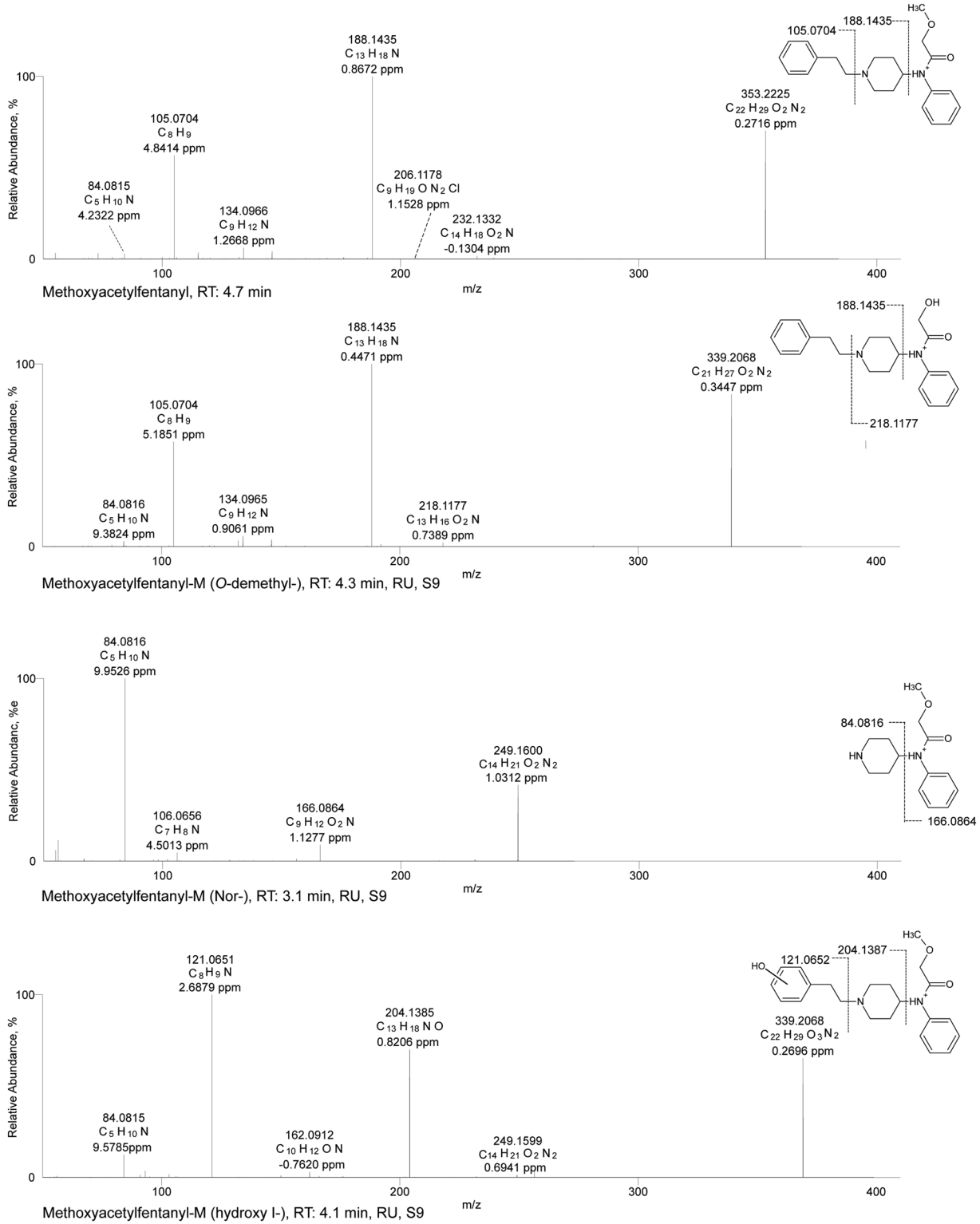

Figure 3. HR-MS/MS spectra of methoxyacetylfentanyl and selected phase I metabolites. The spectra with proposed structures, retention times (RT), detected in rat urine (RU) and/or pooled human S9 fraction incubations (S9), and predominant fragmentation patterns of methoxyacetylfentanyl and metabolites are arranged according to their presentation in the text.

206.1163 ($C_{12}H_{16}O_2N$), and 232.1332 ($C_{14}H_{18}O_2N$). Amide cleavage resulted in the fragment ion at *m/z* 166.0857 (2-methoxy *N*-phenylacetamide, $C_9H_{12}O_2N$). Another low-abundant characteristic fragment ion was derived from the 4-anilio-*N*-phenethyl-piperidine part (4-ANPP) of the molecule (281.2014, $C_{19}H_{25}N_2$) and could not be

ID	Analyte	Elemental composition	Monoisotopic exact masses	Monoisotopic accurate masses	Error (ppm)	Accurate fragment masses (*m/z*)								
						Product 1	Error (ppm)	Product 2	Error (ppm)	Product 3	Error (ppm)	Product 4	Error (ppm)	RT (min)
	Methoxyacetylfentanyl	$C_{22}H_{29}O_2N_2$	353.2223	353.2225	0.272	188.1435	0.867	134.0966	1.267	105.0704	4.841	84.0811	4.232	4.69
C1	*N*-dealkyl- (Nor)	$C_{14}H_{21}O_2N_2$	249.1597	249.1600	1.031	166.0864	1.128	106.0656	4.501	84.0816	9.953			3.07
C2	*N*-dealkyl-*O*-demethyl-	$C_{13}H_{19}O_2N_2$	235.1441	235.1442	−0.600	152.0707	0.878	94.0657	5.665	81.0812	9.881			1.84
C3	Amide hydrolyzed-	$C_{19}H_{25}N_2$	281.2012	281.2014	0.679	188.1434	0.187	134.0965	0.823	105.0703	3.931	84.0811	3.675	4.98
C4	Amide hydrolyzed hydroxy I-	$C_{19}H_{25}ON_2$	297.1961	297.1963	0.426	205.1337	0.554	188.1438	2.238	134.096	1.619	105.0706	6.817	3.06
C5	Amide hydrolyzed hydroxy II-	$C_{19}H_{25}ON_2$	297.1961	297.1962	0.211	204.1385	1.053	121.0651	2.394	84.0815	8.749			4.41
C6	*O*-demethyl-	$C_{21}H_{25}O_2N_2$	339.2067	339.2068	0.345	218.1177	0.739	188.1435	−0.447	134.0965	0.906	105.0704	5.185	4.31
C7	*O*-demethyl-hydroxy I-	$C_{21}H_{25}O_3N_2$	355.2016	355.2020	1.033	235.1439	−0.705	204.1385	1.022	121.0651	2.509	84.0815	8.876	3.65
C8	*O*-demethyl-hydroxy II-	$C_{21}H_{25}O_3N_2$	355.2016	355.2016	−0.056	337.1910	−0.133	204.1384	0.446	186.1272	−2.796	91.0548	5.897	3.94
C9	*O*-demethyl-hydroxy III-	$C_{21}H_{25}O_3N_2$	355.2016	355.2018	1.046	188.1434	0.183	134.0965	0.874	105.0703	3.831	84.0815	8.475	4.01
C10	*O*-demethyl-hydroxy-methoxy-	$C_{22}H_{29}O_4N_2$	385.2121	385.2124	0.823	234.1488	−0.389	192.1019	−0.105	151.0756	1.330	119.0494	2.289	3.87
C11	Hydroxy I-	$C_{22}H_{29}O_3N_2$	369.2172	369.2176	0.795	249.1598	0.089	204.1385	0.968	121.0651	2.270	84.0815	8.648	4.09
C12	Hydroxy II-	$C_{22}H_{29}O_3N_2$	369.2172	369.2175	0.704	351.2068	0.322	204.1383	0.073	186.1272	−3.071	105.0703	4.436	4.38
C13	*N*-oxide I-	$C_{22}H_{29}O_3N_2$	369.2172	369.2180	2.020	261.1598	0.136	189.1386	0.085	146.0965	0.170	105.0703	4.218	5.10
C14	*N*-oxide II-	$C_{22}H_{29}O_3N_2$	369.2172	369.2178	1.382	261.1599	0.596	186.1279	0.786	158.0965	0.309	105.0703	4.366	5.22
C15	Hydroxy-methoxy-	$C_{23}H_{31}O_4N_2$	399.2278	575.2580	0.528	234.1490	0.441	151.0755	1.054	119.0494	2.016	84.0815	8.082	4.19
C16	Amide hydrolysed hydroxy-glucuronide	$C_{25}H_{33}O_7N_2$	473.2282	473.2283	0.214	297.1963	0.540	188.1436	1.229	105.0705	4.800			3.06
C17	*O*-demethyl-glucuronide	$C_{27}H_{35}O_8N_2$	515.2387	515.2393	0.952	339.2069	0.444	218.1177	0.436	188.1435	0.759	105.0703	4.500	4.03
C18	*O*-demethyl-hydroxy-glucuronide	$C_{27}H_{35}O_9N_2$	531.2387	531.2340	0.496	355.2022	1.635	204.1386	1.716	121.0652	3.012	84.0816	9.696	3.47
C19	*O*-demethyl-hydroxy-methoxy-glucuronide	$C_{29}H_{35}O_{10}N_2$	561.2442	561.2447	0.696	385.2124	0.681	234.1488	−0.331	151.0755	0.995	119.0493	0.979	3.31
C20	Hydroxy-glucuronide	$C_{28}H_{35}O_9N_2$	545.2493	545.2501	1.314	369.2177	1.221	249.1600	1.123	204.1386	1.523	121.0652	3.047	3.65
C21	Hydroxy-methoxy-glucuronide	$C_{29}H_{39}O_{10}N_2$	575.2599	575.2599	−0.089	399.2281	0.684	234.1491	0.881	192.1019	0.111	151.0755	0.757	3.73

Table 3. Identification (ID), methoxyacetylfentanyl and its metabolites as well as elemental composition, exact mass, accurate mass, characteristic product ions, mass errors, and retention time (RT) of the compounds detected in pS9 incubations and in rat urine after oral administration. Elemental composition and all given masses are protonated forms.

observed in all metabolite spectra. In general, methoxyacetylfentanyl showed a fragmentation pattern according to previous published metabolism studies of methoxyacetylfentanyl and other 4-anilinopiperidine-type fentanyl analogues[18,29,30].

***O*-demethyl-methoxyacetylfentanyl.** The main metabolic pathway seemed to be *O*-demethylation (**C6**, PM of *m/z* 339.2068). According to Fig. 3, the MS^2 spectrum showed the same characteristic fragment ions as the parent compound except for the mass of the parent compound showing a loss of a methyl group (−14.0156 u). As described above, the fragments of the phenylethylpiperidine, phenethyl chain or methoxy-*N*-phenylacetamide were used for identification. The fragment ion of the phenylethylpiperidine at *m/z* 188.1435 represented the unmodified part of the molecule. On the other hand, the methoxy-*N*-phenylacetamide showed loss of methyl (−14.0156 u), producing the fragment ion at *m/z* 218.1177 instead of 232.1332.

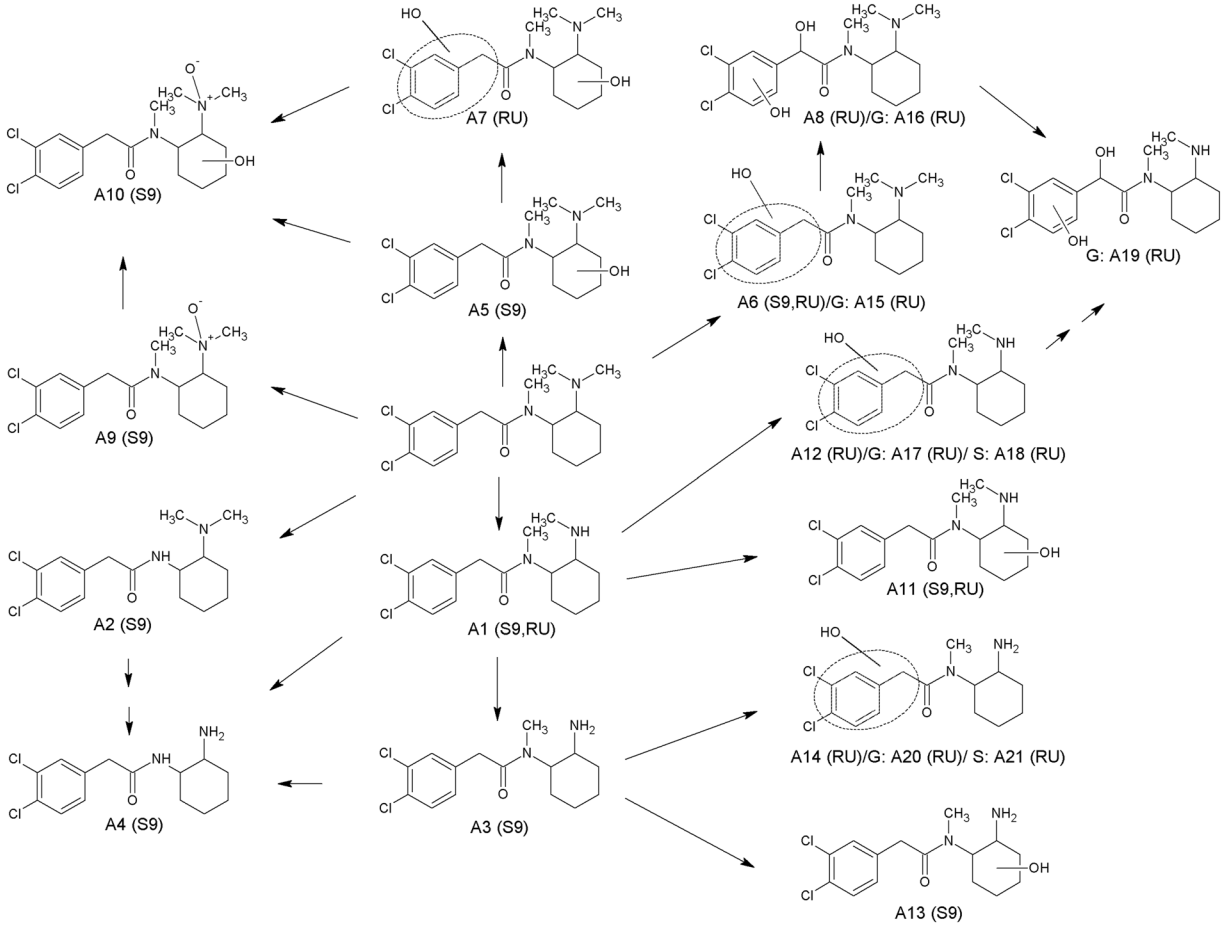

Figure 4. Metabolic pathways of U-51754 studied in rat urine (RU) and pooled human S9 fraction incubations (S9). Phase II metabolites: glucuronides (G), and sulfates (S). Numbering according to Table 1.

Nor-methoxyacetylfentanyl. Compared with the parent compound, the nor-methoxyacetylfentanyl metabolite (*N*-dealkylated derivative, **C1**, PM at *m/z* 249.1600) exhibited only few fragment ions. However, this metabolite could be identified by characteristic fragment ions for the 2-methoxy *N*-phenylacetamide part of the molecule. Identification was carried out by the concise fragment ion at *m/z* 84.0816, related to the piperidine ring, as well as the fragment ion at *m/z* 166.0864, indicating an unchanged 2-methoxy *N*-phenylacetamide. Furthermore, no fragment ions belonging to the phenylethylpiperidine part of the molecule could be detected, indicating a cleavage of the molecule between the phenethylchain and the piperidine nitrogen.

Hydroxy-methoxyacetylfentanyl. Regarding hydroxylation, several metabolites could be identified. Two monohydroxylated metabolites were found (**C11**, **C12**, PM at *m/z* 369.2179). **C11** showed the characteristic fragment ions of the phenylethylpiperidine part with a mass shift of oxygen (+15.9946 u, O) forming the fragment ions at *m/z* 121.0652 and 204.1387, indicating a hydroxylation at the phenethyl chain. Conversely, the hydroxy metabolite **C12** (EMS) showed initial loss of water forming the fragment ion at *m/z* 351.2054. The fragment ion at *m/z* 204.1387 represented hydroxylation at the phenylethylpiperidine part. However, the absence of the fragment ion at *m/z* 121.0652 and the presence of a mass shift of oxygen at the fragment at *m/z* 84.0815 resulted in the fragment at *m/z* 100.0763 and indicated a modified piperidine ring. Thus, hydroxylation might have occurred at the piperidine ring. Two other metabolites with the same *m/z* ratio were detected at 5.25 min (**C13**, **C14**, EMS) and could not be identified as hydroxy metabolites. Both spectra showed similar fragment ions to the parent spectrum, representing cleavage of oxygen without loss of water. These facts exclude the piperidine ring as the site of hydroxylation. The aromatic systems are also unlikely to undergo loss of hydroxy groups. Furthermore, the fragment ions formed are in accordance with those already described by Steuer *et al.* for *N*-oxide metabolites[31]. Those metabolites eluted after the parent compound, which has been frequently described for *N*-oxides[1,29,32]. Thus, *N*-oxidation at the nitrogen of the piperidine ring is the likeliest metabolic step. Owing to the molecular structure, two diastereomers could be formed with probably minimally different chromatographic properties, resulting in two detectable peaks.

ESI$^+$ HR-MS/MS for identification of the phase II metabolites based on MS/MS fragmentation. Most fragments in the spectra of the conjugates were also present in those of the corresponding phase I

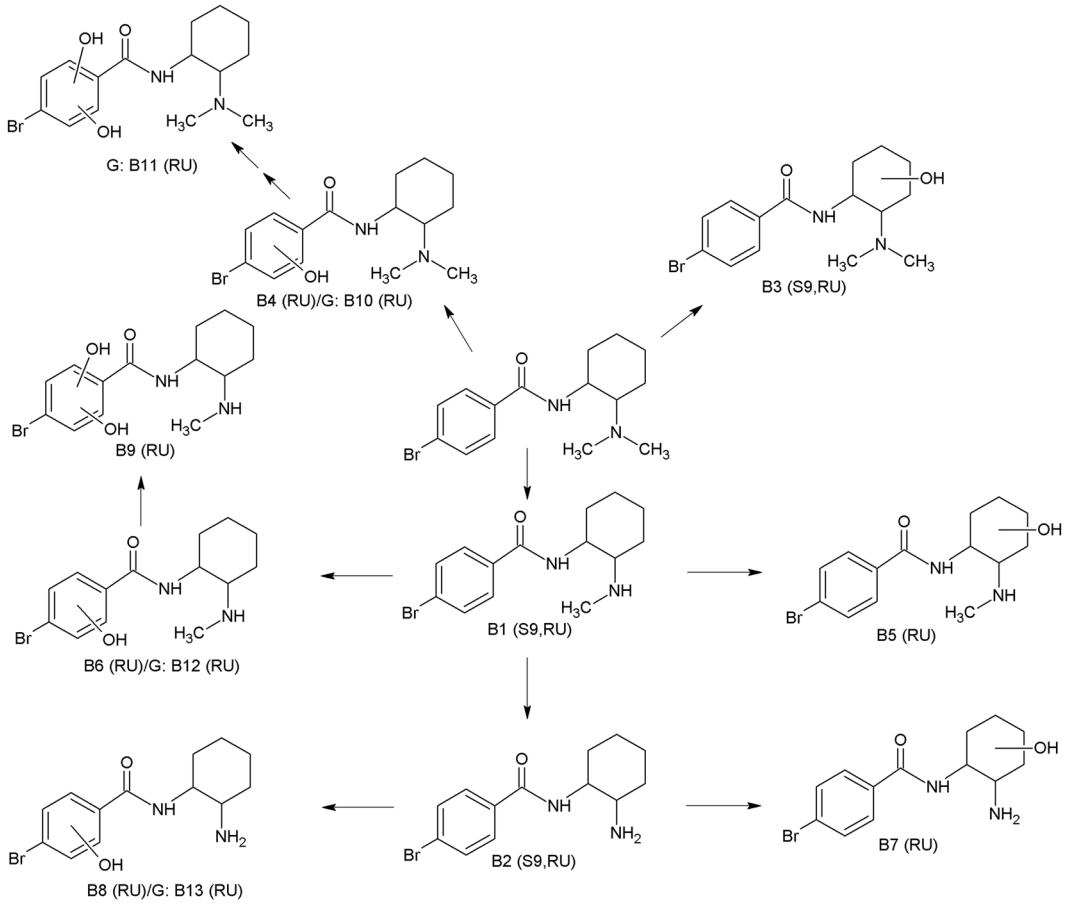

Figure 5. Metabolic pathways of U-47931E studied in rat urine (RU) and pooled human S9 fraction incubations (S9). Phase II metabolites: glucuronides (G). Numbering according to Table 2.

metabolites and are not discussed here. As shown in Tables 1–3, all glucuronides eliminated dehydrated glucuronic acid (−176.0321 u) and all sulphates dehydrated sulphuric acid (−79.9568 u). In total, seven corresponding phase II metabolites of U-51754 could be identified and four for U-47931E. Despite conjugate cleavage prior to extraction for some phase II metabolites (**A19**, **B11**, EMS), only trace amounts of the aglyca have been detected. However, the spectra of these metabolites showed characteristic fragment ions, so metabolite identification was possible. The aglycon of the hydroxy-glucuronide of U-47931E (**B10**, EMS) could not be identified in the urinary samples, possibly due to low stability. Nevertheless, reliable identification by characteristic fragment ions was possible for this metabolite. As described above, more than one isomer with similar MS^2 spectra could be detected for all *N*-demethylated and hydroxylated metabolites of the U-substances. Caused by multiple sites of hydroxylation, more isomers could be formed after conjugation with glucuronic acid or sulphuric acid.

In total, six phase II metabolites of methoxyacetylfentanyl could be identified; all formed through conjugation of their corresponding phase I metabolite with glucuronic acid. For some phase II metabolites, fragment ions still containing the corresponding conjugate helped to evaluate the position of the conjugate. The fragment ion at *m/z* 380.1704 represented the hydroxy-4-ANPP conjugated with glucuronic acid after loss of the hydroxyacetaldehyde and could be found in the spectrum of the hydroxy-glucuronide (**C20**, EMS) and the *O*-demethyl-hydroxy-glucuronide (**C18**, EMS). The fragmentation ion at *m/z* 410.1818 represented the metabolised 4-ANPP part conjugated with glucuronic acid and could be found in the MS^2 spectrum of the *O*-demethylated hydroxy-methoxy-glucuronide (**C19**, EMS). Sulphates of methoxyacetylfentanyl could not be detected, probably as a consequence of the generally reduced formation of sulphate conjugates in rats[30]. In line with our results, sulphates were only sparsely detected in previous studies as well[18].

Proposed metabolic pathways. The proposed metabolic pathways of U-51754 are shown in Fig. 4. The predominant pathway was single or multiple *N*-demethylation of the amine moiety (**A1**, **A2**, **A3**, **A4**) and hydroxylation of the cyclohexyl ring (**A5**). Hydroxylation to the respective *N*-oxide (**A9**) was also observed, as well as further hydroxylation of this metabolite at the hexyl ring (**A10**). After *N*-demethylation, the metabolites underwent further oxidation to the respective hydroxy derivates (**A11**, **A13**). Another metabolic pathway included hydroxylation of either the benzyl ring or the methylene linker, also combined with *N*-demethylations or further hydroxylation (**A6**, **A7**, **A8**, **A12**, **A14**). The main hydroxylated phase I metabolites underwent further glucuronidation (**A15**, **A16**, **A17**, **A19**, **A20**) or sulphation (**A18**, **A21**).

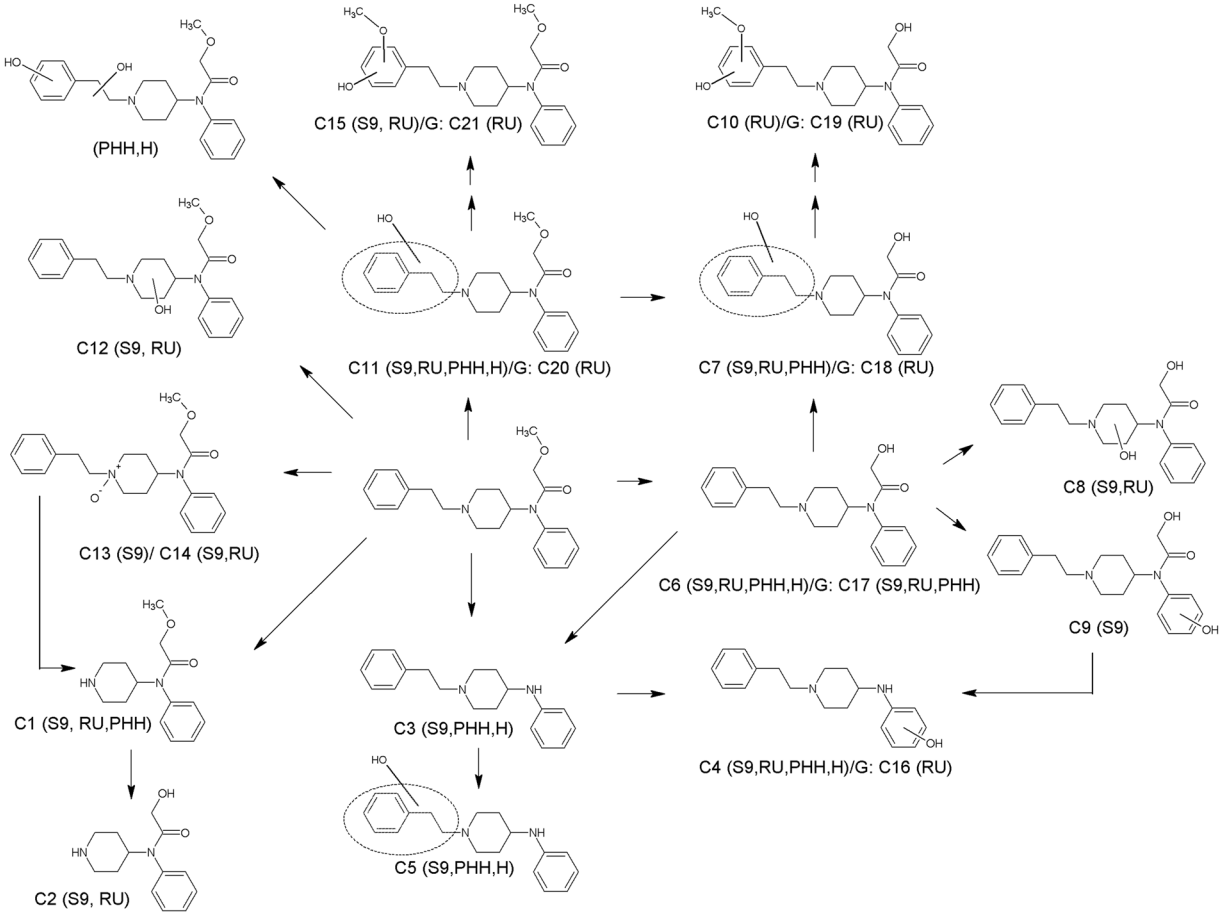

Figure 6. Metabolic pathways of methoxyacetylfentanyl studied in rat urine (RU), pooled human S9 fraction incubations (S9), pooled human hepatocytes (PHH)[18] and/or various biological human samples (H)[18]. Phase II metabolites: glucuronides (G). Numbering according to Table 3.

Figure 5 shows the proposed metabolic pathway of U-47931E. The main initial step in the metabolic pathways was *N*-demethylation (**B1**). Further metabolism steps were an additional *N*-demethylation (**B2**) or hydroxylation at the cyclohexyl ring (**B5**, **B7**) or the cyclophenyl ring (**B6**, **B8**). The *N*-demethylated hydroxy metabolite with hydroxylation at the aromatic system (**B6**) could be further hydroxylated (**B9**). Hydroxylation of the parent compound could occur at either the cyclohexyl (**B3**) or the benzyl ring (**B4**), forming two different metabolic pathways. All phase I metabolites with hydroxylation at the benzyl ring were conjugated to glucuronic acid (**B10**, **B11**, **B12**, **B13**), except for the *N*-demethylated dihydroxylated metabolite. Interestingly, no conjugates were formed after hydroxylation at the cyclohexyl ring even if higher amounts of corresponding phase I metabolites were found. Contrary to U-51754, no sulphated metabolites could be observed.

Figure 6 shows the proposed metabolic pathways for methoxyacetylfentanyl. Five initial metabolic steps could be postulated. One metabolic pathway was the *N*-dealkylation (**C1**). After *N*-dealkylation, the nor-metabolite was *O*-demethylated further (**C2**). On the other hand, one initial metabolic step was the *O*-demethylation (**C6**) itself, which was followed by further alkyl, piperidine or aryl hydroxylation (**C7**, **C8**, **C9**) or underwent methylation after two-fold hydroxylation (**C10**). The third metabolic pathway included the amide hydrolysis to the 4-ANPP derivative (**C3**) followed by hydroxylation (**C4**, **C5**). One additional metabolic pathway was the hydroxylation of the parent compound at either the alkyl moiety (**C11**) or the piperidine ring (**C12**) followed by methylation after two-fold hydroxylation (**C15**). Furthermore, hydroxylation to the respective *N*-oxide (**C13**, **C14**) could be observed. Some hydroxylated metabolites were further conjugated to glucuronic acid (**C16**, **C17**, **C18**, **C19**, **C20**, **C21**), whereas sulphates could not be detected.

Discussion

The parent compounds U-51754 and U-47931E as well as methoxyacetylfentanyl showed only very low signal abundances in rat urine. Concerning other U-substances, comparable results were found in previous studies[33]. In the case of fentanyl, less than 8% is excreted unchanged and approximately 85% is eliminated metabolised in faeces and urine within 72 h[34]. It can be assumed that fentanyl analogues will show a comparable behaviour. Following the administration of isofentanyl and 3-methylfentanyl, Meyer *et al.* could not detect the parent drugs in urine either[30]. In other urinary metabolism studies, the parent compounds could be detected with high

abundances[35,36]. However, since urinary excretion of parent compounds predominantly occurs via metabolites, it is essential to determine metabolites that can serve as targets for urine screening.

After administration of U-51754, the *N*-demethyl-hydroxy metabolite was the most abundant one in the urine specimens, which is a rough assessment considering possible differences in abundance in different MS types. In addition, the *N*,*N*-bisdemethylated and hydroxylated metabolite were abundant, likewise the monohydroxylated metabolite and *N*-demethyl-U-51754. All these metabolites showed a distinctively higher abundance compared with the parent compound. In line with our results, the *N*-demethylated metabolite provided abundant signal intensities for other U-substances as well in previous studies and, as a consequence, should be used as a target[28,37]. However, even the *N*-demethyl-hydroxy metabolite and the hydroxy metabolite might be suitable as targets. In contrast, conjugated metabolites only showed low signal abundance and could be excluded.

For U-47931E, the most abundant metabolites were the one- and two-fold *N*-demethylated metabolites with or without further hydroxylation and the hydroxy metabolite. However, all metabolites exhibited signal intensities lower than that of the parent compound. Nonetheless, the *N*-demethylated metabolite reached good detectability in human *in vitro* assays as well and might be preferentially used as an additional urinary marker. Conjugated metabolites were the least abundant metabolites and thus excluded as possible targets.

The alkyl hydroxy metabolite was the most abundant metabolite in rat urine samples after administration of methoxyacetylfentanyl, showing a much higher signal abundance than that of the parent compound. Hydroxy metabolites were found to be one of the main metabolites of different fentanyl analogues in other studies as well, but not yet for methoxyacetylfentanyl[18,33]. Furthermore, the nor-metabolite and the *O*-demethylated metabolite were also abundant metabolites. In line with these results, the nor-metabolite has already been described as the main metabolite of many fentanyl analogs[31,34]. As far as humans are concerned, Mardal *et al*. observed the parent compound, together with the *O*-demethylated metabolite and the amide hydrolysis product 4-ANPP, as representing the highest signal intensities in different biological samples[18]. However, this result was obtained by studying different tissue and blood samples and only one urine sample. This fact could have affected the detectability of different metabolites, as in our study. Furthermore, 4-ANPP was found to be a minor metabolite in other metabolism studies for other fentanyls[38–40]. Taking these findings together, the nor-metabolite and the *O*-demethylated metabolite might be the most suitable targets for urine screening approaches. Supporting this, the *O*-demethylated metabolite was also elucidated as the main metabolite for the structurally related fentanyl analogue Ocfentanil[41]. Conjugated metabolites showed only low signal abundance, turning out to be neglected as possible targets.

Owing to the lack of authentic human urine samples, incubations with phS9 incubations were performed in this study and compared with the metabolites formed by rats. Incubations with phS9 fraction are one alternative model to HLM or hepatocyte cell cultures for the assessment of toxicokinetic data.[1,21,31,42]. However, *in vitro* models are limited, running the risk of missing metabolites. As a comprehensive model, an animal[25] might be used, but the potential of interspecies differences in enzyme activity has to be considered[43,44]. Well-established models for metabolism studies are rats. In accordance with previous studies, this animal model can be used for urinary identification of metabolites after oral administration and thus was used in this study[23,24,45]. A comparison of all metabolites formed *in vivo* and *in vitro* is shown in Table 4. In general, major phS9 metabolites were in good agreement with major rat urine metabolites for all NSOs tested and the same biotransformations were observed. Many deviations between phS9 and urine metabolites can be explained by the different time allowed for metabolism and the missing recirculation of metabolites *in vitro* compared with *in vivo*. This leads to fewer metabolites *in vitro* in general and a lower prevalence of second- or third-generation metabolites. This is in accordance with previous studies comparing *in vitro* and *in vivo* metabolism using rat urine and phS9[22]. The low formation of phase II metabolites in phS9 incubations might be caused by the low formation of underlying phase I metabolites.

For U-51754, seven out of 14 phase I metabolites could be detected in rat urine and 10 out of 14 in phS9 incubations. Only three metabolites were identical in both models. The different sites of hydroxylation were one of the main differences between both models, but the main metabolic steps such as single *N*-demethylation, hydroxylation, and single *N*-demethylation combined with hydroxylation were comparable for both models. As already mentioned, different hydroxylation sites might be a species-related difference. Phase II metabolites were only detected in rat urine.

In summary, for U-47931E, more metabolites could be detected *in vivo* than *in vitro*. Only three out of nine metabolites were found in phS9 incubates. In particular, the formation of multiple-step metabolites was more dominant in the *in vivo* system. Phase II metabolites were again only found *in vivo*. However, the most abundant metabolites were comparable in both models.

For methoxyacetylfentanyl, eleven out of 15 phase I metabolites were found in rat urine and 14 out of 15 in phS9. Ten metabolites were identical in both models. The alkyl hydroxylated 4-ANPP could only be observed in phS9 incubations as well as the *O*-demethylated metabolite with further aryl hydroxylation. In rat urine, six phase II metabolites were found, whereas in phS9 incubations only one glucuronide could be identified. This is in accordance with findings published by Richter *et al.*[21]. In summary, most metabolic steps, particularly the main reactions such as the *N*-dealkylation, *O*-demethylation, and hydroxylation, were comparable in both models.

In general, the results of this study are in good agreement with those concerning comparable compounds. Owing to the lack of data from further metabolism studies on U-51754 or U-47931E, the results of this study must be compared with data from U-47700 or other U-substances such as U-49900. In terms of *N*-demethylation as a major metabolic pathway for U-51754 and U-47931E, our results are in good agreement with data already published on the metabolism of U-47700 in human liver microsomes (HLM) and human case samples[28,37,46,47]. Compared with previous studies[33,47], this is the first study detecting phase II metabolites in this class of substances. Only for AH-7921, a structurally related compound, a glucuronide has already been described[48]. Contrary to U-51754, no sulphated metabolites could be observed for U-47931E, but the main phase I pathways determined

ID	Analyte	phS9	Rat urine	PHH	Human samples
U-51754					
A1	*N*-demethyl I-	+	+		
A2	*N*-demethyl II-	+			
A3	*N*,*N*-bisdemethyl-	+			
A4	*N*,*N*,*N*-tridemethyl-	+			
A5	Hydroxy I-	+			
A6	Hydroxy II-	+	+		
A7	Dihydroxy I-		+		
A8	Dihydroxy II-		+		
A9	*N*-oxide-	+			
A10	*N*-oxide-hydroxy-	+			
A11	*N*-demethyl-hydroxy I-	+	+		
A12	*N*-demethyl-hydroxy II-		+		
A13	*N*,*N*-bisdemethyl-hydroxy I-	+			
A14	*N*,*N*-bisdemethyl-hydroxy II-		+		
A15	hydroxy-glucuronide		+		
A16	dihydroxy-glucuronide		+		
A17	*N*-demethyl-hydroxy-glucuronide		+		
A18	*N*-demethyl-hydroxy-sulfate		+		
A19	*N*-demethyl-dihydroxy-glucuronide		+		
A20	*N*,*N*-bisdemethyl-hydroxy-glucuronide		+		
A21	*N*,*N*-bisdemethyl-hydroxy-sulfate		+		
U-47931E					
B1	*N*-demethyl-	+	+		
B2	*N*,*N*-bisdemethyl-	+	+		
B3	Hydroxy I-	+	+		
B4	Hydroxy II-		+		
B5	*N*-demethyl-hydroxy I-		+		
B6	*N*-demethyl-hydroxy II-		+		
B7	*N*,*N*-bisdemethyl-hydroxy I-		+		
B8	*N*,*N*-bisdemethyl-hydroxy II-		+		
B9	*N*-demethyl-dihydroxy-		+		
B10	Hydroxy-glucuronide		+		
B11	Dihydroxy-glucuronide		+		
B12	*N*-demethyl-hydroxy-glucuronide		+		
B13	*N*,*N*-bisdemethyl-hydroxy-glucuronide		+		
Methoxyacetylfentanyl					
C1	*N*-dealkyl- (Nor)	+	+	+	
C2	*N*-dealkyl-*O*-demethyl-	+	+		
C3	Amide hydrolyzed-	+		+	+
C4	Amide hydrolyzed hydroxy I-	+	+	+	+
C5	Amide hydrolyzed hydroxy II-	+		+	+
C6	*O*-demethyl-	+	+	+	+
C7	*O*-demethyl-hydroxy I-	+	+	+	
C8	*O*-demethyl-hydroxy II-	+	+		
C9	*O*-demethyl-hydroxy III-	+			
C10	*O*-demethyl-hydroxy-methoxy-		+		
C11	Hydroxy I-	+	+	+	+
C12	Hydroxy II-	+	+		
C13	*N*-oxide I-	+			
C14	*N*-oxide II-	+	+		
C15	Hydroxy-methoxy-	+	+		
C16	Amide hydrolysed hydroxy-glucuronide		+		
C17	*O*-demethyl-glucuronide	+	+	+	
C18	*O*-demethyl-hydroxy-glucuronide		+		
C19	*O*-demethyl-hydroxy-methoxy-glucuronide		+		

Continued

ID	Analyte	phS9	Rat urine	PHH	Human samples
C20	Hydroxy-glucuronide		+		
C21	Hydroxy-methoxy-glucuronide		+		

Table 4. Phase I and II metabolites of U-51754, U-47931E, and methoxyacetylfentanyl found *in vitro* (phS9 fractions) and *in vivo* (rat urine) compared to those detected in pooled human hepatocytes (PHH) and various biological human samples published by Mardal *et al.*[18].

for this substance were in accordance with our results for U-51754 or further studies on other U-substances[33]. In total, fewer metabolites of U-47931E were formed in comparison to U-51754.

In general, the findings concerning the formation of metabolites of methoxyacetylfentanyl showed, on the one hand, similarities to other fentanyl-analogue metabolism studies[1,18], but, on the other, differences regarding the formation of dihydroxylated metabolites. *N*-dealkylation was already found to be a common metabolic reaction for other fentanyls[49,50]. Further, the formation of 4-ANPP has already been described as a metabolic pathway for many other fentanyl analogues[51–53]. Other initial metabolic steps such as *O*-demethylation and hydroxylation have been published for methoxyacetylfentanyl by Mardal *et al.* or in previous studies of other fentanyls as well[18,31]. However, Mardal *et al.* did not detect *N*-oxidation. In contrast, they found the dihydroxylated metabolite. Furthermore, they could distinguish between hydroxylation at the ethyl side chain and the phenyl ring of this moiety by means of mass spectrometry. These differences could be an effect of different settings of the mass spectrometry analysis used in that study.

Conclusions

The major phase I and II metabolites of the three NSOs, U-51754, U-47931E, and methoxyacetylfentanyl, were tentatively identified in phS9 as well as in rat urine specimens after oral administration. Concerning U-51754 and U-47931E, *N*-demethylation of the amine moiety and hydroxylation of the hexyl ring as well as combinations thereof led to the most abundant metabolites. *N*-dealkylation to the nor-metabolite, *O*-demethylation, and hydroxylation at the alkyl part of the molecule were observed to be the most abundant metabolites of methoxyacetylfentanyl. These findings indicate that metabolites are essential urinary targets for detecting these NSOs and confirm their consumption, as most of the parent compounds could only be detected with minor abundance in rat urine. In general, the results of this study are in good agreement with those concerning comparable compounds obtained from HLM incubations, human hepatocytes, and/or human cases.

Compliance with ethical standards. The authors declare that the experiments have been conducted in accordance with all applicable institutional, national, or international guidelines for care and use of rats.

Data Availability

Datasets generated during and/or analyzed during the current study are not publicly available but are available from the corresponding author on reasonable request.

References

1. Watanabe, S. *et al. In Vitro* and *In Vivo* Metabolite Identification Studies for the New Synthetic Opioids Acetylfentanyl, Acrylfentanyl, Furanylfentanyl, and 4-Fluoro-Isobutyrylfentanyl. *AAPS J* **19**, 1102–1122 (2017).
2. Fentanils and synthetic cannabinoids: driving greater complexity into the drug situation. An update from the EU Early Warning System, http://www.emcdda.europa.eu/system/files/publications/8870/2018-2489-td0118414enn.pdf (2018).
3. Marchei, E. *et al.* New synthetic opioids in biological and non-biological matrices: A review of current analytical methods. *TrAC* **102**, 1–15 (2018).
4. Prekupec, M. P., Mansky, P. A. & Baumann, M. H. Misuse of Novel Synthetic Opioids: A Deadly New Trend. *J Addict Med* **11**, 256–265 (2017).
5. Armenian, P., Vo, K. T., Barr-Walker, J. & Lynch, K. L. Fentanyl, fentanyl analogs and novel synthetic opioids: A comprehensive review. *Neuropharmacology* **134**, 121–132 (2018).
6. European Drug Report 2017. Trends and Develops, http://www.emcdda.europa.eu/system/files/publications/4541/TDAT17001ENN.pdf (2017).
7. Coopman, V. *et al.* A case of acute intoxication due to combined use of fentanyl and 3,4-dichloro-N-[2-(dimethylamino)cyclohexyl]-N-methylbenzamide (U-47700). *Forensic Sci Int* **266**, 68–72 (2016).
8. Domanski, K. *et al.* Two cases of intoxication with new synthetic opioid, U-47700. *Clin Toxicol (Phila)* **55**, 46–50 (2017).
9. Dziadosz, M., Klintschar, M. & Teske, J. Postmortem concentration distribution in fatal cases involving the synthetic opioid U-47700. *Int J Legal Med* **131**, 1555–1556 (2017).
10. Hikin, L. *et al.* Multiple fatalities in the North of England associated with synthetic fentanyl analogue exposure: Detection and quantitation a case series from early 2017. *Forensic Sci Int* **282**, 179–183 (2018).
11. Amlani, A. *et al.* Why the FUSS (Fentanyl Urine Screen Study)? A cross-sectional survey to characterize an emerging threat to people who use drugs in British Columbia, Canada. *Harm Reduct J* **12**, 54 (2015).
12. Seither, J. & Reidy, L. Confirmation of Carfentanil, U-47700 and Other Synthetic Opioids in a Human Performance Case by LC-MS-MS. *J Anal Toxicol* **41**, 493–497 (2017).
13. Reddit - researchchemicals, https://www.reddit.com/r/researchchemicals/comments/7avo0o/bromadoline_u47931e_review_of_2_samples/.
14. Bluelight - (RC's) Novel opioid U-51754, http://www.bluelight.org/vb/threads/793107-Novel-opioid-U-51754.
15. TripSit Factsheets - U-51754, http://drugs.tripsit.me/u-51754.
16. Sharma, V. & McNeill, J. H. To scale or not to scale: the principles of dose extrapolation. *Br J Pharmacol* **157**, 907–921 (2009).
17. Methoxyacetylfentanyl. EMCDDA-Europol Joint Report on a new psychoactive substance: 2-methoxy-N-phenyl-N-[1-(2-phenylethyl)piperidin-4-yl]acetamide (methoxyacetylfentanyl), http://www.emcdda.europa.eu/system/files/publications/7925/20181015_TDAS18002ENN_PDF.pdf.

18. Mardal, M. *et al*. Postmortem analysis of three methoxyacetylfentanyl-related deaths in Denmark and *in vitro* metabolite profiling in pooled human hepatocytes. *Forensic Sci Int* **290**, 310–317 (2018).
19. EVE and Rave - The Swiss Drug Forum. (2018). https://www.eve-rave.ch/wordpress/Forum/viewtopic.php?t=59342.
20. TripSitFactsheets-Methoxyacetylfentanyl. http://drugs.tripsit.me/methoxyacetyl-fentanyl.
21. Richter, L. H. J., Flockerzi, V., Maurer, H. H. & Meyer, M. R. Pooled human liver preparations, HepaRG, or HepG2 cell lines for metabolism studies of new psychoactive substances? A study using MDMA, MDBD, butylone, MDPPP, MDPV, MDPB, 5-MAPB, and 5-API as examples. *J Pharm Biomed Anal* **143**, 32–42 (2017).
22. Caspar, A. T., Westphal, F., Meyer, M. R. & Maurer, H. H. LC-high resolution-MS/MS for identification of 69 metabolites of the new psychoactive substance 1-(4-ethylphenyl-)-N-[(2-methoxyphenyl)methyl] propane-2-amine (4-EA-NBOMe) in rat urine and human liver S9 incubates and comparison of its screening power with further MS techniques. *Anal Bioanal Chem* **410**, 897–912 (2018).
23. A Michely, J. A. *et al*. New Psychoactive Substances 3-Methoxyphencyclidine (3-MeO-PCP) and 3-Methoxyrolicyclidine (3-MeO-PCPy): Metabolic Fate Elucidated with Rat Urine and Human Liver Preparations and their Detectability in Urine by GC-MS, "LC-(High Resolution)-MSn" and "LC-(High Resolution)-MS/MS". *Curr Neuropharmacol* **15**, 692–712 (2017).
24. Welter, J. *et al*. 2-methiopropamine, a thiophene analogue of methamphetamine: studies on its metabolism and detectability in the rat and human using GC-MS and LC-(HR)-MS techniques. *Anal Bioanal Chem* **405**, 3125–3135 (2013).
25. Caspar, A. T. *et al*. Metabolic fate and detectability of the new psychoactive substances 2-(4-bromo-2,5-dimethoxyphenyl)-N-[(2-methoxyphenyl)methyl]ethanamine (25B-NBOMe) and 2-(4-chloro-2,5-dimethoxyphenyl)-N-[(2-methoxyphenyl)methyl] ethanamine (25C-NBOMe) in human and rat urine by GC-MS, LC-MS(n), and LC-HR-MS/MS approaches. *J Pharm Biomed Anal* **134**, 158–169 (2017).
26. Michely, J. A., Meyer, M. R. & Maurer, H. H. Dried urine spots - A novel sampling technique for comprehensive LC-MS(n) drug screening. *Anal Chim Acta* **982**, 112–121 (2017).
27. Caspar, A. T. *et al*. Metabolism of the tryptamine-derived new psychoactive substances 5-MeO-2-Me-DALT, 5-MeO-2-Me-ALCHT, and 5-MeO-2-Me-DIPT and their detectability in urine studied by GC-MS, LC-MS(n), and LC-HR-MS/MS. *Drug Test Anal* **10**, 184–195 (2018).
28. Krotulski, A. J., Mohr, A. L. A., Papsun, D. M. & Logan, B. K. Metabolism of novel opioid agonists U-47700 and U-49900 using human liver microsomes with confirmation in authentic urine specimens from drug users. *Drug Test Anal* **10**, 127–136 (2018).
29. Astrand, A. *et al*. Correlations between metabolism and structural elements of the alicyclic fentanyl analogs cyclopropyl fentanyl, cyclobutyl fentanyl, cyclopentyl fentanyl, cyclohexyl fentanyl and 2,2,3,3-tetramethylcyclopropyl fentanyl studied by human hepatocytes and LC-QTOF-MS. *Arch Toxicol* **93**, 95–106 (2019).
30. Meyer, M. R. *et al*. Qualitative studies on the metabolism and the toxicological detection of the fentanyl-derived designer drugs 3-methylfentanyl and isofentanyl in rats using liquid chromatography-linear ion trap-mass spectrometry (LC-MS(n). *Anal Bioanal Chem* **402**, 1249–1255 (2012).
31. Steuer, A. E., Williner, E., Staeheli, S. N. & Kraemer, T. Studies on the metabolism of the fentanyl-derived designer drug butyrfentanyl in human *in vitro* liver preparations and authentic human samples using liquid chromatography-high resolution mass spectrometry (LC-HRMS). *Drug Test Anal* **9**, 1085–1092 (2017).
32. Feasel, M. G. *et al*. Metabolism of Carfentanil, an Ultra-Potent Opioid, in Human Liver Microsomes and Human Hepatocytes by High-Resolution Mass Spectrometry. *AAPS J* **18**, 1489–1499 (2016).
33. Concheiro, M., Chesser, R., Pardi, J. & Cooper, G. Postmortem Toxicology of New Synthetic Opioids. *Front Pharmacol* **9**, 1210 (2018).
34. McClain, D. A. & Hug, C. C. Jr. Intravenous fentanyl kinetics. *Clin Pharmacol Ther* **28**, 106–114 (1980).
35. Melent'ev, A. B., Kataev, S. S. & Dvorskaya, O. N. Identification and analytical properties of acetyl fentanyl metabolites. *Journal of Analytical Chemistry* **70**, 240–248 (2015).
36. Patton, A. L. *et al*. Quantitative measurement of acetyl fentanyl and acetyl norfentanyl in human urine by LC-MS/MS. *Anal Chem* **86**, 1760–1766 (2014).
37. Jones, M. J., Hernandez, B. S., Janis, G. C. & Stellpflug, S. J. A case of U-47700 overdose with laboratory confirmation and metabolite identification. *Clin Toxicol (Phila)* **55**, 55–59 (2017).
38. Goromaru, T. *et al*. Identification and Quantitative Determination of Fentanyl Metabolites in Patients by Gas Chromatography-Mass Spectrometry. *Anesthesiology.* **61**, 73–7 (1984).
39. Mahlke, N. S., Ziesenitz, V., Mikus, G. & Skopp, G. Quantitative low-volume assay for simultaneous determination of fentanyl, norfentanyl, and minor metabolites in human plasma and urine by liquid chromatography-tandem mass spectrometry (LC-MS/MS). *Int J Legal Med* **128**, 771–778 (2014).
40. Staeheli, S. N. *et al*. Time-dependent postmortem redistribution of butyrfentanyl and its metabolites in blood and alternative matrices in a case of butyrfentanyl intoxication. *Forensic Sci Int* **266**, 170–177 (2016).
41. Allibe, N. *et al*. Fatality involving ocfentanil documented by identification of metabolites. *Drug Test Anal* **10**, 995–1000 (2018).
42. Peters, F. T. & Meyer, M. R. *In vitro* approaches to studying the metabolism of new psychoactive compounds. *Drug Test Anal* **3**, 483–495 (2011).
43. Martignoni, M., Groothuis, G. M. & de Kanter, R. Species differences between mouse, rat, dog, monkey and human CYP-mediated drug metabolism, inhibition and induction. *Expert Opin Drug Metab Toxicol* **2**, 875–894 (2006).
44. Turpeinen, M. *et al*. Predictive value of animal models for human cytochrome P450 (CYP)-mediated metabolism: a comparative study *in vitro*. *Xenobiotica* **37**, 1367–1377 (2007).
45. Montesano, C. *et al*. Identification of MT-45 Metabolites: In Silico Prediction, *In Vitro* Incubation with Rat Hepatocytes and *In Vivo* Confirmation. *J Anal Toxicol* **41**, 688–697 (2017).
46. Elliott, S. P., Brandt, S. D. & Smith, C. The first reported fatality associated with the synthetic opioid 3,4-dichloro-N-[2-(dimethylamino)cyclohexyl]-N-methylbenzamide (U-47700) and implications for forensic analysis. *Drug Test Anal* **8**, 875–879 (2016).
47. Fleming, S. W. *et al*. Analysis of U-47700, a Novel Synthetic Opioid, in Human Urine by LC-MS-MS and LC-QToF. *J Anal Toxicol* **41**, 173–180 (2017).
48. Wohlfarth, A. *et al*. Metabolic characterization of AH-7921, a synthetic opioid designer drug: *in vitro* metabolic stability assessment and metabolite identification, evaluation of in silico prediction, and *in vivo* confirmation. *Drug Test Anal* **8**, 779–791 (2016).
49. Kanamori, T. *et al*. Metabolism of Fentanyl and Acetylfentanyl in Human-Induced Pluripotent Stem Cell-Derived Hepatocytes. *Biol Pharm Bull* **41**, 106–114 (2018).
50. Sato, S., Suzuki, S., Lee, X. P. & Sato, K. Studies on 1-(2-phenethyl)-4-(N-propionylanilino)piperidine (fentanyl) and related compounds VII. Quantification of alpha-methylfentanyl metabolites excreted in rat urine. *Forensic Sci Int* **195**, 68–72 (2010).
51. Goggin, M. M., Nguyen, A. & Janis, G. C. Identification of Unique Metabolites of the Designer Opioid Furanyl Fentanyl. *J Anal Toxicol* **41**, 367–375 (2017).
52. Labroo, R. B., Paine, M. F., Thummel, K. E. & Kharasch, E. D. Fentanyl metabolism by human hepatic and intestinal cytochrome P450 3A4: implications for interindividual variability in disposition, efficacy, and drug interactions. *Drug Metab Dispos* **25**, 1072–1080 (1997).
53. Martucci, H. F. H., Ingle, E. A., Hunter, M. D. & Rodda, L. N. Distribution of furanyl fentanyl and 4-ANPP in an accidental acute death: A case report. *Forensic Sci Int* **283**, e13–e17 (2018).

Acknowledgements

The authors would like to thank the staff of the Institute of Experimental and Clinical Toxicology at Saarland University for their support and/or helpful discussions. We acknowledge support by the Deutsche Forschungsgemeinschaft (DFG, German Research Foundation) and Saarland University within the funding programme Open Access Publishing.

Author Contributions

F.N., L.H.J.R., N.S. and M.R.M. designed and conducted the research. F.N. wrote the manuscript, performed the experiments and analysed the data. P.H.S., N.S. and M.R.M. supervised the research. All authors approved the final manuscript.

Additional Information

Supplementary information accompanies this paper at https://doi.org/10.1038/s41598-019-50196-y.

Competing Interests: The authors declare no competing interests.

Publisher's note Springer Nature remains neutral with regard to jurisdictional claims in published maps and institutional affiliations.

3.2 Are pigs a suitable animal model for in vivo metabolism studies of new psychoactive substances? A comparison study using different in vitro/in vivo tools and U-47700 as model drug (104)

(DOI: 10.1016/j.toxlet.2020.04.001)

Authors Contributions Frederike Nordmeier conducted and evaluated the experiment as well as composed the manuscript; Adrian Doerr assisted at the execution of the animal experiments; Matthias W. Laschke and Michael D. Menger carried out and enabled the animal experiments and assisted with scientific discussions; Nadine Schaefer, Markus R. Meyer, and Peter H. Schmidt assisted with scientific discussions and the development of the experiments as well as supervised the research.

Toxicology Letters 329 (2020) 12–19

Contents lists available at ScienceDirect

Toxicology Letters

journal homepage: www.elsevier.com/locate/toxlet

Are pigs a suitable animal model for in vivo metabolism studies of new psychoactive substances? A comparison study using different in vitro/in vivo tools and U-47700 as model drug

Frederike Nordmeier[a], Adrian Doerr[a], Matthias W. Laschke[b], Michael D. Menger[b], Peter H. Schmidt[a], Nadine Schaefer[a], Markus R. Meyer[c,*]

[a] Institute of Legal Medicine, Saarland University, 66421 Homburg, Germany
[b] Institute for Clinical and Experimental Surgery, Saarland University, 66421 Homburg, Germany
[c] Department of Experimental and Clinical Toxicology, Institute of Experimental and Clinical Pharmacology and Toxicology, Center for Molecular Signaling (PZMS), Saarland University, 66421 Homburg, Germany

GRAPHICAL ABSTRACT

In vitro and in vivo metabolism studies of the new synthetic opioid U-47700 were elucidated using LC-HR-MS/MS. The pig urinary metabolic pattern was compared to different metabolizing systems (human and pig liver microsomes, human liver S9 fraction, rat) and to human data. In total, 12 phase I and 8 phase II metabolites were identified. Main metabolic reactions were *N*-demethylation and hydroxylation predominantly catalyzed by CYP2B6, CYP2C19, CYP3A4, and CYP3A5.

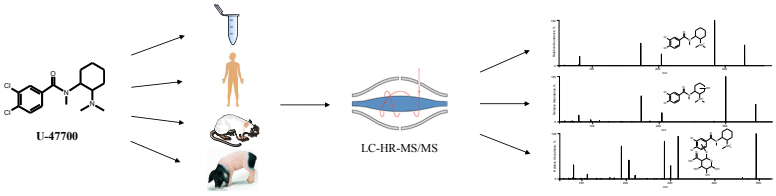

ARTICLE INFO

Keywords:
New synthetic opioids
U-47700
Pigs
Urinary metabolic patterns
LC-HR-MS/MS

ABSTRACT

Being highly potent, New Synthetic Opioids (NSO) have become a public health concern. Little is known though about the metabolism and toxicokinetics (TK) of many of the non fentanyl NSO such as U-47700. Obtaining such data in humans is challenging and so we investigated if pigs were a suitable model species as TK model for U-47700. The metabolic fate of U-47700 was elucidated after intravenous administration to one pig in vivo and results were compared to metabolic patterns formed by different other in vitro systems (human and pig liver microsomes, human liver S9 fraction) and compared to rat and human in vivo data. Furthermore, monooxygenase isozymes responsible for the major metabolic steps were elucidated.

In total, 12 phase I and 8 phase II metabolites of U-47700 could be identified. The predominant reactions were *N*-demethylation, hydroxylation, and combination of them followed by glucuronidation or sulfation. The most predominant monooxygenase catalyzed conversions were *N*-demethylation, and hydroxylation by CYP3A4 and 2B6, and FMO3 catalyzed *N*-oxidation. Similar main phase I metabolites were found in vitro as compared to in vivo (pig/human). The metabolic pattern elucidated in the pig was comparable to human in vivo data. Thus, pigs seem to be a suitable animal model for metabolism and further TK of U-47700.

* Corresponding author.
E-mail address: markus.meyer@uks.eu (M.R. Meyer).

https://doi.org/10.1016/j.toxlet.2020.04.001
Received 16 January 2020; Received in revised form 27 March 2020; Accepted 2 April 2020
Available online 04 May 2020
0378-4274/

1. Introduction

New Psychoactive Substances (NPS) are synthetic alternatives to the traditional drugs of abuse and widespread on the drugs of abuse market (Baumann et al., 2018; Meyer, 2016). Nowadays, an increasing number of New Synthetic Opioids (NSO) became available (http://www.emcdda.europa.eu/system/files/publications/11364/20191724_TDAT19001ENN_PDF.pdf, 2019). The non-fentanyl NSO U-47700 (3,4-dichloro-*N*-[2-(diemthylamino)cyclohexyl]-*N*-methylbenzamide) was developed by the Upjohn Company in the 1970s and first reports were released by the European Monitoring Center for Drugs and Drug Addiction in 2014 (Koch et al., 2018). The abuse of NSO, in particular U-47700, has led to a recent rise in severe intoxications due to their high potencies (Coopman et al., 2016; Dziadosz et al., 2017; Elliott et al., 2016; Fleming et al., 2017; Mohr et al., 2016; Ruan et al., 2016). U-47700 was scheduled in the United States and some European countries including Germany (https://www.gesetze-im-internet.de/btmg_, 1981/anlage_ii.html).

However, still little is known about the in vivo toxicodynamics and toxicokinetics (TK) of U-47700 (Nikolaou et al., 2017). In vitro toxicodynamic studies demonstrated that it is a selective μ-opioid receptor agonist. Its binding affinity is about 7.5 fold higher than that of morphine and their antinoceptive activity and side effects are similar (Cheney et al., 1985; Harper et al., 1974; Lehmann et al., 2018). However, there are only few in vivo TK data of U-47700 available in the literature, mostly from fatal intoxications with unknown dosage, time of intake, and time of death (Coopman et al., 2016; Koch et al., 2018; Nikolaou et al., 2017). Due to the increasing number of abuse and intoxication cases with U-47700, the knowledge of in vivo TK data of this NSO is essential. One TK issue is the knowledge of analytical targets for toxicological analysis. This is of particular importance for the analysis of urine samples, where the analytical target (usually the main urinary metabolite) needs to be known. Thus, the metabolic pathway needs to be elucidated. For identification of phase I and II metabolites, human in vitro models such as pooled human liver microsomes (pHLM) and cytosol, pooled human liver S9 fraction (pHS9) or hepatocyte cell cultures might be used (Peters and Meyer, 2011; Richter et al., 2017). In vivo animal models are a further tool to elucidate the urinary excretion profile (Caspar et al., 2017), but the potential of interspecies differences in enzyme activity has to be considered (Martignoni et al., 2006; Turpeinen et al., 2007). One well established animal model for metabolism studies is the rat. However, this animal model is fraught with the disadvantage of limited amounts of body fluids being available as well as the restricted routes of administration (Parasuraman et al., 2010; Zhang et al., 2012). To overcome these disadvantages, other animal models have to be established such as pigs. They have already been used for TK studies of synthetic cannabinoids (Schaefer et al., 2017a, b; Schaefer et al., 2015, 2019; Schaefer et al., 2018). One benefit is the close relation of pigs to humans in terms of metabolism particularly via cytochrome P450 (CYP) enzymes but also by anatomical structure and physiological properties (Anzenbacher et al., 1998; Swindle et al., 2012).

The identification of in vitro phase I metabolites of U-47700 has already been performed in pHLM and confirmed with human urine and blood samples from intoxications and post-mortem cases (Krotulski et al., 2018). However, there is no knowledge about the extent of phase II metabolites excreted in vivo into urine (Elliott et al., 2016; Jones et al., 2017; Krotulski et al., 2018; Vogliardi et al., 2018).

Therefore, the aim of the following study was to elucidate the metabolic pattern of U-47700 after intravenous administration to pig. Data was then compared to results obtained using other in vivo models (human and rat), other in vitro models (pig and human liver microsomes, pHS9), and previously published data. In addition, the involvement of single monooxygenases in the initial metabolic steps was elucidated.

2. Material and methods

2.1. Chemicals and reagents

U-47700 hydrochloride (purity 92.6%) was provided by the German Federal Crime Police Office (Wiesbaden, Germany) for research purposes. Isocitrate, isocitrate dehydrogenase, superoxide dismutase, 3′-phosphoadenosine-5′-phosphosulfate (PAPS), S-(5′-adenosyl)-L-methionine (SAM), dithiothreitol (DTT), reduced glutathione (GSH), acetyl carnitine, and acetyl coenzyme A (AcCoA) were purchased from Sigma (Taufkirchen, Germany), nicotinamide adenine dinucletide phosphate ($NADP^+$) from Biomol (Hamburg, Germany), and acetonitrile (LC-MS grade), ammonium formate (analytical grade), formic acid (LC-MS grade), methanol (LC-MS grade), glucuronidase (EC No. 3.2.1.32)/arylsulfatase (EC No. 3.1.6.1) from Helix pomatia L, and all other chemicals and reagents (analytical grade) from VWR (Darmstadt, Germany). pHLM from 25 donors (20 mg microsomal protein/mL 330 pmol total P450/mg protein), pHS9 (20 mg protein/mL, from 30 individual donors), UGT (uridine diphosphate (UDP-)glucuronosyltransferase) reaction mix solution A (25 mM UDP-glucuronic acid), UGT reaction mix solution B (250 mM Tris–HCl, 40 mM $MgCl_2$, and 0.125 mg/mL alamethicin), and baculovirus-infected insect cell microsomes (Supersomes) containing 1 nmol/mL of human complementary DNA-expressed cytochrome-P450 monooxygenases (CYP) 1A2, CYP2A6, CYP2B6, CYP2C8, CYP2C9, CYP2C19, CYP2D6, CYP2E1 (1 nmol/mL), CYP3A4, CYP3A5 (2 nmol/mL), or flavin-containing monooxygenase (FMO) 3 (5 mg protein/mL) were obtained from Corning (Amsterdam, The Netherlands). After delivery, the enzyme preparations and CYPs were thawed at 37 °C, aliquoted, snap-frozen in liquid nitrogen, and stored at −80 °C until use.

Pig liver microsomes (PLM) were freshly isolated from a single pig liver. The preparation is described in the electronic supplementary material (ESM).

2.2. Identification of phase I and II metabolites in pHS9 incubates

The incubation conditions were in accordance to the experimental design developed by Richter et al. (Richter et al., 2017). After 10 min pre-incubation at 37 °C with 25 μg/mL alamethicin (UGT reaction mix solution B), 90 mM phosphate buffer (pH 7.4), 2.5 mM Mg^{2+}, 2.5 mM isocitrate, 0.6 mM $NADP^+$, 0.8 U/mL isocitrate dehydrogenase, 100 U/mL superoxide dismutase, 0.1 mM AcCoA, and 2.3 mM acetyl carnitine, incubations of pHS9 (final protein concentration of 2 mg/mL) were performed. Afterward, 2.5 mM UDP-glucuronic acid (UGT reaction mix solution A), 40 μM aqueous PAPS, 1.2 mM SAM, 1 mM DTT, 10 mM GSH, and 25 μM U-47700 in phosphate buffer were added. All given concentrations are final concentrations. The reaction was initiated by adding the substrate. The mixture was incubated for 60 and 360 min. After 60 min, a 60 μL aliquot of the mixture was transferred into a reaction tube. Reactions were terminated by adding 20 μL of ice-cold acetonitrile. The remaining mixture was incubated for additional 300 min and thereafter the reactions were stopped by adding 30 μL of ice-cold acetonitrile. The solutions were cooled for 30 min at −18 °C and centrifuged for 2 min at 14,000 rpm. The supernatants were transferred into autosampler vials and 5 μL injected onto an Orbitrap-based liquid chromatography (LC) high-resolution (HR) mass spectrometry (MS) system as described below. To confirm the absence of interfering compounds and to identify non-metabolically originated compounds, additional blank incubations without substrate and control samples without pHS9 were prepared.

2.3. Identification of phase I and II metabolites in pHLM and PLM incubates as well as monooxygenase activity screening studies

According to standard procedures (Caspar et al., 2018a), 25 μM U-47700 was incubated with pHLM and PLM (1 mg protein/mL, each) and

the isoenzymes (50 pmol/mL, each) CYP1A2, CYP2A6, CYP2B6, CYP2C8, CYP2C9, CYP2C19, CYP2D6, CYP2E1, CYP3A4, CYP3A5 or FMO3 (0.25 mg protein/mL) for 30 min at 37 °C. Besides enzymes and substrates, the incubation mixtures (final volume, 50 µL) consisted of 90 mM phosphate buffer (pH 7.4), 5 mM Mg^{2+}, 5 mM isocitrate, 1.2 mM $NADP^+$, 0.5 U/mL isocitrate dehydrogenase, and 200 U/mL superoxide dismutase. Phosphate buffer was replaced with 90 mM Tris buffer (pH 7.4) for incubations with CYP2A6 and CYP2C9, according to the Gentest manual. The incubations were performed for 30 min. Reactions were initiated by addition of pre-warmed mixture of isocitrate dehydrogenase, isocitrate, $MgCl_2$ and $NADP^+$ and stopped with 50 µL of ice-cold acetonitrile. After centrifugation for 2 min at 14,000 rpm, 50 µL of the supernatants were transferred to autosampler vials and 5 µL injected onto the LC-HR-MS/MS system.

2.4. Human urine sample

One post mortem human urine sample was collected during autopsy in the context of a fatal intoxication. A 19-year-old male was found dead in his flat after a mixed intoxication of U-47700, 3-methoxyphencyclidine (3-MeO-PCP), 4-methoxybutyrfentanyl (4-MeO-butyrfentanyl), and diclazepam. The concentration of U-47700 detected in heart blood serum was about 1.1 mg/L. The concentrations of the other substances in heart blood serum were as follows: 0.0068 mg/L of 3-MeoPCP, 0.0088 mg/L of 4-Meo-butyrfentanyl, and < 0.001 mg/L of diclazepam. The urine sample was stored at −20 °C until analysis.

2.5. Rat urine samples

All animal experiments were performed in accordance with the German legislation on protection of animals and the National Institute of Health Guide for the Care and Use of Laboratory Animals. According to an established study design (Caspar et al., 2018b; Michely et al., 2017; Welter et al., 2013), the investigations were performed using rat urine samples from one male Wistar rat (Charles River, Sulzfeld, Germany) for toxicological diagnostic reasons according to German law. For identification of metabolites, the compound was administered in an aqueous suspension by gastric intubation of a single 0.6 mg/kg body weight dose.

The dose was calculated based on common user doses reported in trip reports (http://neuepsychoaktivesubstanzen.de/u-47700/#U-47700_Dosis_Dosierung, 2017) and scaled by dose-by-factor approach from man to rat according to Sharma and McNeill (Sharma and McNeill, 2009). The rats were housed in metabolism cages for 24 h, having water ad libitum. Over a period of 24 h, the urine was collected separately from feces. To verify that the samples were free of interfering compounds, blank urine samples were collected before drug administration. The samples were aliquoted and stored at −20 °C before analyzing.

2.6. Pig study design

One single domestic male pig (Swabian Hall strain, body weight 40.2 kg) was used for the study. The animal had water ad libitum and daily standard chow. A night before the experiment, it was kept fasting but still had free access to water.

The pig received a 100 µg/kg body weight dose of U-47700. A stock solution of 4 mg/mL was first prepared in ethanol for i.v. drug administration. A volume of 1005 µL was used to obtain a 100 µg/kg body weight dose. The volume was filled up with sodium chloride 0.9% to a volume of 10 mL and administered into the jugular vein within 30 s. The surgical procedure was performed according to already published procedures (Schaefer et al., 2017a, b) and was described in detail in the ESM. Urine specimens were collected before administration and then in the following intervals: t = 0–60, t = 60 − 120, t = 120 − 180, t = 180–240, t = 240–300, t = 300–360, t = 360–420, and t = 420 − 480 min. All samples were stored at −20 °C until analysis.

2.7. Sample preparation of urine samples for identification of phase I and II metabolites

In accordance to published procedures (Wissenbach et al., 2011), 100 µL of urine was mixed with 500 µL of acetonitrile for protein precipitation. After shaking and centrifugation for 2 min at 14,000 rpm, the supernatant was transferred into new vials and evaporated to dryness under a gentle stream of nitrogen. Afterward the extract was reconstituted in 50 µL of eluent A and eluent B (1:1, v/v) and transferred into autosampler vials.

Additionally and prior to the extraction procedure, urine samples were treated with β-glucuronidase/arylsulfatase for conjugate cleavage (Michely et al., 2017). For this purpose, 200 µL of urine were incubated with 20 µL β-glucuronidase/arylsulfatase in 180 µL 100 mM aqueous ammonium acetate buffer (pH 5.2) for 2 h at 55 °C. The extracts were precipitated by adding of 1 mL acetonitrile and stored for 5 min at – 20 °C. After shaking and centrifugation, the supernatant was gently evaporated and reconstituted with 100 µL of eluent A and eluent B (1:1, v/v). An aliquot of 1 µL of the extract was injected onto the LC-HR-MS/MS system with conditions described below.

2.8. LC-HR-MS/MS instrumentation

As described previously (Caspar et al., 2018b; Michely et al., 2017), a ThermoFisher Scientific (TF, Dreieich, Germany) Dionex UltiMate 3000 RS pump consisting of a degasser, a quaternary pump, and an UltiMate autosampler, coupled to a TF Q-Exactive Plus system (Dreieich, Germany) equipped with a heated electrospray ionization (HESI)-II source was used for analysis.

Gradient elution was performed on a TF Accucore PhenylHexyl column (100 mm x 2.1 mm, 2.6 µm, Dreieich, Germany) with a column oven temperature of 60 °C. The mobile phase consisted of 2 mM aqueous ammonium formate containing 0.1% (v/v) formic acid and 1% (v/v) acetonitrile (pH 3, eluent A) and 2 mM ammonium formate solution with acetonitrile/methanol (50:50, v/v), containing 0.1% (v/v) formic acid and 1% (v/v) water (eluent B). The gradient and flow rate were programmed as follows: 0 − 1 min hold 99% A, 1 − 10 min 99% A to 1% A, both with flow rate 0.5 mL/min, 10 − 11.5 min hold, 11.5–13.5 min hold 99% A, both with flow rate 0.8 mL/min. The HESI-II source conditions were as follows: sheath gas, 60 arbitrary units (AU); auxiliary gas, 10 AU; spray voltage, 3.00 kV; heater temperature, 320 °C; ion transfer capillary temperature, 320 °C; and S-lense RF level, 60.0. The MS was operated in positive ionization mode using full scan (FS) and subsequent data dependent acquisition (DDA) mode with inclusion list containing the *m/z* values of 43 theoretically expected metabolites. The mass calibration was done according to the manufacture's recommendations using external mass calibrators. The settings for FS data were as follows: resolution, 35,000; microscans, 1: automatic gain control (AGC) target, 1e6; maximum injection time (IT), 120 ms; scan range for FS data *m/z* 100 − 600. The settings for the DDA mode were as follows: option "do not pick others", enabled; dynamic exclusion, off; resolution 17,500; microscans, 1; loop count, 5; AGC target, 2e5; maximum IT, 250 ms; isolation window, 1.0 *m/z*, high collision dissociation (HCD) with stepped normalized collision energy (NCE), 17.5, 35, and 52.5%; spectrum data type, profile; underfill ratio, 0.5. For data handling Xcalibur Qual Browser software version 3.0.63 was used.

3. Results and discussion

3.1. LC-HR-MS/MS identification of U-47700 and its phase I and II metabolites based on MS/MS fragmentation

The LC-HR-MS/MS-fragmentation patterns of U-47700 and its metabolites will be discussed in the following. Due to the high number of metabolites and that some metabolites were already discussed in previous studies (Krotulski et al., 2018; Vogliardi et al., 2018), not all

Table 1
U-47700 and all tentatively identified metabolites as well as their elemental composition (EC), monoisotopic exact mass (EM), monoisotopic accurate mass (AM), characteristic product ions (PI), mass errors (in ppm), and retention time (RT, in min). Elemental composition and all given masses are protonated forms. Hydroxylation at the hexyl ring is indicated by [1] and hydroxylation at the phenyl ring by [2].

No.	compound	EC	EM	AM	Error	PI 1	Error	PI 2	Error	PI 3	Error	PI 4	Error	RT
	U-47700	$C_{16}H_{23}ON_2Cl_2$	329.1181	329.1180	−0.626	284.0601	0.742	203.9977	0.216	172.9555	−0.244	126.1276	−1.131	5.25
	Phase I													
M1	*N*-demethyl-	$C_{15}H_{21}ON_2Cl_2$	315.1025	315.1022	0.403	284.0601	−0.742	203.9977	−0.191	172.9555	−0.246	112.1125	3.499	5.21
M2	*N,N*-bisdemethyl-	$C_{14}H_{19}ON_2Cl_2$	301.0868	301.0868	−0.387	284.0601	−0.742	270.0446	−0.481	189.9822	−0.294	172.9556	0.220	5.21
M3	*N,N,N*-tridemethyl-	$C_{13}H_{17}ON_2Cl_2$	287.0712	287.0708	−1.5074	270.0445	−0.206	189.9815	−2.931	172.9552	−1.844	98.0966	2.105	5.06
M4	Hydroxy-[1]	$C_{16}H_{23}O_2N_2Cl_2$	345.1131	345.1134	0.825	300.0553	0.203	203.9980	1.163	172.9557	0.956	110.0968	3.486	4.18
M5	N-oxide-	$C_{16}H_{23}O_2N_2Cl_2$	345.1131	345.1133	0.615	284.0606	0.745	203.9978	0.171	172.9557	0.967	112.1125	3.627	5.27
M6	N-oxide hydroxy-	$C_{16}H_{23}O_3N_2Cl_2$	361.1080	361.1070	−2.782	300.0553	0.148	282.0449	0.793	203.9979	0.993	110.0968	3.610	4.50
M7	*N*-demethyl-hydroxy-[1]	$C_{15}H_{21}O_2N_2Cl_2$	331.0974	331.0974	−0.243	300.0554	0.299	282.0447	0.074	203.9978	0.171	172.9556	0.121	4.42
M8	*N*-demethyl-hydroxy-[2]	$C_{15}H_{21}O_2N_2Cl_2$	331.0974	331.0970	−0.710	300.0549	−0.451	219.9925	−1.775	188.9501	−2.388	112.1122	1.419	4.89
M9	*N,N*-bisdemethyl-hydroxy-[1]	$C_{14}H_{19}O_2N_2Cl_2$	317.0818	317.0809	−2.756	300.0546	−2.318	286.0371	−2.491	203.9974	−0.536	172.9552	−2.106	4.32
M10	*N,N*-bisdemethyl-hydroxy-[2]	$C_{14}H_{19}O_2N_2Cl_2$	317.0818	317.0813	−1.611	286.0390	−2.023	205.9767	−1.582	188.9501	−1.814	162.9711	−0.782	4.22
M11	*N,N,N*-tridemethyl-hydroxy-[1]	$C_{13}H_{17}O_2N_2Cl_2$	303.0661	303.0659	−0.942	286.0390	−2.167	189.9815	−3.440	172.9552	−2.048	96.0812	3.948	4.84
M12	*N,N,N*-tridemethyl-hydroxy-[2]	$C_{13}H_{17}O_2N_2Cl_2$	303.0661	303.0646	−5.173	286.0389	−2.522	205.9768	−1.083	188.9499	−2.863	81.0705	7.409	4.80
	Phase II													
M13	Hydroxy-glucuronide-[1]	$C_{22}H_{31}O_8N_2Cl_2$	521.1451	521.1423	−3.583	476.0863	−2.244	345.1115	−1.886	300.0547	−1.935	172.9552	−2.210	4.26
M14	*N*-demethyl-hydroxy-glucuronide-[1]	$C_{21}H_{29}O_8N_2Cl_2$	507.1295	507.1295	−0.144	476.0861	−2.676	300.0545	−1.700	203.9971	−0.679	110.0965	0.478	4.24
M15	*N*-demethyl-hydroxy-glucuronide-[2]	$C_{21}H_{29}O_8N_2Cl_2$	507.1295	507.1294	−0.211	476.0871	−0.612	331.0969	−1.166	300.0548	−1.669	219.9923	−1.502	4.42
M16	*N*-demethyl-hydroxy-sulfate-[1]	$C_{15}H_{21}O_5N_2Cl_2S$	411.0542	411.0526	−4.049	380.0111	−2.593	282.0439	−1.093	203.9971	−0.683	172.9552	−2.286	4.75
M17	*N,N*-bisdemethyl-hydroxy-glucuronide-[1]	$C_{20}H_{27}O_8N_2Cl_2$	493.1138	493.1124	−0.679	317.0814	−4.450	286.0389	−2.310	189.9816	−2.452	172.9553	−1.699	4.39
M18	*N,N*-bisdemethyl-hydroxy-glucuronide-[2]	$C_{20}H_{27}O_8N_2Cl_2$	493.1138	493.1129	−1.983	317.0813	−1.450	300.0547	−2.370	286.0389	−2.310	188.9500	−2.321	4.45
M19	*N,N*-bisdemethyl-hydroxy-sulfate-[1]	$C_{14}H_{19}O_5N_2Cl_2S$	397.0386	397.0380	−1.466	380.0166	−1.147	268.0283	−1.910	203.9972	−0.610	172.9552	−1.947	4.70
M20	*N,N*-bisdemethyl-hydroxy-sulfate-[2]	$C_{14}H_{19}O_5N_2Cl_2S$	397.0386	397.0381	−1.433	317.0812	−1.324	286.0930	2.1766	205.9766	−1.156	188.9501	−1.973	4.91

metabolites were discussed in detail. A list of all identified phase I and II metabolites is given in Table 1 including exact mass, accurate mass, elemental composition, characteristic fragment ions, mass error, and retention time.

Metabolite identification was performed by comparison of their MS^2 spectra to the MS^2 spectrum of U-47700. In total, 12 phase I and eight phase II metabolites of U-47700 were identified in the in vitro incubations or in rat, pig, or human urine. The MS^2 spectra of U-47700 and its metabolites are given in Figure S1 in the ESM. The predominant metabolic reactions were *N*-demethylation, hydroxylation, and combination of them followed by glucuronidation or sulfation. The proposed metabolic pathway is shown in Fig. 1.

U-47700 (protonated mass, precursor mass (PM) of *m/z* 329.1180) showed a fragmentation pattern according to already published data (Elliott et al., 2016; Fleming et al., 2017; Krotulski et al., 2018). Loss of dimethylamine at the cyclohexyl ring led to the most abundant and characteristic fragment ion at *m/z* 284.0601. Cleavage of the C−N bond next to the carbonyl group occurs at both sides of the nitrogen and formed the two other characteristic fragments at *m/z* 203.9977 and 172.9555. A low-abundant fragment ion at *m/z* 126.1276 is related to the cyclohexyl ring with the tertiary amine. The cyclohexyl ring was represented by the fragment ion at *m/z* 81.0704.

M1 (PM at *m/z* 315.1022), which was formed by *N*-demethylation of the tertiary amine, showed a fragmentation pattern closely to that of U-47700 and literature data (Elliott et al., 2016; Fleming et al., 2017; Krotulski et al., 2018; Richeval et al., 2019), as well as the *N,N*-bisdemethylated metabolite M2. The fragmentation pattern of M2 differed from those of U-47700 and M1 through presence of the fragment ions at *m/z* 270.0446 and 189.9822. This led to the hypothesis that demethylation occurred at both, the tertiary amide and the tertiary amine. However, previous studies described *N,N*-bisdemethylation at the tertiary amine confirmed with the analysis of reference material (Krotulski et al., 2018). The *N,N,N*-tridemethylated metabolite M3 was identified by the fragment ion at *m/z* 270.0445 and 189.9815 which corresponded to the fragment ions at *m/z* 284.0601 and 203.9977 both altered in one CH_2 group. M4 (PM at *m/z* 345.1134) was hydroxylated at the cyclohexyl ring, characterized by the fragment ion at *m/z* 110.0968 and 79.0550 indicating loss of water at the cyclohexyl ring. This metabolite, even as other hydroxylated metabolites, gives rise to multiple chromatographic peaks, which was expected due to multiple sites at the cyclohexyl ring where hydroxylation could occur. In previous published data, hydroxylation cloud only be identified in combination with *N*-demethylation (Jones et al., 2017). However, hydroxylated metabolites were already described for structural related compound as U-48800 or U-51754 (Gampfer et al., 2019; Nordmeier et al., 2019). M5 showed the same fragment ions as U-47700 and was associated with *N*-oxidation at the tertiary amine. The spectrum of M6 showed the same fragment ions as the hydroxy metabolite M4 and was characterized by the fragment ion at *m/z* 361.1070, which corresponded to the fragment ion at *m/z* 345.1133 shifted by an oxygen. Thus, this metabolite might be formed due to *N*-oxidation with additional hydroxylation at the cyclohexyl ring. The *N*-demethyl-hydroxy metabolite M7 (PI at *m/z* 331.0974) and the *N,N*-bisdemethyl-hydroxy metabolite M9 (PI at *m/z* 317.0818) showed the same characteristic fragmentation patterns as their corresponding hydroxy metabolite M4 and were already described in the literature by Jones et al. (Jones et al., 2017). M11 (PI at *m/z* 303.0659) was identified by the fragment ions at *m/z* 286.0390 and is the corresponding *N,N,N*-tridemethyl-hydroxy isomer to M3. Their fragmentation pattern was in accordance to each other. The *N*-demethylated and hydroxylated metabolites M8 and M10 were formed by single or double *N*-demethylation at the tertiary amine and hydroxylation at the phenyl ring characterized by the fragment ions at *m/z* 188.9499 which consisted of the dichlorobenzaldehyde shifted by an oxygen. The *N,N,N*-tridemethyl-hydroxy metabolite M12 showed the same characteristic fragment ions related to hydroxylation at the phenyl ring as M8 and M10. Hydroxylation at the phenyl ring was not described for U-47700,

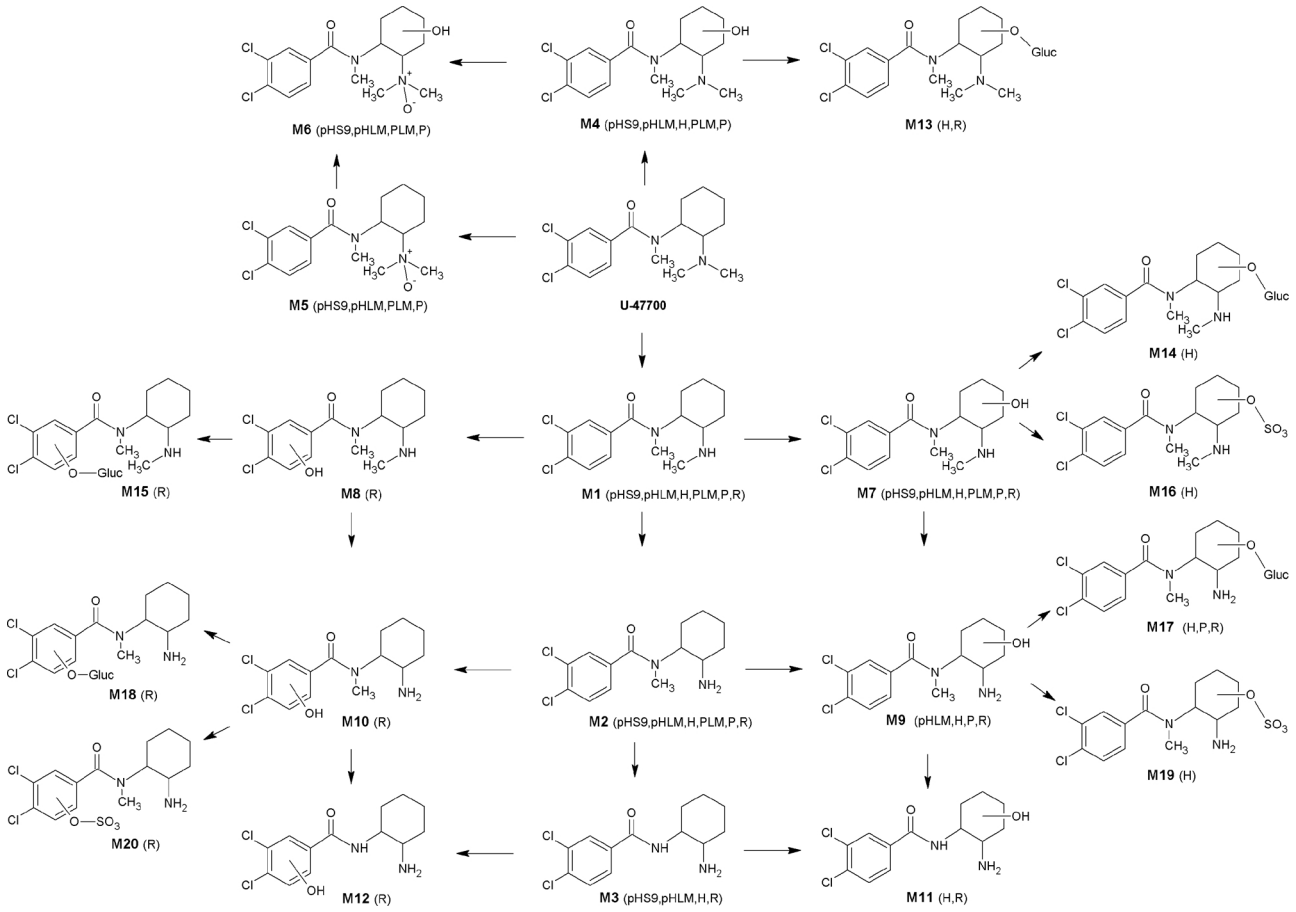

Fig. 1. Metabolic pathways of U-47700 studied in rat urine (R), pig urine (P), human urine (H), pooled human liver microsomes (pHLM), pig liver microsomes (PLM), and pooled human liver S9 fraction incubations (phS9). Numbering according to Table 1.

yet but could be found for U-48800, U-51754, and U-47931E (Gampfer et al., 2019; Nordmeier et al., 2019). For hydroxylated metabolites as well as for *N*-demethylated and hydroxylated metabolites, additional phase II conjugation could be identified. M13, M14, M15, M17 and M18 originated by glucuronidation and M16, M19 and M20 by sulfation. All glucuronides eliminated dehydrated glucuronic acid (−176.0321 u) and all sulfates dehydrated sulfuric acid (−79.9568 u). All mass spectra of phase II metabolites formed by conjugation of either glucuronic or sulfuric acid were in accordance to those of their corresponding phase I metabolites.

3.2. Monooxygenase activity screening

The incubation conditions allowed a statement of the qualitative involvement of a particular monooxygenase. Studies were also performed to elucidate whether the main metabolic steps in pigs are comparable to those in humans, based on monooxygenase contribution. Initial metabolic steps in pig for U-47700 were *N*-demethylation, hydroxylation, and *N*-oxidation. All steps could be confirmed to be identical with those in man. As summarized in Table 2, *N*-demethylation was catalyzed by most of the CYPs and hydroxylation by CYP2C19, CYP2A6, CYP2B6, CYP2C19, CYP2C8, CYP3A4, and CYP3A5. *N*-oxidation was catalyzed by CYP3A4 and CYP3A5 as well as FMO3, already known to be involved in metabolism of several NPS (Wagmann et al., 2016). *N*-demethylation in combination with hydroxylation was formed only in CYP2B6, CYP2C19, and CYP3A4 incubates. In total, CYP2B6, CYP2C19, CYP3A4, and CYP3A5 were predominantly involved in the metabolism of U-47700. Isozyme mapping of the structurally related compound U-48800 also showed that CYP2C19 and CYP3A4 were the isozymes catalyzing most reactions (Gampfer et al., 2019).

3.3. Comparison of metabolism studies in the different in vitro and in vivo systems and comparison to the literature

3.3.1. In vitro metabolism by pHLM, PLM and pHS9

All tested in vitro tools were in good agreement to each other as summarized in Table 3. All phase I metabolites (M1-M7) could be identified with the exception of M3 in PLM. *N*,*N*-bisdemethyl-hydroxy-U-47700 could additionally be found in pHLM. Surprisingly, no phase II metabolites were detected in pHS9 but a low formation of phase II

Table 2
General involvement of monooxygenases in the formation of the given initial metabolic reactions of U-47700.

	CYP											
Metabolic reaction	1A2	2A6	2B6	2C8	2C9	2C19	2D6	2E1	3A4	3A5	FMO3	HLM
N-demethylation	+		+	+	+	+	+		+	+		+
Hydroxylation		+	+		+	+			+	+		+
N-oxidation									+	+	+	+

Table 3
U-47700 and its phase I and II metabolites found in pig urine compared to different in vitro and in vivo models (pig liver microsomes (PLM) pooled human liver microsomes (pHLM) pooled human liver S9 fraction (pHS9), rat) as well as human urine. Hydroxylation at the hexyl ring is indicated by [1] and hydroxylation at the phenyl ring by [2]. Most abundant metabolites are highlighted in grey.

		pig		rat	human		
		in vitro	in vivo	in vivo	in vitro		in vivo
ID	Metabolite	PLM	urine	urine	pHLM	pS9	urine
Phase I							
M1	*N*-demethyl	+	+	+	+	+	+
M2	*N*,*N*-bisdemethyl	+	+	+	+	+	+
M3	*N*,*N*,*N*-tridemethyl			+	+	+	+
M4	Hydroxy[1]	+	+		+	+	+
M5	N-oxide	+	+		+	+	
M6	N-oxide hydroxy	+	+		+	+	
M7	*N*-demethyl-hydroxy[1]	+	+	+	+	+	+
M8	*N*-demethyl-hydroxy[2]			+			
M9	*N*,*N*-bisdemethyl-hydroxy[1]		+	+	+		+
M10	*N*,*N*-bisdemethyl-hydroxy[2]			+			
M11	*N*,*N*,*N*-tridemethyl-hydroxy[1]			+			+
M12	*N*,*N*,*N*-tridemethyl-hydroxy[2]			+			
Phase II							
M13	Hydroxy-glucuronide[1]		+				+
M14	*N*-demethyl-hydroxy-glucuronide[1]						+
M15	*N*-demethyl-hydroxy-glucuronide[2]			+			
M16	*N*-demethyl-hydroxy-sulfate[1]						+
M17	*N*,*N*-bisdemethyl-hydroxy-glucuronide[1]		+	+			+
M18	*N*,*N*-bisdemethyl-hydroxy-glucuronide[2]			+			
M19	*N*,*N*-bisdemethyl-hydroxy-sulfate[1]						+
M20	*N*,*N*-bisdemethyl-hydroxy-sulfate[2]			+			

metabolites in pHS9 was already described for other NPS (Caspar et al., 2018b). Lower formation of phase II metabolites in pHS9 could be caused by low formation of underlying phase I metabolites. Furthermore, most of the phase II metabolites are built by multiple reaction steps which are not very pronounced in rigid systems such as in vitro incubations. pHLM showed a higher metabolic activity than PLM and pHS9, despite longer incubation time used in pHS9 incubations. However, pHS9 is known to have a lower activity than pHLM due to the fact of lower metabolizing enzyme content in pHS9 (Richter et al., 2017). PLM incubates showed the lowest enzymatic activity and all metabolites had a much lower abundance than the parent drug. Nevertheless, main metabolites were in accordance to the other in vitro systems.

3.3.2. *In vivo metabolism by rat, pig, or human*

As shown in Table 3, metabolite formation was comparable in all in vivo models. The same most abundant metabolites (*N*-demethyl-, *N*,*N*-bisdemethyl, *N*-demethyl-hydroxy- and *N*,*N*-bisdemethyl-hydroxy-U-47700) were detected in urine, respectively. In contrast to pig and human, rat samples contained lower amounts of the parent compound, which may be due to the way of administration and different doses. Furthermore, metabolites after hydroxylation at the phenyl ring were found exclusively in rat urine samples. This could be caused by species related differences in metabolism. Nevertheless, hydroxylation at the phenyl ring was observed for other U-substances in human (Gampfer et al., 2019; Nordmeier et al., 2019). In pig specimens as well as in the in vitro samples, *N*-oxides could be found. This metabolite was not found in human or rat urine but species related differences concerning the involved enzymes were described (Yamazaki et al., 2014). Yamazaki et al. showed that the content of FMO3 in minipig liver microsomes and HLM should be comparable but that pig FMO3 shows a higher activity (Yamazaki et al., 2014). Thus, FMO3-dependent *N*-oxygenation reactions are more likely to occur in pig than in human. Phase II metabolites of U-47700 were found in all samples. In all analyzed species, phase II metabolites were formed by glucuronidation and/or sulfation, but these metabolites were less abundant than their corresponding phase I metabolites. In pig and rat, glucuronidation was more pronounced than sulfation. No sulfates could be detected in pig and only one in rat. Low formation of sulfated metabolites in rats was already described (Meyer et al., 2012). However, sulfation was described as a metabolic reaction of synthetic cannabinoids occurring in pigs (Schaefer et al., 2017a). In vitro and in vivo results of phase I metabolism were in good agreement particularly within the same species. Formation of phase II metabolites was lacking in the in vitro models and in vivo models should be preferred to answer related questions.

In general, the comparability of the results is better applying same study settings, but the formation of metabolites was comparable in all in vivo models despite different routes of administration. U-47700 is consumed both orally and intravenously. In rat studies gastric intubations are the easiest way for drug administration and an already well established model (Caspar et al., 2018b; Michely et al., 2017; Welter et al., 2013). As far as the pig study is concerned, an i.v. administration was chosen to figure out, whether the pig is suitable for TK studies of NSO, because a bioavailability of 100% is guaranteed. Regarding the ethical need of a preferably little number of experimental animals no further administration routes were applied. Furthermore, the aim of this study was to generate qualitative data of metabolism of U-47700. For ethical reasons, only one rat was used in this study to keep the number of experimental animals as low as possible. In alignment to only one rat urine, only one pig urine was used, too. Thus, it should be kept in mind that these results only reflect one individual and no pool of

each species. For further TK studies a higher number of animals would be necessary.

3.4. Comparison of metabolism in pig and human

The results showed a good correlation between both species even if the setting of the human dosage or administration was not known. Considering the high serum concentration of U-47700 in the human sample, the deceased had presumably taken a higher dose than that used in pig, resulting in a maximum concentration of 109 ng/mL in serum. However, similar most abundant metabolites could be found in the urine samples. The pattern of phase I metabolites in the pig urine was in agreement with those in human except for the *N*,*N*,*N*-tridemethylated metabolites, which could only be detected in the human urine samples and the exclusively formed *N*-oxide metabolite in the pig urine sample. Nevertheless, this was only a less abundant metabolite. Thus, the pig should be a suitable model for metabolism studies of NPS but at least for NSO. Furthermore, this model might be suitable for further TK studies of U-47700 and NSO/NPS.

3.5. Analytical implications and recommended analytical urinary targets

The parent compound was detectable at high abundances in all pig samples until 8 h after drug administration. However, abundance declined over time. Amongst the metabolites, *N*,*N*-bisdemethyl-hydroxy U-47700 was the most abundant, whereas *N*-demethyl-U-47700 was the most abunndant metabolite in the human urine samples (Jones et al., 2017; Krotulski et al., 2018; Richeval et al., 2019; Smith et al., 2019). *N*,*N*-bisdemethyl-hydroxy U-47700 appeared 2 − 3 h after administration and was predominantly present also in the last pig sample. The same was true for *N*-demethyl U-47700. More polar metabolites as the *N*-oxide or the hydroxy metabolite were only found at the first time points (until 3 h or 5 h, respectively). *N*-oxide-hydroxy U-47700 and the hydroxy glucuronide were the least abundant metabolites. In addition to the parent drug, suitable urinary targets for proof of U-47700 intake should therefore be *N*-demethyl-, *N*,*N*-bisdemethyl-, *N*-demethyl-hydroxy- and *N*,*N*-bisdemethyl-hydroxy-U-47700.

4. Conclusions

Several phase I and II metabolites of U-47700 could be identified in pig urine after intravenous administration, in PLM, pHLM, pHS9 incubations, and in rat and human urine. *N*-demethylation, hydroxylation, and the combination of both led to the most abundant metabolites. CYP2B6, CYP2C19, CYP3A4, and CYP3A5 were predominantly involved in the initial phase I metabolism of U-47700 in vitro. In general and despite minor differences, results showed that the pig model was in good agreement with those obtained applying other tools. Particularly the good correlation to human data underlined the suitability of pigs as TK model for elucidation of the metabolic pattern and probably further TK data of U-47700 and other NSO/NPS.

Transparency document

The Transparency document associated with this article can be found in the online version.

Declaration of Competing Interest

The authors declare that they have no known competing financial interests or personal relationships that could have appeared to influence the work reported in this paper.

Acknowledgments

The authors would like to thank Benjamin Peters, Christine Wesley, the staff of the Institute for Clinical and Experimental Surgery at Saarland University and the Institute of Experimental and Clinical Toxicology at Saarland University for their support, help and/or helpful discussions. We acknowledge the EU funded project ADEBAR (IZ25-5793-2016-27).

Appendix A. Supplementary data

Supplementary material related to this article can be found, in the online version, at doi:https://doi.org/10.1016/j.toxlet.2020.04.001.

References

Anzenbacher, P., Soucek, P., Anzenbacherova, E., Gut, I., Hruby, K., Svoboda, Z., Kvetina, J., 1998. Presence and activity of cytochrome P450 isoforms in minipig liver microsomes. Comparison with human liver samples. Drug Metab. Dispos. 26 (1), 56–59.

Baumann, M.H., Majumdar, S., Le Rouzic, V., Hunkele, A., Uprety, R., Huang, X.P., Xu, J., Roth, B.L., Pan, Y.X., Pasternak, G.W., 2018. Pharmacological characterization of novel synthetic opioids (NSO) found in the recreational drug marketplace. Neuropharmacology 134 (Pt A), 101–107.

Caspar, A.T., Brandt, S.D., Stoever, A.E., Meyer, M.R., Maurer, H.H., 2017. Metabolic fate and detectability of the new psychoactive substances 2-(4-bromo-2,5-dimethoxyphenyl)-N-[(2-methoxyphenyl)methyl]ethanamine (25B-NBOMe) and 2-(4-chloro-2,5-dimethoxyphenyl)-N-[(2-methoxyphenyl)methyl]ethanamine (25C-NBOMe) in human and rat urine by GC-MS, LC-MS(n), and LC-HR-MS/MS approaches. J. Pharm. Biomed. Anal. 134, 158–169.

Caspar, A.T., Gaab, J.B., Michely, J.A., Brandt, S.D., Meyer, M.R., Maurer, H.H., 2018a. Metabolism of the tryptamine-derived new psychoactive substances 5-MeO-2-Me-DALT, 5-MeO-2-Me-ALCHT, and 5-MeO-2-Me-DIPT and their detectability in urine studied by GC-MS, LC-MS(n), and LC-HR-MS/MS. Drug Test. Anal. 10 (1), 184–195.

Caspar, A.T., Westphal, F., Meyer, M.R., Maurer, H.H., 2018b. LC-high resolution-MS/MS for identification of 69 metabolites of the new psychoactive substance 1-(4-ethylphenyl-)-N-[(2-methoxyphenyl)methyl] propane-2-amine (4-EA-NBOMe) in rat urine and human liver S9 incubates and comparison of its screening power with further MS techniques. Anal. Bioanal. Chem. 410 (3), 897–912.

Cheney, B.V., Szmuszkovicz, J., Lahti, R.A., Zichi, D.A., 1985. Factors affecting binding of trans-N-[2-(methylamino)cyclohexyl]benzamides at the primary morphine receptor. J. Med. Chem. 28 (12), 1853–1864.

Coopman, V., Blanckaert, P., Van Parys, G., Van Calenbergh, S., Cordonnier, J., 2016. A case of acute intoxication due to combined use of fentanyl and 3,4-dichloro-N-[2-(dimethylamino)cyclohexyl]-N-methylbenzamide (U-47700). Forensic Sci. Int. 266, 68–72.

Dziadosz, M., Klintschar, M., Teske, J., 2017. Postmortem concentration distribution in fatal cases involving the synthetic opioid U-47700. Int. J. Legal Med. 131 (6), 1555–1556.

Elliott, S.P., Brandt, S.D., Smith, C., 2016. The first reported fatality associated with the synthetic opioid 3,4-dichloro-N-[2-(dimethylamino)cyclohexyl]-N-methylbenzamide (U-47700) and implications for forensic analysis. Drug Test. Anal. 8 (8), 875–879.

Fleming, S.W., Cooley, J.C., Johnson, L., Frazee, C.C., Domanski, K., Kleinschmidt, K., Garg, U., 2017. Analysis of U-47700, a Novel Synthetic Opioid, in Human Urine by LC-MS-MS and LC-QToF. J. Anal. Toxicol. 41 (3), 173–180.

Gampfer, T.M., Richter, L.H.J., Schaper, J., Wagmann, L., Meyer, M.R., 2019. Toxicokinetics and analytical toxicology of the abused opioid U-48800 - in vitro metabolism, metabolic stability, isozyme mapping, and plasma protein binding. Drug Test. Anal. 11 (10), 1572–1580.

Harper, N.J., Veitch, G.B., Wibberley, D.G., 1974. 1-(3,4-Dichlorobenzamidomethyl)cyclohexyldimethylamine and related compounds as potential analgesics. J. Med. Chem. 17 (11), 1188–1193.

http://neuepsychoaktivesubstanzen.de/u-47700/#U-47700_Dosis_Dosierung, 2017.

http://www.emcdda.europa.eu/system/files/publications/11364/20191724_TDAT19001ENN_PDF.pdf, 2019. EMCDDA: European Monitoring Center of Drugs and Drug Addiction. European Drug Report – Trends and Developments.

Jones, M.J., Hernandez, B.S., Janis, G.C., Stellpflug, S.J., 2017. A case of U-47700 overdose with laboratory confirmation and metabolite identification. Clin. Toxicol. Phila. (Phila) 55 (1), 55–59.

Koch, K., Auwarter, V., Hermanns-Clausen, M., Wilde, M., Neukamm, M.A., 2018. Mixed intoxication by the synthetic opioid U-47700 and the benzodiazepine flubromazepam with lethal outcome: Pharmacokinetic data. Drug Test Anal in press. https://doi.org/10.1002/dta.2391.

Krotulski, A.J., Mohr, A.L.A., Papsun, D.M., Logan, B.K., 2018. Metabolism of novel opioid agonists U-47700 and U-49900 using human liver microsomes with confirmation in authentic urine specimens from drug users. Drug Test. Anal. 10 (1), 127–136.

Lehmann, S., Teifel, D., Alexander Rothschild, M., Andresen-Streichert, H., 2018. Tödliche Intoxikation mit dem Designer-Opioid U-47700. Toxichem Krimtech 85 (1), 36–43.

Martignoni, M., Groothuis, G.M., de Kanter, R., 2006. Species differences between mouse, rat, dog, monkey and human CYP-mediated drug metabolism, inhibition and

induction. Expert Opin. Drug Metab. Toxicol. 2 (6), 875–894.
Meyer, M.R., 2016. New psychoactive substances: an overview on recent publications on their toxicodynamics and toxicokinetics. Arch. Toxicol. 90 (10), 2421–2444.
Meyer, M.R., Dinger, J., Schwaninger, A.E., Wissenbach, D.K., Zapp, J., Fritschi, G., Maurer, H.H., 2012. Qualitative studies on the metabolism and the toxicological detection of the fentanyl-derived designer drugs 3-methylfentanyl and isofentanyl in rats using liquid chromatography-linear ion trap-mass spectrometry (LC-MS(n)). Anal. Bioanal. Chem. 402 (3), 1249–1255.
Michely, J.A., Manier, S.K., Caspar, A.T., Brandt, S.D., Wallach, J., Maurer, H.H., 2017. New psychoactive substances 3-methoxyphencyclidine (3-meo-pcp) and 3-methoxyrolicyclidine (3-MeO-PCPy): metabolic fate elucidated with rat urine and human liver preparations and their detectability in urine by GC-MS, "LC-(high resolution)-MSn" and "LC-(high resolution)-MS/MS". Curr. Neuropharmacol. 15 (5), 692–712.
Mohr, A.L., Friscia, M., Papsun, D., Kacinko, S.L., Buzby, D., Logan, B.K., 2016. Analysis of novel synthetic opioids U-47700, U-50488 and Furanyl Fentanyl by LC-MS/MS in postmortem casework. J. Anal. Toxicol. 40 (9), 709–717.
Nikolaou, P., Katselou, M., Papoutsis, I., Spiliopoulou, C., Athanaselis, S., 2017. U-47700. An old opioid becomes a recent danger. Forensic Toxicol. 35 (1), 11–19.
Nordmeier, F., Richter, L.H.J., Schmidt, P.H., Schaefer, N., Meyer, M.R., 2019. Studies on the in vitro and in vivo metabolism of the synthetic opioids U-51754, U-47931E, and methoxyacetylfentanyl using hyphenated high-resolution mass spectrometry. Sci. Rep. 9 (1), 13774.
Parasuraman, S., Raveendran, R., Kesavan, R., 2010. Blood sample collection in small laboratory animals. J. Pharmacol. Pharmacother. 1 (2), 87–93.
Peters, F.T., Meyer, M.R., 2011. In vitro approaches to studying the metabolism of new psychoactive compounds. Drug Test. Anal. 3 (7–8), 483–495.
Richeval, C., Gaulier, J.M., Romeuf, L., Allorge, D., Gaillard, Y., 2019. Case report: relevance of metabolite identification to detect new synthetic opioid intoxications illustrated by U-47700. Int. J. Legal Med. 133 (1), 133–142.
Richter, L.H.J., Flockerzi, V., Maurer, H.H., Meyer, M.R., 2017. Pooled human liver preparations, HepaRG, or HepG2 cell lines for metabolism studies of new psychoactive substances? A study using MDMA, MDBD, butylone, MDPPP, MDPV, MDPB, 5-MAPB, and 5-API as examples. J. Pharm. Biomed. Anal. 143, 32–42.
Ruan, X., Chiravuri, S., Kaye, A.D., 2016. Comparing fatal cases involving U-47700. Forensic Sci. Med. Pathol. 12 (3), 369–371.
Schaefer, N., Kettner, M., Laschke, M.W., Schlote, J., Peters, B., Bregel, D., Menger, M.D., Maurer, H.H., Ewald, A.H., Schmidt, P.H., 2015. Simultaneous LC-MS/MS determination of JWH-210, RCS-4, (9)-tetrahydrocannabinol, and their main metabolites in pig and human serum, whole blood, and urine for comparing pharmacokinetic data. Anal. Bioanal. Chem. 407 (13), 3775–3786.
Schaefer, N., Helfer, A.G., Kettner, M., Laschke, M.W., Schlote, J., Ewald, A.H., Meyer, M.R., Menger, M.D., Maurer, H.H., Schmidt, P.H., 2017a. Metabolic patterns of JWH-210, RCS-4, and THC in pig urine elucidated using LC-HR-MS/MS: Do they reflect patterns in humans? Drug Test. Anal. 9 (4), 613–625.
Schaefer, N., Kettner, M., Laschke, M.W., Schlote, J., Ewald, A.H., Menger, M.D., Maurer, H.H., Schmidt, P.H., 2017b. Distribution of synthetic cannabinoids JWH-210, RCS-4 and delta 9-tetrahydrocannabinol after intravenous administration to pigs. Curr. Neuropharmacol. 15 (5), 713–723.
Schaefer, N., Wojtyniak, J.G., Kroell, A.K., Koerbel, C., Laschke, M.W., Lehr, T., Menger, M.D., Maurer, H.H., Meyer, M.R., Schmidt, P.H., 2018. Can toxicokinetics of (synthetic) cannabinoids in pigs after pulmonary administration be upscaled to humans by allometric techniques? Biochem. Pharmacol. 155, 403–418.
Schaefer, N., Kroll, A.K., Korbel, C., Laschke, M.W., Menger, M.D., Maurer, H.H., Meyer, M.R., Schmidt, P.H., 2019. Distribution of the (synthetic) cannabinoids JWH-210, RCS-4, as well as 9-tetrahydrocannabinol following pulmonary administration to pigs. Arch. Toxicol. 93 (8), 2211–2218.
Sharma, V., McNeill, J.H., 2009. To scale or not to scale: the principles of dose extrapolation. Br. J. Pharmacol. 157 (6), 907–921.
Smith, C.R., Truver, M.T., Swortwood, M.J., 2019. Quantification of U-47700 and its metabolites in plasma by LC-MS/MS. J. Chromatogr. B Analyt. Technol. Biomed. Life Sci. 1112, 41–47.
Swindle, M.M., Makin, A., Herron, A.J., Clubb Jr., F.J., Frazier, K.S., 2012. Swine as models in biomedical research and toxicology testing. Vet. Pathol. 49 (2), 344–356.
Turpeinen, M., Ghiciuc, C., Opritoui, M., Tursas, L., Pelkonen, O., Pasanen, M., 2007. Predictive value of animal models for human cytochrome P450 (CYP)-mediated metabolism: a comparative study in vitro. Xenobiotica 37 (12), 1367–1377.
Vogliardi, S., Stocchero, G., Maietti, S., Tucci, M., Nalesso, A., Snenghi, R., Favretto, D., 2018. Non-fatal overdose with U-47700: identification in biological matrices. Curr. Pharm. Biotechnol. 19 (2), 180–187.
Wagmann, L., Meyer, M.R., Maurer, H.H., 2016. What is the contribution of human FMO3 in the N-oxygenation of selected therapeutic drugs and drugs of abuse? Toxicol. Lett. 258, 55–70.
Welter, J., Meyer, M.R., Wolf, E.U., Weinmann, W., Kavanagh, P., Maurer, H.H., 2013. 2-methiopropamine, a thiophene analogue of methamphetamine: studies on its metabolism and detectability in the rat and human using GC-MS and LC-(HR)-MS techniques. Anal. Bioanal. Chem. 405 (10), 3125–3135.
Wissenbach, D.K., Meyer, M.R., Remane, D., Weber, A.A., Maurer, H.H., 2011. Development of the first metabolite-based LC-MS(n) urine drug screening procedure-exemplified for antidepressants. Anal. Bioanal. Chem. 400 (1), 79–88.
Yamazaki, M., Shimizu, M., Uno, Y., Yamazaki, H., 2014. Drug oxygenation activities mediated by liver microsomal flavin-containing monooxygenases 1 and 3 in humans, monkeys, rats, and minipigs. Biochem. Pharmacol. 90 (2), 159–165.
Zhang, D., Luo, G., Ding, X., Lu, C., 2012. Preclinical experimental models of drug metabolism and disposition in drug discovery and development. Acta Pharm. Sin. B 2 (6), 549–561.

3.3 Toxicokinetics of U-47700, tramadol and their main metabolites in pigs following intravenous administration – Is a multiple species allometric scaling approach useful for the extrapolation of toxicokinetic parameters to humans?

(Submitted 07/2021, DOI not yet provided)

Authors Contributions Frederike Nordmeier conducted and evaluated the experiment as well as composed the manuscript; Adrian Doerr, and Nadja Walle assisted at the execution of the animal experiments; Iryna Sihinevich and Thorsten Lehr assisted with the calculation and modulation of the pharmacokinetic data; Matthias W. Laschke and Michael D. Menger carried out and enabled the animal experiments and assisted with scientific discussions; Nadine Schaefer, Markus R. Meyer, and Peter H. Schmidt assisted with scientific discussions and the development of the experiments as well as supervised the research.

Archives of Toxicology

Toxicokinetics of U-47700, tramadol, and their main metabolites in pigs following intravenous administration – Is a multiple species allometric scaling approach useful for the extrapolation of toxicokinetic parameters to humans?

--Manuscript Draft--

Manuscript Number:	
Full Title:	Toxicokinetics of U-47700, tramadol, and their main metabolites in pigs following intravenous administration – Is a multiple species allometric scaling approach useful for the extrapolation of toxicokinetic parameters to humans?
Article Type:	Original Article
Corresponding Author:	Nadine Schaefer Institute of Legal Medicine, Saarland University GERMANY
Corresponding Author Secondary Information:	
Corresponding Author's Institution:	Institute of Legal Medicine, Saarland University
Corresponding Author's Secondary Institution:	
First Author:	Frederike Nordmeier
First Author Secondary Information:	
Order of Authors:	Frederike Nordmeier
	Iryna Sihinevich
	Adrian A. Dörr
	Nadja Walle
	Matthias W. Laschke, Prof. Dr.
	Thorsten Lehr, Prof. Dr.
	Michael D. Menger, Prof. Dr.
	Peter H. Schmidt, Prof. Dr.
	Markus R. Meyer, Prof. Dr.
	Nadine Schaefer
Order of Authors Secondary Information:	
Funding Information:	
Abstract:	New synthetic opioids (NSOs) pose a public health concern since their emergence on the illicit drug market and are gaining increasing importance in forensic toxicology. Like many other new psychoactive substances, NSOs are consumed without any preclinical safety data or any knowledge on toxicokinetic (TK) data. Due to ethical reasons, controlled human TK studies cannot be performed for the assessment of these relevant data. As an alternative animal experimental approach, six pigs per drug received a single intravenous dose of 100 µg/kg body weight (BW) of U-47700 or 1000 µg/kg BW of tramadol to evaluate, whether this species is suitable to assess the TK of NSOs. The drugs were determined in serum and whole blood using a fully validated method based on solid-phase extraction and LC-MS/MS. The concentration-time profiles and a population (pop) TK analysis revealed that a three-compartment model best described the TK data of both opioids. Central volumes of distribution were 0.94 L/kg for U-47700 and 1.25 L/kg for tramadol and central (metabolic) clearances were estimated at 1.57 L/h/kg and 1.85 L/h/kg for U-47700 and tramadol, respectively. The final popTK model parameters for pigs were upscaled via allometric scaling techniques. In comparison to published human data, concentration-time profiles for

	tramadol could successfully be predicted with single species allometric scaling. Furthermore, possible profiles for U-47700 in human were simulated. The findings of this study indicate that unlike a multiple species scaling approach, pigs in conjunction with TK modeling are a suitable tool for the assessment of TK data of NSOs and the prediction of human TK data.
Suggested Reviewers:	Kraemer Michael, Dr. Institute of Legal Medicine, Bonn michael.kraemer@uni-bonn.de Expertise in forensic toxicology and toxicokinetics

Toxicokinetics of U-47700, tramadol, and their main metabolites in pigs following intravenous administration – Is a multiple species allometric scaling approach useful for the extrapolation of toxicokinetic parameters to humans?

Frederike Nordmeier[a], Iryna Sihinevich[b], Adrian A. Doerr[a], Nadja Walle[a], Matthias W. Laschke[c], Thorsten Lehr[b], Michael D. Menger[c], Peter H. Schmidt[a], Markus R. Meyer[d], and Nadine Schaefer[a*]

[a]Institute of Legal Medicine, Saarland University, 66421 Homburg, Germany

[b]Clinical Pharmacy, Saarland University, 66123 Saarbruecken, Germany

[c]Institute for Clinical and Experimental Surgery, Saarland University, 66421 Homburg, Germany

[d]Department of Experimental and Clinical Toxicology, Institute of Experimental and Clinical Pharmacology and Toxicology, Center for Molecular Signaling (PZMS), Saarland University, 66421 Homburg, Germany

---

*Corresponding author: phone: +49 6841 16 26336; fax: +49 6841 16 26314

E-Mail address: nadine.schaefer@uks.eu (N. Schaefer)

Abstract

New synthetic opioids (NSOs) pose a public health concern since their emergence on the illicit drug market and are gaining increasing importance in forensic toxicology. Like many other new psychoactive substances, NSOs are consumed without any preclinical safety data or any knowledge on toxicokinetic (TK) data. Due to ethical reasons, controlled human TK studies cannot be performed for the assessment of these relevant data. As an alternative animal experimental approach, six pigs per drug received a single intravenous dose of 100 µg/kg body weight (BW) of U-47700 or 1000 µg/kg BW of tramadol to evaluate, whether this species is suitable to assess the TK of NSOs. The drugs were determined in serum and whole blood using a fully validated method based on solid-phase extraction and LC-MS/MS. The concentration-time profiles and a population (pop) TK analysis revealed that a three-compartment model best described the TK data of both opioids. Central volumes of distribution were 0.94 L/kg for U-47700 and 1.25 L/kg for tramadol and central (metabolic) clearances were estimated at 1.57 L/h/kg and 1.85 L/h/kg for U-47700 and tramadol, respectively. The final popTK model parameters for pigs were upscaled via allometric scaling techniques. In comparison to published human data, concentration-time profiles for tramadol could successfully be predicted with single species allometric scaling. Furthermore, possible profiles for U-47700 in human were simulated. The findings of this study indicate that unlike a multiple species scaling approach, pigs in conjunction with TK modeling are a suitable tool for the assessment of TK data of NSOs and the prediction of human TK data.

Keywords: New Synthetic Opioids, U-47700, Pigs, Population Toxicokinetic Modeling, Toxicokinetics, LC-MS/MS

Introduction

A large and increasing number of new psychoactive substances (NPS) with similar effects as compared to classical drugs of abuse have been released in Europe for about a decade. The most frequently consumed substance classes are synthetic cannabinoids and cathinones, whereas new synthetic opioids (NSOs) remained absent from the illicit drug market for a relatively long time but have increasingly appeared over the last years (EMCDDA 2019).

For a few years now, one of the most popular NSO U-47700 has emerged on the drugs of abuse market (World Health Organization 2016). It was initially sold via the internet as a legal alternative to common opioid drugs, such as heroin or morphine (Mohr et al. 2016; Rohrig et al. 2017). Being cheaper than heroin and having a more potent receptor binding strength to the μ-opioid receptor than morphine, U-47700 has continuously been consumed, although it was scheduled in many European countries and the USA (Koch et al. 2018, Lehmann et al. 2018).

The much higher binding affinities of NSOs result in strong psychoactive and unpredictable toxic effects, even if small doses are consumed. Numerous cases of intoxications have been reported with life-threatening conditions expressed by the classical triad of opioid intoxications, that is to say, respiratory depression, sedation, and miosis (Coopman et al. 2016; Alzghari et al. 2017; Fleming et al. 2017; Rambaran et al. 2017).

The structure of U-47700 is most likely related to tramadol. Unlike tramadol, whose toxicokinetic (TK) properties have extensively been elucidated using different animal models or controlled human studies with different routes of administration (Murthy et al. 2000; Vullo et al. 2014; Evangelista Vaz et al. 2018), preclinical safety data of U-47700 are still lacking except for data from multiple metabolism studies and one animal study in rats (Solimini et al. 2018; Truver et al. 2020). Yet, TK data are important for the interpretation of analytical data, e.g. with respect to time of intake or concentration in real samples. Due to ethical reasons,

these data must usually not be elucidated in controlled human studies. Thus, standardized and controlled animal studies remain the only tool for the assessment of TK properties.

TK studies often include repetitive sampling of body fluids or tissues to establish complete concentration-time profiles and, thus, demand large animals like pigs with sufficient blood volume for multiple blood sampling. Furthermore, the anatomical structure and physiological properties (e.g. cardiovascular, urogenital, digestive system) of pigs correlate with those of humans (Puccinelli et al. 2011). Finally, pigs display a comparable cytochrome P450 (CYP) monooxygenase pattern resulting in a similar metabolism (Anzenbacher et al. 1998), as shown for U-47700 in a previous study (Nordmeier et al. 2020a). In addition, pigs have already been proven to be suitable for TK studies of different synthetic cannabinoids and Δ^9-tetrahydrocannabinol (Schaefer et al. 2015, 2016, 2017, 2018, 2020).

Therefore, the aims of the present study were to i) elucidate TK data of U-47700, ii) examine whether domestic pigs can be used for the prediction of human TK of this substance and tramadol and iii) evaluate a multiple species allometric scaling approach. For this study, a novel liquid chromatography-tandem mass spectrometry (LC-MS/MS) method was developed and fully validated for pig serum and whole blood. The concentration-time profile of U-47700 after intravenous (i.v.) administration to pigs should be set up and compared to that of tramadol. Thereafter, the concentration-time profiles should be modeled to assess whether this model can predict already published tramadol data in humans.

Materials and methods

Chemicals and reagents

Chemicals and reagents used in this study are given in the Electronic Supplementary Material (ESM, S1).

Experimental preparation

The preparation of the used buffer and drug-free pig blood samples as well as the preparation of stock solutions, calibration standards, and quality control samples was performed according to a previously published study (Nordmeier et al. 2021). The preparations are described in detail in the ESM (S1).

Sample preparation

According to a previous study (Nordmeier et al. 2021), solid-phase extraction (SPE) was performed with Bond Elut HCX cartridges (130 mg/3 mL; Agilent, Waldbronn, Germany). Condition of the columns was carried out by two washing steps with 3 mL methanol and one with 3 mL phosphate buffer (0.1 M, pH 6). For the validation experiments, 1 mL serum or whole blood was added to a mixture of 50 µL of an ethanolic stable-isotope-labeled internal standard mixture solution (SIL-IS; 10 ng/50 µL of *N*-desmethyl-U-47700-d_3, tramadol-C_{13}-d_3, and *O*-desmethyltramadol (ODT)-d_6), 50 µL spiking solution, and 2 mL phosphate buffer for validation experiments. For authentic samples, the spiking solution was replaced by ethanol. After vortexing, the samples were centrifuged at 3200 g for 8 min and loaded onto the cartridges. Subsequently, two washing steps with 2 mL phosphate buffer and 2.75 mL hydrochloric acid (0.01 M) were carried out. The columns were carefully dried with swabs and then exposed for 10 min to maximum vacuum (10 inHg). Then, they were dried another time for 3 min under maximum vacuum following the treatment with 2 mL of methanol. Analyte elution was achieved using 1.75 mL dichloromethane-methanol-ammonia solution (25%) (30:15:1.25, v/v). Subsequently, the eluates were evaporated under a gentle stream of nitrogen (N_2) at 60 °C. The dry residues were reconstituted in 100 µL of mobile phase A (50 mM ammonium formate, pH 3.5) and shaken for 15 min. Twenty µL were injected onto the LC-MS/MS system.

LC-MS/MS conditions

As already described in a previous study (Nordmeier et al. 2021), an AB SCIEX (Darmstadt, Germany) API 3200 QTrap-MS/MS was coupled to a Shimadzu Prominance HPLC equipped with two solvent delivery units (LC-20AD), a communication bus module (CBM-20A), an autosampler (SIL-20AC), a degasser (DGU-20), and a column oven (CTO-10AC) for the analyzation of serum and whole blood samples. Positive ionization was reached using electrospray ionization (ESI).

Chromatographic separation was performed with a Waters (Wexford, Ireland) Sunfire C_{18} (150 x 2.1 mm, 3.5 µm) analytical column and gradient elution using mobile phase A and B (0.1% formic acid in acetonitrile). The total runtime was about 16 min. The gradient was as follows: starting with 25% eluent B, min 1.5 to 10 ramping to 36% eluent B, min 10 to 11 ramping to 95% eluent B, holding 95% eluent B for 1 min, min 12 to 12.5 reducing to 25% eluent B, min 12.5 to 16 holding 25% eluent B. The flow rate was adjusted at 0.3 mL/min, the injection volume at 20 µL, and the oven temperature at 30 °C.

In positive ESI mode, multiple-reaction monitoring (MRM) was used with a dwell time of 100 ms. Detection of the compounds was applied with three transitions per precursor ion for U-47700 and *N*-desmethyl-U-47700, and two for tramadol and ODT, respectively. Method parameters are provided in the ESM (Table S1). The source and gas parameters were set as follows: curtain gas (N_2) – 35 psi, collision gas (N_2) – medium, temperature – 500 °C, ion source gas 1 (N_2) – 50 psi, ion source gas 2 (N_2) – 80 psi, ion spray voltage – 5500 V. Data acquisition was performed with Analyst software Version 1.6.

Method validation

Validation was carried out according to the guidelines of the Society of Toxicological and Forensic Chemistry (GTFCh) and international guidelines (Peters et al. 2007, 2009).

A full validation was performed for pig serum and whole blood, including selectivity, recovery (RE), matrix effects (ME), process efficiency (PE), determination of limits of

detection (LODs), linearity, and lower limits of quantification (LLOQs), intra- and interday accuracy and precision tests, processed sample stability, freeze and thaw stability, and carry-over effects. RE, ME, and PE were estimated according to Matuszewski et al. (2003). A detailed description is given in the ESM (S1).

Animals

As already described in previous studies (Schaefer et al. 2016, 2017, 2018; Nordmeier et al. 2020a, 2021), the experiments were carried out according to the German legislation on protection of animals and the National Institute of Health Guide for the Care and Use of Laboratory Animals (Permission no: 32/2018). For this TK study, 12 domestic male pigs (Swabian Hall strain, mean body weight (BW) 42.8 ± 1.9 kg) were used. The pigs had free access to water and daily standard chow. A night prior to the experiment the animals were kept fasting, but still received water ad libitum.

Surgical procedure

The surgical procedure was performed according to previous studies (Schaefer et al. 2016, 2017, 2018; Nordmeier et al. 2020a, 2021) and is provided in detail in the ESM (S1). In brief, anesthesia of the animals was done with ketamine/xylanzine and maintained with isoflurane under the supply of oxygen. Blood sample collection occurred via a triple-lumen central venous catheter in the jugular vein.

Study design

As already described (Nordmeier 2020a,b, 2021), the TK study included two different groups. Six pigs received a 100 µg/kg BW dose of U-47700 and six other pigs a 1000 µg/kg BW dose of tramadol. For i.v. drug administration, a stock solution of 4 mg/mL U-47700 was prepared by dissolving the solid compound in ethanol. To reach a 100 µg/kg BW dose, appropriate

volumes of 1005-1120 µL were used and filled up with 0.9% sodium chloride to obtain a final volume of 10 mL.

As for tramadol, volumes of 906-1134 µL of a purchased tramadol-HCl solution were administered to obtain a 1000 µg/kg BW dose. Prior to administration, those volumes were filled up with 0.9% sodium chloride as well. Administration of the prepared solutions occurred into the jugular vein within 30 s. Blood sampling (about 10 mL each) was carried out before and 1, 2, 5, 10, 15, 30, 45, 60, 90, 120, 180, 240, 300, 360, 420, and 480 min after the administration via the central venous catheter. To obtain serum, an aliquot of each sample (7 mL) was centrifuged at 1250 g for 15 min. All samples were stored at - 20 °C until analysis.

Calculation of half-lives

The calculation of half-lives ($t_{1/2}$) was performed for serum and whole blood data using the non-compartmental method (first-order elimination kinetics). The mean of the measured concentrations was plotted on a semi-logarithmic scale lg c(A) against the time after dose t. For linear regression, the curve was split into three parts (α-, β-, γ-phase) enabling the best coverage of the data points. Linear regression was performed for each part and each part was described by Eq. 1

$$\lg c(\mathrm{A}) = \lg c_0\,(\mathrm{A}) - k/2{,}303 \times t \qquad (1)$$

with k as elimination rate constant and c_0 (A) as initially concentration of A.

Based on that, k was calculated via the slope of the regression curves and $t_{1/2}$ as shown in Eq. 2:

$$t_{1/2} = \ln(2) / k \qquad (2)$$

The calculation was performed using Microsoft Office Excel 2003 (Redmond, WA, USA).

Population (pop) TK model development for U-47700 and tramadol

PopTK modeling and simulations as well as model evaluations were performed for serum data of the parent compounds using non-linear mixed-effects modeling techniques implemented in NONMEM® (version 7.4.3, ICON Development Solutions, Ellicott City, MD, USA) (Beal et al. 2009). These techniques allow to estimate the typical values of the model parameters for a population and to quantify inter-individual variability (IIV) and residual (unexplained) variability. The first-order conditional estimation with interaction (FOCE-I) method was used in NONMEM®. IIV was modeled using exponential random effects models. Model selection was based on several criteria, including differences in objective function values (dOFV), visual inspection of goodness-of-fit (GOF) plots, and precision of parameter estimates provided by NONMEM®. One nested model was considered superior to another when the OFV was reduced by 3.84 points (chi-square value, $p < 0.05$, one degree of freedom). For internal model evaluation, a visual predictive check (VPC) was performed based on 1000 simulations using fixed- and random-effects parameters of the final TK models. Median and 90% confidence interval (CI) simulated serum concentrations were calculated, plotted against time, and overlaid with the observed data. Statistical analyses and data visualization were performed in R version 3.6.1 and higher (The R Foundation for Statistical Computing) (R.C. Team 2018) using Rstudio version 1.2.1335 (RStudio, Inc.) and ggplot2 R package (Wickham 2009). PopTK analyses in NONMEM® were performed using Pirana™ version 2.9.5 as a modeling environment.

Prediction of human tramadol and U-47700 exposure

To predict human exposure, different allometric scaling techniques using single (pig) and multiple species, selected to cover a wide range of BWs (mouse, rat, rhesus macaque, dog, pig, llama, and horse), were evaluated (Huh et al. 2011). Tramadol TK profiles for species other than a pig (Cox et al. 2011; Knych et al. 2013; Kelly et al. 2015; Jamali et al. 2017;

Evangelista Vaz et al. 2018) as well as human i.v. pharmacokinetic (PK) studies (Campanero et al. 1999; Quetglas et al. 2007; Yılmaz and Erdem 2015; United States Patent 2018) used for the evaluation of human exposure predictions were obtained during the literature search, digitized, and are listed in Table S5. An appropriate scaling technique for human predictions was selected based on several statistical and graphical criteria (dOFV, GOF plots, and VPCs as in 2.11). The reported dosing regimens, as well as the subjects' BW were included in the simulation scenarios. If no BW was stated, the population mean BW was used. For human profiles, which had no BW values stated at all, a mean BW of 70 kg was assumed.

For the multiple species allometric scaling approach, simple allometry with a power function correlating model parameters (such as clearance and volume of distribution) with BW ($P = aBW^b$) was used, where *P* is the parameter of interest, *a* is the coefficient and *b* is the allometry exponent, respectively (Huh et al. 2011). In an attempt to improve the overall performance of the simple allometric scaling, different correction factors, such as maximum life-span potential (MLP), brain weight (BRW), liver blood flow (LBF), bile flow, and liver weight (LW) on central clearance were tested, given that the relevant values were available in the literature for the selected species.

For the single allometric scaling approach, the final popTK model parameters for pigs were fixed and at first upscaled via allometric scaling techniques, which incorporated BW as an exponential covariate for all model parameters (Eq. 3) (Huh et al. 2011):

$$Parameter_{human} = Parameter_{pig} \times (BW_{human}/BW_{pig})^b \quad (3)$$

The allometry exponents (b) fixed at values between 0.6 and 1.6 were tested as the most commonly estimated values for small-molecule drugs used for interspecies scaling found in the literature (Huh et al. 2011). BW_{pig} was set to the mean value of 42.83 kg.

The incorporation of LBF into the model as a correction factor on central clearance helped further optimize the description of human data (Table S5) (Campanero et al. 1999; Quetglas et al. 2007; Yılmaz and Erdem 2015; United States Patent 2018). Hence, the human clearance was estimated, as shown in Eq. 4:

$$Clearance_{human} = Clearance_{pig} \times (BW_{human}/BW_{pig})^{b} \times (LBF_{human}/LBF_{pig}) \quad (4)$$

Single species scaling using LBF was proposed by Ward and Smith (2004). LBF [mL/min/kg] values per kg BW were used, as BW was already incorporated into the equation with the allometric exponent of 1.0. As there was no value for pig LBF in the original paper, the LBF values were set to 4.986 mL/min/kg for humans and 20.286 mL/min/kg for pigs respectively, as provided by Hall et al. (2012). To be used in Eq. 2, LBF_{human} and LBF_{pig} values were divided by the corresponding BW provided in the paper.

Finally, using the scaling method selected for tramadol prediction in humans, simulations of i.v. human dosing for U-47700 were performed in NONMEM®. For this purpose, the serum concentration-time profile for an individual with a BW of 70 kg given an i.v. bolus dose of 100 µg/kg was simulated 1000 times.

Results

Method validation

All validation parameters were in the acceptable range according to the guidelines of the GTFCh (Peters et al. 2009). Detailed results of the validation and a discussion are given in the ESM (S2 and S3).

Concentration-time profiles

After single i.v. administration, mean maximum concentrations (c_{max}) in serum of 103 ± 26 ng/mL U-47700 and 802 ± 329 ng/mL tramadol were reached immediately (t = 1 min)

(Fig. S1). The drug concentrations rapidly decreased within the first hour. After 60 min, mean concentrations of 17 ± 5 ng/mL U-47700 and 141 ± 34 ng/mL tramadol were found. Thereafter, the concentrations decreased slowly. At the end of the experiment, 8 h after administration, concentrations (c_{last}) of 0.8 ± 0.3 ng/mL U-47700 and 6.6 ± 2.3 ng/mL tramadol were still determined in serum samples.

C_{max} values measured in whole blood samples amounted to 86 ± 23 ng/mL U-47700 and 936 ± 295 ng/mL tramadol (Fig. S2). Showing a similar concentration decrease, c_{last} values of 0.4 ± 0.3 ng/mL for U-47700 and 4.6 ± 3.4 ng/mL for tramadol were reached after 8 h.

In Fig. 1 the mean drug concentration-time profiles of U-47700 and tramadol in serum after single i.v. administration are plotted on a semi-logarithmic scale. The plot for U-47700 as well as for tramadol indicated a triphasic decline. These phases consisted of a tissue distribution (α) phase, an elimination (β) phase, and a tissue release (γ) phase. Half-lives ($t_{1/2}$) for the α phase were 5.6 min for U-47700 and 6.8 min for tramadol. Calculated $t_{1/2}$ for the β phase were 37.6 min for U-47700 and 49.3 min for tramadol. For the γ phase, $t_{1/2}$ of 136.7 min for U-47700 and 115.7 min for tramadol could be determined. $T_{1/2}$ of U-47700 and tramadol calculated in whole blood were in the same range for all three phases. The mean drug concentration-time profiles in whole blood are shown in Fig. S3.

C_{max} of *N*-desmethyl-U-47700 was 6.8 ± 3.2 ng/mL (Fig. S1) in serum samples and 5.0 ± 2.2 ng/mL in whole blood samples (Fig. S2) and was reached after 60 min. Afterward, the concentration of this metabolite slowly decreased in a monophasic decline. Based on this, the calculated $t_{1/2}$ was 214 min in serum and 250 min in whole blood.

As for ODT a mean c_{max} of 32 ± 8 ng/mL could be determined 15 min after administration in serum samples (Fig. S1) and a c_{max} of 38 ± 10 ng/mL after 30 min in whole blood (Fig. S2). ODT concentrations decreased slowly afterward in a monophasic decline, as well. The calculated $t_{1/2}$ was 103 min in serum and 107 min in whole blood.

PopTK model development for U-47700 and tramadol

During the model development process, one-, two- and three-compartment models with linear and Michaelis-Menten elimination kinetics were tested. A three-compartment model with first order elimination processes described the data of both tramadol and U-47700 in serum the best. Model parameters in pig serum were precisely estimated with reasonable residual standard errors (RSEs) (Table 1). GOF plots (Fig. S4) and VPCs (Fig. 2) for both tramadol and U-47700 revealed no significant trend and were in good agreement with the observed data. Moderate IIV was identified on clearances (CL, Q2) and volumes of distribution ($V_{central}$, V2, and V3) parameters as shown in Table 1. The differential equations and parameter calculations are provided in the ESM (S4). Individual TK profiles (n = 6) for tramadol and U-47700 can also be found in the ESM (Fig. S5).

Prediction of human tramadol and U-47700 exposure

The human tramadol exposure was predicted using the final popTK pig model and different scaling techniques, described above. Multispecies allometric scaling failed to adequately predict human data, as it became clear that the interspecies variability in metabolic clearance is too large and this parameter cannot be scaled appropriately using only BW as an exponential covariate (Fig. S6). Adding the further correction factors on CL failed to sufficiently improve the situation. Using simple single species (pig, BW only) allometric scaling resulted in the substantial underprediction of the human tramadol profiles. Thus, the human tramadol exposure was best predicted using the final popTK model parameters for pigs upscaled via allometric scaling technique, which incorporated BW as an exponential covariate for all model parameters and LBF as a correction factor on metabolic clearance. The allometry exponent of 1.0 on each TK parameter described the data best and was therefore incorporated. For all five human studies (Table S5) (Campanero et al. 1999; Quetglas et al. 2007; Yılmaz and Erdem 2015; United States Patent 2018), the concentration-time profiles

were predicted adequately (Fig. 3). Observed data points were mostly within the 90% prediction interval for profiles 2 and 3, slightly underpredicted for profiles 4 and 5, and slightly overpredicted for profile 1.

The scaling technique that was considered best for tramadol was adopted for U-47700 and simulation of an i.v. bolus dose of 100 µg/kg of U-47700 for a human with BW of 70 kg was performed as shown in Fig. 4. No human profiles for U-47700 were available from the literature and therefore these predictions could not be verified with observed data.

Discussion

Dosage

All animals received an i.v. dose of 100 µg/kg BW U-47700 or 1000 µg/kg BW tramadol, respectively. Hence, total doses of 4.2 ± 0.1 mg of U-47700 and 42.8 ± 2.1 mg of tramadol were reached. As already described in a previous study (Nordmeier et al. 2021), the tramadol dose was similar to common human therapeutic i.v. dosages (Gelbe Liste 2020). A common (low) users' dosage of U-47700 for the i.v. administration is about 3-5 mg (Neuepsychoaktivesubstanzen 2017). In this context, a similar net dose was chosen for this TK study. Thereby, it was assured that the animals remained under the influence of measurable concentrations. On the other hand, they should not be exposed to great toxic effects.

Concentration-time profiles

U-47700 and *N*-desmethyl-U-47700

Regarding U-47700, TK data are sparsely available. Yet, only one controlled animal study (Truver et al. 2020) was performed and one case report provides human TK data of this substance in serum (Koch et al. 2018).

Our results are in good agreement with those of Truver et al. (2020). The authors administered U-47700 (0.3, 1.0 or 3.0 mg/kg BW, n = 6 each) subcutaneously to male Sprague-Dawley rats. Sampling occurred from 15 until 480 min post-injection. C_{max} levels rose linearly from 40, 110 to 173 ng/mL for the different doses. Thus, they were in the same range as our c_{max} values considering the given doses. The calculated $t_{1/2}$ were comparable as well.

Koch et al. (2018) reported the case of a 24-year-old man who suffered apnea after consumption of U-47700 in combination with the benzodiazepine flubromazepam. During hospitalization, a serum concentration of 370 ng/mL was detected 42 min after the admission to the hospital. In comparison, in our study, a maximum serum concentration of 103 ± 26 ng/mL was reached immediately after administration. This discrepancy could be a hint at a much higher dosage in the authentic case. Koch et al. (2018) estimated two elimination phases by visual inspection of the semi-logarithmic concentration-time profile of U-47700. Yet, we estimated a 3-phasic decline. Koch et al. (2018) calculated a $t_{1/2}$ of approximately 6 h for the first phase, which is comparable to that of morphine. $T_{1/2}$ calculated in the present study were in the range of minutes for the distribution phase and up to one-half hour for the elimination phase. $T_{1/2}$ of the tissue release phase was about 2.3 h and therefore differs from the values calculated by Koch et al. (2018). These high deviations may be explained by the fact that Koch et al. (2018) obtained the first serum samples 42 min after admission to the hospital. Especially, the unknown period of time between consumption and the first sampling could have a great impact on the estimated TK data. In particular, Koch et al. (2018) did not consider the first decline of U-47700. The following sampling extended up to 81 h post-admission. Hence, also late phase TK data of U-47700 were included, whereas in our study the sampling time was only up to 8 h. The TK parameter c_{max} is dose-dependent and concerning linear TK, assessed in the present study as well as by Koch et al. (2018), it is proportional to the dosage. However, in terms of linear TK, dose and concentration

dependences do not apply to $t_{1/2}$. Another issue that has to be considered in this context is that the route of administration in that case report was unknown, which could have a great impact on the TK.

TK parameters for the main metabolite *N*-desmethyl-U-47700 are only sparsely available in the literature, as well. In our study, the level of metabolite showed a medium increase with a c_{max} 60 min after drug administration. Subsequently, the concentration slowly decreased, which led to slightly higher metabolite concentrations and a higher $t_{1/2}$ in comparison to U-47700 at the end of the experiment. This behavior indicates a high metabolism rate of U-47700 to *N*-desmethyl-U-47700, but a slow distribution/elimination of the metabolite. In the study of Truver et al. (2020), a slower kinetic for *N*-desmethyl-47700 was observed, as well. However, a longer $t_{1/2}$ of *N*-desmethyl-U-47700 compared to U-47700 makes this metabolite interesting as a target for routine blood analysis, especially if a long time period between consumption and analysis has to be considered.

Tramadol and ODT

The concentration-time profile of tramadol observed in this study is in good agreement with that found by Bortolami et al. (2015), administering tramadol i.v. to sheep. They observed higher maximum serum concentrations in comparison with our values, but this difference may have resulted from higher dosages. In agreement with our data, tramadol serum concentrations decreased rapidly, but in contrast to our study, tramadol could not anymore be detected in every treated sheep 6 h following administration. The concentration-time-profile for ODT was comparable as well.

Moreover, our estimated TK parameters were partly in the same range as those determined after single controlled intramuscular (i.m.) administration of tramadol to piglets (Vullo et al. 2014). Higher dosage and a different route of administration may explain some deviations mainly concerning c_{max}. Considering the dose administered, the relative c_{max}

determined in our study was much higher as compared to the values by Vullo et al. (2014). In both studies, high ODT levels were found over a short time period after administration. In comparison with other animals, such as dogs and goats, piglets and pigs formed higher levels of the active metabolite (Vullo et al. 2014). These differences might be due to variations in drug metabolism between different species (Martignoni et al. 2006). As ODT is an active metabolite with a higher affinity to the μ-opioid receptor, a faster metabolism in pigs and piglets has great toxicodynamic importance.

Generally, values for $t_{1/2}$ of tramadol appeared to be very species-related and, thus, indicate differences in metabolism and TK in different species as well. The $t_{1/2,\gamma}$ of tramadol observed in this study (1.9 h) was a little bit higher than terminal $t_{1/2}$ reported for piglets (1.34 h) (Vullo et al. 2014), horses (1.5 h) (Shilo et al. 2008), and dogs (0.73 h) (Giorgi et al. 2010) but lower than that reported in llama (2.54 h) (Cox et al. 2011). Regarding the human terminal $t_{1/2}$ of tramadol published in the literature (Murthy et al. 2000; Grond and Sablotzki 2004; World Health Organization 2014), values between 5 and 6 h were mostly determined. In the present study, a quite shorter terminal $t_{1/2}$ of about 2 h was estimated. Of course, a faster metabolization and elimination of tramadol may have a big influence on this parameter. Another explanation for this possible underestimation is the much shorter sampling period of 8 h in our study as compared to other studies covering a sampling period up to 48-72 h (Meyer et al. 2015; Skinner-Robertson et al. 2015; DeLemos et al. 2017). Thus, the $t_{1/2}$ of this study only reflects the elimination within the first 8 h following administration, and the real terminal $t_{1/2}$ could only be estimated in a long-term elimination study.

Regarding human studies, the concentration-time profile of our study was in good agreement with that of Murthy et al. (2000), administering a 2 mg/kg i.v. dose to children. However, in our study, a faster increase in the metabolite concentration was observed. Maximum concentrations were reached after 15 min, whereas Murthy et al. (2000) observed maximum concentrations 4.9 h following the administration. A slower metabolism in humans

than in animals has already been reported in the literature (Grond and Sablotzki 2004) and our results indicate a faster metabolization in pigs as well. In our study, estimated TK parameters as V and CL also differ from those calculated in those human studies (Murthy et al. 2000). As already shown in other animal studies, CL values of pigs were higher than those obtained for humans after i.v. administration, supporting the assumption of a faster metabolism of tramadol in pigs compared to human (Grond and Sablotzki 2004; Vullo et al. 2014). On the other hand, in humans, a higher V (~3L/kg) was observed as compared to our study (V = ~1.25 L/kg) indicating a higher distribution in deep compartments (Murthy et al. 2000).

Comparing c_{max} values of tramadol after i.v. administration reported in the literature with our results substantially lower substance plasma concentrations of about 400 ng/mL were determined in studies using comparable dosages (100 mg/~70 kg for humans vs. 1 mg/kg in our study) (Lintz et al. 1986, 1998a,b). However, differences in analytics in serum and plasma need to be taken into consideration comparing serum and plasma concentrations. Plasma could be contaminated with cells, lysed cells could release their content into plasma or cells could be still metabolically active in plasma (Bowen et al. 2010). These processes might have an influence on the compound concentration determined in plasma and could result in higher concentrations if substances have a prevalence for binding to blood cells or it could affect the ratio of the concentrations of the parent compound to metabolite. Furthermore, in humans a higher V (~3L/kg) (World Health Organization 2014) was determined as compared to pigs (~1.25 L/kg). A higher tissue affinity and distribution into deep compartments result in lower blood concentrations of tramadol and therefore could be an explanation for this phenomenon.

General findings and TK parameters of U-47700 and tramadol

The choice of the matrix (plasma, serum, or whole blood) is an important aspect of the drug quantification for the TK/PK studies. Currently, the majority of the PK studies are using plasma (or serum) as a matrix of choice rather than whole blood. Concerning drugs with high

binding to erythrocytes, this difference can influence some TK parameters (e.g. increased volume of distribution), as less drug is left in the plasma compared to the whole blood (Dash et al. 2020). For this reason, in the current study both serum and whole blood were used as matrices. In general, the concentration-time profiles of U-47700 and its metabolite in serum and whole blood illustrated that the determined concentrations in serum samples were higher than those in whole blood samples, leading to the suggestion that U-47700 and its metabolite might not accumulate in red blood cells. In contrast, tramadol and ODT generally displayed lower concentrations in serum than in whole blood, indicating the binding of those substances to red blood cells. Some literature data are available signifying the formation of tramadol complexes with human hemoglobin (Tunç et al. 2013), but its relevance for the tramadol PK remains unclear.

In misuse and poisoning cases in clinical and forensic toxicology, serum samples are the matrix of choice for analytics, and serum TK data are of special interest. Since tramadol PK studies have almost exclusively used plasma as a matrix rather than whole blood, the popTK modeling and simulations were only performed for serum data of the parent compounds. Thus, the possibility of a slight difference between plasma and serum concentrations must be considered, when interpreting the modeling results.

TK parameters of U-47700 and tramadol determined in pig serum showed similar behavior. In both cases, the three-compartment model described the data best. Central CL was estimated to be 1.9 L/h/kg and 1.6 L/h/kg for tramadol and U-47700, respectively, indicating a moderate to fast elimination of both substances. The $V_{central}$ was estimated to be 1.3 L/kg for tramadol and 0.9 L/kg for U-47700. The determined V values of both substances indicate a slight distribution into deep compartments. The smaller $V_{central}$ values compared to the first peripheral V2 suggest a rapid distribution from the central compartment into highly perfused tissues, whereas the higher $V_{central}$ values compared to the second peripheral V3 suggest a slower distribution into deep compartments (scarcely perfused tissues). Thus, higher

concentrations of both substances in different tissues as compared to blood concentrations are possible regarding postmortem toxicological cases. Furthermore, an accumulation in adipose tissue has to be taken into consideration (Nordmeier et al. 2021).

In general, estimated TK parameters for tramadol tend to be very similar, but slightly higher than for U-47700.

Prediction of human tramadol exposure

To predict the human exposure of drugs from animal studies, the allometric scaling technique is commonly used. This method is an empirical approach that is based on the assumption of the similarities in the physiology across different species and correlates physiological parameters, such as CL and V with body size using a power function. The method is widely used in drug development (e.g. first in human studies) (Hunter 2010).

In the current analysis both multiple and single (pig) species allometry scalings were attempted. Multiple species allometry (Fig. S6) was challenging, as the interspecies variability in metabolic clearance between species, as well as in humans was very large despite adjusting for the differences in BW. This can be attributed to the interspecies differences in the expression of CYPs, which are the most important family of drug-metabolizing enzymes and the major cause of species differences in hepatic drug metabolism (Martignoni et al. 2006). Though additional correction factors (MLP, BRW, LBF, bile flow, and LW) were tested to address this issue, they either did not improve the prediction or were only available for some of the species. Due to these issues, we have proceeded with single (pig) species allometry (Fig. 3).

An empirical allometric exponent for the majority of the small-molecule drugs lay between 0.4 and 1.5, dependent on the elimination pathway (renal, hepatic, or mixed) and characteristic of the drug (Huh et al. 2011). Huh et al. (2011) reported no value for tramadol, but substances that have similar elimination and characteristics as tramadol (base,

hepatic/mixed elimination) had an exponent value around 0.7-0.8 (e.g., 0.805 for fentanyl, 0.775 for methadone). Huang et al. (2015) reported the allometric exponent b for tramadol to be around 1.14 (based on the linear regressions of the log‐log transformed clearance vs. BW data). For the current analysis, allometric exponents between 0.5 and 1.6 were tested, and b = 1.0 was found to fit the best (evaluated using dOFV, %RSE, and GOF plots). This value is close to the values found in the literature for tramadol and similar substances.

The simple allometric scaling generally works well for small-molecule drugs that are mainly renally eliminated. However, for hepatically eliminated drugs with a large between-species variability in hepatic metabolism, simple allometric scaling may not work very well in the extrapolation of hepatic metabolic CL from animals to humans. Thus, to improve the predictions, liver metabolism should be incorporated as well as BW (Huh et al. 2011). This seems to be the case for tramadol, as it is primarily eliminated through metabolism by the liver (by CYP2D6, CYP3A4, and CYP2B6 in humans). The incorporation of the LBF on CL significantly improved human predictions for tramadol. LBF was previously reported to be directly proportional to liver weight in the majority of the mammalian species. Accordingly, liver weight (and therefore hepatic blood flow) could be related to BW (Boxenbaum 1980). In human, LBF depends not only on liver and BW, but also changes with age and with disease progression in chronic liver disease, which make extrapolation of hepatic metabolic CL from animals to humans even more challenging (Woodhouse and Wynne 1988). Thus, the current analysis shows that even with the incorporation of both BW and LBF, not all profiles could have been described perfectly. The literature data used for human predictions provided further difficulties, as for 3 of 5 available profiles no BW data were reported, so it was assumed, that BW = 70 kg. This assumption, by all means, can affect the accuracy of the prediction, if the individual/mean BW varies greatly from the assumed 70 kg. A further limitation of the current analysis lies in the availability and inconsistency of the physiological parameters used as correction factors on CL for a pig. For example, there were multiple values of LBF for pigs

available in the literature: Boxenbaum et al. (1980) reported hepatic blood flow of 43.75 mL/min/kg, though the LBF_{pig} value of 20.286 mL/min/kg was provided by Hall et al. (2012). In the case of our analysis, the value that provided the best fit was used, nevertheless one should be aware of heterogeneity of the available animal data, as well as of a strain of the animal being used (e.g., different pig strains, minipig, or micropig). Nevertheless, despite some limitations, single species scaling from pig to human using LBF was shown to be able to predict human data reasonably well.

As there were a lot of similarities between tramadol and U-47700 popTK in pigs, we assumed that the same scaling method could be applied to simulate the potential concentration-time curve of U-47700 for humans. This approach applies that we also assume a faster metabolism of U-47700 in pigs compared to human, as shown in Fig. 4. The main limitation here was a lack of human TK data for U-47700 so far. Therefore, further research of human TK for U-47700 is needed to evaluate the human prediction using observed human data.

Conclusion

In the present study, serum and whole blood concentration-time profiles were successfully determined for U-47700, tramadol, and their main metabolites in pigs after i.v. administration using a fully validated LC-MS/MS method. A three-compartment popTK model with first-order elimination described the serum concentration-time profiles for U-47700 and tramadol the best. Parameter estimates for U-47700 and tramadol are very similar but slightly higher for tramadol than for U-47700. The $V_{central}$ indicates a slight distribution of both substances into deep compartments and central clearances a medium to fast elimination. A higher $t_{1/2}$ of *N*-desmethyl-U-47700 compared to its parent compound U-47700 makes this metabolite interesting as a target for analytical approaches in forensic and clinical toxicology. To draw a conclusion: whilst a multiple species scaling approach failed to adequately predict human

tramadol TK data, the successful prediction of human tramadol TK data based on this popTK pig model proposes that pigs in combination with a single species TK modeling technique provide a helpful tool for the prediction of human TK of NSOs. Hereby generated data might offer an enhancement in the interpretation of analytical results in clinical and forensic misuse or poisoning cases.

Acknowledgements The authors thank Benjamin Peters and the staff of the Institute for Clinical and Experimental Surgery at Saarland University for their support and help during the study. Furthermore, we acknowledge the EU funded project ADEBAR (IZ25-5793-2016-27).

Compliance with ethical standards

Conflicts of interest The authors declare that there are no financial or other relations that could lead to a conflict of interest.

Ethical Approval All experiments were performed in accordance with the German legislation on protection of animals and the National Institutes of Health Guide for the Care and Use of Laboratory Animals (permission number: 32/2018).

References

Alzghari SK, Fleming SW, Rambaran KA, et al (2017) U-47700: An emerging threat. Cureus 9(10):e1791. doi:https://doi.org/10.7759/cureus.1791

Anzenbacher P, Soucek P, Anzenbacherova E, et al (1998) Presence and activity of cytochrome P450 isoforms in minipig liver microsomes comparison with human liver samples. Drug Metab Dispos 26:56–59

Beal SL, Boeckmann A, Bauer RJ (2009) NONMEM user's guides. Icon Development Solutions, Ellicott City

Bortolami E, Della Rocca G, Di Salvo A, et al (2015) Pharmacokinetics and antinociceptive effects of tramadol and its metabolite O-desmethyltramadol following intravenous administration in sheep. Vet J 205(3):404-9. doi:https://doi.org/10.1016/j.tvjl.2015.04.011

Bowen RAR, Hortin GL, Csako G, et al (2010) Impact of blood collection devices on clinical chemistry assays. Clin Biochem 43:4–25. doi:https://doi.org/https://doi.org/10.1016/j.clinbiochem.2009.10.001

Boxenbaum H (1980) Interspecies variation in liver weight, hepatic blood flow, and antipyrine intrinsic clearance: Extrapolation of data to benzodiazepines and phenytoin. J Pharmacokinet Biopharm 8:165–176. doi:https://doi.org/10.1007/BF01065191

Campanero MA, Calahorra B, Valle M, et al (1999) Enantiomeric separation of tramadol and its active metabolite in human plasma by chiral high-performance liquid chromatography: Application to pharmacokinetic studies. Chirality 11:272–279. doi:https://doi.org/https://doi.org/10.1002/(SICI)1520-636X(1999)11:4<272::AID-CHIR3>3.0.CO;2-I

Coopman V, Blanckaert P, Van Parys G, Van Calenbergh S, Cordonnier J (2016) A case of acute intoxication due to combined use of fentanyl and 3,4-dichloro-N-[2-(dimethylamino)cyclohexyl]-N-methylbenzamide (U-47700). Forensic Sci Int 266:68–72. doi:https://doi.org/10.1016/J.FORSCIINT.2016.05.001

Cox S, Martín-Jiménez T, Amstel S, Doherty T (2011) Pharmacokinetics of intravenous and intramuscular tramadol in llamas. J Vet Pharmacol Ther 34:259–264. doi:https://doi.org/10.1111/j.1365-2885.2010.01219.x

Dash RP, Veeravalli V, Thomas JA, et al (2020) Whole blood or plasma: what is the ideal matrix for pharmacokinetic-driven drug candidate selection? Future Med Chem 13:157–171. doi:https://doi.org/10.4155/fmc-2020-0187

DeLemos B, Richards HM, Vandenbossche J, et al (2017) Safety, tolerability, and pharmacokinetics of therapeutic and supratherapeutic doses of tramadol hydrochloride in healthy adults: A randomized, double-blind, placebo-controlled multiple-ascending-dose study. Clin Pharmacol Drug Dev 6:592-603. doi:https://doi.org/10.1002/cpdd.378

EMCDDA: European Monitoring Center of Drugs and Drug Addiction (2019) European drug report – Trends and developments. http://www.emcdda.europa.eu/system/files/publications/11364/20191724_TDAT19001ENN_PDF.pdf. Accessed June 2021

Evangelista Vaz R, Draganov DI, Rapp C, et al (2018) Preliminary pharmacokinetics of tramadol hydrochloride after administration via different routes in male and female B6 mice. Vet Anaesth Analg 45:111–122. doi:https://doi.org/10.1016/j.vaa.2016.09.007

Fleming SW, Cooley JC, Johnson L, et al (2017) Analysis of U-47700, a novel synthetic opioid, in human urine by LC-MS-MS and LC-QToF. J Anal Toxicol 41(3):173-180. doi:https://doi.org/10.1093/jat/bkw131

Grond S, Sablotzki A (2004) Clinical pharmacology of tramadol. Clin Pharmacokinet 43:879–923. doi:https://doi.org/10.2165/00003088-200443130-00004

Hall C, Lueshen E, Mošat' A, Linninger AA (2012) Interspecies scaling in pharmacokinetics: A novel whole-body physiologically based modeling framework to discover drug biodistribution mechanisms in vivo. J Pharm Sci 101(3):1221–1241. doi:https://doi.org/10.1002/jps.22811

Huang Q, Gehring R, Tell LA, Li M, Riviere JE (2015) Interspecies allometric meta-analysis of the comparative pharmacokinetics of 85 drugs across veterinary and laboratory animal species. J Vet Pharmacol Ther 38(3):214–226. doi:https://doi.org/https://doi.org/10.1111/jvp.12174

Huh Y, Smith DE, Rose Feng M (2011) Interspecies scaling and prediction of human clearance: comparison of small- and macro-molecule drugs. Xenobiotica 41:972–987. doi:https://doi.org/10.3109/00498254.2011.598582

Hunter R (2010) Interspecies Allometric Scaling. Handb Exp Pharmacol 199:139–157. doi:https://doi.org/10.1007/978-3-642-10324-7_6

Jamali B, Sheikholeslami B, Hosseinzadeh Ardakani Y, et al (2017) Evaluation of the ecstasy influence on tramadol and its main metabolite plasma concentration in rats. Drug Metab Pers Ther 32:137–145. doi:https://doi.org/doi:10.1515/dmpt-2017-0018

Kelly KR, Pypendop BH, Christe KL (2015) Pharmacokinetics of tramadol following intravenous and oral administration in male rhesus macaques (Macaca mulatta). J Vet Pharmacol Ther 38:375–382. doi:https://doi.org/https://doi.org/10.1111/jvp.12194

Knych HK, Corado CR, Mckemie DS, Steffey EP (2013) Pharmacokinetics and selected pharmacodynamic effects of tramadol following intravenous administration to the horse. Equine Vet J 45:490–496. doi:https://doi.org/https://doi.org/10.1111/j.2042-3306.2012.00688.x

Koch K, Auwaerter V, Hermanns-Clausen M, Wilde M, Neumann MA (2018) Mixed intoxication by the synthetic opioid U-47700 and the benzodiazepine flubromazepam with lethal outcome: Pharmacokinetic data. Drug Test. Anal 10(8):1336-1341. doi:https://doi.org/10.1002/dta.2391

Gelbe Liste (2020). Pharmindex. https://www.gelbe-liste.de/wirkstoffe/Tramadol_1406. Accessed June 2021

Giorgi M, Del Carlo S, Łebkowska-Wieruszewska B, Kowalski CJ, Saccomanni G (2010) Pharmacokinetics of tramadol and metabolites after injective administrations in dogs. Pol J Vet Sci 13(4):639-44. doi:https://doi.org/10.2478/v10181-010-0027-y

Lehmann S, Teifel D, Rothschild MA, Andresen-Streichert H (2018) Tödliche Intoxikation mit dem Designer-Opioid U-47700. Tochichem Krimtech 85(1):36

Lintz W, Barth H, Becker R, et al (1998a) Pharmacokinetics of tramadol and bioavailability of enteral tramadol formulations. 2nd communication: drops with ethanol. Arzneimittelforschung 48:436–445

Lintz W, Barth H, Osterloh G (1998b) Pharmacokinetics of tramadol and bioavailability of enteral tramadol formulations. 43rd communication: suppositories. Arzneimittelforschung 48:889–899

Lintz W, Barth H, Osterloh G, Schmidt-Boethelt E (1986) Bioavailability of enteral tramadol formulations. 1st communication: capsules. Arzneimittelforschung 36:1278—1283

Martignoni M, Groothuis GMM, de Kanter R (2006) Species differences between mouse, rat, dog, monkey and human CYP-mediated drug metabolism, inhibition and induction. Expert Opin Drug Metab Toxicol 2:875–894. doi:https://doi.org/10.1517/17425255.2.6.875

Matuszewski BK, Constanzer ML, Chavez-Eng CM (2003) Strategies for the assessment of matrix effect in quantitative bioanalytical methods based on HPLC-MS/MS. Anal Chem 75(13):3019-30. doi:https://doi.org/10.1021/ac020361s

Meyer MR, Rosenborg S, Stenberg M, Beck O (2015) First report on the pharmacokinetics of tramadol and O-desmethyltramadol in exhaled breath compared to plasma and oral fluid after a single oral dose. Biochem Pharmacol 98:502–510. doi:https://doi.org/https://doi.org/10.1016/j.bcp.2015.09.008

Mohr ALA, Friscia M, Papsun D, Kacinko SL, Buzby D, Logan BK (2016) Analysis of novel synthetic opioids U-47700, U-50488 and furanyl fentanyl by LC-MS/MS in postmortem casework. J Anal Toxicol 40(9):709-717. doi:https://doi.org/10.1093/jat/bkw086

Murthy B, Pandya K, Booker P, Murray A, Lintz W, Terlinden R (2000) Pharmacokinetics of tramadol in children after IV or caudal epidural administration. Br J Anaesth 84:346–349. doi:https://doi.org/10.1093/oxfordjournals.bja.a013437

Neue Psychoaktive Substanzen (2017) http://neuepsychoaktivesubstanzen.de/u-47700/#U-47700_Dosis_Dosierung. Accessed June 2021

Nordmeier F, Doerr A, Laschke MW, et al (2020a) Are pigs a suitable animal model for in vivo metabolism studies of new psychoactive substances? A comparison study using different in vitro/in vivo tools and U-47700 as model drug. Toxicol Lett 329:12-19. doi:https://doi.org/https://doi.org/10.1016/j.toxlet.2020.04.001

Nordmeier F, Doerr A, Laschke MW, et.al (2020b) Erhebung toxikokinetischer Daten der synthetischen Opioide U-47700 und Tramadol sowie der Hauptmetabolite im Schwein nach intravenöser Verabreichung. 99. Jahrestagung der Deutschen Gesellschaft für Rechtsmedizin. Abstracts. Rechtsmedizin 30:361-412

Nordmeier F, Doerr AA, Potente S, et al (2021) Perimortem distribution of U-47700, tramadol and their main metabolites in pigs following intravenous administration. J Anal Toxicol (*in press*). doi:https://doi.org/10.1093/jat/bkab044

Peters FT, Drummer OH, Musshoff F (2007) Validation of new methods. Forensic Sci Int 165:216–224. doi:https://doi.org/10.1016/J.FORSCIINT.2006.05.021

Peters F, Paul L, Musshoff F, et al (2009) Anhang B zur Richtlinie der GTFCh zur Qualitätssicherung bei forensisch-toxikologischen Untersuchungen Anforderungen an die Validierung von Analysemethoden. Toxichem Krimtech. https://www.gtfch.org/cms/images/stories/files/GTFCh_Richtlinie_Anhang B_Validierung_Version 1.pdf. Accessed June 2021

Puccinelli E, Gervasi P, Longo V (2011) Xenobiotic metabolizing cytochrome P450 in pig, a promising animal model. Curr Drug Metab 12:507–525. doi:https://doi.org/10.2174/138920011795713698

Quetglas EG, Azanza JR, Cardenas E, et al (2007) Stereoselective pharmacokinetic analysis of tramadol and its main phase I metabolites in healthy subjects after intravenous and oral administration of racemic tramadol. Biopharm Drug Dispos 28:19–33. doi:https://doi.org/https://doi.org/10.1002/bdd.526

R.C. Team (2018) R: A language and environment for statistical computing. R foundation for Statistical computing. Vienna

Rambaran KA, Fleming SW, An J, et al (2017) U-47700: A clinical review of the literature. J Emerg Med 53:509–519. doi:https://doi.org/10.1016/J.JEMERMED.2017.05.034

Rohrig TP, Miller SA, Baird TR (2017) U-47700: A not so new opioid. J Anal Toxicol 42(1):e12-e14. doi:https://doi.org/10.1093/jat/bkx081

Schaefer N, Kettner M, Laschke MW, et al (2015) Simultaneous LC-MS/MS determination of JWH-210, RCS-4, Δ9-tetrahydrocannabinol, and their main metabolites in pig and human serum, whole blood, and urine for comparing pharmacokinetic data. Anal Bioanal Chem 407:3775–3786. doi:https://doi.org/10.1007/s00216-015-8605-6

Schaefer N, Kettner M, Laschke MW, et al (2017) Distribution of synthetic cannabinoids JWH-210, RCS-4 and Δ 9-tetrahydrocannabinol after intravenous administration to pigs. Curr Neuropharmacol 15:713–723. doi:https://doi.org/10.2174/1570159X15666161111114214

Schaefer N, Kroell A-K, Koerbel C, et al (2020) Time- and temperature-dependent postmortem concentration changes of the (synthetic) cannabinoids JWH-210, RCS-4, as well as Δ9-tetrahydrocannabinol following pulmonary administration to pigs. Arch Toxicol 94:1585-1599. doi:https://doi.org/10.1007/s00204-020-02707-4

Schaefer N, Wojtyniak J-G, Kettner M, et al (2016) Pharmacokinetics of (synthetic) cannabinoids in pigs and their relevance for clinical and forensic toxicology. Toxicol Lett 253:7–16. doi:https://doi.org/10.1016/J.TOXLET.2016.04.021

Schaefer N, Wojtyniak J-G, Kroell A-K, et al (2018) Can toxicokinetics of (synthetic) cannabinoids in pigs after pulmonary administration be upscaled to humans by allometric techniques? Biochem Pharmacol 155:403–418. doi:https://doi.org/10.1016/J.BCP.2018.07.029

Shilo Y, Britzi M, Eytan B, Lifschitz T, Soback S, Steinmann A (2008) Pharmacokinetics of tramadol in horses after intravenous, intramuscular and oral administration. J Vet Pharmacol Ther 31:60–65. doi:https://doi.org/10.1111/j.1365-2885.2007.00929.x

Skinner-Robertson S, Fradette C, Bouchard S, Mouksassi MS, Varin F (2015) Pharmacokinetics of tramadol and O-desmethyltramadol enantiomers following administration of extended-release tablets to elderly and young subjects. Drugs Aging 32:1029–1043. doi:https://doi.org/10.1007/s40266-015-0315-4

Solimini R, Pichini S, Pacifici R, Busardò FP, Giorgetti R (2018) Pharmacotoxicology of non-fentanyl derived new synthetic opioids. Front Pharmacol 9:654. doi:https://doi.org/10.3389/fphar.2018.00654

Truver MT, Smith CR, Garibay N, Kopajtic TA, Swortwood MJ, Baumann MH (2020) Pharmacodynamics and pharmacokinetics of the novel synthetic opioid, U-47700, in male rats. Neuropharmacology 177:108195. doi:https://doi.org/https://doi.org/10.1016/j.neuropharm.2020.108195

Tunç S, Çetinkaya A, Duman O (2013) Spectroscopic investigations of the interactions of tramadol hydrochloride and 5-azacytidine drugs with human serum albumin and human hemoglobin proteins. J Photochem Photobiol B Biol 120:59–65. doi:https://doi.org/https://doi.org/10.1016/j.jphotobiol.2013.01.011

United States Patent (2018). Intravenous administration of tramadol. US 10,022, 321 B2. Accessed June 2021.

Vullo C, Kim TW, Meligrana M, Marini C, Giorgi M (2014) Pharmacokinetics of tramadol and its major metabolite after intramuscular administration in piglets. J Vet Pharmacol Ther 37:603–606. doi:https://doi.org/10.1111/jvp.12133

Ward KW, Smith BR (2004) A comprehensive quantitative and qualitative evaluation of extrapolation of intravenous pharmacokinetic parameters from rat, dog, and monkey to humans. I. Clearance. Drug Metab Dispos 32:603-611. doi:https://doi.org/10.1124/dmd.32.6.603

Wickham H (2009) ggplot2: Elegant Graphics for Data Analysis. Springer-Verlag. New York

Woodhouse KW, Wynne HA (1988) Age-related changes in liver size and hepatic blood flow. Clin Pharmacokinet 15:287–294. doi:https://doi.org/10.2165/00003088-198815050-00002

World Health Organization (2014), Expert committee on drug dependence thirty‑sixth meeting. Tramado l update review report agenda item 6.1. https://www.who.int/medicines/areas/quality_safety/6_1_Update.pdf. Accessed June 2021

World Health Organization (2016) Expert committee on drug dependence thirty-eighth meeting. U-47700 critical review report agenda item 4.1. https://www.who.int/medicines/access/controlled-substances/4.1_U-47700_CritReview.pdf?ua=1. Accessed June 2021

Yılmaz B, Erdem AF (2015) Simultaneous determination of tramadol and its metabolite in human Plasma by GC/MS. J AOAC Int 98:56–61. doi:https://doi.org/10.5740/jaoacint.14-085

Legends to figures

Fig. 1 Semi-logarithmic plot of the mean concentration-time profiles including standard deviation (SD) of **A.** U-47700 (blue line) and *N*-desmethyl-U-47700 (orange line) after single i.v. administration of a 100 µg/kg body weight (BW) dose, and **B.** Tramadol (blue line) and *O*-desmethyltramadol (orange line) after single i.v. administration of a 1000 µg/kg BW dose determined in pig serum.

Fig. 2 Visual predictive checks (VPCs) of final popTK models for tramadol (upper panel) and U-47700 (lower panel) on the **A.** linear and **B.** semi-logarithmic scale. The dots represent observed concentrations. The lines depict the median of the predicted concentrations and the shaded area is the 90% confidence interval of the predictions after 1000 simulations.

Fig. 3 Prediction of human tramadol concentration-time profiles on the **A.** linear and **B.** semi-logarithmic scale. Simulated median and 90% confidence interval of the predictions after 1000 simulations shown as a solid line and shaded area respectively. Observed values digitized from literature 1-5 (Table S5) are displayed as dots.

Fig. 4 Simulation of human U-47700 serum concentration-time profile (i.v. bolus dose of 100 µg/kg, BW = 70 kg) on the **A.** linear and **B.** semi-logarithmic scale. Simulated median and 90% confidence interval of the predictions after 1000 simulations shown as a solid line and shaded area respectively. The dotted line shows the median U-47700 serum concentration in pig, given the same dose (100 µg/kg, i.v bolus).

Figure 1

Click here to access/download;Figure;Fig1_log-serum-Konz-Zeitprofil.png

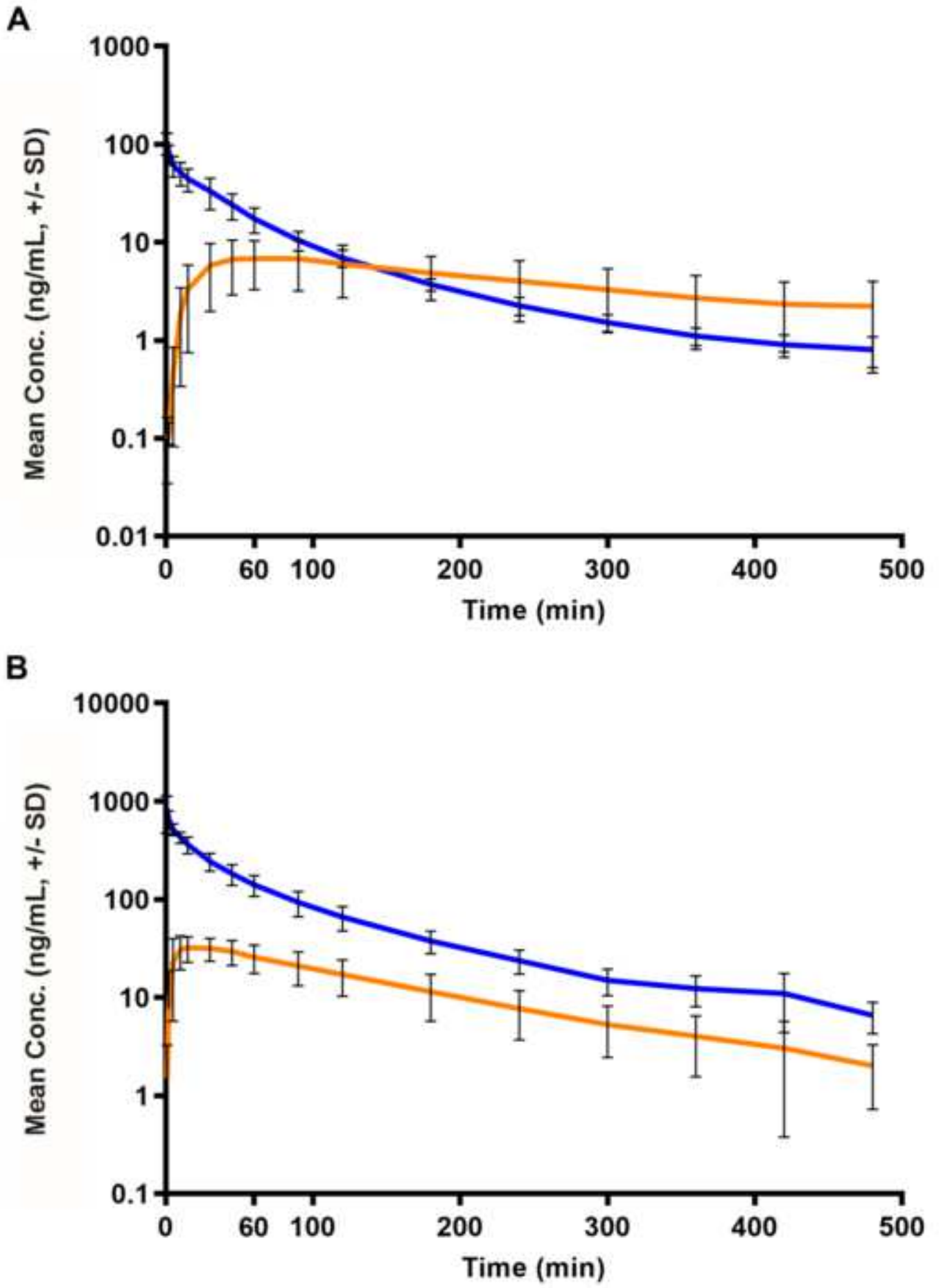

Figure 2

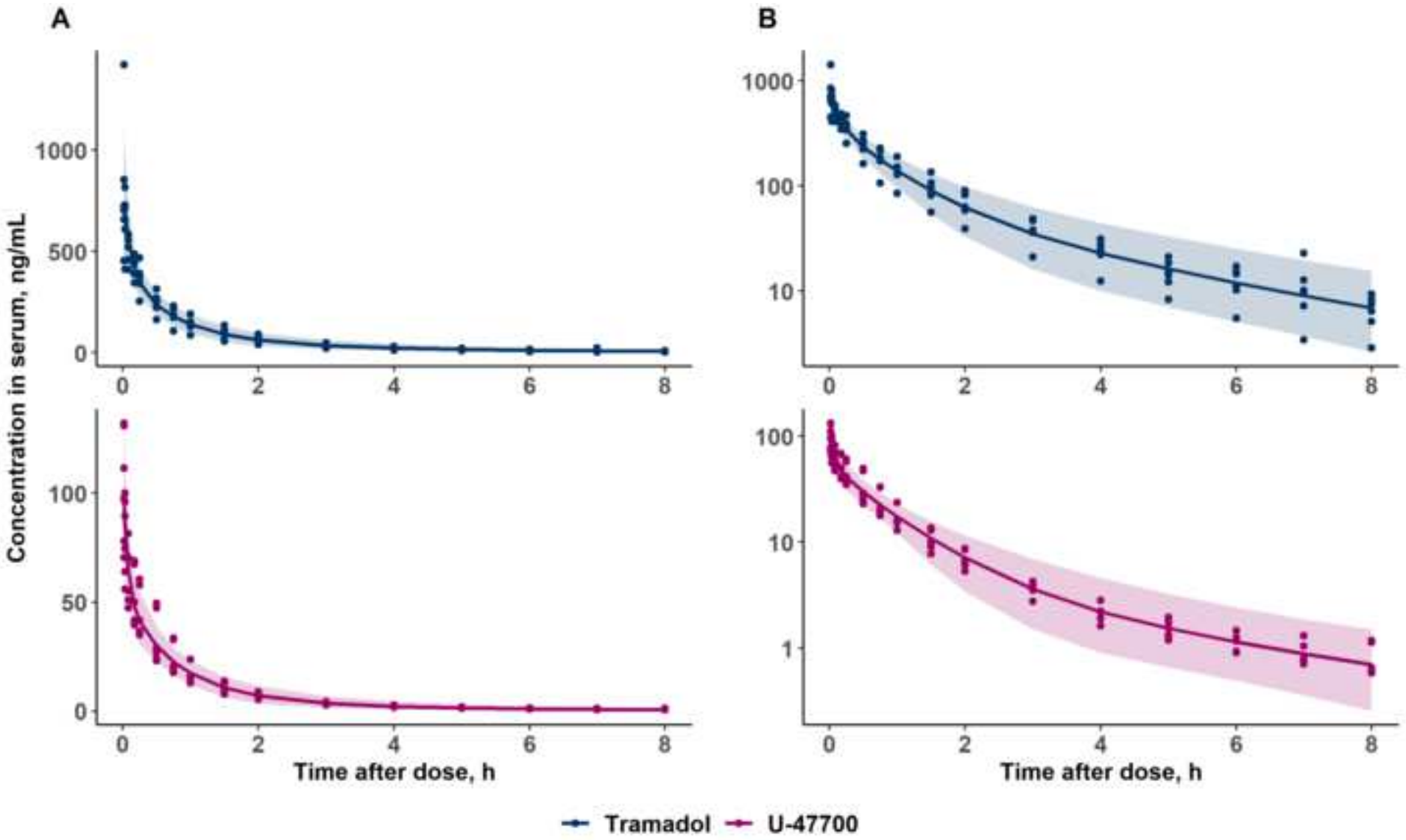

Figure 3

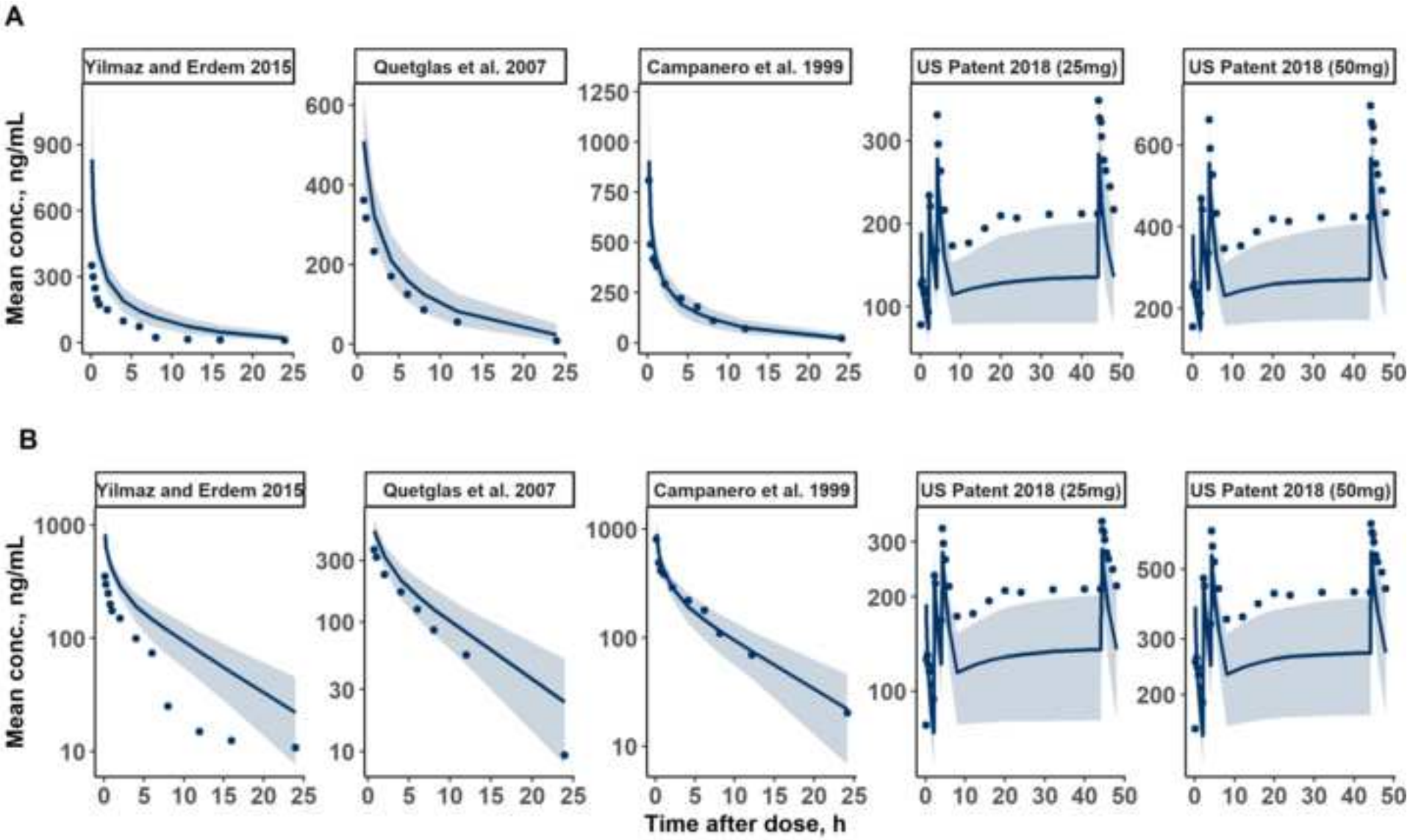

Figure 4

Click here to access/download;Figure;Fig4_VPC_U47700_human.png

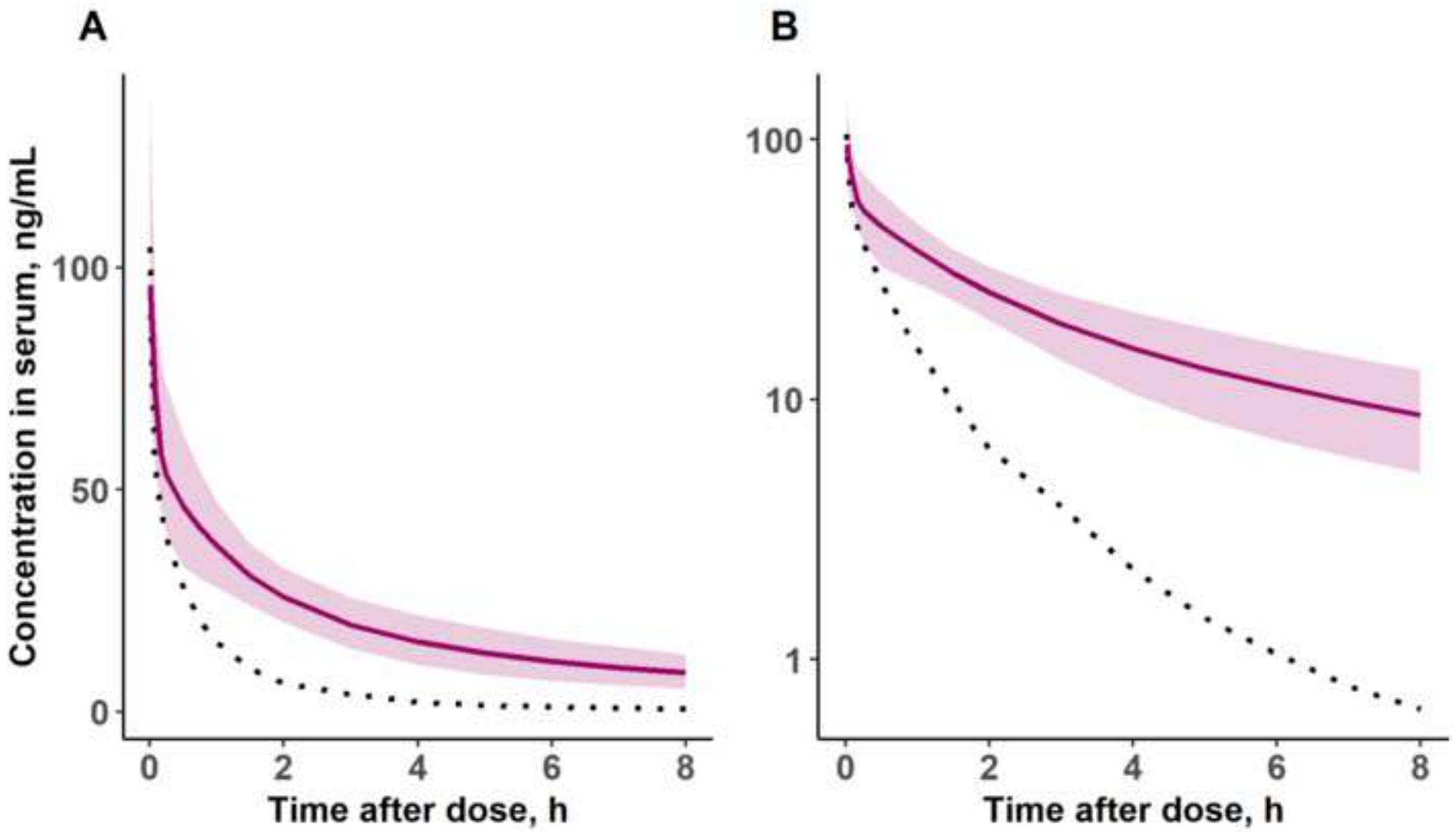

Table 1 Toxicokinetic parameters of tramadol and U-47700 estimated in serum from a three-compartment pig model. RSE: relative standard error; CL: clearance from central compartment; V: volumes of distribution; Q: intercompartmental clearance; IIV: interindividual variability; CV: coefficient of variation; n.a.: not applicable.

Parameter	Unit	Tramadol		U-47700	
		Estimate	RSE (%)	Estimate	RSE (%)
Structural model parameters					
$V_{central}$	(L/kg)	1.3	17.8	0.9	15.5
CL	(L/h/kg)	1.9	7.6	1.6	7.9
V2	(L/kg)	1.7	17.3	1.5	19.7
Q2	(L/h/kg)	0.7	13.9	0.4	18.0
V3	(L/kg)	0.7	18.9	0.6	19.0
Q3	(L/h/kg)	3.4	51.6	5.2	44.7
Variability					
IIV $V_{central}$	(%CV)	27.9	33.8	24.8	9.5
IIV CL	(%CV)	16.6	31.9	19.2	15.5
IIV V2	(%CV)	30.5	49.6	54.0	33.9
IIV Q2	(%CV)	31.5	32.0	28.2	13.9
IIV V3	(%CV)	n.a.	n.a	47.7	25.4
IIV Q3	(%CV)	n.a	n.a	n.a	n.a
Proportional residual error	(%)	15.0	17.8	8.5	8.1

Electronic Supplementary Material

Toxicokinetics of U-47700, tramadol, and their main metabolites in pigs following intravenous administration – Is a multiple species allometric scaling approach useful for the extrapolation of toxicokinetic parameters to humans?

Frederike Nordmeier[1], Iryna Sihinevich[2], Adrian A. Doerr[1], Nadja Walle[1], Matthias W. Laschke[3], Thorsten Lehr[2], Michael D. Menger[3], Peter H. Schmidt[1], Markus R. Meyer[4], and Nadine Schaefer[1*]

[1]Institute of Legal Medicine, Saarland University, 66421 Homburg, Germany

[2]Clinical Pharmacy, Saarland University, 66123 Saarbruecken, Germany

[3]Institute for Clinical and Experimental Surgery, Saarland University, 66421 Homburg, Germany

[4]Department of Experimental and Clinical Toxicology, Institute of Experimental and Clinical Pharmacology and Toxicology, Center for Molecular Signaling (PZMS), Saarland University, 66421 Homburg, Germany

S1 Methods

Chemicals and reagents

Hydrochloric acid, di-potassium hydrogen phosphate, ammonia solution 25% EMSURE, potassium hydroxide, and formic acid EMSURE were purchased from Merck (Darmstadt, Germany). Na_2EDTA, dichloromethane, and ammonium formate were obtained from Sigma-Aldrich (Steinheim, Germany). From Fisher chemicals (Loughborough, UK) HPLC-grade water, acetonitrile, methanol, and ethanol were bought. Standards as *N*-desmethyl-U-47700

(solid), methanolic solutions of dehydrocodeine, fentanyl, norfentanyl, morphine (0.1 mg/mL each), tramadol-HCl, *O*-desmethyltramadol-HCl (ODT), codeine, EDDP, hydromorphone, hydrocodone, 6-monoacetylmorphine (6-MAM), methadone, oxycodone, tilidin, and nortilidin (1 mg/mL each), U-51754 hydrochloride (solid), U-47931E (solid), methoxyacetylfentanyl hydrochloride (solid), tramadol-HCl-C_{13}-d_3 (1 mg/mL), and ODT-d_6 (0.1 mg/mL) were from LGC (Wesel, Germany). *N*-desmethyl-U-47700-d_3 (0.1 mg/mL in acetonitrile) was purchased from Sigma-Aldrich (Taufkirchen, Germany). Tramadol-HCl solution used for drug administration (Tramadol Denk 100 mg in 2 mL) was bought from Denk Pharma (Munich, Germany). U-47700 hydrochloride (purity 92.6%) was offered by the German Federal Crime Police Office (Wiesbaden, Germany) for research purposes.

Experimental preparation

Buffers

For the preparation of the phosphate buffer (0.1 M, pH 6), 13.61 g di-potassium hydrogen phosphate was dissolved in 1 L deionized water. Potassium hydroxide solution (1 M) was added for pH adjustment.

Blank serum, and whole blood samples

Blank blood samples used for method development and validation were taken from drug-free pigs (Swabian Hall strain, Emil Faerber GmbH & Co. KG, Zweibruecken, Germany). Before freezing, blood samples were divided into two aliquots. One aliquot was centrifuged at 1250 g for 15 min to obtain serum samples. Na_2EDTA (1.64 mg/mL) was given to the whole blood samples for prevention of clotting. All samples were stored at - 20 °C until analysis.

Stock solutions, calibration standards, and quality control samples

The solid compound was dissolved in methanol to generate standard stock solutions of U-47700 and *N*-desmethyl-U-47700 (1 mg/mL). Working standard solutions (0.001, 0.01, 0.1 mg/mL) were generated by the dilution of the stock solutions or liquid reference standards with ethanol, respectively. Spiking solutions for calibration standards were prepared in serum at concentrations of 0.25, 0.5, 1, 5, 10, 15, 20, 50, and 100 ng/mL, and in whole blood in concentrations of 0.5, 1, 5, 10, 15, 20, 50, and 100 ng/mL through the dilution of working solutions with ethanol. Quality control (QC) LOW, MID, and HIGH samples were prepared in the same way. QC concentrations are shown in Table S3 and S4. All solutions were stored at - 20 °C.

Method validation

Six blank serum or whole blood samples from different drug-free pigs were analyzed to check for interfering signals at the multiple reaction monitoring (MRM) transitions of the analytes or stable-isotope-labeled internal standard (SIL-IS). Two zero samples per matrix containing only SIL-IS were analyzed to check for interference at the retention time of the SIL-IS. In addition, two blank serum or whole blood samples and two zero samples spiked with several opioids were analyzed as described before. The following drugs were tested: U-51754, U-47931E, methoxyacetylfentanyl, fentanyl, norfentanyl, oxycodone, morphine, hydromorphone, hydrocodone, codeine, 6-MAM, methadone, dihydrocodeine, EDDP, tilidin, nortilidin (100 ng/mL each).

Recovery (RE), matrix effects (ME), and process efficiency (PE) were estimated according to Matuszewski et al. (2003) by preparing three different sets of quality control (QC) LOW and HIGH samples. Sample set one represented neat standard solution, sample set two blank matrices spiked after extraction, and sample set three was spiked before extraction.

Drug-free serum and blood from different pigs were used to achieve six different sets per matrix. RE was calculated by comparison of the absolute peak areas of sample set three and two. ME was estimated by comparison of the peak areas of set two with those of set one. PE was obtained by comparing peak areas of set three with those of set one.

The linearity of the calibration range was examined by spiking blank serum or whole blood samples with 50 µL of the corresponding calibration standard. Each calibration level was analyzed six times and the peak area ratios between analyte and SIL-IS were plotted against the drug concentration. Linear regression was performed via the Valistat 2.0 software (Arvecon, Walldorf, Germany) using non-weight, a weighted [1/concentration], and a weighted least-square [1/(concentration)^2] regression model and different statistical tests (Grubbs test, F test, Mandel test). The lowest point of the calibration curve determined in serum or whole blood was defined as lower limits of quantification (LLOQ).

Limits of detection (LODs) were estimated by preparing different concentrations in drug-free serum or whole blood. For U-47700, tramadol and their metabolites concentrations of 0.02, 0.05, 0.07, 0.1, 0.12, 0.15, 0.17, 0.2, 0.25, 0.05, 1.0, 1.5, 2.0 2.5, 3.0, 3.5, 4.0, 4.5, and 5.0 ng/mL were prepared in serum. In whole blood, concentrations of 0.1, 0.15, 0.2, 0.25, 0.3, 0.35, 0.4, 0.45, 0.5, 3.5, 4.0, 4.5, 5.0, 5.5, and 6.0 ng/mL were prepared. LODs were determined by signal-to-noise ratios of the quantifier and qualifier MRM transitions of 3:1.

For accuracy and precision tests, 1 mL aliquots of blank pig serum or whole blood were spiked freshly on each of 8 days with 50 µL of QC LOW or HIGH solution. They were analyzed in duplicates and calculated via daily calibration curves. Calculation of bias values, repeatability, and intermediate precision was performed using Valistat 2.0 software.

For determination of the dilution integrity for concentrations higher than the calibration range, blank serum or whole blood samples were spiked with analyte concentrations tenfold the QC HIGH, diluted 1:10 and analyzed in duplicates on 8 days.

In order to estimate the stability of processed samples under conditions of a liquid chromatography-tandem mass spectrometry (LC-MS/MS) analysis session, QC LOW and HIGH samples (n = 6 each) were prepared in blank serum or whole blood and then pooled at each concentration level. They were analyzed at time intervals of 60 min over a total run time of 15 h. Stability was calculated by linear regression with the Valistat 2.0 software by comparison of absolute peak areas.

For determination of freeze/thaw stability, QC LOW and HIGH samples (n = 6 each) were prepared in blank serum or whole blood and analyzed before and after three freeze and thaw cycles. Each freeze/thaw cycle was processed as a 21 h freezing period at - 20 °C followed by a thawing period over 3 h at room temperature. For determination of long-term stability QC LOW and HIGH samples (n = 6 each) were prepared in blank serum or whole blood and analyzed before and after a freezing period of 30 days at - 20 °C.

Carry-over effects were estimated during the analysis of the authentic pig serum and whole blood samples obtained from the toxicokinetic study. Therefore, one blank sample was analyzed between two authentic samples with high concentrations.

Surgical Procedure

In accordance with previous studies (Schaefer et al. 2016, 2017, 2018; Nordmeier et al. 2020, 2021), the animals were treated with ketamine hydrochloride (30 mg/kg, Ursotamin; Serumwerk Bernburg, Bernburg, Germany), xylazine hydrochloride (2.5 mg/kg, Rompun; Bayer, Leverkusen, Germany), and 1 mg atropine (Braun, Melsungen, Germany) by intramuscular injection. Anesthesia was maintained with isoflurane (2-4%, Forene, AbbVie, Ludwigshafen, Germany) and mechanically ventilation occurred with a mixture of oxygen and air (1:2 v/v; FiO_2 of 0.30; Respirator ABV-U; F. Stephan GmbH, Gackenbach, Germany) and a tidal volume of 10-12 mL/kg. A catheter was placed in the left ear vein for fluid

(sodium chloride 0.9% [8 mL/kg/h], Braun, Melsungen, Germany) replacement. Sample collection, i.v. drug administration, and monitoring of mean central venous pressure was made sure by the placement of a triple-lumen 7F central venous catheter (Certofix Trio, Braun, Melsungen, Germany) into the jugular vein. For assurance of urine collection, a suprapubic catheter (Cystofix, Braun, Melsungen, Germany) was placed into the bladder. Prior to the drug administration, the pigs were allowed to stabilize for 10-15 min.

S2 Results

Method validation

The analysis of blank pig serum, whole blood, or zero samples revealed no interferences. There were also no interferences in analyzed samples spiked with several opioids.

The full ME, RE, and PE data are shown in Table S2. In general, the matrix effects were in the acceptable range of ± 25% according to the guidelines of the GTFCh (Peters et al. 2009) except for tramadol and ODT in serum QC LOW and whole blood QC LOW and HIGH samples.

LOD values and the calibration ranges are shown in Table S3 and S4. For the calibration, a weighted ($1/x^2$) quadratic regression model was applied for all analytes in both matrices.

The accuracy bias and the relative standard deviation (RSD) values from intra- and interday precision tests are listed in Table S2 and S3. Bias values were within the acceptable interval of ± 15%. The RSD values ≤ 15% are acceptable (Peters et al. 2009). RSD values for all analytes were in this range as well. Sample dilution did not affect these criteria.

All analytes were stable for at least 12 h at 15 °C. A decrease in the peak area > 25% during the tested period indicates instability of the analyte (Peters et al. 2009). During three

freeze/thaw cycles, no degradation of any analyte was observed as well as after a freezing period of 30 days at - 20 °C. Mean values of stability samples should be in a range of 90-100% of the control samples (Peters et al. 2009).

During analysis, no carry-over effects were observed.

S3 Discussion

Validation and applicability of the method

A novel LC-MS/MS method for simultaneous determination of U-47700, tramadol, and their main metabolites was developed. All criteria for a successful validation according to the guidelines of the GTFCh (Peters et al. 2009) were fulfilled with minor exceptions in terms of ME and RE. In general, ME was in the acceptable range, but especially in the whole blood samples, signals were suppressed by the matrix. In the case of tramadol and ODT, a markable suppression of the signals was determined in whole blood samples, whereas in serum samples suppression was not that pronounced. One reason for that could be the difference in the composition of whole blood and serum. Whole blood contains more solid components, which aggravate SPE and maybe affect analyte extraction as well. However, in the context that ME data were carried out without the usage of SIL-IS, ME probably will be compensated in routine analysis using SIL-IS and for both compound, tramadol and ODT, SIL-IS was used. Furthermore, the low standard deviation (SD) indicates a good reproducibility of the method and its results. Nevertheless, ME in serum were acceptable and TK data were manly collected in serum. Another conspicuousness was the low RE in terms of U-47700 and its metabolite in the whole blood QC HIGH samples. Values of RE > 50% are permitted by the GTFCh (Peters et al. 2009) and in our method only values of about 35% were reached in whole blood samples, whereas values for serum samples were about twice as high und thus in the

acceptable range. PE values were low, too. Hence, a signal suppression by whole blood alone might not be the reason for the low RE. As described above in terms of ME, also in this case the combination of whole blood and SPE might be responsible for the low RE of this substance. However, SD values were very low for this RE values, indicating results of a very good reproducibility. Furthermore, all signals of the whole blood samples showed acceptable intensities, low concentrations were less influenced by this effect and, thus, a quantification of low concentrations in whole blood could be guaranteed. In addition, as for ME, these data were carried out without the usage of and SIL-IS and, thus, RE might be compensated in routine analysis using SIL-IS as well.

Regarding U-47700 and its metabolite, LOD and LLOQ values obtained for serum in this study were in the same range as those determined in the study by Smith et al. (2019) with the exception of some minor differences. LOD and LLOQ values were slightly higher in our study. LOD values for whole blood for both substances were in agreement with those from the method developed by Seither et al. (2017), whereas LLOQ values were lower in our method compared to that of Gerace et al. (2018), who applied a fast protein precipitation approach. In terms of tramadol, LOD and LLOQ values were slightly lower in our study compared to that of Fernández et al. (2013), who established a quantification method for 26 opioids in whole blood after SPE. LLOQ values in serum were in the same range for tramadol and ODT, as determined in the study of Meyer et al. (2015).

The validated method was applied to a TK study following i.v. administration of U-47700 or tramadol to 6 pigs, respectively. The results obtained in one group of the pigs receiving the same drug were in good agreement with each other and the method was suitable to determine the serum and whole blood concentration-time profiles of both substances as well as the metabolites. Regarding U-47700, only a few samples had to be diluted due to concentrations above the calibration range. Eight hours following administration, most whole

blood samples displayed higher concentrations than the LOD, whereas some concentrations were lower than the LLOQ, but the analytes were still detectable. Regarding the serum samples, all determined concentrations were higher than the LLOQ. In terms of tramadol, many samples had to be diluted due to much higher concentrations above the calibration range. Caused by the higher dosage, higher serum/whole blood concentrations were estimated, but also low concentrations at the end of the experiment because of a great concentration decrease in the organism during the experiment. However, in terms of the linearity of the calibration curve, a broader calibration range was not possible. Due to the medium sensitivity of tramadol and ODT within this applied method and the used MS/MS, many samples showed concentrations lower than the LOD/LLOQ at the end of the experiment in terms of whole blood samples, but both substances were still detectable in each sample. In terms of serum samples, most of the determined concentrations were higher than the LLOQ.

S4 popTK modeling: differential equations and parameter calculation

A three-compartment linear mammillary model was implemented in NONMEM® using ADVAN11 TRANS4 subroutine as described below:

```
1 = CENTRAL: DADT(1) = - CL/V1*A(1) + Q2/V2*A(2) -Q2/V1*A(1) + Q3/V3*A(3) - Q3/V1*A(1)
2 = PERIPHERAL 1:  DADT(2) = Q2/V1*A(1) - Q2/V2*A(2)
3 = PERIPHERAL 2:  DADT(3) = Q3/V1*A(1) - Q3/V3*A(3)
4 = OUTPUT
```

NONMEM model file and **parameters calculation** used in the single species scaling from pig to human for tramadol using LBF on CL and WGT on all patameters:

```
$PROBLEM PK
$INPUT ID TIME AMT RATE CMT DV MDV WGT AMTKG SPECIES BRAIN BrainWGT WGT1 BILE UDPGT ENQ BRAINTOWGT DOSE DUR WGT2 MLP GFR CF
$DATA Human_all.csv IGNORE=@
$SUBROUTINES ADVAN11 TRANS4

$PK
```

```
TVCL = THETA(1)*((WGT/42.83)**THETA(7))*((364/73)/(517.3/25.5))
CL = TVCL * EXP(ETA(1))
TVV1 = THETA(2)*((WGT/42.83)**THETA(8))
V1 = TVV1 * EXP(ETA(2))
TVQ2 = THETA(3)*((WGT/42.83)**THETA(9))
Q2  = TVQ2 * EXP(ETA(3))
TVV2 = THETA(4)*((WGT/42.83)**THETA(10))
V2 = TVV2 * EXP(ETA(4))
TVQ3 = THETA(5)*((WGT/42.83)**THETA(11))
Q3  = TVQ3 * EXP(ETA(5))
TVV3 = THETA(6)*((WGT/42.83)**THETA(12))
V3 = TVV3 * EXP(ETA(6))
S1 = V1

$ERROR
IPRED=F
DEL=0
IF (IPRED.EQ.0) DEL=0.0001
W=F
IRES=DV-IPRED
IWRES=IRES/(W+DEL)
Y=IPRED+W*EPS(1)

$THETA
(0, 78.9) FIX ; CL (L/h)
(0, 53.6) FIX ; V1 (L)
(0, 30.8) FIX ; Q2 (L/h)
(0, 74.7) FIX ; V2 (L)
(0, 147) FIX ; Q3 (L/h)
(0, 28.4) FIX ; V3 (L)
(1) FIX ; WGT on CL
(1) FIX ; WGT on V1
(1) FIX ; WGT on Q2
(1) FIX ; WGT on V2
(1) FIX ; WGT on Q3
(1) FIX ; WGT on V3

$OMEGA
0.0394 FIX ; IIV CL
0.0745 FIX ; IIV V1
0.133 FIX ; IIV Q2
0.102 FIX ; IIV V2
0 FIX ; IIV Q3
0 FIX ; IIV V3

$SIGMA
0.0226 ; RV Proportional error

$EST METHOD=1 INTER MAXEVAL=9999 NOABORT PRINT=1 POSTHOC
$COV
$TABLE ID TIME IPRED IWRES CWRES FILE=sdtab3105_015 ONEHEADER NOPRINT
$TABLE CL V1 V2 V3 Q2 Q3 ONEHEADER NOPRINT FIRSTONLY FILE=patab3105_015
```

Table S1 MRM transitions and MS conditions for all analytes and the stable-isotope-labeled internal standard with collision energy (CE), declustering potential (DP), entrance Potential (EP), and collision cell exit potential (CXP).

Analyte	RT (min)	Precursor Ion (Q1, m/z)	Product Ion (Q3, m/z)	DP (V)	EP (V)	CE (V)	CXP (V)
U-47700	7.99	329.0	173.0	41	6.5	39	6
		329.0	284.2	41	6.5	19	16
		329.0	204.1	41	6.5	33	6
N-desmethyl-U-47700	7.42	314.9	284.0	41	7	21	12
		314.9	173.1	41	7	35	6
		314.9	204.1	41	7	35	8
Tramadol	2.88	264.3	58.2	21	6.5	37	4
		264.3	57.4	21	6.5	37	58
O-desmethyltramadol	2.33	250.2	57.9	21	10	39	8
		250.2	57.1	21	10	77	4
N-desmethyl-U-47700-d_3	7.36	318.1	287.2	41	9	21	10
		318.1	176.1	41	9	39	6
		318.1	148.1	41	9	65	4
Tramadol-C_{13}-d_3	2.84	268.2	58.0	31	4	37	8
		268.2	57.1	31	4	89	56
O-desmethyltramadol-d_6	2.32	256.2	64.1	36	3	29	4
		256.2	77.0	36	3	79	4

Table S2 Drug, matrix effects (ME), recovery (RE), and process efficiency (PE) including their relative standard deviation (RSD) for pig serum/whole blood QC LOW and QC HIGH samples.

Analyte	Serum			Whole blood		
	ME% (RSD%)	RE% (RSD%)	PE% (RSD%)	ME% (RSD%)	RE% (RSD%)	PE% (RSD%)
OC LOW						
U-47700	77.1 (5.6)	74.9 (7.3)	57.7 (4.8)	101.4 (11.3)	70.2 (15.4)	71.1 (16.5)
N-desmethyl-U-47700	78.0 (5.5)	72.5 (5.5)	56.5 (11.6)	104.1 (10.6)	68.4 (17.4)	71.2 (16.9)
Tramadol	71.8 (8.9)	81.0 (4.0)	58.1 (7.9)	67.2 (28.1)	76.1 (17.2)	51.2 (15.6)
O-desmethyltramadol	63.7 (8.2)	89.8 (6.4)	57.2 (9.3)	36.1 (17.5)	77.6 (10.0)	28.0 (9.5)
QC HIGH						
U-47700	92.7 (2.7)	67.0 (6.0)	62.1 (5.3)	110.5 (14.5)	33.2 (2.0)	36.6 (6.8)
N-desmethyl-U-47700	91.8 (4.7)	66.1 (6.0)	60.7 (6.2)	115.4 (15.0)	36.3 (4.2)	42.0 (9.08)
Tramadol	83.9 (6.6)	80.5 (4.4)	67.5 (4.9)	76.1 (20.8)	78.2 (26.4)	59.5 (14.0)
O-desmethyltramadol	77.3 (7.5)	86.5 (3.7)	66.8 (6.3)	48.7 (17.7)	85.6 (37.4)	41.7 (10.7)

Table S3 Drug, used stable-isotope-labeled internal standard (SIL-IS), limit of detection (LOD), calibration range with lower limits of quantification (LLOQ) as lowest point, nominal concentration, accuracy bias, and the relative standard deviation (RSD) values for repeatability and intermediate precision for pig serum CQ LOW and QC HIGH samples.

Analyte	SIL-IS	LOD [ng/mL]	Calibration range [ng/mL]	QC LOW				QC HIGH			
				Nominal conc. [ng/mL]	Accuracy bias [%]	Repeatability RSD [%]	Intermediate Precision RSD [%]	Nominal conc. [ng/mL]	Accuracy bias [%]	Repeatability RSD [%]	Intermediate Precision RSD [%]
U-47700	*N*-desmethyl-U-47700-d_3	0.05	0.25-50	0.75	1.0	9.6	9.6	35	-0.04	7.4	11.1
N-desmethyl-U-47700	*N*-desmethyl-U-47700-d_3	0.1	0.25-50	0.75	9.3	7.0	7.0	35	-0.3	8.6	8.6
Tramadol	Tramadol-C_{13}- d_3	0.05	0.5-100	1.5	8.0	6.2	8.5	75	9.6	3.9	3.9
O-desmethyl-tramadol	*O*-desmethyl-tramadol-d_6	1.5	5-100	7.5	8.7	7.6	7.6	75	2.2	7.0	10.1

Table S4 Drug, used stable-isotope-labeled internal standard (SIL-IS), limit of detection (LOD), calibration range with lower limits of quantification (LLOQ) as lowest point, nominal concentration, accuracy bias, and the relative standard deviation (RSD) values repeatability and intermediate precision for pig whole blood CQ LOW and QC HIGH samples.

Anaylte	SIL-IS	LOD [ng/mL]	Calibration range [ng/mL]	QC LOW				QC HIGH			
				Nominal conc. [ng/mL]	Accuracy bias [%]	Repeatability RSD [%]	Intermediate Precision RSD [%]	Nominal conc. [ng/mL]	Accuracy bias [%]	Repeatability RSD [%]	Intermediate Precision RSD [%]
U-47700	*N*-desmethyl-U-47700-d_3	0.1	0.5-50	2	11.28	4.02	4.94	35	4.89	3.46	6.94
N-desmethyl-U-47700	*N*-desmethyl-U-47700-d_3	0.1	0.5-50	2	4.84	3.45	4.62	35	-1.19	4.03	5.75
Tramadol	Tramadol-C_{13}- d_3	0.1	1-100	8	4.13	3.77	6.23	80	3.30	2.05	3.36
O-desmethyl-tramadol	*O*-desmethyl-tramadol-d_6	3.5	10-100	20	4.46	2.68	4.96	80	1.81	3.36	6.12

Table S5 Overview of the digitized tramadol literature data, used in the prediction of human tramadol concentration-time profiles and interspecies scaling analysis. NA not available, i.v. intravenous

ID	Species	Sex	n	Weight	Administration	Dose	Matrix	Sampling times	Reference
Human studies									
1	Volunteers (immediately after operation)	NA	6	71.2 ± 2.5 kg	single i.v. infusion (over 2 min)	100 mg	measured in plasma	0, 0.1, 0.25, 0.5, 0.75, 1, 2, 4, 6, 8, 12, 16, 20, and 24 h after drug administration.	(Yılmaz and Erdem 2015)
2	Healthy volunteers	male	12	50 to 80 kg (65 kg mean value)	single i.v. infusion (over 10 min)	100 mg (racemic tramadol)	R(+) and S(-) tramadol enantiomers measured in plasma (forearm vein)	0, 0.25, 0.5, 0.75, 1, 2, 4, 6, 8, 12 and 24 h after the end of the infusion	(Quetglas et al. 2007)
3	Healthy volunteers	NA	12	NA (assumed 70 kg)	single i.v. infusion (over 10 min)	100 mg (racemic tramadol)	R(+) and S(-) tramadol enantiomers measured in plasma	0, 10, 25, 40, and 55 min; and 1, 2, 4, 6, 8, 12, and 24 h after start of infusion.	(Campanero et al. 1999)
4	Healthy volunteers	NA	17	NA (assumed 70 kg)	multiple i.v. infusion (assumed bolus)	25 mg at 0h, followed by 25 mg at 2h, 25 mg at 4h, and 25 mg every 4 hours thereafter through 44h	measured in plasma	0, 0.15,0.25, 0.5, 0.75, 1, 1.5, 2, 2.25, 2.5, 4, 4.25, 4.5, 5, 6, 8, 12, 16, 20, 24, 32, 40, 44, 44.3, 44.5, 44.8, 45, 45.5, 46, 47, 48 h	(United States Patent 2018)
5	Healthy volunteers	NA	17	NA (assumed 70 kg)	multiple i.v. infusion (assumed bolus)	50 mg at 0h, followed by 50 mg at 2h, 50 mg at 4h, and 50 mg every 4 hours thereafter through 44h	measured in plasma	0, 0.15,0.25, 0.5, 0.75, 1, 1.5, 2, 2.25, 2.5, 4, 4.25, 4.5, 5, 6, 8, 12, 16, 20, 24, 32, 40, 44, 44.3, 44.5, 44.8, 45, 45.5, 46, 47, 48 h	(United States Patent 2018)
Animal studies									
6	C57Bl/6 Mice	3 male/ 3 female	6	20 - 30 g (25 g mean value)	i.v. bolus	25 mg/kg	measured in plasma (from tail-vein)	composite PK profile: 2 samples per mouse: 5, 15, 30 min and 1, 2, 4 hours post i.v.	(Evangelista Vaz et al. 2018)
7	Sprague-Dawley rats	male	6	250 - 300 g (275 g mean	single i.v. bolus	10 mg/kg	measured in plasma (from jugular vein)	tramadol 18 h after pretreatment with	(Jamali et al. 2017)

				value)				either MDMA or normal saline, blood samples at appropriate time intervals (0–300 min)	
8	Rhesus Macaques (Macaca Mulatta)	male	4	17 ± 2 kg	single i.v. bolus	1.50 mg/kg	measured in serum (from cephalic vein)	prior and 2, 5, 10, 15, 23, 45 min and 1, 1.5, 2, 3, 4, 6, 8, 10 h after drug administration	(Kelly et al. 2015)
9	Mixed breed dogs	male	6	22 to 32 kg (28.8 kg mean value)	single i.v. bolus	1.0 mg/kg	measured in plasma (from jugular vein)	0, 1, 2, 5, 10, 20, 40, and 60 min and at 2, 4, 6, 12, and 24 h.	(McMillan et al. 2008)
10	Adult llamas	male	6	107 to 140 kg (123.5 kg mean value)	single i.v. bolus (over 1 min.)	2.0 mg/kg	measured in plasma (from jugular vein)	0, 1, 3, 5, 10, 15, 20, 30, 45 min and 1, 1.5, 2, 4, 8, 12, 18, 24 and 48 h following administration	(Cox et al. 2011)
11	Healthy adult horses	4 male / 5 female	9	563.7 ± 49.1 kg	single i.v. bolus	0.5, 1.5 and 3 mg/kg	measured in plasma (from jugular vein)	at time 0 and at 5, 10, 15, 30 and 45 min and 1, 1.5, 2, 2.5, 3, 3.5, 4, 5, 6, 8, 12, 18, 24, 36, 48 and 72 h post administration	(Knych et al. 2013)

A

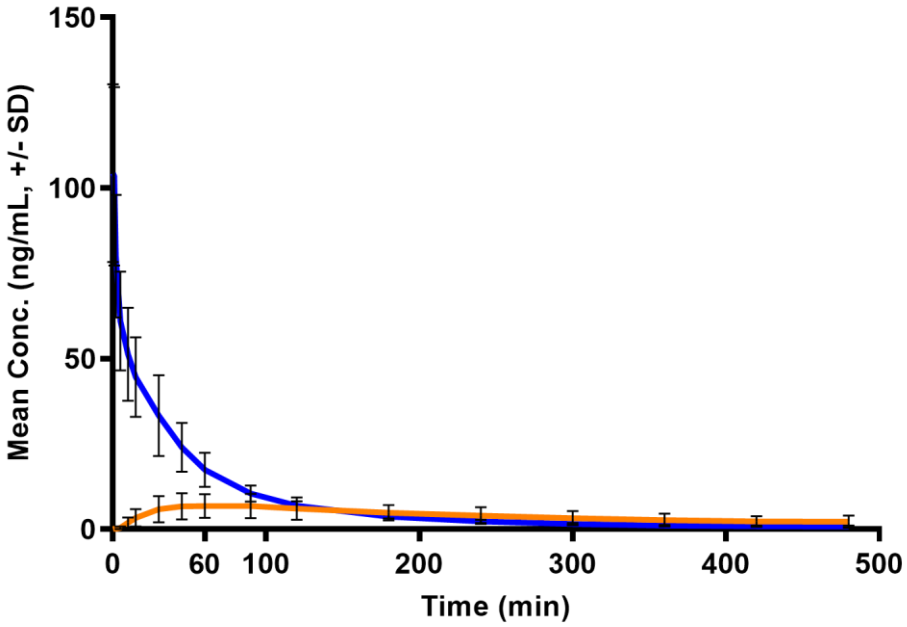

B

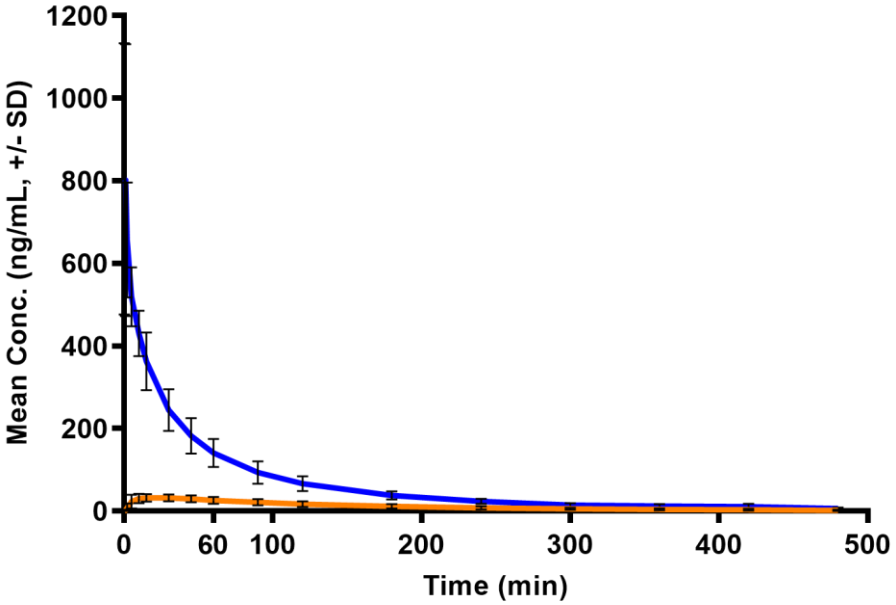

Fig. S1 Mean concentration-time profiles (n = 6 each) including standard deviation (SD) of **A.** U-47700 (blue line) and *N*-desmethyl-U-47700 (orange line) after single i.v. administration of a100 µg/kg body weight (BW) dose, and **B.** Tramadol (blue line) and *O*-desmethyltramadol (orange line) after single i.v. administration of a 1000 µg/kg BW dose determined in pig serum.

A

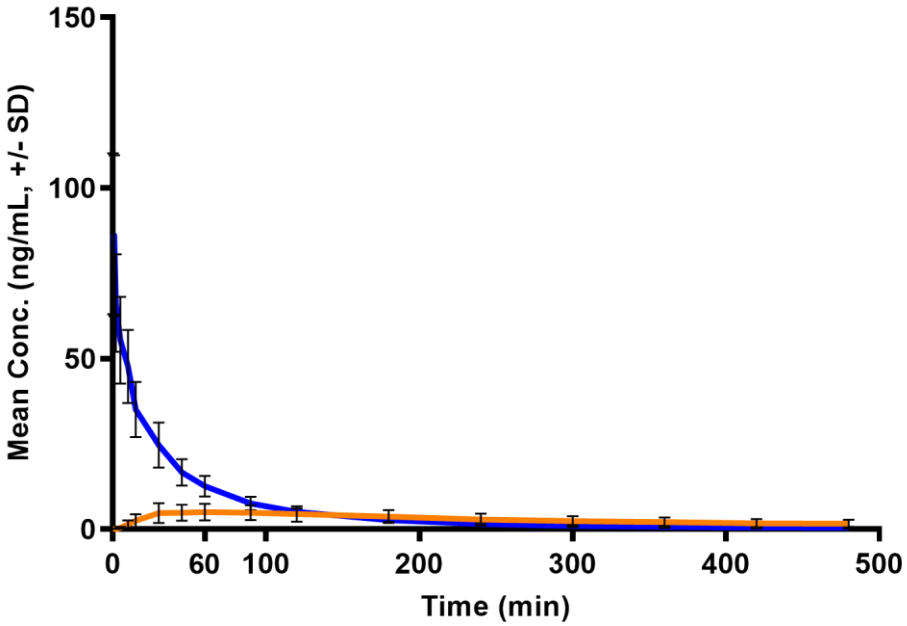

B

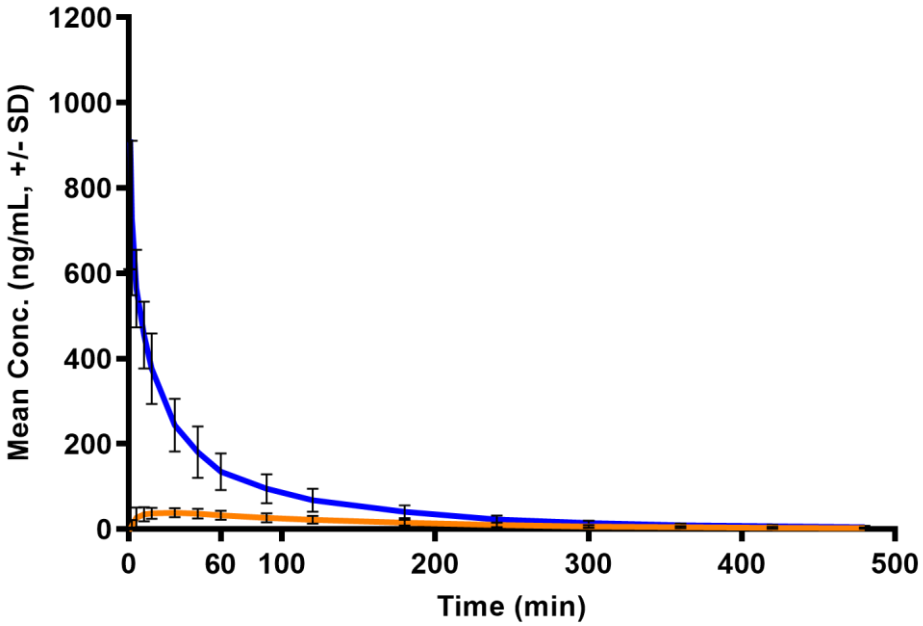

Fig. S2 Mean concentration-time profiles (n = 6 each) including standard deviation (SD) of **A.** U-47700 (blue line) and *N*-desmethyl-U-47700 (orange line) after single i.v. administration of a 100 µg/kg body weight (BW) dose, and **B.** Tramadol (blue line) and *O*-desmethyltramadol

(orange line) after single i.v. administration of a 1000 µg/kg BW dose determined in pig whole blood.

A

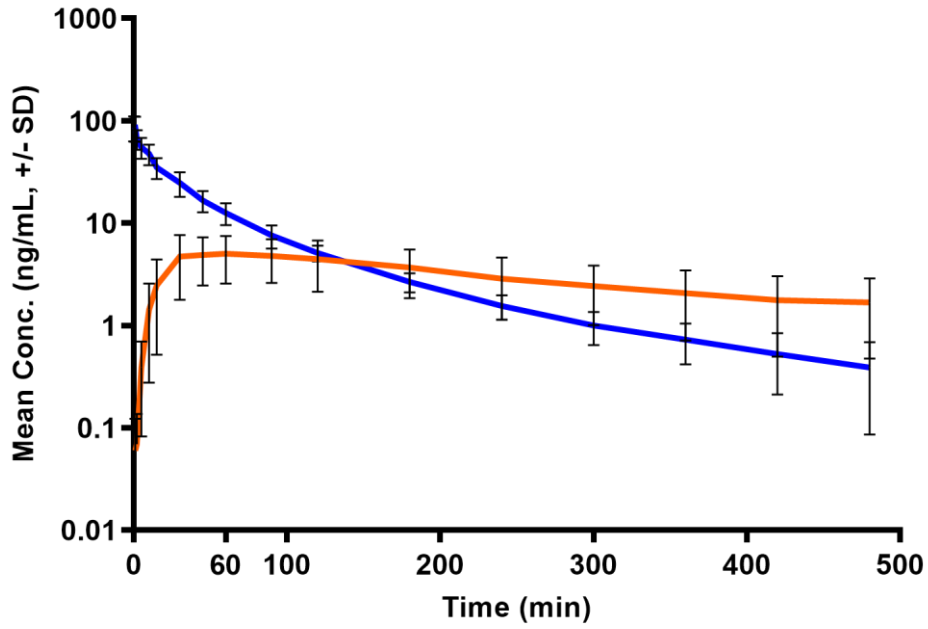

B

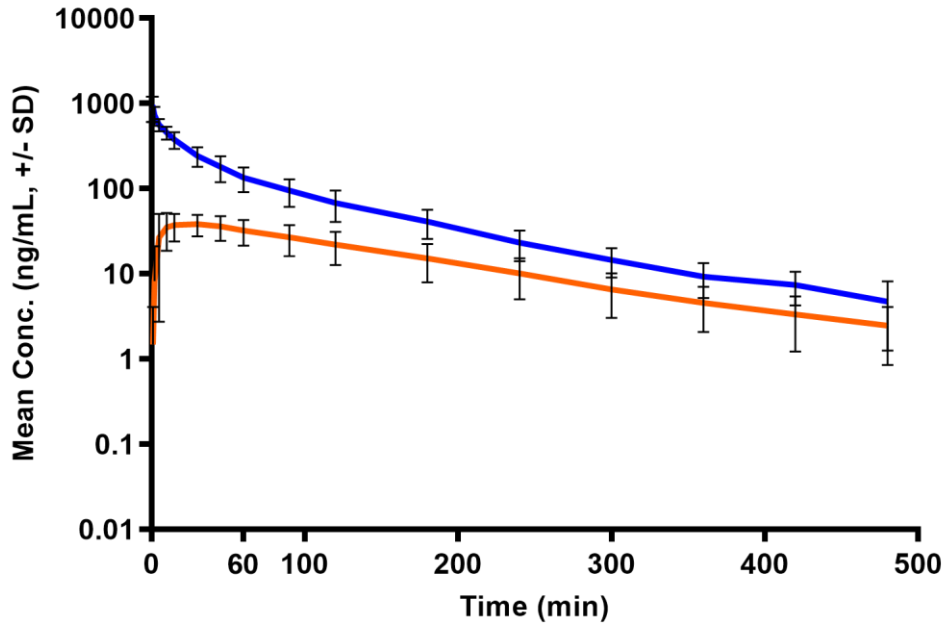

Fig. S3 Semi-logarithmic plot of the mean concentration-time profiles including standard deviation (SD) of **A.** U-47700 (blue line) and *N*-desmethyl-U-47700 (orange line) after single i.v. administration of a 100 µg/kg body weight (BW) dose, and **B.** Tramadol (blue line) and

O-desmethyltramadol (orange line) after single i.v. administration of a1000 µg/kg BW dose determined in pig whole blood.

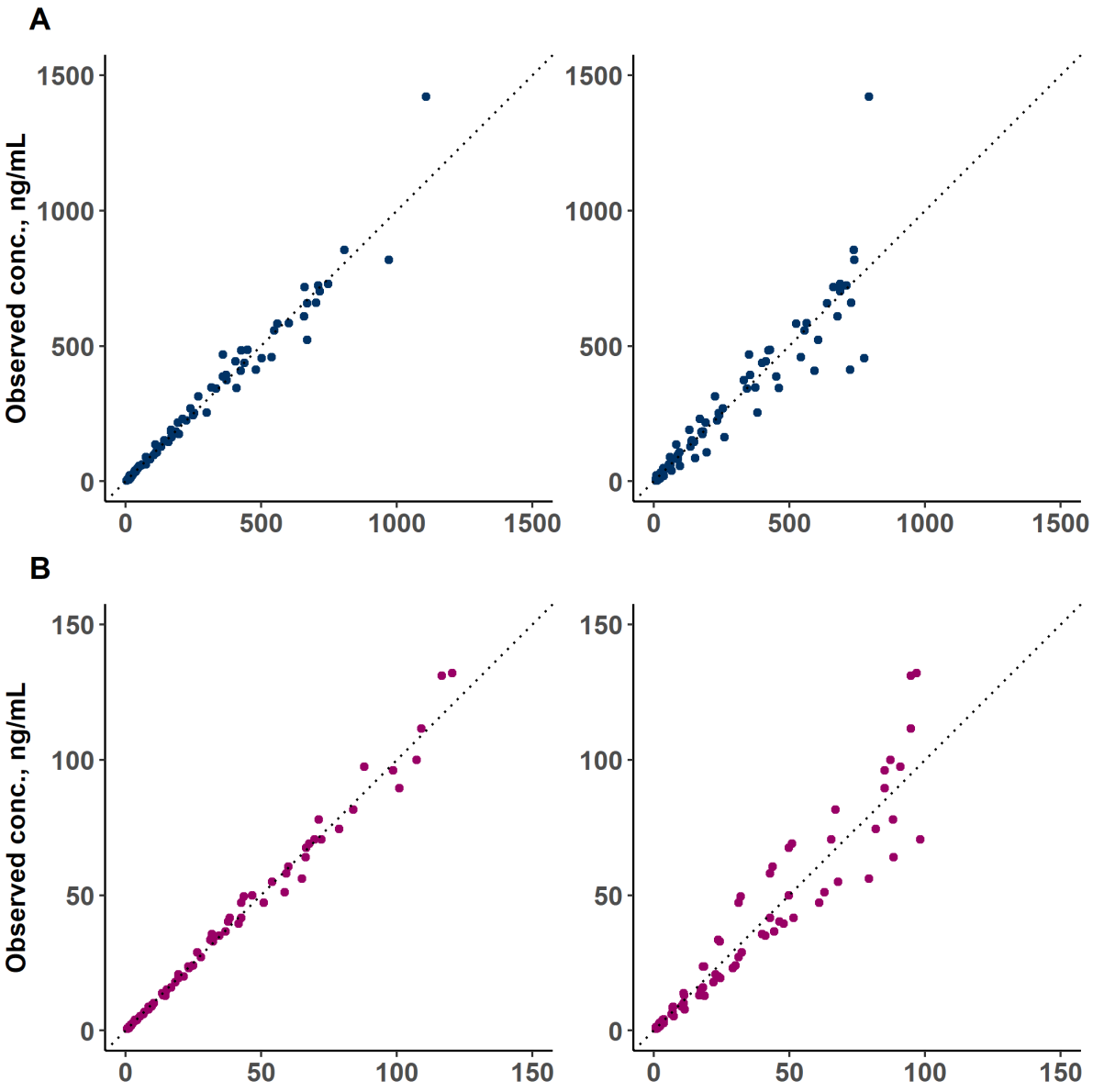

Fig. S4 Goodness-of-fit plots for the final population (pop) toxicokinetic (TK) model for tramadol (**A**) and U-47700 (**B**). On the left-hand side are plots of observations versus individual predictions. On the right-hand side are plots of observed serum concentrations versus population predictions. The black dotted line represents the line of identity.

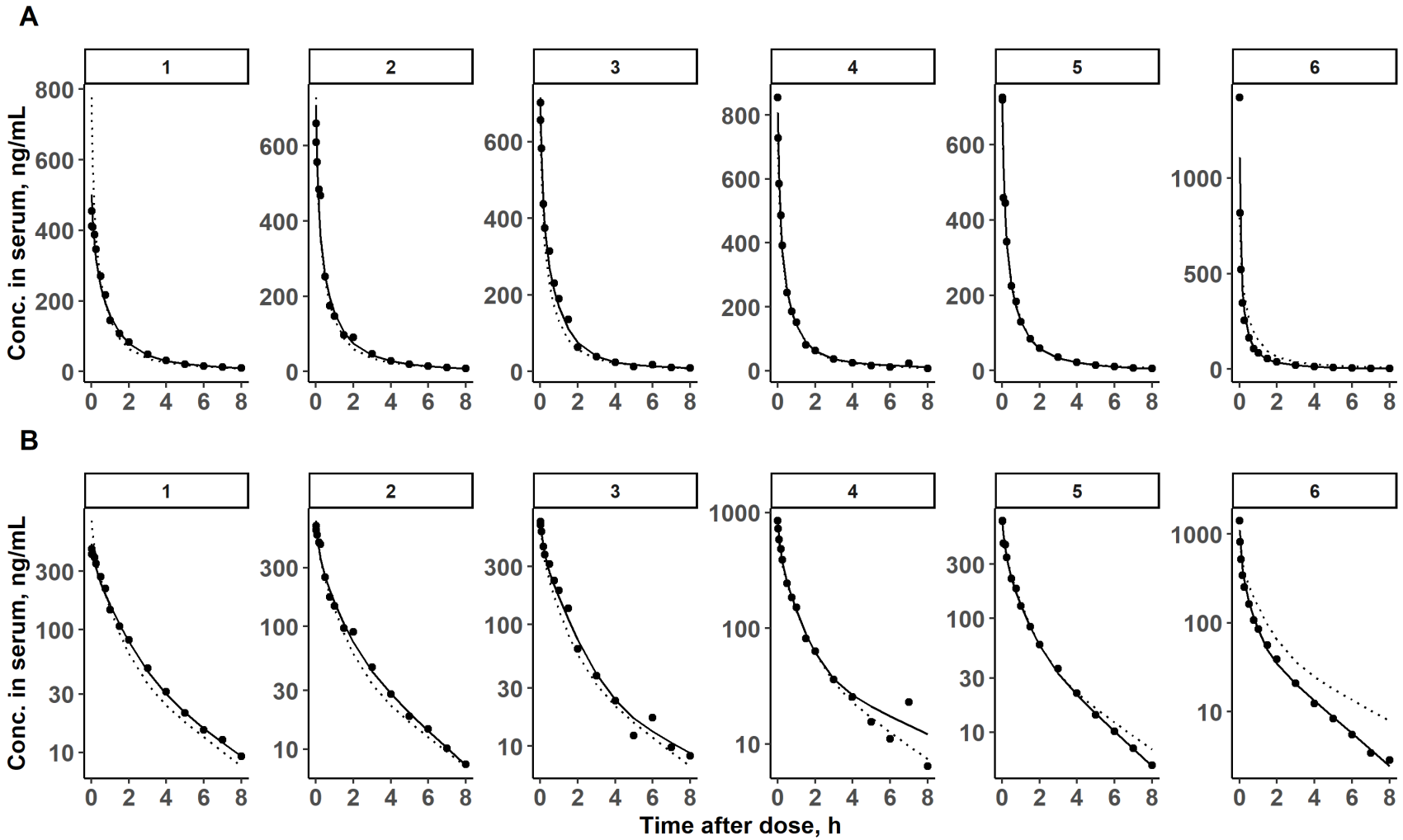

Fig. S5a Individual plots for tramadol serum concentration in pigs (n = 6; pig 1-6) on the **A.** linear and **B.** semi-logarithmic scale. The dots represent observed concentrations. Solid lines depict individual predictions (IPRED), dotted lines show population predictions (PRED).

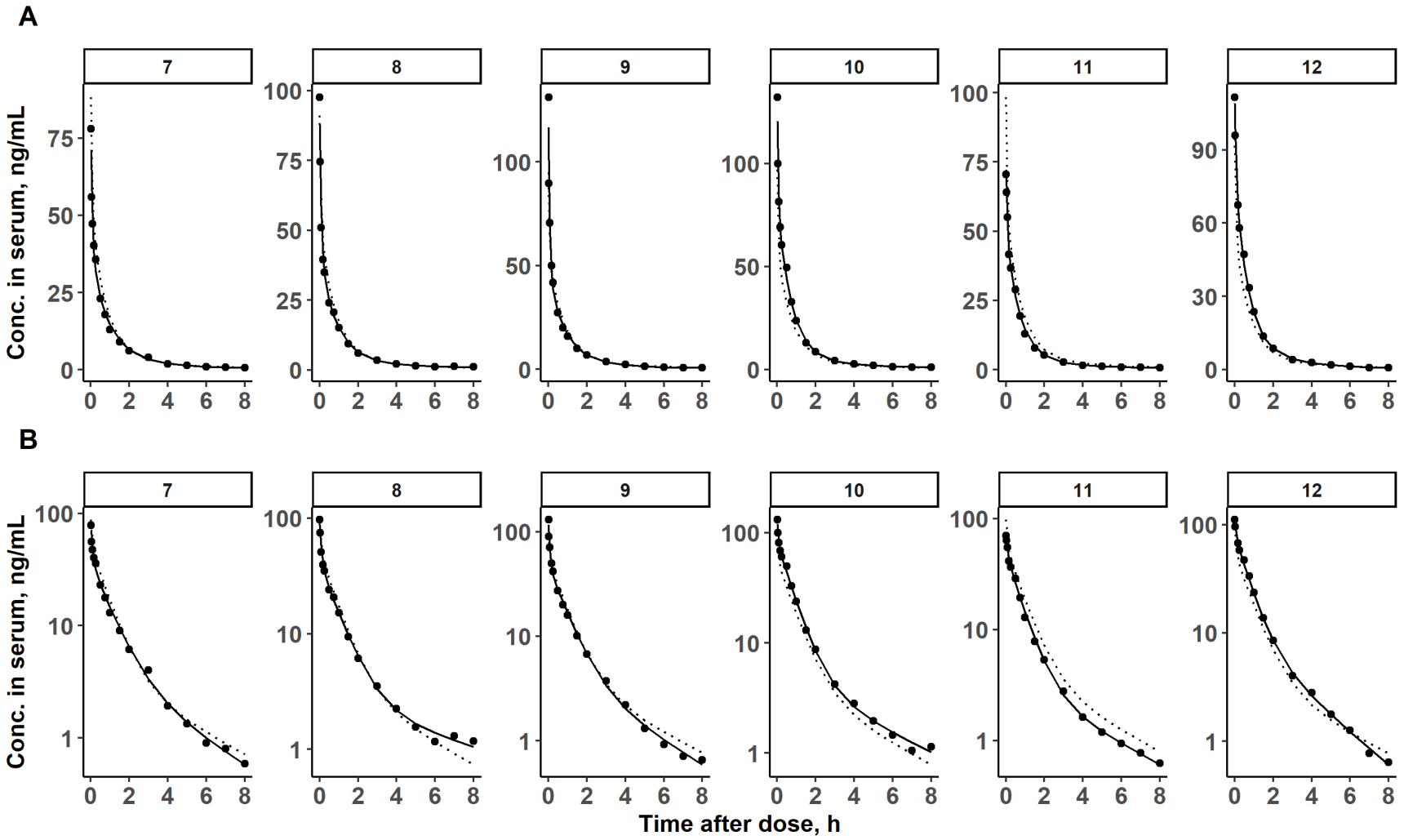

Fig. S5b Individual plots for U-47700 serum concentration in pigs (n = 6; pig 7-12) on the **A.** linear and **B.** semi-logarithmic scale. The dots represent observed concentrations. Solid lines depict individual predictions (IPRED), dotted lines show population predictions (PRED).

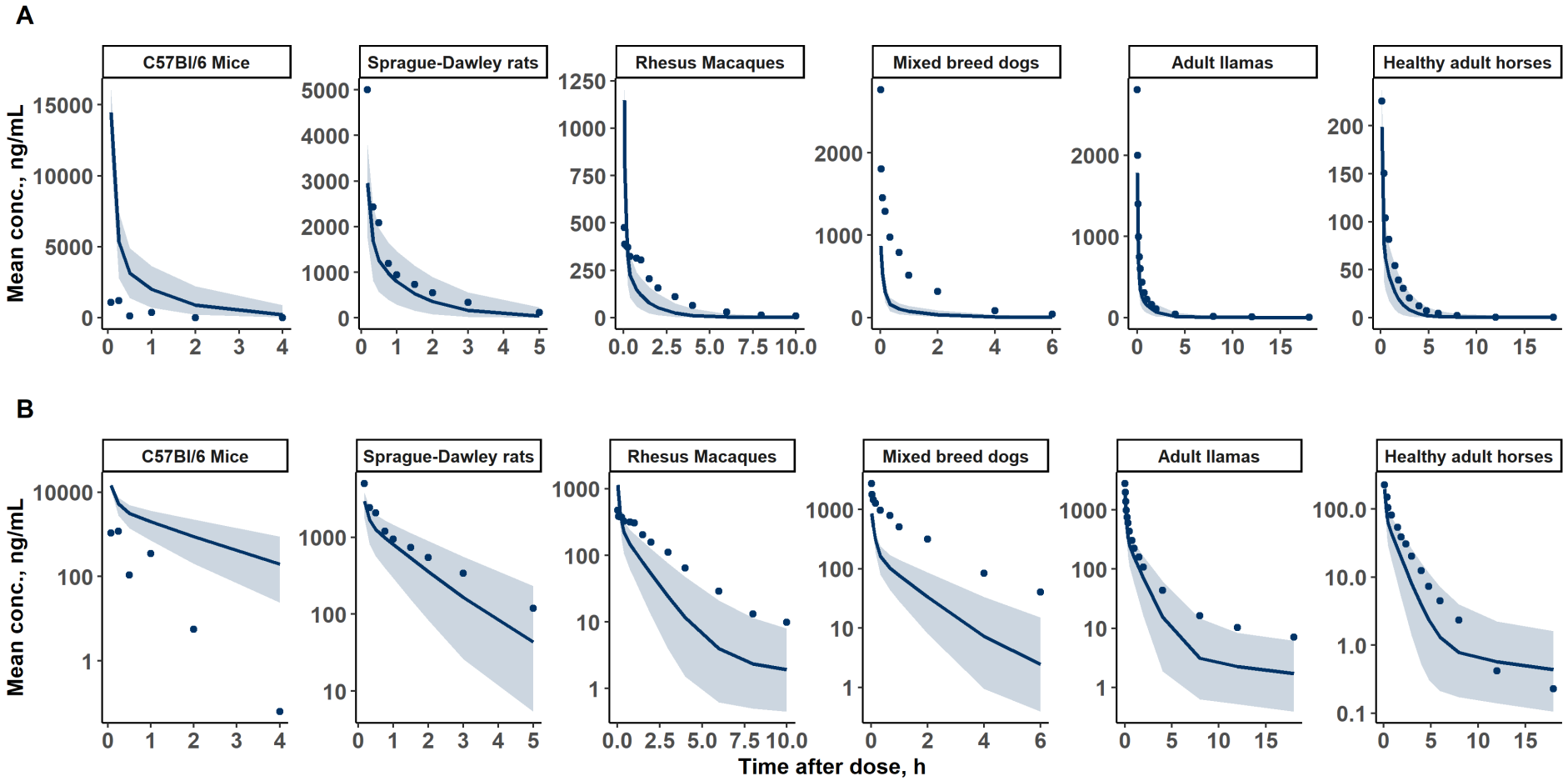

Fig. S6 Visual predictive checks (VPCs) of three-compartmental popTK model (with IIV on central clearance) for tramadol in different animal species on the **A.** linear and **B.** semi-logarithmic scale. The dots represent observed concentrations. The lines depict the median of the predicted concentrations and the shaded area is the 90% confidence interval of the predictions after 1000 simulations.

References

Campanero MA, Calahorra B, Valle M, Troconiz IF, Honorato J (1999) Enantiomeric separation of tramadol and its active metabolite in human plasma by chiral high-performance liquid chromatography: Application to pharmacokinetic studies. Chirality 11:272–279. https://doi.org/https://doi.org/10.1002/(SICI)1520-636X(1999)11:4<272::AID-CHIR3>3.0.CO;2-I

Cox S, Martín-Jiménez T, Amstel S, Doherty T (2011) Pharmacokinetics of intravenous and intramuscular tramadol in llamas. J Vet Pharmacol Ther 34:259–264. https://doi.org/10.1111/j.1365-2885.2010.01219.x

Evangelista Vaz R, Draganov DI, Rapp C, Avenel F, Steiner G, Arras M, Bergadano A (2018) Preliminary pharmacokinetics of tramadol hydrochloride after administration via different routes in male and female B6 mice. Vet Anaesth Analg 45:111-112. https://doi.org/10.1016/j.vaa.2016.09.007

Fernandez M, Wille SMR, Kummer N, Di Fazio V, Ruyssinckx E, Samyn N (2013) Quantitative analysis of 26 opioids, cocaine, and their metabolites in human blood by ultra performance liquid chromatography–tandem mass spectrometry. Ther Drug Monit 35:510-521. https://doi.org/10.1097/FTD.0b013e31828e7e6b

Gerace E, Salomone A, Luciano C, Di Corcia D, Vincenti M (2018) First case in italy of fatal intoxication involving the new opioid U-47700. Front Pharmacol 9:747. https://doi.org/10.3389/fphar.2018.00747

Jamali B, Sheikholeslami B, Hosseinzadeh Ardakani Y, Lavasani H, Rouini MR (2017) Evaluation of the ecstasy influence on tramadol and its main metabolite plasma concentration in rats. Drug Metab Pers Ther 32:137–145. https://doi.org/doi:10.1515/dmpt-2017-0018

Kelly KR, Pypendop BH, Christe KL (2015) Pharmacokinetics of tramadol following intravenous and oral administration in male rhesus macaques (Macaca mulatta). J Vet Pharmacol Ther 38:375–382. https://doi.org/10.1111/jvp.12194

Knych HK, Corado CR, Mckemie DS, Steffey EP (2013) Pharmacokinetics and selected pharmacodynamic effects of tramadol following intravenous administration to the horse. Equine Vet J 45:490–496. https://doi.org/https://doi.org/10.1111/j.2042-3306.2012.00688.x

Matuszewski BK, Constanzer ML, Chavez-Eng CM (2003) Strategies for the assessment of matrix effect in quantitative bioanalytical methods based on HPLC-MS/MS. Anal Chem 75:3019-3030. https://doi.org/10.1021/ac020361s

McMillan CJ, Livingston A, Clark CR, Dowling PM, Taylor SM, Duke T, Terlinden R (2008) Pharmacokinetics of intravenous tramadol in dogs. Can J Vet Res 72:325–331

Meyer MR, Rosenborg S, Stenberg M, Beck O (2015) First report on the pharmacokinetics of tramadol and O-desmethyltramadol in exhaled breath compared to plasma and oral fluid after a single oral dose. Biochem Pharmacol 98:502–510. https://doi.org/https://doi.org/10.1016/j.bcp.2015.09.008

Nordmeier F, Doerr A, Laschke MW, et al (2020) Are pigs a suitable animal model for in vivo metabolism studies of new psychoactive substances? A comparison study using

different in vitro/in vivo tools and U-47700 as model drug. Toxicol Lett 329:12-19. https://doi.org/https://doi.org/10.1016/j.toxlet.2020.04.001

Nordmeier F, Doerr AA, Potente S, et al (2021) Perimortem distribution of U-47700, tramadol and their main metabolites in pigs following intravenous administration. J Anal Toxicol (*submitted*)

Peters F, Paul L, Musshoff F, et al (2009) Anhang B zur Richtlinie der GTFCh zur Qualitätssicherung bei forensisch-toxikologischen Untersuchungen Anforderungen an die Validierung von Analysemethoden. Toxichem Krimtech. https://www.gtfch.org/cms/images/stories/files/GTFCh_Richtlinie_Anhang B_Validierung_Version 1.pdf. Accessed March 2021

Quetglas EG, Azanza JR, Cardenas E, Sádaba B, Campanero MA (2007) Stereoselective pharmacokinetic analysis of tramadol and its main phase I metabolites in healthy subjects after intravenous and oral administration of racemic tramadol. Biopharm Drug Dispos 28:19–33. https://doi.org/https://doi.org/10.1002/bdd.526

Schaefer N, Kettner M, Laschke MW, et al (2017) Distribution of synthetic cannabinoids JWH-210, RCS-4 and Δ 9-tetrahydrocannabinol after intravenous administration to pigs. Curr Neuropharmacol 15:713–723. https://doi.org/10.2174/1570159X15666161111114214

Schaefer N, Wojtyniak J-G, Kettner M, et al (2016) Pharmacokinetics of (synthetic) cannabinoids in pigs and their relevance for clinical and forensic toxicology. Toxicol Lett 253:7–16. https://doi.org/10.1016/J.TOXLET.2016.04.021

Schaefer N, Wojtyniak J-G, Kroell A-K, et al (2018) Can toxicokinetics of (synthetic) cannabinoids in pigs after pulmonary administration be upscaled to humans by allometric techniques? Biochem Pharmacol 155:403–418. https://doi.org/10.1016/J.BCP.2018.07.029

Seither J, Reidy L (2017) Confirmation of carfentanil, U-47700 and other synthetic opioids in a human performance case by LC-MS-MS. J Anal Toxicol 41:493-497. https://doi.org/10.1093/jat/bkx049

Smith CR, Truver MT, Swortwood MJ (2019) Quantification of U-47700 and its metabolites in plasma by LC-MS/MS. J Chromatogr B 1112:41–47. https://doi.org/https://doi.org/10.1016/j.jchromb.2019.02.026

United States Patent (2018). Intravenous administration of tramadol. US 10,022, 321 B2. Accessed March 2021.

Yılmaz B, Erdem AF (2015) Simultaneous determination of tramadol and its metabolite in human plasma by GC/MS. J AOAC Int 98:56–61. https://doi.org/10.5740/jaoacint.14-085

3.4 Perimortem distribution of U-47700, tramadol and their main metabolites in pigs following intravenous administration (105)

This is a pre-copyedited, author-produced version of an article accepted for publication in Journal of Analytical Toxicology following peer review. The version of record (105) and the Electronic Supplement Material is available online at:

(DOI: 10.1093/jat/bkab044; accepted by mail of 02.05.2021)

Authors Contributions Frederike Nordmeier conducted and evaluated the experiment as well as composed the manuscript; Adrian Doerr, Nadja Walle, and Stefan Potente assisted at the execution of the animal experiments; Matthias W. Laschke and Michael D. Menger carried out and enabled the animal experiments and assisted with scientific discussions; Nadine Schaefer, Markus R. Meyer, and Peter H. Schmidt assisted with scientific discussions and the development of the experiments as well as supervised the research.

Perimortem distribution of U-47700, tramadol and their main metabolites in pigs following intravenous administration

Frederike Nordmeier[1], Adrian A. Doerr[1], Stefan Potente[1], Nadja Walle[1], Matthias W. Laschke[2], Michael D. Menger[2], Peter H. Schmidt[1], Markus R. Meyer[3], and Nadine Schaefer[1*]

[1]Institute of Legal Medicine, Saarland University, 66421 Homburg, Germany

[2]Institute for Clinical and Experimental Surgery, Saarland University, 66421 Homburg, Germany

[3]Department of Experimental and Clinical Toxicology, Institute of Experimental and Clinical Pharmacology and Toxicology, Center for Molecular Signaling (PZMS), Saarland University, 66421 Homburg, Germany

*Author to whom correspondence should be addressed. Email: nadine.schaefer@uks.eu

Abstract

In spite of a decreasing number of new releases, New Synthetic Opioids (NSO) are gaining increasing importance in postmortem (PM) forensic toxicology. For the interpretation of analytical results, toxicokinetic (TK) data, e.g. on tissue distribution, are helpful. Concerning NSO, such data are usually not available due to the lack of controlled human studies. Hence, a controlled TK study using pigs was carried out and the tissue distribution of U-47700 and tramadol as reference was examined. Twelve pigs received an intravenous dose of 100 µg/kg body weight (BW) U-47700 or 1000 µg/kg BW tramadol, respectively. Eight hours after administration, the animals were put to death with T61. Relevant organs, body fluids and tissues were sampled. After homogenization and solid-phase extraction, quantification was performed applying standard addition and liquid chromatography-tandem mass spectrometry. At the time of death, the two parent compounds were determined in all analyzed specimens. Regarding U-47700, concentrations were highest in duodenum content, bile fluid and adipose tissue (AT). Concerning tramadol, next to bile fluid and duodenum content, highest concentrations were determined in the lung. Regarding the metabolites, *N*-desmethyl-U-47700 and *O*-desmethyltramadol (ODT) were detected in all analyzed specimens except for AT (ODT). Higher metabolite concentrations were found in specimens involved in metabolism. *N*-desmethyl-U-47700 showed much higher concentrations in routinely analyzed organs (lung, liver, kidney) than U-47700. To conclude, besides the routinely analyzed specimens in PM toxicology, AT, bile fluid and duodenum content could serve as alternative matrices for blood, urine or standard specimens such as kidney or liver. In case of U-47700, quantification of the main metabolite *N*-desmethyl-U-47700 is highly recommendable.

Introduction

Although the number of new releases of New Psychoactive Substances and following also the number of appearances of New Synthetic Opioids (NSO) decreases, NSO still pose a public health concern (1). One of the most discussed non-fentanyl NSO is U-47700 (3,4-dichloro-*N*-[2-(dimethylamino)cyclohexyl]-*N*-methylbenzamide), patented by the Upjohn Company in 1978. U-47700 is structurally not related to classical opioids such as morphine or heroine, but demonstrated a 7.5-fold higher binding affinity to the μ-opioid receptor (MOR) than morphine (2,3). Due to its high toxic potential, U-47700 is scheduled in Germany and many other European countries (4).

Several fatalities attributable to this substance were reported in the literature (5–8). In the context of postmortem (PM) toxicology, the knowledge concerning the tissue distribution of a substance is important when interpreting analytical results, especially if commonly analyzed body fluids as blood or urine are not available.

However, published data on U-47700 provide only little information on toxicokinetic (TK) properties such as tissue distribution (9). Furthermore, it has to be kept in mind that authentic PM data are always fraught with some uncertainties, e.g. the missing knowledge on the dose, time and route of administration as well as the PM interval (10–14). Additionally, in most case reports (15), only the parent compound was studied whilst the distribution of metabolites was not investigated. Indeed, in case of a longer survival time after drug intake, parent compounds might have diminished completely, and analysis of the metabolites would therefore gain major importance.

As controlled human TK studies cannot be performed, animal models may serve as alternative. However, commonly used small animals such as mice or other rodents are rather unsuitable for extensive and multiple sampling due to their small organ size. In contrast, pigs enable extensive tissue sampling. Generally, pigs display a great similarity to the human

species in terms of metabolism due to a comparable cytochrome P450 monooxygenase pattern (16), as well as anatomical and physiological properties (17). Moreover, pigs have been proven to be a suitable TK model for different (synthetic) cannabinoids (18–23). By means of the established pig model, prediction of human THC exposure was successful (21). In addition, the tissue distribution in the pig model was comparable to published data (22). Therefore, a TK model in pig serum has previously been developed for U-47700 and tramadol as a reference (24). This model appeared to be a suitable tool for the assessment of TK data in serum. Furthermore, metabolic patterns of U-47700 in pigs were comparable to human patterns (25).

In this context, the aim of the present study was to elucidate the distribution of U-47700, tramadol and their main metabolites in various tissues and fluids in pigs following controlled intravenous (i.v.) administration. Furthermore, possible differences of drug concentrations in adipose tissue (AT) collected from different anatomical sites should be assessed.

Materials and Methods

Chemicals and reagents

The chemicals and reagents as well as the preparation of the buffers and blank whole blood specimens are described in the Supplementary data.

Stock solutions, calibration standards, and quality control samples

The standard stock solutions, calibration standards and quality control samples were prepared as described in the Supplementary data.

Liquid chromatography-tandem mass spectrometry (LC-MS/MS) conditions

The LC-MS/MS conditions including instrumentation, chromatographic and mass spectrometric conditions are described in detail in the Supplementary data.

Animals

As already described in previous studies (19–23,25), all experiments were performed in accordance with the German legislation on protection of animals and the National Institute of Health Guide for the Care and Use of Laboratory Animals (permission number: 32/2018). Twelve domestic male pigs (Swabian Hall strain, mean body weight (BW) 42.8 ± 1.9 kg) were used for the study. The animals had daily standard chow and water ad libitum. The pigs were kept fasting a night before the experiment, but still had free access to water.

Surgical procedure

The surgical procedure has already been described elsewhere (19,25) and is described in detail in the Supplementary data.

Study design

As previously described (24), the study included 12 pigs, which were divided into two different groups. Six pigs received a 100 µg/kg body weight (BW) dose of U-47700. The pigs of the other group (n = 6) received a 1000 µg/kg BW dose of tramadol. A stock solution of 4 mg/mL U-47700 (solid) was prepared in ethanol for i.v. drug administration. Volumes of 1005-1120 µL were applied to obtain a 100 µg/kg BW dose. For tramadol, volumes of 906-1134 µL of a tramadol-HCl solution were used to reach a 1000 µg/kg BW dose. All volumes were filled up with sodium chloride 0.9% to a volume of 10 mL. The dose was administered within 30 sec by i.v. administration of the prepared solutions into the jugular vein. Eight hours after administration, the animals were euthanized with T61 (embutramide, mebenzonium,

tetracaine; 0.12 mL/kg BW, Intervent Deutschland GmbH, Unterschleissheim, Germany) and the following organs, tissues, and body fluids were collected: brain, lung, liver, kidney, skeletal muscle tissue from the hind leg, bile fluid, duodenum content, peripheral blood from the jugular vein (PB), central blood (CB) and AT (subcutaneous (s.c.) from ventral, perirenal as well as dorsal).

Sample preparation

Blood specimens

The PB and CB samples were prepared according to a fully validated method. Validation (selectivity, specificity, linearity, limit of detection/quantification, matrix effects, accuracy, precision, stability) was carried out according to the guidelines of the German Society of Toxicological and Forensic Chemistry (26). Limits of detection were 0.1 ng/mL for U-47700, *N*-desmethyl-U-47700 and tramadol, and 3.5 ng/mL for ODT. Lower limits of quantification were assessed at 0.5 ng/mL for U-47700 and metabolite, at 1 ng/mL for tramadol and at 10 ng/mL for ODT. Briefly, an aliquot of 1 mL whole blood was added to a mixture of 50 µL of an ethanolic stable-isotope-labeled internal standard mixture solution (SIL-IS; 10 ng/50 µL of *N*-desmethyl-U-47700-d_3, tramadol-C_{13}-d_3, and *O*-desmethyltramadol- d_6), 50 µL of ethanol and 2 mL phosphate buffer. For the preparation of calibrators and quality controls, 50 µL of ethanol were replaced by 50 µL of the appropriate spiking solution. After vortexing and centrifugation at 3,200 g for 8 min, SPE was carried out as described in the Supplementary data. Quantification was applied with calibration curves for whole blood.

Tissue specimens

An amount of 2 g solid tissue (brain, lung, liver, kidney, skeletal muscle tissue), bile or duodenum content was homogenized (tissue/fluid/content:water 1:5, w/w). For AT specimens, an amount of 2 g tissue was homogenized with acetonitrile (tissue/acetonitrile 1:5,

w/w). Afterwards, the homogenized tissue was centrifuged for 8 min at 3,200 g. For the standard addition approach, four 1 mL portions of the supernatants were prepared with or without addition of 50 µL of the three different calibrator concentrations of U-47700 and *N*-desmethyl-U-477700 or tramadol and *O*-desmethyltramadol (Supplementary Table S1). In case of the pigs having received the U-47700 dose, the supernatant of homogenized duodenum content was diluted with phosphate buffer 1:2 (v/v) prior to analysis. Considering the pigs with the tramadol dose, supernatants of homogenized lung and duodenum content were diluted 1:2 (v/v) and supernatants of homogenized bile fluid 1:10 (v/v) with phosphate buffer prior to analysis. To all prepared homogenates, a mixture of 50 µL of the ethanolic SIL-IS solution (20 ng/50 µL) and 2 mL phosphate buffer was added. After vortexing, the samples were centrifuged at 3,200 g for 8 min and SPE was carried out as described in the Supplementary data.

Standard addition approach

For quantification of the drugs and their metabolites, a standard addition approach was chosen. A detailed description is given in the Supplementary.

Statistical tests

For the comparison of concentrations detected in AT samples collected from different regions, a one-way ANOVA followed by a Bonferroni posthoc-test was performed. An unpaired two-tailed Student's t-test followed by an f-test was applied to compare *N*-desmethyl-U-47700 tissue concentrations of pig S4 with the mean concentration. Statistics were carried out using GraphPad Prism 5.00 (GraphPad Software, San Diego, CA, USA).

Prediction of octanol-water partition coefficient (LogP)

LogP values for U-47700, *N*-desmethyl-U-47700, and ODT were calculated with the ACD/ChemSketch 2018.1.1 software (Toronto, Canada).

Results

Standard addition approach

A standard addition approach was applied for quantification of U-47700, tramadol and their metabolites. Regression coefficients (r^2) for U-47700 and tramadol as well as for their metabolites ranged between 0.98 and 1.0. A discussion about the applicability of this approach is given in the Supplementary.

Distribution patterns

Mean concentrations of the drugs and their metabolites including standard error of mean (SEM) are presented in Figure 1 and 2. Concentrations for each pig are given in Supplementary Table S3 and S4.

At the time of death, the two parent compounds could be determined in all analyzed tissues or body fluids. Regarding U-47700, the highest concentrations were found in duodenum content followed by bile fluid, and the AT specimens (Figure 1). The highest tramadol concentrations were detected in bile fluid followed by duodenum content and lung (Figure 2). The lowest concentrations of the parent compounds were found in PB and CB, but the concentrations in most cases were still higher than the limit of detection of the method (Supplementary Table S3/S4).

The metabolites could be detected in every analyzed specimen with one exception. ODT was not found in all AT specimens. In general, higher concentrations of the metabolites were found in tissues/body fluids involved in metabolism or excretion such as lung, liver, kidney, bile and duodenum content. Highest concentrations of *N*-desmethyl-U-47700 were detected in

duodenum content followed by lung and liver (Figure 1). Conversely, this metabolite could only be detected in very low concentrations in the blood specimens as well as in skeletal muscle tissue. Regarding ODT, highest concentrations were found in bile fluid as well as in duodenum content and kidney (Figure 2). Concerning the metabolites, an overall higher interindividual variability was observed compared to the parent compounds. Especially regarding pig S4, metabolite concentrations were significantly ($p<0.05$) higher in many tissue specimens (kidney, brain, and muscle) compared to those of the other pigs receiving U-47700 (Supplementary Table S3). Possible explanations are given in the Supplementary.

Concentrations in AT specimens collected from different regions

In case of U-47700 and *N*-desmethyl-U-47700 no significant differences in concentrations could be specified regarding AT specimens sampled from different regions. Tramadol concentrations in perirenal AT were lower than the respective dorsal and s.c. concentrations, but differences were not significant ($p>0.05$). ODT could not be detected in dorsal and s.c. AT and only low concentrations could be determined in the perirenal AT of 4 pigs.

Discussion

Dosage

The current study on the perimortem tissue distribution of U-47700 is part of a comprehensive TK study assessing different TK parameters of U-47700. Tramadol is an opioid structurally most closely related to U-47700. In addition, it has already been well studied in animals and men with regard to its pharmacokinetic properties. Thus, tramadol was administered as reference compound in this study to compare the TK data with those assessed for U-47700 and to verify, whether the pig model is suitable for the elucidation of TK parameters of opioids. For this purpose, a 100 µg/kg BW or 1000 µg/kg BW dose of U-47700 or tramadol

was administered intravenously to pigs, respectively. This resulted in total doses of 4.2 ± 0.1 mg of U-47700 and 42.8 ± 2.1 mg of tramadol. Regarding U-47700, common users' (low) dosage for i.v. administration are in the range of a few mg (27). Thus, a comparable net dose was chosen in this study to assure that the animals remained under the influence of measurable concentrations but were not exposed to relevant toxic effects. The tramadol concentration was comparable to common therapeutic i.v. dosages (28).

Distribution patterns

U-47700 and *N*-desmethyl-U-47700

In general, higher concentrations of the metabolite *N*-desmethyl-U-47700 were detected in most organs in comparison to U-47700. On the contrary, U-47700 displayed higher concentrations in bile and duodenum content. Previous studies demonstrated that both compounds do not undergo glucuronidation (25). Thus, a conjugate cleavage would not change this ratio. A higher parent compound concentration in bile as compared to the metabolite supports the suggestion of a renal excretion of *N*-desmethyl-U-47700 and no predisposition of this metabolite for enterohepatic circulation with a biliary excretion. In addition, bile and duodenum content showed very high U-47700 concentrations compared to other organs (Figure 1). Combined with the lower U-47700 concentration in the kidney a biliary excretion of the unmetabolized compound is conceivable.

As far as AT specimens are concerned, low metabolite concentrations were found as compared to U-47700. The lower lipophilicity of *N*-desmethyl-U-47700 (LogP = 2.65) compared to U-47700 (LogP = 3.14) could be one explanation for a minor accumulation in AT.

Regarding the volume of distribution (V_d) of U-47700 estimated in a previous study (24), a preliminary value of 0.97 L/kg (calculated by linear regressions of a non-compartment model) indicates an affinity to tissues with following accumulation and a medium distribution

into deep compartments. Hence, a distribution from central compartments into peripheral compartments as AT is also suggested by this value. Furthermore, U-47700 seemed to be high-grade metabolized. Together with the preliminary value for the clearance of 0.017 L/min*kg (24) a (rapid) decrease of the serum level of U-47700 is likely.

Lungs showed a very high concentration of the metabolite compared to the concentration of U-47700. A general high affinity of lipophilic and basic substances to lung tissue has already been observed (29,30). Since U-47700 contains a tertiary amine with strong basic properties, metabolization of U-47700 in lungs and accumulation of its even more basic metabolite might be possible.

Additionally, liver and kidney tissue displayed much higher concentrations of the metabolite than of the parent compound. This might be caused by metabolization of U-47700 in the liver and subsequent renal excretion via the kidney. Due to the higher hydrophilicity of *N*-desmethyl-U-47700, an excretion of this metabolite into urine is likely.

Apart from this, lung, liver and kidney tissue are standard specimens and should be analyzed in routine PM toxicology. Considering the moderate concentration of the parent compound and a much higher metabolite concentration, *N*-desmethyl-U-47700 should be analyzed in a routine approach, as well. Analyzing pig urine specimens (data not shown) as part of this comprehensive TK study (25), concentrations of the metabolite were also higher throughout the whole experiment and *N*-desmethyl-U-47700 showed an increased serum half-life as compared to U-47700 (31). Thus, particularly in intoxication cases with long term intervals between consumption and death, the sole detection of *N*-desmethyl-U-47700 could be used as evidence of a consumption of U-47700 which might not be detectable anymore. Even though a direct appraisal from tissue concentrations to a possible blood concentration or time of consumption might not be possible, the inclusion of the metabolite as additional target for the analysis of those specimens is useful.

Another noticeable finding is the higher concentration of the metabolite in brain tissue. Diffusion processes through the blood-brain-barrier (BBB) are facilitated by higher lipophilicity and a smaller molecule size (32). Loss of one methyl group has no relevant effect in terms of molecule size, but *N*-desmethyl-U-47700 (LogP = 2.65) is less lipophilic than U-47700 (LogP = 3.14). If the transfer via the BBB was driven by diffusion processes and not by specified transporters, a higher concentration of *N*-desmethyl-U-47700 than of U-47700 would be surprising. However, specified transporters with a higher affinity to the metabolite as well as local metabolism of U-47700 within the brain tissue could be a possible explanation for this phenomenon. A previous study showed an involvement of a wide range of human cytochrome-P450 (CYP) monooxygenases in the formation of *N*-desmethyl-U-47700 (25). Yet, involvement of porcine CYP enzymes is difficult to constitute. Meanwhile, different studies about CYP enzymes have been published using different pig breeds (17,33). A high sequence homology between conventional pig CYPs and those of minipigs is expected, but differences in e.g. expression levels or substrate specificity have to be considered (33). However, there is a high sequence homology between many human and porcine CYPs (17), also between those monooxygenases involved in *N*-demethylation of U-47700. Thus, *N*-demethylation might be catalyzed by a widespread range of porcine CYPs, as well. Brain tissue is rich in CYPs (17). Hence, *N*-demethylation of U-47700 in brain tissue is conceivable.

Tramadol and ODT

Tramadol and ODT showed similar distribution patterns throughout all analyzed tissues and fluids with general higher parent compound concentrations as compared to those of ODT. There are only two exceptions. First, the liver showed similar to slightly higher concentrations of ODT as compared to tramadol. It is well known that *O*-demethylation of tramadol to the active metabolite ODT primarily occurs in the human liver via CYP2D6 (34-36), but porcine

CYP2D monooxygenases probably differ from human enzymes. However, primary metabolism of tramadol in pigs might also occur in the liver.

Second, AT showed high tramadol concentrations, whilst nearly no ODT was detectable in this tissue. One possible explanation for high concentrations of tramadol in AT as composed to lower concentrations in the liver might be the high V_d. Tramadol displayed a V_d of 2.6-2.9 L/kg in human (37) and a much higher value of 6.7 L/kg in piglets (40). These high values indicate a distribution into deep compartments.

Another peculiarity deserving further explanations is the much higher tramadol/ODT content in lung tissue as compared to kidney. Tramadol and its metabolites are nearly completely excreted via the kidneys (34). Therefore, higher concentrations in lung tissue compared to those in kidney tissue are unusual at first sight. Speculating about probable reasons one has to keep in mind, that especially lipophilic and basic substances have a high affinity to lung tissue with subsequent metabolization (29,30). Hence, accumulation and metabolism of tramadol and thus high concentrations of tramadol/ODT are possible, since tramadol has basic properties (39). Furthermore, a high concentration of tramadol in lung might also have resulted from the administration of the substance via the jugular vein. The blood flow from the jugular vein via the right heart into the pulmonary artery and the lung before returning to the left heart and reaching the body circulation may have facilitated the drug uptake as well. However, the mean concentrations in lung tissue showed a high SD caused by one pig outlier showing a much higher concentration of tramadol and ODT in lungs compared to all other. Apart from this value, the tramadol/ODT concentrations in lung and kidney specimens are comparable.

Additionally, very high concentrations of tramadol were found in bile and duodenum content compared to all other specimens. This is another surprising fact, keeping in mind that tramadol is not subject to enterohepatic circulation and biliary excretion (34).

It is known, that tramadol shows a very fast tissue distribution within minutes to hours and a high tissue affinity (40,41). Furthermore, tramadol is metabolized much more rapidly in animals than in humans (34). In a previous study, maximum serum concentrations of ODT were reached after only 15 min (24), whereas in human maximum metabolite concentrations were usually reached after hours (42). This finding indicates a rapid metabolism of tramadol in pigs followed by a possible fast excretion of tramadol/ODT. Thus, an extensive metabolism and excretion before the end of the experiment (faster than 8 h) might explain the only low to moderate concentrations of tramadol/ODT in the different tissue specimens, especially in those, which are involved in metabolism.

In a first view, a higher concentration of tramadol than that of ODT in brain tissue seemed to be unexpected, keeping in mind that ODT is showing much higher MOR affinity than tramadol. However, both, tramadol and ODT pass the BBB, but the transport of tramadol is supported and facilitated through higher lipophilicity. In addition, metabolism also occurs in brain (44-46). Furthermore, Tao et al. (43) showed a preferential brain versus plasma distribution of tramadol over ODT in mice and rats.

Comparison of U-47700 and tramadol and their metabolites

At the time of death, U-47700 and tramadol were still detectable in PB and CB. However, concerning only low to moderate concentrations of U-47700, tramadol, and their metabolites, standard specimens such as kidney or liver should additionally be analyzed in routine PM toxicology.

Regarding U-47700, tramadol and their metabolites, in routine specimens rather similar distribution patterns were determined with little exceptions. First, higher metabolite concentrations of U-47700 were detected in different organs whereas tramadol displayed higher concentrations than ODT in most tissues. As mentioned before, this difference could be explained by faster metabolization and elimination of tramadol. Second, U-47700

concentrations in liver tissue were significantly higher compared to other organs than tramadol concentrations, which were comparable to those determined in skeletal muscle tissue. A rapid metabolization and transport out of the liver might be a possible explanation for this low tramadol concentration. Furthermore, tramadol displayed a very high concentration in duodenum content and much higher concentration in bile. On the contrary, U-47700 showed very high concentrations in bile fluid as well, but much higher concentrations in duodenum content.

The data of the current study showed a high concentration of U-47700 and tramadol in AT specimens compared to the moderate tissue concentrations indicating a persistence of these drugs in AT. In addition, *N*-desmethyl-U-47700 (LogP = 2.65) was present in moderate concentrations in AT specimens, but ODT (LogP = 1.86) was not detectable. Betschart et al. (47) established the hypothesis that drugs with a LogP value below 2 are unlikely to be stored in AT. In comparison to the concentrations in other organs, U-47700 showed much higher concentrations in AT than its metabolite and tramadol. This difference corresponds to the descending order of the LogP values: 3.14 (U-47700), 2.65 (*N*-desmethyl-U-47700), and 2.51 (tramadol) (39). Compared to another study examining an opioid (48), fentanyl showed a lower distribution into AT despite a higher lipophilicity (LogP = 4.05) (49). This fact indicates that accumulation in AT is not simply a matter of lipid solubility and other factors such as basic properties of the chemical structure play an important role as well (50).

Comparison with published data

In general, published human PM data on tissue distribution of U-47700 and tramadol are derived from case reports and thus from case-by-case observations. In contrast to our experimental concept of a controlled animal study, in which a moderate dose was deliberately chosen to ensure that the animals were not exposed to toxic effects of the drug, most of the case reports are dealing with fatal intoxications mainly resulting in much higher drug

concentrations as compared to our study. Furthermore, data were only obtained analyzing blood, urine, or a limited choice of specimens in most of the cases. In addition, analytical methods differed from case to case. Because of an unknown background, case reports often suffer from uncertainties such as the unknown dosage and time of intake and thus an unknown survival time, unknown user habits or unspecified postmortem interval. Amongst other variables, the route of consumption could have an impact on the tissue distribution. With respect to other common consumption manners (especially orally and nasally for U-47700), the distribution pattern reported in those case reports could differ from our results. In general, other routes of administration might lead to lower concentrations of the parent compounds and the metabolites in different specimens as compared to concentrations following i.v. administration due to first pass effects and a bioavailability less than 100% (22). Furthermore, an i.v. administration could lead to higher concentrations in lung and heart as already mentioned above. On the other hand, after oral consumption, higher concentrations of the metabolite in liver, bile and duodenum content are conceivable. For these reasons, a comparison of the case reports with our study is only possible to a limited extent. It is even more astonishing that parallels between our data and those of different case reports were observed.

In most of the published human case reports on intoxications with U-47700 only blood concentrations were reported and the tissue distribution of this NSO has not been discussed (10,11,13,51-53). Just a few data were published regarding the tissue distribution in PM cases (5,6,15,54-56). Nevertheless, none of these mentioned case reports described metabolite tissue distribution as in our study and no controlled animal studies for examination of tissue distribution of U-47700 have been performed, yet. In alignment with our results, most of them reported much higher tissue concentrations than blood concentrations. Dziadosz et al. (15) reported two cases of lethal intoxications with U-47700 with a rather similar tissue distribution as in our pig study and thus with higher concentrations found in liver, lung and

kidney as compared to concentrations in brain. As in our study, in other case reports high concentrations of U-47700 were determined in liver and bile fluid as well (5,55,56).

Regarding tramadol, data from human fatalities have already been reported regarding both, only blood/urine concentrations or blood and tissue distribution (48,57-62). Concerning metabolite concentrations, in all cases higher tramadol than ODT concentrations were found as in our study. A few dedicated studies on the topic shall be discussed in more detail: Brockbals et al. (48) identified higher compound concentrations in tissue specimens than in blood in two PM cases. In alignment to our results, high concentrations of tramadol were determined in lung, followed by kidney and liver. ODT distribution was similar to the tramadol distribution. In correlation to our findings, Musshoff et al. (61) identified highest concentrations of tramadol in bile fluid compared to moderate tissue concentrations in liver and kidney. Furthermore, in different cases concentrations in muscle tissue and in the brain were only low to moderate (60,61). In contrary to U-47700, several controlled animal studies on tissue distribution of tramadol were performed, as well. In acutely poisoned rats, similar distribution patterns were observed as compared to our study (63). Our results were in good agreement with those of Lamia et al. (64), determining tramadol concentrations in rabbit tissue in a controlled study after oral administration of lethal dosages. The same distribution pattern was estimated with some minor exceptions. Firstly, higher brain and slightly higher blood concentrations were assessed in the rabbit study as compared to our study. On the other hand, in our study much higher concentrations of tramadol were detected in bile fluid as compared to all other tissues. However, it has to be taken into consideration that the lethal dose in the rabbit study may have resulted in a shorter survival time that is to say a shorter period of time between the administration of the drug and sampling of the tissue specimens. Differences in the route of administrations would have an impact on the tissue distribution, too.

Summary and resulting recommendations for routine forensic PM analysis

In summary, besides routine samples of lung, liver and kidney, AT, bile fluid and duodenum content could serve as alternative matrices for the detection of the synthetic opioids U-47700 and tramadol in PM toxicology. Both substances were also detectable in brain and muscle tissue at the time of death. Regarding U-47700, determination of the main metabolite *N*-desmethyl-U-47700 should be preferred due to a much higher concentration in routinely analyzed specimens. Despite higher doses in intoxication cases, the blood concentration of both parent compounds and metabolites are expected to be very low. Especially with long term PM intervals, the detection in blood might be difficult and the analysis of the recommended specimens would be a good alternative.

Conclusion

Distribution patterns of the two synthetic opioids U-47700 and tramadol as well as their main metabolites *N*-desmethyl-U-47700 and ODT following i.v. administration were investigated in domestic pigs. The results suggest a rapid distribution of both parent compounds into tissues involved in absorption, metabolism, and excretion. As a conclusion, besides routinely analyzed tissue specimens (lung, liver, and kidney) bile fluid and duodenum content could serve as alternative matrices. In addition, both parent compounds showed an accumulation in AT. Therefore, this specimen might also be a recommendable matrix. In terms of U-47700, the main metabolite *N*-desmethyl-U-47700 showed much higher concentrations in all analyzed tissues/body fluids as compared to the parent compound. Thus, this metabolite should also be analyzed in PM cases.

Acknowledgements

The authors thank Benjamin Peters, the staff of the Institute for Legal Medicine at Saarland University and the staff of the Institute for Clinical & Experimental Surgery at Saarland University for their support and help during the study. We acknowledge the EU funded project ADEBAR (IZ25-5793-2016-27).

Conflict of Interest

The authors declare no conflict of interest.

Funding

This work has not received any financial support.

Ethical Approval

All experiments were performed in accordance with the German legislation on protection of animals and the National Institutes of Health Guide for the Care and Use of Laboratory Animals (permission number: 32/2018).

Data Availability Statement

The data underlying this article are available in the article and in its online supplementary material.

References

1. (2019) European drug report – Trends and developments. EMCDDA: European monitoring center of drugs and drug addiction. http://www.emcdda.europa.eu/system/files/publications/11364/20191724_TDAT19001ENN_PDF.pdf (accessed December 29, 2020).
2. (2016) U-47700 Critical review report agenda item 4.1. Expert committee on drug dependence. thirty-eighth meeting. World health organization. http://www.who.int/medicines/access/controlled-substances/4.1_U-47700_CritReview.pdf (accessed December 29, 2020).
3. Koch, K., Auwaerter, V., Hermanns-Clausen, M., Wilde, M. and Neukamm, M.A. (2018) Mixed intoxication by the synthetic opioid U-47700 and the benzodiazepine flubromazepam with lethal outcome: Pharmacokinetic data. *Drug Testing and Analysis*, 10, 1336-1341.
4. Bundesministerium der Justiz und für Verbraucherschutz Gesetz über den Verkehr mit Betäubungsmitteln (Betäubungsmittelgesetz - BtMG) Anlage II (zu § 1 Abs. 1). https://www.gesetze-im-internet.de/btmg_1981/anlage_ii.html (accessed October 29, 2020).
5. Mcintyre, I.M., Gary, R.D., Joseph, S. and Stabley, R. (2017) A Fatality Related to the Synthetic Opioid U-47700: Postmortem concentration distribution. *Journal of Analytical Toxicology*, 41, 158–160.
6. Chesser, R., Pardi, J., Concheiro, M. and Cooper, G. (2019) Distribution of synthetic opioids in postmortem blood, vitreous humor and brain. *Forensic Science International*, 305, 109999.
7. Armenian, P., Vo, K.T., Barr-Walker, J. and Lynch, K.L. (2017) Fentanyl, fentanyl analogs and novel synthetic opioids: A comprehensive review. *Neuropharmacology*, 134, 121-132.
8. Seither, J. and Reidy, L. (2017) Confirmation of carfentanil, U-47700 and other synthetic opioids in a human performance case by LC-MS-MS. *Journal of Analytical Toxicology*, 41, 493-497.
9. Solimini, R., Pichini, S., Pacifici, R., Busardò, F.P. and Giorgetti, R. (2018) Pharmacotoxicology of non-fentanyl derived new synthetic opioids. *Frontiers in Pharmacology*, 9, 654.
10. Mohr, A.L.A., Friscia, M., Papsun, D., Kacinko, S.L., Buzby, D. and Logan, B.K. (2016) Analysis of novel synthetic opioids U-47700, U-50488 and furanyl fentanyl by LC-MS/MS in postmortem casework. *Journal of Analytical Toxicology*, 40, 709-717.
11. Elliott, S.P., Brandt, S.D. and Smith, C. (2016) The first reported fatality associated with the synthetic opioid 3,4-dichloro-N-[2-(dimethylamino)cyclohexyl]-N-methylbenzamide (U-47700) and implications for forensic analysis. *Drug Testing and Analysis*, 8, 875-789.
12. Fleming, S.W., Cooley, J.C., Johnson, L., Clinton Frazee, C., Domanski, K., Kleinschmidt, K., et al. (2017) Analysis of U-47700, a novel synthetic opioid, in human urine by LC-MS-MS and LC-QToF. *Journal of Analytical Toxicology*, 41, 173-180.
13. Coopman, V., Blanckaert, P., Van Parys, G., Van Calenbergh, S. and Cordonnier, J. (2016) A case of acute intoxication due to combined use of fentanyl and 3,4-dichloro-N-[2-(dimethylamino)cyclohexyl]-N-methylbenzamide (U-47700). *Forensic Science International*, 266, 68–72.
14. Ruan, X., Chiravuri, S. and Kaye, A.D. (2016) Comparing fatal cases involving U-47700. *Forensic Science, Medicine, and Pathology*, 12, 369-371
15. Dziadosz, M., Klintschar, M. and Teske, J. (2017) Postmortem concentration distribution in fatal cases involving the synthetic opioid U-47700. *International Journal of Legal Medicine*, 131, 1555-1556.

16. Anzenbacher, P., Soucek, P., Anzenbacherova, E., Gut, I., Hrubý, K., Svoboda, Z., et al. (1998) Presence and activity of cytochrome P450 isoforms in minipig liver microsomes comparison with human liver samples. *Drug Metabolism and Disposition: The Biological Fate of Chemicals*, 26, 56–59.
17. Puccinelli, E., Gervasi, P. and Longo, V. (2011) Xenobiotic metabolizing cytochrome P450 in pig, a promising animal model. *Current Drug Metabolism*, 12, 507–525.
18. Schaefer, N., Kettner, M., Laschke, M.W., Schlote, J., Peters, B., Bregel, D., et al. (2015) Simultaneous LC-MS/MS determination of JWH-210, RCS-4, Δ9-tetrahydrocannabinol, and their main metabolites in pig and human serum, whole blood, and urine for comparing pharmacokinetic data. *Analytical and Bioanalytical Chemistry*, 407, 3775–3786.
19. Schaefer, N., Wojtyniak, J.-G., Kettner, M., Schlote, J., Laschke, M.W., Ewald, A.H., et al. (2016) Pharmacokinetics of (synthetic) cannabinoids in pigs and their relevance for clinical and forensic toxicology. *Toxicology Letters*, 253, 7–16.
20. Schaefer, N., Kettner, M., Laschke, M.W., Schlote, J., Ewald, A.H., Menger, M.D., et al. (2017) Distribution of synthetic cannabinoids JWH-210, RCS-4 and Δ 9-tetrahydrocannabinol after intravenous administration to pigs. *Current Neuropharmacology*, 15, 713–723.
21. Schaefer, N., Wojtyniak, J.-G., Kroell, A.-K., Koerbel, C., Laschke, M.W., Lehr, T., et al. (2018) Can toxicokinetics of (synthetic) cannabinoids in pigs after pulmonary administration be upscaled to humans by allometric techniques? *Biochemical Pharmacology*, 155, 403–418.
22. Schaefer, N., Kroell, A.-K., Koerbel, C., Laschke, M.W., Menger, M.D., Maurer, H.H., et al. (2019) Distribution of the (synthetic) cannabinoids JWH-210, RCS-4, as well as Δ9-tetrahydrocannabinol following pulmonary administration to pigs. *Archives of Toxicology*, 93, 2211–2218.
23. Schaefer, N., Kroell, A.-K., Koerbel, C., Laschke, M.W., Menger, M.D., Maurer, H.H., et al. (2020) Time- and temperature-dependent postmortem concentration changes of the (synthetic) cannabinoids JWH-210, RCS-4, as well as Δ9-tetrahydrocannabinol following pulmonary administration to pigs. *Archives of Toxicology*, 94, 1585-1599.
24. Nordmeier, F., Doerr, A., Laschke, M.W., Walle, N., Menger, M.D., Schmidt, P.H., et al. (2020) Erhebung toxikokinetischer Daten der synthetischen Opioide U-47700 und Tramadol sowie der Hauptmetabolite im Schwein nach intravenöser Verabreichung. 99. Jahrestagung der Deutschen Gesellschaft für Rechtsmedizin. Abstracts. *Rechtsmedizin*, 30, 361-412.
25. Nordmeier, F., Doerr, A., Laschke, M.W., Menger, M.D., Schmidt, P.H., Schaefer, N., et al. (2020) Are pigs a suitable animal model for in vivo metabolism studies of new psychoactive substances? A comparison study using different in vitro/in vivo tools and U-47700 as model drug. *Toxicology Letters*, 329, 12-19.
26. Peters F.T., Paul L.D., Musshoff F., Aebi B., Auwaerter V., et al (2009) Anhang B zur Richtlinie der GTFCh zur Qualitätssicherung bei forensisch-toxikologischen Untersuchungen Anforderungen an die Validierung von Analysemethoden. *Toxichem Krimtech*, 76, 185-208. https://www.gtfch.org/cms/images/stories/files/GTFCh_Richtlinie_Anhang B_Validierung_Version 1.pdf. (accessed December 29, 2020).
27. (2017) http://neuepsychoaktivesubstanzen.de/u-47700/#U-47700_Dosis_Dosierung (accessed December 29, 2020).
28. (2020) Gelbe Liste. Pharmindex https://www.gelbe-liste.de/wirkstoffe/Tramadol_1406 (accessed December 29, 2020).
29. Bakhle, Y.S. (1990) Pharmacokinetic and metabolic properties of lung. *British Journal of Anaesthesia*, 65, 79–93.

30. Ryan, U.S. and Grantham, C.J. (1989) Metabolism of endogenous and xenobiotic substances by pulmonary vascular endothelial cells. *Pharmacology & Therapeutics*, 42, 235–250.
31. Truver, M.T., Smith, C.R., Garibay, N., Kopajtic, T.A., Swortwood, M.J. and Baumann, M.H. (2020) Pharmacodynamics and pharmacokinetics of the novel synthetic opioid, U-47700, in male rats. *Neuropharmacology*, 177, 108195.
32. Dhopeshwarkar, G.A. and Mead, J.F. (1973) Uptake and transport of fatty acids into the brain and the role of the blood–brain barrier system. *Advances in Lipid Research*, 11, 109–142.
33. Helke, K.L., Nelson, K.N., Sargeant, A.M., Jacob, B., McKeag, S., Haruna, J., et al. (2016) Pigs in toxicology: Breed differences in metabolism and background findings. *Toxicologic Pathology*, 44, 575–590.
34. Grond, S. and Sablotzki, A. (2004) Clinical pharmacology of tramadol. *Clinical Pharmacokinetics*, 43, 879–923.
35. Paar, W.D., Frankus, P. and Dengler, H.J. (1992) The metabolism of tramadol by human liver microsomes. *The Clinical Investigator*, 70, 708–710.
36. Subrahmanyam, V., Renwick, A.B., Walters, D.G., Young, P.J., Price, R.J., Tonelli, A.P., et al. (2001) Identification of cytochrome P-450 isoforms responsible for cis-tramadol metabolism in human liver microsomes. *Drug Metabolism and Disposition*, 29, 1146.
37. (2014) Tramadol update review. Report agenda item 6.1. World health organization and expert committeeon drug dependence thirty-sixth Meeting Geneva. https://www.who.int/medicines/areas/quality_safety/6_1_Update.pdf (accessed December, 2020)
38. Vullo, C., Kim, T.-W., Meligrana, M., Marini, C. and Giorgi, M. (2014) Pharmacokinetics of tramadol and its major metabolite after intramuscular administration in piglets. *Journal of Veterinary Pharmacology and Therapeutics*, 37, 603–606.
39. Riviere, J.E. and Papich, M.G. (2017) Veterinary pharmacology and therapeutics. 10th ed. Wiley-Blackwell. Hoboken, NJ.
40 Lee, C.R., McTavish, D. and Sorkin, E.M. (1993) Tramadol. *Drugs*, 46, 313–340.
41. Lintz, W., Barth, H., Osterloh, G. and Schmidt-Böthelt, E. (1986) Bioavailability of enteral tramadol formulations. 1st communication: capsules. *Arzneimittel-Forschung*, 36, 1278—1283.
42. Murthy, B., Pandya, K., Booker, P., Murray, A., Lintz, W. and Terlinden, R. (2000) Pharmacokinetics of tramadol in children after iv or caudal epidural administration. *British Journal of Anaesthesia*, 84, 346–349.
43. Tao, Q., Stone, D.J., Borenstein, M.R., Codd, E.E., Coogan, T.P., Desai-Krieger, D., et al. (2002) Differential tramadol and O-desmethyl metabolite levels in brain vs. plasma of mice and rats administered tramadol hydrochloride orally. *Journal of Clinical Pharmacy and Therapeutics*, 27, 99–106.
44. Kitamura, A., Higuchi, K., Okura, T. and Deguchi, Y. (2014) Transport characteristics of tramadol in the blood-brain barrier. *Journal of Pharmaceutical Sciences*, 103, 3335–41.
45. Liu, H., Hu, Y., Liu, J., Wang, N. and Hou, Y. (2001) Transportation of the enantiomers of trans tramadol and O-demethyltramadol across blood-brain barrier. *Yao xue xue bao = Acta Pharmaceutica Sinica*, 36, 644–647.
46. Wang, Q., Han, X., Li, J., Gao, X., Wang, Y., Liu, M., et al. (2015) Regulation of cerebral CYP2D alters tramadol metabolism in the brain: interactions of tramadol with propranolol and nicotine. *Xenobiotica*, 45, 335–344.
47. Betschart, H.R., Jondorf, W.R. and Bickel, M.H. (1988) Differences in adipose tissue distribution of basic lipophilic drugs between intraperitoneal and other routes of

administration. *Xenobiotica*, 18, 113–121.
48. Brockbals, L., Staeheli, S.N., Gascho, D., Ebert, L.C., Kraemer, T. and Steuer, A.E. (2018) Time-dependent postmortem redistribution of opioids in blood and alternative matrices. *Journal of Analytical Toxicology*, 42, 365–374.
49. Niesel, H.C. (2003) Lokalanästhesie, Regionalanästhesie, Regionale Schmerztherapie. 2nd ed., Thieme Verlagsgruppe, Stuttgard.
50. Moor, M.J., Steiner, S.H., Jachertz, G. and Bickel, M.H. (1992) Adipose tissue distribution and chemical structure of basic lipophilic drugs: Desipramine, N-acetyldesipramine, and haloperidol. *Pharmacology & Toxicology*, 70, 121–124.
51. Gerace, E., Salomone, A., Luciano, C., Di Corcia, D. and Vincenti, M. (2018) First case in italy of fatal intoxication involving the new opioid U-47700. *Frontiers in Pharmacology*, 9, 747.
52. Židková, M., Horsley, R., Hloch, O. and Hložek, T. (2019) Near-fatal intoxication with the "new" synthetic opioid U-47700: The first reported case in the czech republic. *Journal of Forensic Sciences*, 64, 647–650.
53. Richeval, C., Gaulier, J.-M., Romeuf, L., Allorge, D. and Gaillard, Y. (2019) Case report: relevance of metabolite identification to detect new synthetic opioid intoxications illustrated by U-47700. *International Journal of Legal Medicine*, 133, 133–142.
54. Rohrig, T.P., Miller, S.A. and Baird, T.R. (2017) U-47700: A not so new opioid. *Journal of Analytical Toxicology*, 42, e12-e14. doi:10.1093/jat/bkx081.
55. Fels, H., Lottner-Nau, S., Sax, T., Roider, G., Graw, M., Auwärter, V., et al. (2019) Postmortem concentrations of the synthetic opioid U-47700 in 26 fatalities associated with the drug. *Forensic Science International*, 301, e20–e28. doi:10.1016/ J.FORSCIINT.2019.04.010.
56. Strehmel, N., Duempelmann, D., Vejmelka, E., Strehmel, V., Roscher, S., Scholtis, S., et al. (2018) Another fatal case related to the recreational abuse of U-47700. *Forensic Science, Medicine and Pathology*, 14, 531–535.
57. Costa, I., Oliveira, A., Guedes de Pinho, P., Teixeira, H.M., Moreira, R., Carvalho, F., et al. (2013) Postmortem redistribution of tramadol and O-desmethyltramadol. *Journal of Analytical Toxicology*, 37, 670–675.
58. Bynum, N.D., Poklis, J.L., Gaffney-Kraft, M., Garside, D. and Ropero-Miller, J.D. (2005) Postmortem distribution of tramadol, amitriptyline, and their metabolites in a suicidal overdose. *Journal of Analytical Toxicology*, 29, 401–406.
59. Levine, B., Ramcharitar, V. and Smialek, J.E. (1997) Tramadol distribution in four postmortem cases. *Forensic Science International*, 86, 43–48.
60. Oertel, R., Pietsch, J., Arenz, N., Zeitz, S.G., Goltz, L. and Kirch, W. (2011) Distribution of metoprolol, tramadol, and midazolam in human autopsy material. *Journal of Chromatography A*, 1218, 4988–4994.
61. Moore, K.A., Cina, S.J., Jones, R., Selby, D.M., Levine, B. and Smith, M.L. (1999) Tissue distribution of tramadol and metabolites in an overdose fatality. *The American Journal of Forensic Medicine and Pathology*, 20, 98-100.
62. Musshoff, F. and Madea, B. (2001) Fatality due to ingestion of tramadol alone. *Forensic Science International*, 116, 197–199.
63. Liang, M., Cai, X. and Jin, M. (2010) Distribution of tramadol in acute poisoned rats. *Fa Yi Xue Za Zhi*, 26, 436–439.
64. Lamia, M.E., Zeinab, A.E. and Hassan, M.M. (2001) Effects of tramadol on the development of lucilia sericata (diptera: calliphoridae) and detection of the drug concentration in postmortem rabbit tissues and larvae. *Journal of Entomology*, 8, 353–364.

Legends to Figures

Figure 1. Distribution of U-47700 (dotted bars) and *N*-desmethyl-U-47700 (squared bars) in tissues and body fluids 8 h after intravenous administration of a 100 µg/kg body weight dose of U47700 to 6 pigs. Concentrations are displayed as mean in ng/g or ng/mL ± standard error of mean (SEM); *PB* peripheral blood, *CB* central blood, *A.T.* adipose tissue.

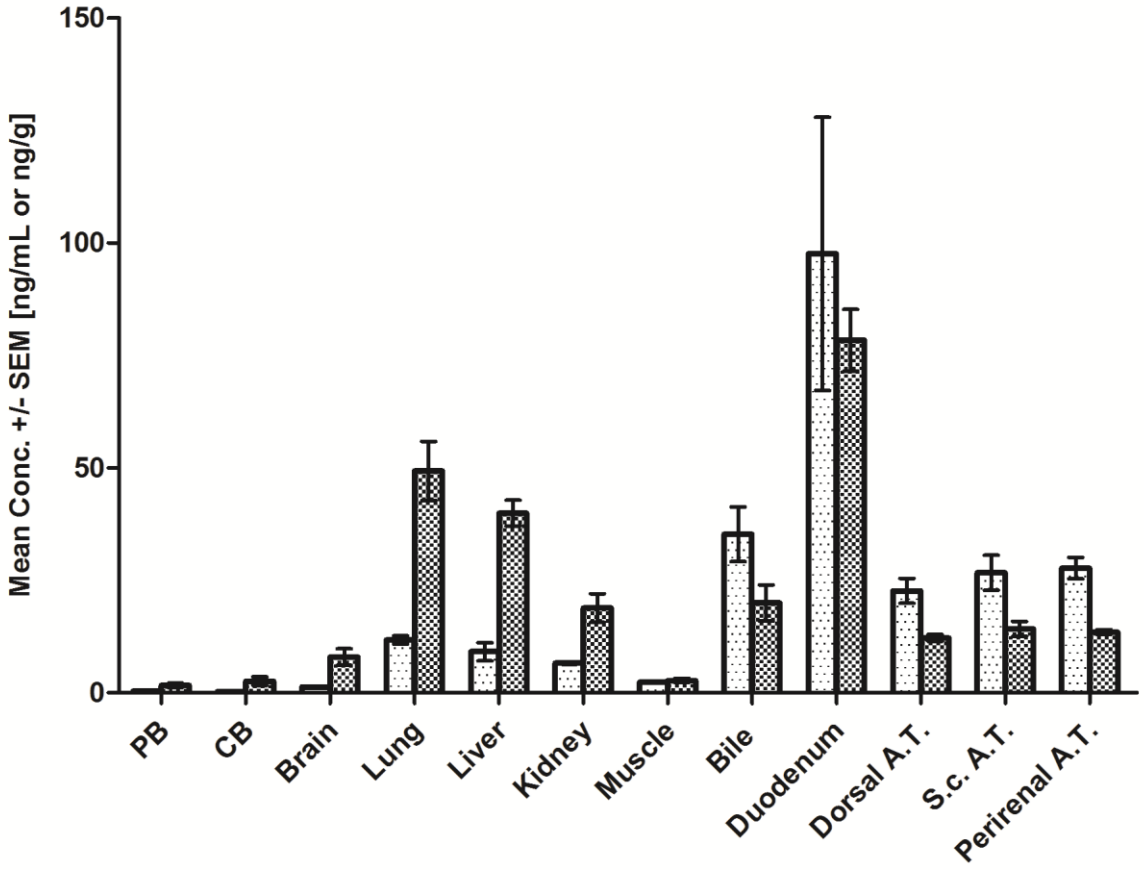

Figure 2. Distribution of tramadol (dotted bars) and *O*-desmethyltramadol (squared bars) in tissues and body fluids 8 h after intravenous administration of a 1000 µg/kg body weight dose of tramadol to 6 pigs. Concentrations are displayed as mean in ng/g or ng/mL ± standard error of mean (SEM); *PB* peripheral blood, *CB* central blood, *A.T.* adipose tissue.

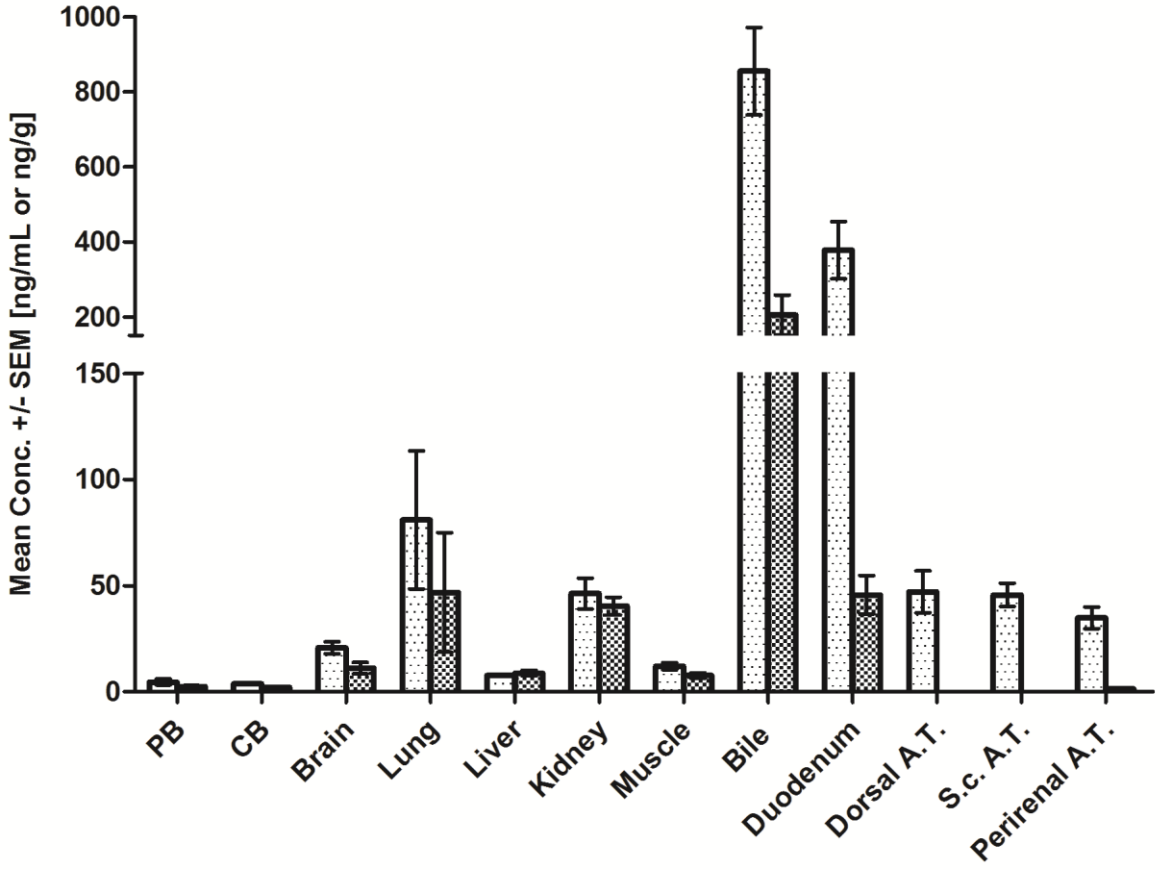

3.5 Are the (new) synthetic opioids U-47700, tramadol and their main metabolites prone to time-dependent postmortem redistribution? – A systematic study using an in vivo pig model

(Submitted 08/2021, DOI not yet provided)

Authors Contributions Frederike Nordmeier conducted and evaluated the experiment as well as composed the manuscript; Adrian Doerr, Nadja Walle and Stefan Potente assisted at the execution of the animal experiments; Matthias W. Laschke and Michael D. Menger carried out and enabled the animal experiments and assisted with scientific discussions; Nadine Schaefer, Markus R. Meyer, and Peter H. Schmidt assisted with scientific discussions and the development of the experiments as well as supervised the research.

Archives of Toxicology

Are the (new) synthetic opioids U-47700, tramadol and their main metabolites prone to time-dependent postmortem redistribution? – A systematic study using an in vivo pig model

--Manuscript Draft--

Manuscript Number:	
Full Title:	Are the (new) synthetic opioids U-47700, tramadol and their main metabolites prone to time-dependent postmortem redistribution? – A systematic study using an in vivo pig model
Article Type:	Original Article
Corresponding Author:	Nadine Schaefer Institute of Legal Medicine, Saarland University GERMANY
Corresponding Author Secondary Information:	
Corresponding Author's Institution:	Institute of Legal Medicine, Saarland University
Corresponding Author's Secondary Institution:	
First Author:	Frederike Nordmeier
First Author Secondary Information:	
Order of Authors:	Frederike Nordmeier
	Doerr A. Doerr
	Stefan Potente
	Nadja Walle
	Matthias W. Laschke
	Michael D. Menger
	Peter H. Schmidt
	Markus R. Meyer
	Nadine Schaefer
Order of Authors Secondary Information:	
Funding Information:	
Abstract:	The interpretation of analytical results in forensic postmortem (PM) cases often poses a great challenge, in particular due to possible PM redistribution (PMR) phenomena. In terms of new synthetic opioids, such data are usually not available and if so, they are from case reports without the exact knowledge of dose, user habits, time of consumption or PM interval. Hence, a controlled toxicokinetic pig study was performed allowing the examination of PM tissue distribution and possible PMR of U-47700, tramadol and the main metabolites N -desmethyl-U-47700 and O -desmethyltramadol (ODT). For this purpose, twelve domestic pigs received an intravenous dose of 100 µg/kg body weight (BW) U-47700 or 1000 µg/kg BW tramadol, respectively. The animals were put to death with T61 eight hours after administration and relevant organs, tissues and body fluids were sampled. Subsequently, the animals were stored at room temperature (RT) and samples were taken again after 24, 48, and 72 hours PM. Following homogenization and solid-phase extraction, quantification was performed applying a standard addition approach and liquid-chromatography tandem mass spectrometry. Only low to moderate concentration changes of U-47700, tramadol and their main metabolites were found in the analyzed tissue specimens and body fluids during storage at RT depending on the chosen PM interval. On the contrary, a remarkable concentration increase of tramadol was observed in liver tissue. These

	findings indicate that both synthetic opioids as well as their main metabolites are only slightly prone to PMR and central blood might be the matrix of choice for quantification of these substances.
Suggested Reviewers:	Jessica Welter-Luedeke Jessica.Welter-Luedeke@med.uni-muenchen.de Expertise in postmortem toxicology

Are the (new) synthetic opioids U-47700, tramadol and their main metabolites prone to time-dependent postmortem redistribution? – A systematic study using an in vivo pig model

Frederike Nordmeier[1], Adrian A. Doerr[1], Stefan Potente[1], Nadja Walle[1], Matthias W. Laschke[2], Michael D. Menger[2], Peter H. Schmidt[1], Markus R. Meyer[3], and Nadine Schaefer[1*]

[1]Institute of Legal Medicine, Saarland University, 66421 Homburg, Germany

[2]Institute for Clinical and Experimental Surgery, Saarland University, 66421 Homburg, Germany

[3]Department of Experimental and Clinical Toxicology, Institute of Experimental and Clinical Pharmacology and Toxicology, Center for Molecular Signaling (PZMS), Saarland University, 66421 Homburg, Germany

---

*Corresponding author: phone: +49 6841 16 26336; fax: +49 6841 16 26314

E-Mail address: nadine.schaefer@uks.eu (N. Schaefer)

Abstract

The interpretation of analytical results in forensic postmortem (PM) cases often poses a great challenge, in particular due to possible PM redistribution (PMR) phenomena. In terms of new synthetic opioids, such data are usually not available and if so, they are from case reports without the exact knowledge of dose, user habits, time of consumption or PM interval. Hence, a controlled toxicokinetic pig study was performed allowing the examination of PM tissue distribution and possible PMR of U-47700, tramadol and the main metabolites *N*-desmethyl-U-47700 and *O*-desmethyltramadol (ODT). For this purpose, twelve domestic pigs received an intravenous dose of 100 µg/kg body weight (BW) U-47700 or 1000 µg/kg BW tramadol, respectively. The animals were put to death with T61 eight hours after administration and relevant organs, tissues and body fluids were sampled. Subsequently, the animals were stored at room temperature (RT) and samples were taken again after 24, 48, and 72 hours PM. Following homogenization and solid-phase extraction, quantification was performed applying a standard addition approach and liquid-chromatography tandem mass spectrometry. Only low to moderate concentration changes of U-47700, tramadol and their main metabolites were found in the analyzed tissue specimens and body fluids during storage at RT depending on the chosen PM interval. On the contrary, a remarkable concentration increase of tramadol was observed in liver tissue. These findings indicate that both synthetic opioids as well as their main metabolites are only slightly prone to PMR and central blood might be the matrix of choice for quantification of these substances.

Keywords: New Synthetic Opioids; U-47700; postmortem redistribution; toxicokinetics; pigs; LC-MS/MS

Introduction

One of the most challenging tasks for forensic toxicologists is the interpretation of postmortem (PM) analytical results, because most parameters necessary for the evaluation of drug concentrations, such as dose and time of intake or the PM interval (PMI), are unknown (Skopp 2010) and numerous complex underlying mechanisms affect the results (Kennedy 2010). By analyzing antemortem specimens, reference values for drug concentrations in blood (e.g., therapeutic, toxic or lethal) are usually available allowing for reasonable interpretation of the findings. However, comparable assessments are not possible in the PM period due to variations in the concentrations according to the sampling site and between time of death and autopsy (Pélissier-Alicot et al. 2003). This difference between PM concentrations and the drug concentrations during lifetime or at the time of death is summarized under the term of PM redistribution (PMR) (Su et al. 2020), which describes a complex interaction between numerous variables. In addition, both during agony and PM interval, substantial concentration changes can occur due to drug degradation, neo-formation or artefactual formation (Skopp 2010) driven by instability or further metabolism via microorganisms in the corpse or the environment (Yarema and Becker 2005). Furthermore, in the agonal phase, substances may be further metabolized and excreted into urine. Major factors influencing the susceptibility to PMR are based on the physicochemical and toxicokinetic (TK) properties of the drug or on environmental conditions (Leikin and Watson 2003; Skopp 2010). Moreover, drugs might be released from several organs acting as drug reservoir into surrounding specimens with lower concentrations promoted by degradation processes in the body (Skopp 2010; Yarema and Becker 2005). Hence, PM blood concentrations can vary, when specimens are collected from different anatomical regions, e.g., central versus peripheral blood (Pélissier-Alicot et al. 2003; Skopp 2010). All these issues should be taken into consideration in the interpretation of PM concentrations to avoid misinterpretations (Leikin and Watson 2003).

Intoxications with new psychoactive substances (NPS) pose additional challenges, since usually no data on TK or toxicodynamic (TD) properties are available (Concheiro et al. 2018). Especially new synthetic opioids (NSO) have become a public health concern within the last few years due to their high potency and, thus, unpredictable toxic effects (EMCDDA 2020). Up to now, numerous fatalities due to NSO have been reported (Zawilska 2017; Concheiro et al. 2018; Chesser et al. 2019). Most of the case reports provide data on concentrations found in blood or urine and only few on tissue distribution. Besides these case reports, controlled animal studies estimating TK and TD data or toxicity were performed only sparsely (Truver et al. 2020; Kyei-Baffour and Lindsley 2020). However, none of these studies provided comprehensive data on PM tissue distribution and possible redistribution, particularly for of 3,4-dichloro-*N*-[2-(dimethylamino)cyclohexyl]-*N*-methylbenzamide (U-47700), which is one of the most popular non-fentanyl NSO. Hundreds of fatal overdoses have been reported since its emergence on the street marked (Elliott et al. 2016; Dziadosz et al. 2017; Rambaran et al. 2017; Kyei-Baffour and Lindsley 2020). Showing a 7.5 – 12-fold higher in vivo activity than morphine, this potent μ-opioid receptor agonist was never advanced to clinic, nor studied in man (Kyei-Baffour and Lindsley 2020) and only little is known concerning TK and TD properties.

We recently establish a pig animal model suitable for TK studies of NSO following intravenous (i.v.) administration of U-47700 and tramadol (as reference) providing data on metabolism, antemortem data on the blood distribution, different TK parameters as well as perimortem data on the tissue distribution (Nordmeier et al. 2020, 2021a, b). Pigs have already been proven to be an appropriate model for the estimation of TK data of other NPS, especially different synthetic cannabinoids (Schaefer et al. 2015, 2016, 2017, 2018, 2019, 2020), and were chosen consequently for the present analyses.

Hence, the aim of this study was to investiagte the PM distribution and time-dependent concentration changes of U-47700, tramadol and their main metabolites followed by a comparison with the perimortem findings and published human or animal data.

Materials and methods

Chemicals and reagents

From Merck (Darmstadt, Germany) the following chemicals were purchased: di-potassium hydrogen phosphate, potassium hydroxide, hydrochloric acid, formic acid EMSURE, and ammonia solution 25 % EMSURE. Ammonium formate, dichloromethane and Na_2EDTA were obtained from Sigma-Aldrich (Steinheim, Germany). Methanol, ethanol, acetonitrile and HPLC-grade water were bought by Fisher chemicals (Loughborough, UK). *N*-desmethyl-U-47700 (solid), and the methanolic solutions of tramadol-HCl, *O*-desmethyltramadol-(ODT-) HCl, (1 mg/mL each), tramadol-HCl-C_{13}-d_3 (1 mg/mL), and ODT-HCl-d_6 (0.1 mg/L) were ordered from LGC (Wesel, Germany). *N*-desmethyl-U-47700-d_3 (0.1 mg/mL in acetonitrile) was obtained from Sigma-Aldrich (Taufkirchen, Germany). Tramadol-HCl for drug administration (Tramadol Denk 100 mg in 2 mL) was purchased from Denk Pharma (Munich, Germany). The German Federal Crime Police Office (Wiesbaden, Germany) provided U-47700 hydrochloride (purity 92.6 %) for research purpose.

The phosphate buffer (0.1 M, pH 6) was prepared as described previously(Nordmeier et al. 2021a, b). In brief, 13.61 g di-potassium hydrogen phosphate was dissolved in 1 L deionized water and by adding 1 M potassium hydroxide solution, the pH was adjusted.

Stock solutions, calibration standards, quality control samples and calibrators for standard addition were prepared as already described in previous studies (Nordmeier et al. 2021a, b). The preparation is described in detail in the Electronic Supplement Material (ESM).

Blank whole blood specimens

Blank whole blood specimens used for the preparation of calibrators and quality controls were obtained from drug free pigs (Swabian Hall strain, Emil Faerber GmbH & Co. KG,

Zweibruecken, Germany). For prevention of clotting, the whole blood samples were spiked with Na_2ETDA (1.64 mg/mL). Afterwards, the samples were stored at -20 °C until analysis.

Animals

As already described (Nordmeier et al. 2021a, b), this TK study was performed using 12 domestic male pigs (Swabian Hall strain, mean body weight (BW) 42.8 ± 1.9 kg). The animal experiments were performed according to the German legislation on protection of animals and the National Institute of Health Guide for the Care and Use of Laboratory Animals (permission number: 32/2018). The animals had free access to standard chow and water each day. The night before the experiment the pigs were not fed any longer but had still free access to water.

Surgical Procedure

The surgical procedure is described in detail in the ESM. In brief, anesthesia of the pigs was maintained with isoflurane following a premedication with ketamine/xylazine. Sample collection, i.v. drug administration and monitoring of the mean central venous pressure were enabled through a triple-lumen 7F central venous catheter placed into the jugular vein.

Study design

As already described elsewhere (Nordmeier et al. 2021a, b), 6 of the 12 pigs received a 100 µg/kg body weight (BW) dose of U-47700. The other pigs (n = 6) received a 1000 µg/kg BW dose of tramadol. Analogous to previous studies (Nordmeier et al. 2021a, b), a stock solution of 4 mg/mL U-47700 (solid) was first prepared in ethanol and appropriate volumes (1005-1120 µL) of this solution were used to obtain a 100 µg/kg BW dose. For tramadol, volumes of 906-1134 µL of a purchased tramadol-HCl solution were applied to reach a 1000 µg/kg BW

dose. For drug administration, all volumes were filled up with sodium chloride 0.9% to a volume of 10 mL and the prepared solutions were i.v. injected into the jugular vein over 30 s. As described in the former TK study (Nordmeier et al. 2021a), the animals were euthanized eight hours after administration (PMI 0) with T61 (0.12 mL/kg BW, Intervent Deutschland GmbH, Unterschleissheim, Deutschland) and the abdominal cavity was opened. Subsequently, biopsies of the following organs, tissues and body fluids were taken by leaving the organs in situ: brain, lung, liver, kidney, skeletal muscle tissue from the hind leg, bile, duodenum content, peripheral blood from the jugular vein (PB), central blood (CB) and adipose tissue (AT; ventral subcutaneous (s.c.), perirenal and dorsal). Then, the abdominal cavity was sutured and the animals were stored at room temperature (RT) in a lateral position. Further specimens were collected 24, 48 and 72 h PM (PMI 1-3) as described above with two exceptions. PM blood at PMI 1-3 was collected from the femoral or brachiocephalic vein. CB was collected from the inferior vena cava or by puncture of the heart. Specimens of PB and bile were not available for all pigs for the whole PMI. Samples were accessible as follows and written in Table 1/2: U-47700: PB PMI 2: n = 5, PB PMI 3: n = 3, bile PMI 2: n = 5, bile PMI 3: n = 3; tramadol: PB PMI 1: n = 5, PB PMI 2: n = 5, PB PMI 3: n = 3, bile PMI 1: n = 5, bile PMI 2: n = 3, bile PMI 3: n = 2. All samples were stored at – 20 °C until analysis.

Sample preparation

Blood specimens

The PB and CB samples were prepared according to a fully validated method already described in a former study (Nordmeier et al. 2021b) as well as in the ESM. Limits of detection were 0.1 ng/mL for U-47700, *N*-desmethyl-U-47700 and tramadol, and 3.5 ng/mL for ODT. Lower limits of quantification were assessed at 0.5 ng/mL for U-47700 and metabolite, at 1 ng/mL for tramadol and at 10 ng/mL for ODT (Nordmeier et al. 2021b).

For extraction of PB samples of less than 1 mL, the whole amount of the sample was homogenized and diluted with blank whole blood until a final volume of 1 mL was reached.

Tissue specimens

The preparation of tissue specimens is described in detail in the ESM. In brief, solid tissue and body fluids were homogenized with water (tissue/fluid/content:water 1:5, w/w) while AT specimens were homogenized with acetonitrile (tissue/acetonitrile 1:5, w/w). After centrifugation, the supernatants were prepared with or without addition of calibrator concentrations of the drugs of interest to create a standard addition calibration curve. The samples were extracted using SPE.

Standard addition method

As already described elsewhere (Nordmeier et al. 2021a), in the current study a standard addition approach was chosen for quantification of the drugs and their metabolites. Except for blood specimens, four portions of each tissue specimen or body fluid were prepared by adding no calibrator solution or different concentrations of calibrator solution as listed in Table S1. The analyte/SIL-IS area ratio was plotted against the calibrator concentration. Based on a linear regression, standard addition calibration equations ($m\ x + b$) were created. Calculation was performed using Microsoft Office Excel 2003 (Redmond, WA, USA). The calculation of the concentrations of the drugs and their metabolites was performed via the slope (m) and intercept ranges (b). The point of interception at the negative side of the x-axis represents the unknown concentration (x).

LC-MS/MS conditions

The LC-MS/MS conditions and the instrumentation were similar to already published studies (Nordmeier et al. 2021a, b) and can be found in detail in the ESM.

Calculation of concentration changes

For the different specimens, mean and median concentration values for both drugs and their metabolites including standard deviation (SD) were calculated using Microsoft Office Excel 2003 (Redmond, WA, USA). Values were calculated for PMI 1-3. The percentage median concentration changes relative to the median perimortem concentrations (PMI 0, values according to Nordmeier et al. 2021a) were calculated as follows (Schaefer et al. 2020):

$$\Delta c\ (\%) = \frac{c(\text{PMI } 1-3) - c(\text{PMI } 0)}{c\ (\text{PMI } 0)} \times 100$$

A concentration increase would be indicated by a value higher than zero and a concentration decrease by a value lower than zero.

Statistical tests

For the examination of time-dependent concentration changes in the different specimens, a non-parametric Friedman-test ($p<0.05$) followed by a Dunn's multiple comparison post-hoc test was performed. Statistics were carried out using GraphPad Prism 9.0.0 (GraphPad Software, San Diego, CA, USA).

Results

Standard addition method

In the present study, a standard addition approach was used for quantification of U-47700, tramadol and their metabolites in the different tissue specimens/contents. The regression coefficients (r^2) for the drugs of interest ranged between 0.94 and 0.99.

General findings

It should be emphasized that high interindividual variations could be observed within the analyzed PM specimens. The mean and median concentrations of the parent drugs and their metabolites as well as the corresponding standard deviations (SD) are listed in Table 1 and 2. The calculation of the median concentration changes was based on the findings published in a previous study (Nordmeier et al. 2021a) and is presented in Fig. 1. The analysis of PM specimens revealed highest concentrations of U-47700 in duodenum content and bile followed by lung and liver. Tramadol was primarily determined in bile, duodenum content, lung and kidney. The lowest concentrations of parent compounds were determined in CB and PB and in the case of U-47700 in muscle and brain additionally. As far as metabolites are concerned, highest concentrations were found in tissues and body fluids involved in metabolism or excretion such as duodenum content, bile, lung and liver.

U-47700 and *N*-desmethyl-U-47700

Concerning U-47700 and its metabolite, both substances could be quantified in all analyzed specimens sampled at all sampling times (when available). Regarding U-44700, only slight concentration changes were observed throughout all tissues and fluids (Fig. 1A). In lung and brain, a slight concentration increase was measured. In muscle, concentrations increased as well within the first 24 h with no further concentration changes during the following PMI. However, concentration changes in these tissues were not significant. PM concentrations in kidney, liver

and dorsal AT presented as rather stable over the examined period. In bile, duodenum content as well as in perirenal and s.c. AT an overall slight decrease of the concentration was observed compared to the median concentration at the time of death (Nordmeier et al. 2021a). In bile, concentrations decreased from PMI 1 to PMI 2, whereas in duodenum content concentrations decreased from PMI 0 to PMI 1. In both specimens, concentrations remained constant after this decrease. Mean concentrations constantly increased in PB until 48 h and then decreased. However, in PB high values were spread broadly with large SD (Table 1). In CB concentrations were regarded to be stable over the examined PMI.

Regarding *N*-desmethyl-U-47700, only minor concentration changes were noticed (Fig. 1B). In comparison with the median concentration after death (Nordmeier et al. 2021a), no relevant concentration changes over the course of PMI were observed in liver, duodenal content as well as in perirenal and dorsal AT. In muscle, concentrations were regarded to be rather constant. In brain and bile, concentrations slightly yet significantly increased in a continuous manner, whereas concentrations in kidney and s.c. AT slightly decreased during the observed PMI. Concentrations in lung were constant within the first 48 h and afterwards increased from PMI 2 to PMI 3. Concentrations in CB and PB slightly increased from PMI 0 to PMI 1, then appeared constant followed by decrease. These concentration changes, however, were only minor.

Tramadol and ODT

Regarding tramadol, quantification was successful for every analyzed specimen collected at the different PMI (when available). Only slight concentration changes were observed in kidney, muscle and brain tissue specimens as well as in CB (Fig. 1C). In lung, dorsal and s.c. AT, a slight to moderate PM concentration decrease was measured. However, changes in lung were not significant. PM concentrations in liver continuously increased, whereas concentrations in

bile and duodenum content considerably decreased from PMI 0 to PMI 1 with no further concentration changes in the following PMI. Concerning perirenal AT, median concentrations decreased from PMI 0 to PMI 1, were constant and then increased from PMI 2 to PMI 3. In PB, a concentration decrease from PMI 0 to PMI 1, an increase from PMI 1 to PMI 2 and a subsequent and a slight decrease from PMI 2 to PMI 3 was measured.

Consistent with the findings at the time of death (Nordmeier et al. 2021a), no ODT was found in the analyzed dorsal and ventral s.c. AT specimens (Table 2), whilst it was detected in all other analyzed specimens (if available). In comparison with the median concentration immediately after death, no relevant concentration changes over the course of the PMI were observed in brain, lung, muscle and PB (Fig. 1D). Concentrations in duodenum content decreased within the first 24 h and then remained stable at a very low concentration level. In liver, kidney, and perirenal AT, concentrations continuously increased significantly. Concentrations slightly increased in CB from PMI 0 to PMI 2 and decreased again. In bile, mean concentrations decreased till 48 h and were significantly lower in PMI 2 as compared to PMI 0. Afterwards, concentrations increased and were comparable to those at the time of death (n = 2) (Nordmeier et al. 2021a, Table 2).

Discussion

PM distribution

The perimortem distribution of U-47700, tramadol and their main metabolites in different tissues and body fluids has already been described elsewhere (Nordmeier et al. 2021a). In brief, highest concentrations of U-47700 were found in duodenum content, bile and AT, whereas highest concentrations of tramadol were determined in bile and duodenum content followed by lung. Concerning the metabolites, *N*-desmethyl-U-47700 and ODT were detected in all

analyzed specimens except for ODT in dorsal and s.c. AT. Higher concentrations were found in specimens involved in metabolism and excretion. PM distribution of U-47700, its metabolite and ODT assessed in the current study is comparable to the perimortem findings (Table 1,2). Regarding tramadol, PM distribution was found to be comparable to the perimortem distribution with the exception of duodenum content, which showed considerably decreasing concentrations (Table 2). These findings will be discussed below. Data on PM tissue distribution are very sparse for synthetic opioids in general and especially for NSO. Published human data on PM distribution derived from case reports usually includes several uncertainties such as an unknown PMI, survival time, time of intake, or dosage.

PM concentration changes

In general, as for U-47700, tramadol and their metabolites showed only slight to moderate concentration changes throughout the analyzed tissues and body fluids (Fig. 1), which changes were in parts statistically significant. In other cases, continuous concentration increases/decreases were observed over the examined PMI suggesting a PMR. However, these changes were not significant. Statistical significance must be taken with caution regarding PM concentrations however because of generally high interindividual variation in PM analytics. Even if fully validated methods were used analyzing both, tissue and blood samples, high interindividual deviations were monitored (Saar et al. 2012; Gleba and Kim 2020). This observation may indicate that PM variances are affected more by the variability of biological PM degradation processes than by the inaccuracy of analytical methods.

To assess the probability of a substance undergoing PMR, several parameters may be taken into consideration. One possible marker is a central-to-peripheral blood concentration ratio (C/P-ratio) of >1 (Han et al. 2012). A previous study (Nordmeier et al. 2021a) showed nearly similar concentrations of U-47700, tramadol, and ODT in PB and CB and a C/P-ratio

only slightly >1 of *N*-desmethyl-U-47700 leading to the conclusion that these substances are not predisposed for PMR. C/P ratios of U-47700 indicating only a minor tendency for PMR have already been found in earlier cases (McIntyre et al. 2016; Rohrig et al. 2017). Similar C/P-ratios for tramadol and ODT were already discussed in literature (Levine et al. 1997; Moore et al. 1999; Musshoff and Madea 2001) indicating that tramadol does not underlie significant PMR. Our data in the present study are in line with the former findings and further support this suggestion (Table 1,2). An additional marker for the estimation of the PMR of a substance is the liver-to-peripheral blood ratio (L/P-ratio) (McIntyre 2014). According to McIntyre et al. (2014), a L/P-ratio less than 5 might be associated with little or no PMR, whereas a greater L/P-ratio support the assumption of a high PMR-potential. L/P-ratios calculated based on the previous data (Nordmeier et al. 2021a) are >5 for U-47700 and its metabolite. Hence, both substances are slightly prone to PMR. Regarding tramadol and ODT, L/P-ratios less than 5 were calculated, indicating that these substances are no candidates for PMR as was also observed in the present study. A high potential for PMR might also be indicated by a large volume of distribution (V_d) (Mantinieks et al. 2020), with a V_d >3 already hinting at PM concentration changes of a substance (Skopp 2010). However, considering the moderate V_d values of U-47700 and tramadol (Nordmeier et al. 2021b), both substances seem less prone to undergo PMR. So far, PMR observed in the present study showed the expected behavior.

While discussing possible explanations for the observed median concentration changes concerning U-47700 and tramadol, the absolute concentrations must be taken into consideration (Table 1,2). Focusing on the median concentrations of tramadol and U-47700 as well as their metabolites in CB and PB (Table 1,2), possible concentration changes during the PMI should be weighed carefully. Concentrations of U-47700 in CB were below 1 ng/mL and all ODT concentrations were below the LOQ leading to the conclusion that discrepancies might be explained by analytical and interindividual variations. In general, a very high SD was maintained in regards of the results for U-47700 in PB especially. Furthermore, in terms of PB,

specimens derived from different veins and were highly diluted by blank whole blood due to only low sample material amounts. In addition, CB specimens were drawn from either the vena cava or the heart chamber which may have impacted the quantified concentrations.

U-47700 and N-desmethyl-U-47700

Regarding U-47700, most concentration changes were minor amounting to less than 100% (Fig. 1A) and, thus, they were potentially attributable mainly to interindividual or analytical variations. As already mentioned, the excessive concentration increase in PB might be affected by dilution processes during the analytical procedure, pronounced interindividual variations (high SD) and a non-standardized sampling of different veins. Furthermore, in only 3 cases PB samples were available throughout the whole PMI and the single values showed an inconsistent PMR. In a previous study (Nordmeier et al. 2021b), the authors determined higher concentrations of U-47700 in serum samples than in whole blood samples leading to the conclusion that U-47700 might not be accumulated in red blood cells. Thus, a release from red blood cells might not be the cause of this obvious concentration increase in PB and CB. One possible explanation for these findings might be a PM release from a possible protein bound form of U-47700 due to PM protein breakdown, but there is no data in the literature about the protein binding of U-47700. However, due to the experimental set-up, a possible PMR in PB is difficult to evaluate and recommendations about its usability for drug quantification should be taken with care. On the contrary, since concentrations in CB were nearly stable, this matrix seems to be suitable for PM quantification of U-47700. A minor increase of median concentration in liver as well as in kidney might be due to diffusion processes from duodenum and bile, where concentrations decreased during the PMI. The low decline of the concentration in s.c. AT might be associated with a diffusion into the directly underlying muscle tissue and, thus, with the observed concentration increase in this tissue. A further remarkable result is the most considerable increase in lung occurring from PMI 2 to PMI 3 (Fig. 1A). A possible

inhomogeneous distribution in lung tissue and practical difficulties to take the repeated biopsies in a standardized way at the same site might be followed by variations in concentrations and could be an explanation for this finding. The same assumption could be made concerning the concentration changes in brain tissue, as we did not differentiate between different brain areas and the brain is well isolated from the remaining body except for the circulatory system. In summary, PM concentration changes of U-47700 could be regarded to be slight to moderate. As already mentioned above, McIntyre et al. (2016) postulated a modest potential for PMR of U-47700 based on C/P- and L/P-ratios. The C/P-ratio observed by Rohrig et al. (2017) supports this suggestion. On the other hand, in some case reports higher CB concentrations in comparison to femoral blood concentrations were discussed (Dziadosz et al. 2017; Strehmel et al. 2018) leading to higher C/P-ratios and thus, a higher predisposition for PMR. However, the reliability of these data cannot seriously be assessed, because information about the dosage, survival time, route of administration or PMI are not available.

In terms of the metabolite *N*-desmethyl-U-47700, the concentration changes in tissues can be considered as minor and, in most specimens, caused again by interindividual or analytical variation. In the early PMI, a minor concentration increase in PB and CB was encountered, but concentrations declined to the initial values again in the later PMI (Table 1, Fig. 1B). Besides a redistribution from surrounding tissues a possible protein binding followed by PM protein breakdown might be a probable explanation for the early increases. As already emphasized regarding U-47700, the mean values in PB in this experiment should be taken with care. Nevertheless, PB and CB might be suitable for PM quantification, if slightly elevated concentrations in the early PMI are considered. Since *N*-desmethyl-U-47700 is accumulated in lung tissue (Nordmeier et al. 2021a) and shows basic properties, a trapping of this drug during acidification of the cells followed by a release out of this drug reservoir and obvious concentration changes were assumed. However, although the metabolite showed very high concentrations in lung at PMI 0 (Nordmeier et al. 2021a, Table 1) only minor concentration

decreases in this tissue and a concentration increase from PMI 2 to PMI 3 were found in the study. The non-differentiated sampling of lung tissue might be a possible explanation for this fact. Furthermore, a drug release from kidney tissue into perirenal AT might have taken place. The last remarkable finding is the concentration increase in bile, which might be caused by redistribution from liver tissue driven by diffusion processes, since drug concentrations were higher in liver tissue than in bile at PMI 0 (Nordmeier et al. 2021a Table 1). However, in liver tissue only a non-significant decrease was observed, but biopsies of liver specimens were indeed taken from different sites and, thus, specimens might be less affected by this redistribution. To conclude, we observed only a low tendency for *N*-desmethyl-U-47700 to undergo PMR.

Tramadol and ODT

Regarding tramadol, mostly minor concentration (less than 100%) changes were observed (Fig. 1C), but a significant concentration increase in liver tissue and a significant concentration decrease in bile and duodenum content were noticed over the course of the PMI. Considering the fact that only low concentrations were found in this tissue at PMI 0 (Nordmeier et al. 2021a, Table 2), diffusion processes especially from the intestine and the bile, in which the amount of tramadol decreased during PMI, might be a possible explanation for this concentration increase. With respect to these findings, quantification of tramadol in liver tissue, routinely analyzed as alternative PM matrix, should be assessed with care. Bile and duodenum content are not commonly used as alternative matrices in PM toxicology. In fact, based on the current data, PM drug quantification of the studied synthetic opioids in those specimens should be avoided. Nevertheless, a qualitative analysis in those specimens is possible due to high PM concentrations. In brain, lung, kidney, muscle and AT only minor concentration changes were observed. As concentration changes in muscle tissue and especially in brain were very slight, both specimens might be used as alternative matrices for PM quantification. Furthermore, a

PMR from lung into the surrounding periphery, e.g., the liver, might be relevant since accumulation of tramadol at PMI 0 and, thus, the determination as drug reservoir was determined in the previous study (Nordmeier et al. 2021a). In addition, tramadol shows basic properties, leading to the suggestion that this drug might also be trapped in the lung after acidification and might be released with the progression of tissue degradation. Our analytical findings suggest this assumption, even if only a minor concentration decrease was measured (Table 2, Fig. 1C). A relevant concentration decrease in PB was detected when the mean values were considered - excluding this matrix as matrix of choice for PM quantification of the studied synthetic opioids. As already mentioned above, these findings have to be assessed with care due to the experimental set-up. Considering the individual values, no consistent trend for PMR of tramadol was identified. Since no obvious concentration changes in CB were determined, this matrix predominantly should be used for PM quantification of tramadol. In line with our results, Levine et. al (1997) and Costa et al. (2013) postulated a low to moderate tendency of tramadol to undergo PMR. Han et al. (2012) observed no clear trend in terms of PMR and postulated a non-consistent PMR of tramadol. However, all these findings are based on the calculation of C/P-ratios or L/P-ratios. Brockbals et al. (2018) examined time-dependent concentration changes using CT-guided organ and fluid specimen biopsies and leaving the organs in situ. They proposed a non-consistent PMR due to the fact that significant time-dependent concentration increases as well as decreases could be observed in PB. These findings are in line with our results if the findings in individual animals are considered. Also in agreement with our results, a controlled PMR study in rats (Su et al. 2020) provided data on low to moderate PMR for tramadol with a concentration increase in liver. In contrast to our study, the authors observed slight concentration increases in kidney and lung as well. However, the different set-up of the study as well as the fact that smaller animals were used might be possible reasons for these discrepancies.

Likewise, in ODT, only minor concentration changes were observed (Fig. 1D). An increase of the median concentrations in lung tissue and a corresponding decrease of the concentrations in duodenum content implicated a diffusion driven by a concentration gradient as already mentioned in the case of tramadol. Since only little concentration differences were found in PB, CB, brain, lung kidney and muscle, these concentration changes could be associated with interindividual variations. Thus, PB and CB as important PM specimen might be suitable for PM quantification. In perirenal AT, an excessive increase of ODT was ascertained. Together with a sudden concentration increase in the kidney tissue at PMI 3, the surrounding sampling situation may be an explanation for this output. Both tissues are located in the abdominal cavity and thus they floated in putrefactive liquid formed during the PMI. By this fact, both specimens got in touch with all other specimens in the abdominal cavity, especially with the intestine where a concentration decrease was observed. To conclude, we observed only a low tendency for ODT to undergo PMR. In line with our results, Brockbals et al. (2018) only observed minor concentration changes in PB as well and, thus, postulated that ODT is less prone to PMR. Based on the lack of obvious differences between CB and PB concentrations and the calculated C/P-ratios, Costa et al (2013) and Bynum et al. (2005) came to the same conclusion.

Limitations of the study

First, it has to be noted that the abdominal cavity had to be opened for the sampling of the different tissue and organ specimens. This has most certainly led to a more aerobic environment and, thus, in a faster occurrence of microorganisms and changes in the microbiome. Furthermore, the sampling of e.g., duodenum content required opening of the organ and the incision was only closed by ligations. Even if these ligations prevent an outlet of the content as far as possible, a contamination of the neighboring putrefactive liquid cannot completely be

ruled out. As a matter of fact, during the PMI, a high proportion of putrefactive liquid was formed, which may have contributed to the redistribution procedure. At last, in voluminous organs like liver, the site of the sampling procedure could not perfectly be standardized for practical reasons. If the drugs might be distributed in an inhomogeneous manner throughout the organs, this behavior might have contributed to the high variability of the results. (However, in CB samples no major changes were observed in the specimens sampled from different sites.)

Conclusion

In the present study, PM distribution patterns as well as time-dependent concentration changes of the (new) synthetic opioids U-47700, tramadol and their main metabolites *N*-desmethyl-U-47700 and ODT were investigated in pigs following i.v. administration. As a conclusion, lung, liver, kidney, duodenum content and bile are suitable matrices for qualitative PM analysis of both parent compounds and their metabolites. In addition, AT could serve as alternative specimen, except for ODT, since this metabolite seems not to be stored in AT. *N*-desmethyl-U-47700 displayed much higher concentrations in tissues/body fluids involved in metabolism compared to U-47700 and thus might be highly recommended as analyte. In general, only low to moderate time-dependent concentration changes were observed throughout the analyzed specimens except for a remarkable concentration decrease of tramadol/(ODT) in duodenum content/bile and an increase in liver tissue. Hence, those specimens should be avoided for PM quantification of tramadol/ODT. Muscle tissue and especially brain could be used as alternative matrices for quantification of tramadol. Concentrations of all analytes were stable in CB during the examined PMI, whereas in PB no clear trend of PMR was identified. Thus, CB might be the matrix of choice for PM quantification of U-47700 and tramadol. To sum up, U-47700 and tramadol as well as their main metabolites show only low to slight tendency for PMR.

Acknowledgements The authors thank Benjamin Peters, the staff of the Institute for Legal Medicine at Saarland University and the staff of the Institute for Clinical and Experimental Surgery at Saarland University for their support and help during the study. We acknowledge the EU funded project ADEBAR (IZ25-5793-2016-27).

Compliance with ethical standards

Conflicts of interest The authors declare that there are no financial or other relations that could lead to a conflict of interest.

Ethical Approval All experiments were performed in accordance with the German legislation on protection of animals and the National Institutes of Health Guide for the Care and Use of Laboratory Animals (permission number: 32/2018).

References

Brockbals L, Staeheli SN, Gascho D, et al (2018) Time-dependent postmortem redistribution of opioids in blood and alternative matrices. J Anal Toxicol 42(6):365–374. https://doi.org/10.1093/jat/bky017

Bynum ND, Poklis JL, Gaffney-Kraft M, Garside D, Ropero-Miller JD (2005) Postmortem distribution of tramadol, amitriptyline, and their metabolites in a suicidal overdose. J Anal Toxicol 29(5):401–406. https://doi.org/10.1093/jat/29.5.401

Chesser R, Pardi J, Concheiro M, Cooper G (2019) Distribution of synthetic opioids in postmortem blood, vitreous humor and brain. Forensic Sci Int 305:109999. https://doi.org/10.1016/J.FORSCIINT.2019.109999

Concheiro M, Chesser R, Pardi J, Cooper G (2018) Postmortem toxicology of new synthetic opioids. Front Pharmacol 9:1210. https://doi.org/10.3389/fphar.2018.01210

Costa I, Oliveira A, Guedes de Pinho P, et al (2013) Postmortem redistribution of tramadol and O-desmethyltramadol. J Anal Toxicol 37(9):670–675. https://doi.org/10.1093/jat/bkt084

Dziadosz M, Klintschar M, Teske J (2017b) Postmortem concentration distribution in fatal cases involving the synthetic opioid U-47700. Int. J. Legal Med 131(6):1555–1556. https://doi.org/10.1007/s00414-017-1593-7

Elliott SP, Brandt SD, Smith C (2016) The first reported fatality associated with the synthetic opioid 3,4-dichloro-N-[2-(dimethylamino)cyclohexyl]-N-methylbenzamide (U-47700) and implications for forensic analysis. Drug Test Anal 8(8):875–879. https://doi.org/10.1002/dta.1984

EMCDDA: European Monitoring Center of Drugs and Drug Addiction (2020) European drug report: Trends and developments. https://doi.org/doi:10.2810/420678

Gleba J, Kim J (2020) A mechanism-based forensic investigation into the postmortem redistribution of morphine. J Anal Toxicol 44(3):256–262. https://doi.org/10.1093/jat/bkz093

Han E, Kim E, Hong H, et al (2012) Evaluation of postmortem redistribution phenomena for commonly encountered drugs. Forensic Sci Int 219(1):265–271. https://doi.org/https://doi.org/10.1016/j.forsciint.2012.01.016

Kennedy MC (2010) Post-mortem drug concentrations. Intern Med J 40(3):183–187. https://doi.org/10.1111/j.1445-5994.2009.02111.x

Kyei-Baffour K, Lindsley CW (2020) DARK classics in chemical neuroscience: U-47700. ACS Chem Neurosci 11(23):3928–3936. https://doi.org/10.1021/acschemneuro.0c00330

Leikin JB, Watson WA (2003) Post-mortem toxicology: What the dead can and cannot tell us. J Toxicol Clin Toxicol 41(1):47–56. https://doi.org/10.1081/CLT-120018270

Levine B, Ramcharitar V, Smialek JE (1997) Tramadol distribution in four postmortem cases. Forensic Sci Int 86(1-2):43–48. https://doi.org/10.1016/S0379-0738(97)02111-7

Mantinieks D, Gerostamoulos D, Glowacki L, et al (2020) Postmortem drug redistribution: A compilation of postmortem/antemortem drug concentration ratios. J Anal Toxicol 45(5):368-377. https://doi.org/10.1093/jat/bkaa107

McIntyre IM (2014) Liver and peripheral blood concentration ratio (L/P) as a marker of

postmortem drug redistribution: a literature review. Forensic Sci Med Pathol 10(1):91–96. https://doi.org/10.1007/s12024-013-9503-x

McIntyre IM, Gary RD, Joseph S, Stabley R (2016) A fatality related to the synthetic opioid U-47700: Postmortem concentration distribution. J Anal Toxicol 41(2):158–160. https://doi.org/10.1093/jat/bkw124

Moore KA, Cina SJ, Jones R, et al (1999) Tissue distribution of tramadol and metabolites in an overdose fatality. Am J Forensic Med Pathol 20(1):98-100. https://doi.org/10.1097/00000433-199903000-00023

Musshoff F, Madea B (2001) Fatality due to ingestion of tramadol alone. Forensic Sci Int 116(2-3):197–199. https://doi.org/10.1016/S0379-0738(00)00374-1

Nordmeier F, Doerr A, Laschke MW, et al (2020) Are pigs a suitable animal model for in vivo metabolism studies of new psychoactive substances? A comparison study using different in vitro/in vivo tools and U-47700 as model drug. Toxicol Lett 329:12-19. https://doi.org/https://doi.org/10.1016/j.toxlet.2020.04.001

Nordmeier F, Doerr AA, Potente S, et al (2021a) Perimortem distribution of U-47700, tramadol and their main metabolites in pigs following intravenous administration. J Anal Toxicol. https://doi.org/10.1093/jat/bkab044

Nordmeier F, Sihinevich I, Doerr A, et al (2021b) Toxicokinetics of U-47700, tramadol, and their main metabolites in pigs following intravenous administration – Is a multiple species allometric scaling approach useful for the extrapolation of toxicokinetic parameters to humans? . Arch Toxicol *submitted*

Pélissier-Alicot A-L, Gaulier J-M, Champsaur P, Marquet P (2003) Mechanisms underlying postmortem redistribution of drugs: A Review. J Anal Toxicol 27(8):533–544. https://doi.org/10.1093/jat/27.8.533

Rambaran KA, Fleming SW, An J, et al (2017) U-47700: A clinical review of the literature. J Emerg Med 53(4):509–519. https://doi.org/10.1016/J.JEMERMED.2017.05.034

Rohrig TP, Miller SA, Baird TR (2017) U-47700: A not so new opioid. J Anal Toxicol42(1):e12-e14. https://doi.org/10.1093/jat/bkx081

Saar E, Beyer J, Gerostamoulos D, Drummer OH (2012) The time-dependant post-mortem redistribution of antipsychotic drugs. Forensic Sci Int 222(1):223–227. https://doi.org/https://doi.org/10.1016/j.forsciint.2012.05.028

Schaefer N, Kettner M, Laschke MW, et al (2017) Distribution of synthetic cannabinoids JWH-210, RCS-4 and Δ 9-tetrahydrocannabinol after intravenous administration to pigs. Curr Neuropharmacol 15(5):713–723. https://doi.org/10.2174/1570159X15666161111114214

Schaefer N, Kettner M, Laschke MW, et al (2015) Simultaneous LC-MS/MS determination of JWH-210, RCS-4, Δ9-tetrahydrocannabinol, and their main metabolites in pig and human serum, whole blood, and urine for comparing pharmacokinetic data. Anal Bioanal Chem 407(13):3775–3786. https://doi.org/10.1007/s00216-015-8605-6

Schaefer N, Kroell A-K, Koerbel C, et al (2019) Distribution of the (synthetic) cannabinoids JWH-210, RCS-4, as well as Δ9-tetrahydrocannabinol following pulmonary administration to pigs. Arch Toxicol 93(8):2211–2218. https://doi.org/10.1007/s00204-019-02493-8

Schaefer N, Kroell A-K, Koerbel C, et al (2020) Time- and temperature-dependent postmortem

concentration changes of the (synthetic) cannabinoids JWH-210, RCS-4, as well as Δ9-tetrahydrocannabinol following pulmonary administration to pigs. Arch Toxicol 95(5):1585-1599. https://doi.org/10.1007/s00204-020-02707-4

Schaefer N, Wojtyniak J-G, Kettner M, et al (2016) Pharmacokinetics of (synthetic) cannabinoids in pigs and their relevance for clinical and forensic toxicology. Toxicol Lett 253:7–16. https://doi.org/10.1016/J.TOXLET.2016.04.021

Schaefer N, Wojtyniak J-G, Kroell A-K, et al (2018) Can toxicokinetics of (synthetic) cannabinoids in pigs after pulmonary administration be upscaled to humans by allometric techniques? Biochem Pharmacol 155:403–418. https://doi.org/10.1016/J.BCP.2018.07.029

Skopp G (2010) Postmortem toxicology. Forensic Sci Med Pathol 6(4):314–325. https://doi.org/10.1007/s12024-010-9150-4

Strehmel N, Duempelmann D, Vejmelka E, et al (2018) Another fatal case related to the recreational abuse of U-47700. Forensic Sci Med Pathol 14(4):531–535. https://doi.org/10.1007/s12024-018-0018-3

Su H, Li Y, Wu M, et al (2020) Dynamic distribution and postmortem redistribution of tramadol in poisoned rats. J Anal Toxicol 45(2):203-210. https://doi.org/10.1093/jat/bkaa035

Truver MT, Smith CR, Garibay N, et al (2020) Pharmacodynamics and pharmacokinetics of the novel synthetic opioid, U-47700, in male rats. Neuropharmacology 177:108195. https://doi.org/https://doi.org/10.1016/j.neuropharm.2020.108195

Yarema MC, Becker CE (2005) Key Concepts in Postmortem Drug Redistribution. Clin Toxicol 43(4):235–241. https://doi.org/10.1081/CLT-58950

Zawilska JB (2017) An expanding world of novel psychoactive substances: Opioids. Front Psychiatry 8:110. https://doi.org/10.3389/fpsyt.2017.00110

Legends to Figures

Fig. 1 Percentage time-dependent postmortem (PM) concentration changes of **A** U-47700, **B** *N*-desmethyl-U-47700, **C** tramadol and **D** *O*-desmethyltramadol (PM interval (PMI) 1 light grey, PMI 2, grey, PMI 3 black) in tissue following administration of a 100 µg/kg body weight (BW) dose of U47700 or a 1000 µg/kg BW dose of tramadol to 6 pigs, each. Concentrations are displayed as median concentration change compared to concentrations calculated at PMI 0 (Nordmeier et al. 2021a). * indicate significant changes either to PMI 0 or between different PMIs ($p < 0.05$); peripheral blood (PB), central blood (CB), adipose tissue (AT), subcutaneous (s.c.).

Figure 1A/B

Click here to access/download;Figure;Fig1_AB.tif

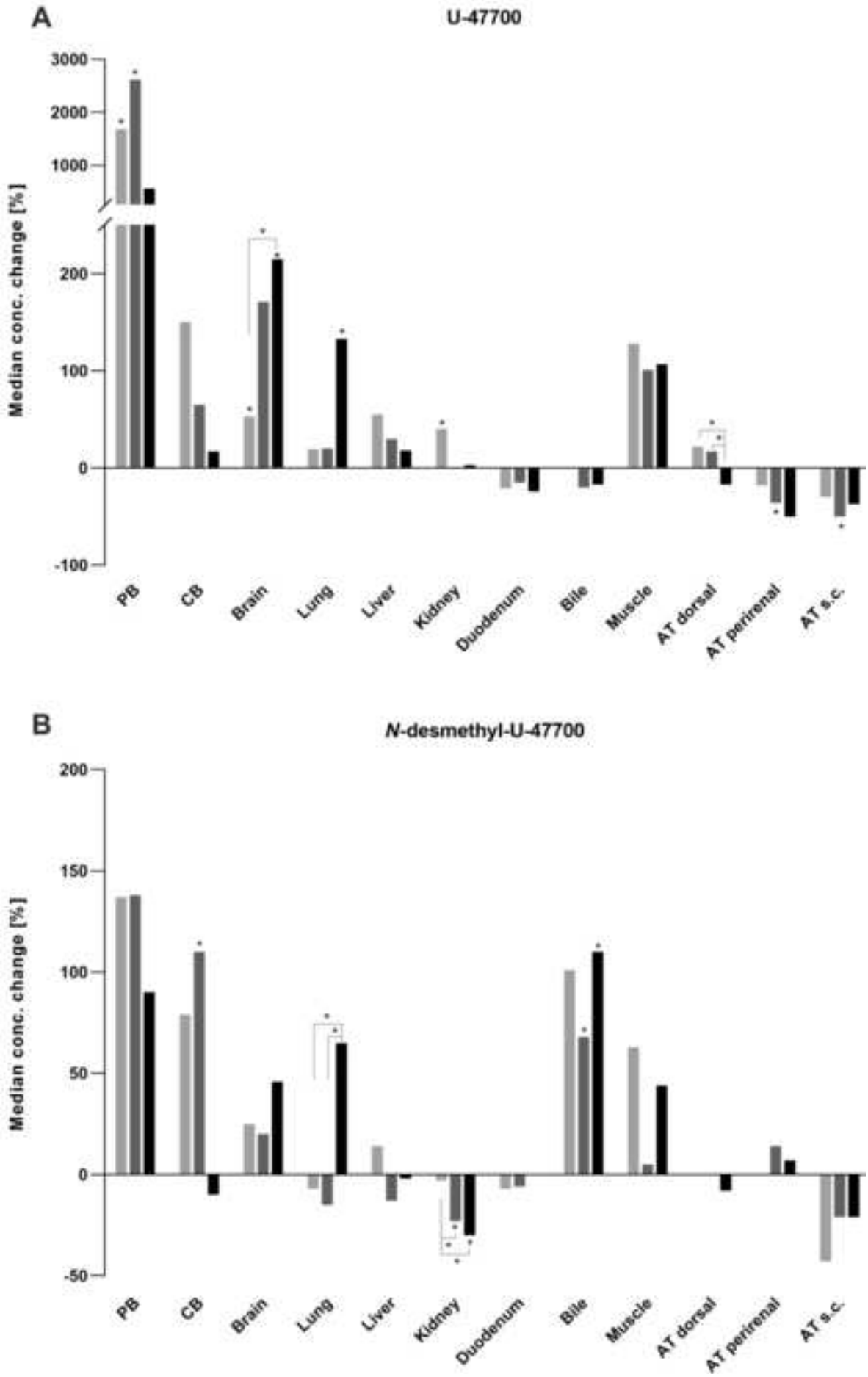

Figure 1C/D

Click here to access/download;Figure;Fig1_CD.tif

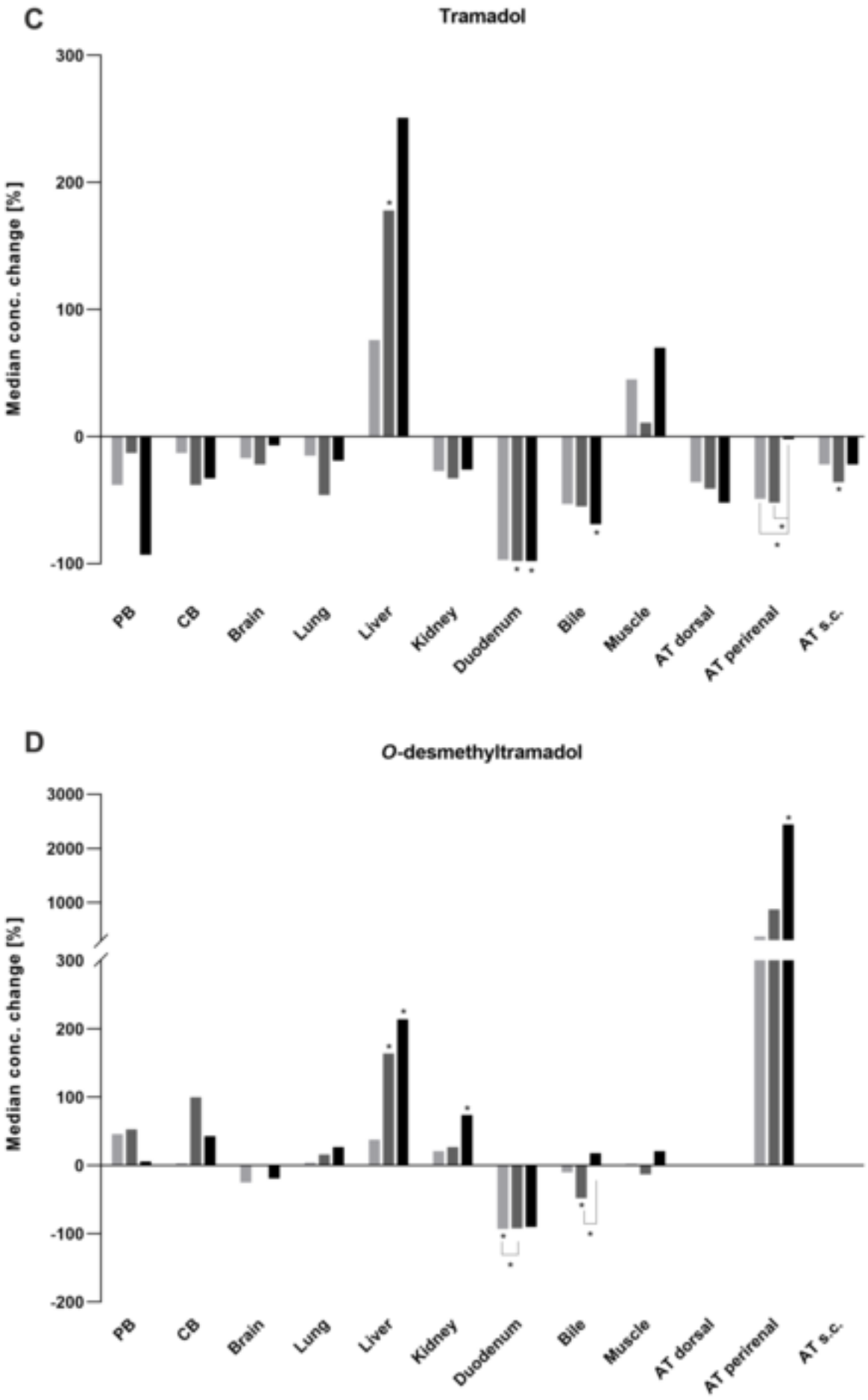

Table 1

Table 1 Median and mean concentrations ± standard deviation (SD) of U-47700 and *N*-desmethyl-U-47700 in tissues and body fluids measured at postmortem interval (PMI) 0 according to Nordmeier et al. 2021a and PMI 1-3; concentrations are approximated except for those marked with asterisk and displayed as one decimal non-zero; concentrations marked with [#] are measured in diluted samples and extrapolated; peripheral blood (PB), central blood (CB), adipose tissue (AT), subcutaneous (s.c.).

Specimen	Median conc. [mean conc. ± SD] in ng/mL or ng/g							
	U-47700				*N*-desmethyl-U-47700			
	PMI 0	PMI 1	PMI 2	PMI 3	PMI 0	PMI 1	PMI 2	PMI 3
PB	0.3* [0.4 ± 0.3] (*n* = 6)	5[#] [5 ± 2] (*n* = 6)	8[#] [9 ± 5] (*n* = 5)	2[#] [3 ± 1] (*n* = 3)	1* [2 ± 1] (*n* = 6)	3[#] [4 ± 3] (*n* = 6)	3[#] [5 ± 4] (*n* = 5)	2[#] [2 ± 1] (*n* = 3)
CB	0.3 [0.3 ± 0.3] (*n* = 6)	0.7* [0.9 ± 0.4] (*n* = 6)	0.5* [0.5 ± 0.1] (*n* = 6)	0.3 [0.5 ± 0.5] (*n* = 6)	2* [3 ± 2] (*n* = 6)	4* [4 ± 3] (*n* = 6)	4* [5 ± 2] (*n* = 6)	2* [3 ± 2] (*n* = 6)
Brain	1 [1±0.5] (*n* = 6)	2 [2 ± 1] (*n* = 6)	4 [4 ± 1] (*n* = 6)	5 [5 ± 1] (*n* = 6)	7 [8 ± 5] (*n* = 6)	8 [8 ± 2] (*n* = 6)	8 [10 ± 4] (*n* = 6)	10 [11 ± 4] (*n* = 6)
Lung	12 [12 ± 2] (*n* = 6)	15 [16 ± 6] (*n* = 6)	15 [17 ± 6] (*n* = 6)	29 [28 ± 9] (*n* = 6)	48 [49 ± 16] (*n* = 6)	44 [47 ± 19] (*n* = 6)	41 [45 ± 23] (*n* = 6)	79 [79 ± 27] (*n* = 6)
Liver	10 [9 ± 5] (*n* = 6)	15 [13 ± 4] (*n* = 6)	13 [13 ± 2] (*n* = 6)	12 [10 ± 5] (*n* = 6)	39 [40 ± 7] (*n* = 6)	44 [41 ± 7] (*n* = 6)	33 [33 ± 7] (*n* = 6)	38 [33 ± 17] (*n* = 6)
Kidney	6 [7 ± 0.7] (*n* = 6)	9 [9 ± 2] (*n* = 6)	6 [7 ± 2] (*n* = 6)	7 [6 ± 2] (*n* = 6)	16 [19 ± 8] (*n* = 6)	15 [20 ± 9] (*n* = 6)	12 [14 ± 7] (*n* = 6)	11 [11 ± 2] (*n* = 6)
Duodenum	73 [98 ± 73] (*n* = 6)	58 [58 ± 12] (*n* = 6)	62 [60 ± 11] (*n* = 6)	55 [54 ± 9] (*n* = 6)	70 [78 ± 17] (*n* = 6)	65 [68 ± 14] (*n* = 6)	65 [71 ± 19] (*n* = 6)	70 [70 ± 12] (*n* = 6)
Bile	34 [36 ± 14] (*n* = 6)	34 [36 ± 11] (*n* = 6)	27 [27 ± 3] (*n* = 5)	28 [28 ± 0.3] (*n* = 2)	19 [21 ± 9] (*n* = 6)	38 [37 ± 17] (*n* = 6)	32 [36 ± 15] (*n* = 5)	39 [39 ± 5] (*n* = 2)
Muscle	2 [2 ± 0.6] (*n* = 6)	6 [6 ± 2] (*n* = 6)	5 [35 ± 3] (*n* = 6)	5 [5 ± 2] (*n* = 6)	3 [3 ± 1] (*n* = 6)	4 [6 ± 4] (*n* = 6)	3 [3 ± 2] (*n* = 6)	4 [4 ± 0.7] (*n* = 6)
AT dorsal	23 [23 ± 7] (*n* = 6)	28 [31 ± 11] (*n* = 6)	27 [32± 16] (*n* = 6)	19 [19 ± 4] (*n* = 6)	12 [22 ± 2] (*n* = 6)	12 [13 ± 3] (*n* = 6)	12 [12 ± 2] (*n* = 6)	11 [12± 2] (*n* = 6)
AT perirenal	28 [28 ± 6] (*n* = 6)	23 [22 ± 5] (*n* = 6)	18 [17 ± 4] (*n* = 6)	14 [15 ± 7] (*n* = 6)	14 [13 ± 1] (*n* = 6)	14 [14 ± 4] (*n* = 6)	16 [17 ± 8] (*n* = 6)	15 [15 ± 3] (*n* = 6)
AT s.c.	30 [27 ± 10] (*n* = 6)	21 [20 ± 8] (*n* = 6)	15 [55 ± 5] (*n* = 6)	19 [19 ± 5] (*n* = 6)	14 [14 ± 4] (*n* = 6)	8 [9 ± 4] (*n* = 6)	11 [10 ± 3] (*n* = 6)	11 [11 ± 2] (*n* = 6)

Table 2 Median and mean concentrations ± standard deviation (SD) of tramadol and *O*-desmethyltramadol in tissues and body fluids measured at postmortem interval (PMI) 0 according to Nordmeier et al. 2021a and PMI 1-3; concentrations are approximated except for those marked with asterisk and displayed as one decimal non-zero; concentrations marked with # are measured in diluted samples and extrapolated; peripheral blood (PB), central blood (CB), adipose tissue (AT), subcutaneous (s.c.), not detectable (n.d.).

Specimen	Median conc. [mean conc. ± SD] in ng/mL or ng/g							
	Tramadol				*O*-desmethyltramadol			
	PMI 0	PMI 1	PMI 2	PMI 3	PMI 0	PMI 1	PMI 2	PMI 3
PB	4* [5 ± 3] (*n* = 6)	3# [2 ± 1] (*n* = 5)	4# [4 ± 3] (*n* = 5)	0.3# [2 ± 2] (*n* = 3)	2 [2 ± 2] (*n* = 6)	3# [3 ± 0.3] (*n* = 5)	3# [3 ± 0.4] (*n* = 5)	2# [2 ± 0.7] (*n* = 3)
CB	4* [4 ± 1] (*n* = 6)	4* [3 ± 1] (*n* = 6)	3* [8 ± 14] (*n* = 6)	3* [3 ± 2] (*n* = 6)	3 [2 ± 1] (*n* = 6)	4 [4 ± 0.7] (*n* = 6)	5 [9 ± 7] (*n* = 6)	4 [4 ± 1] (*n* = 6)
Brain	21 [21 ± 7] (*n* = 6)	17 [18 ± 9] (*n* = 6)	16 [19± 11] (*n* = 6)	20 [20 ± 11] (*n* = 6)	10 [11 ± 6] (*n* = 6)	8 [9 ± 6] (*n* = 6)	10 [11 ± 6] (*n* = 6)	8 [11 ± 9] (*n* = 6)
Lung	52 [81 ± 80] (*n* = 6)	44 [53 ± 27] (*n* = 6)	28 [39 ± 33] (*n* = 6)	43 [49 ± 28] (*n* = 6)	22 [47 ± 63] (*n* = 6)	23 [26 ± 20] (*n* = 6)	26 [27 ± 24] (*n* = 6)	28 [31 ± 23] (*n* = 6)
Liver	7 [8 ± 1] (*n* = 6)	13 [15 ± 5] (*n* = 6)	21 [21 ± 6] (*n* = 6)	26 [23 ± 10] (*n* = 6)	8 [9 ± 3] (*n* = 6)	11 [12 ± 3] (*n* = 6)	21 [22 ± 5] (*n* = 6)	25 [23 ± 5] (*n* = 6)
Kidney	46 [46 ± 18] (*n* = 6)	34 [38 ± 19] (*n* = 6)	31 [41 ± 22] (*n* = 6)	34 [38 ± 18] (*n* = 6)	40 [40 ± 9] (*n* = 6)	48 [52 ± 21] (*n* = 6)	51 [64 ± 36] (*n* = 6)	70 [88 ± 55] (*n* = 6)
Duodenum	341 [378 ± 187] (*n* = 6)	10 [17 ± 20] (*n* = 6)	6 [13 ± 19] (*n* = 6)	6 [7 ± 7] (*n* = 6)	44 [46 ± 20] (*n* = 6)	3 [4 ± 4] (*n* = 6)	3 [4 ± 3] (*n* = 6)	4 [4 ± 2] (*n* = 6)
Bile	914 [855 ± 286] (*n* = 6)	433 [342 ± 187] (*n* = 5)	407 [318 ± 266] (*n* = 3)	282 [282 ± 21] (*n* = 2)	171 [205 ± 120] (*n* = 6)	154 [129 ± 88] (*n* = 5)	88 [68 ± 61] (*n* = 3)	202 [202 ± 76] (*n* = 2)
Muscle	12 [12 ± 4] (*n* = 6)	17 [18 ± 11] (*n* = 6)	13 [19 ± 15] (*n* = 6)	20 [25 ± 19] (*n* = 6)	6 [8 ± 3] (*n* = 6)	7 [9 ± 5] (*n* = 6)	6 [8 ± 5] (*n* = 6)	8 [10 ± 6] (*n* = 6)
AT dorsal	49 [47 ± 24] (*n* = 6)	31 [33 ± 13] (*n* = 6)	29 [30 ± 13] (*n* = 6)	23 [23 ± 8] (*n* = 6)	n.d.	n.d.	n.d.	n.d.
AT perirenal	37 [35 ± 12] (*n* = 6)	19 [18 ± 12] (*n* = 6)	18 [17 ± 8] (*n* = 6)	36 [38 ± 19] (*n* = 6)	1 [1 ± 1] (*n* = 6)	6 [7 ± 6] (*n* = 6)	13 [13 ± 13] (*n* = 6)	34 [31 ± 18] (*n* = 6)
AT s.c.	41 [46 ± 13] (*n* = 6)	32 [31 ± 7] (*n* = 6)	26 [28 ± 7] (*n* = 6)	32 [35 ± 14] (*n* = 6)	n.d.	n.d.	n.d.	n.d.

Electronic Supplementary Material

Are the (new) synthetic opioids U-47700, tramadol and their main metabolites prone to time-dependent postmortem redistribution? – A systematic study using an in vivo pig model

Frederike Nordmeier[1], Adrian A. Doerr[1], Stefan Potente[1], Nadja Walle[1], Matthias W. Laschke[2], Michael D. Menger[2], Peter H. Schmidt[1], Markus R. Meyer[3], and Nadine Schaefer[1*]

[1]Institute of Legal Medicine, Saarland University, 66421 Homburg, Germany

[2]Institute for Clinical and Experimental Surgery, Saarland University, 66421 Homburg, Germany

[3]Department of Experimental and Clinical Toxicology, Institute of Experimental and Clinical Pharmacology and Toxicology, Center for Molecular Signaling (PZMS), Saarland University, 66421 Homburg, Germany

Stock solutions, calibration standards, quality control samples, and calibrators for standard addition

As already described in previous studies (Nordmeier et al. 2021a, b), standard stock solutions with a concentration of 1 mg/mL of U-47700 and *N*-desmethyl-U-47700 were prepared by dissolving the solid compound in methanol. The stock solutions or liquid reference standards were diluted with ethanol to receive working standard solutions (0.001, 0.01, 0.1 mg/mL) of all compounds. Diluting those working solutions with ethanol, spiking solutions for calibration standards were created in whole blood. Concentrations were as follows: 0.5, 1, 5, 10, 15, 20, 50, and 100 ng/mL. In the same manner, quality control (QC) LOW (2 ng/mL for U-47700 and metabolite; 8 ng/mL for tramadol and 20 ng/mL for ODT) and HIGH (35 ng/mL for U-47700 and metabolite; 80 ng/mL for tramadol and metabolite) samples were prepared. All prepared solutions were stored at -20 °C until usage. In Table S1, the concentrations of calibrators used for standard addition are listed.

Surgical Procedure

According to previous studies (Nordmeier et al. 2020, 2021a, b), ketamine hydrochloride (30 mg/kg, Ursotamin; Serumwerke Bernburg, Bernburg, Germany), xylazine hydrochloride (2.5 mg/kg, Rompun; Bayer, Leverkusen, Germany) and 1 mg atropine (Braun, Melsungen, Germany) were used for a premedication by intramuscular injection of the pigs. Analgosedation was preserved with isoflurane (2-4%, Forene, AbbVie, Ludwigshafen, Germany). For mechanical ventilation a mixture of oxygen and air (1:2 v/v; FiO_2 of 0.30; Respirator ABV-U; F. Stephan GmbH, Gackenbach, Germany) and a tidal volume of 10-12 mL/kg was used. The animals got a fluid replacement with sodium chloride 0.9% (8 mL $kg^{-1}h^{-1}$) (Braun, Melsungen, Germany). For this purpose, a catheter was placed in the left ear vein. A triple-lumen 7F central venous catheter (Certofix Trio, Braun, Melsungen, Germany) was placed into the jugular vein

for intravenous (i.v.) drug administration, sample collection and monitoring of mean central venous pressure. Urine collection was ensured by a suprapubic catheter (Cystofix, Braun, Melsungen, Germany) inserted to the bladder. Before drug administration, the animals were allowed to stabilize for 10-15 min.

Sample Preparation

Blood Specimens

According to previous studies (Nordmeier et al. 2021a, b), in a vial, 50 µL of an ethanolic stable-isotope-labeled internal standard mixture solution (SIL-IS; 10 ng/50 µL of *N*-desmethyl-U-47700-d_3, tramadol-C_{13}-d_3, and *O*-desmethyltramadol- d_6) and 50 µL of ethanol were submitted as well as 2 mL phosphate buffer. The homogenized blood samples (1 mL each) were added to this mixture. By a replacement of the 50 µL of ethanol with 50 µL of the appropriate spiking solution and under the usage of blank whole blood samples, the calibrators and quality controls were prepared. The samples were vortexed and centrifugated at 3,200 g for 8 min. Afterwards, solid-phase extraction (SPE) was carried out as described below.

Tissue Specimens

An amount of 2 g solid tissue (brain, lung, liver, kidney, skeletal muscle tissue), bile fluid or duodenum content was homogenized (tissue/fluid/content:water 1:5, w/w) as already described previous (Nordmeier et al. 2021a). In case of AT specimens, water was replaced by acetonitrile (tissue/acetonitrile 1:5, w/w). After centrifugation for 8 min at 3,200 g, the supernatants were split up into four 1 mL portions. The supernatant of homogenized duodenum content of the pigs receiving U-47700 was diluted with phosphate buffer 1:2 (v/v) and the supernatants of homogenized lung and duodenum content of the pigs receiving tramadol were diluted 1:2 (v/v) as well as the supernatants of homogenized bile fluid 1:10 (v/v). For the creation of a standard

addition curve, 50 µL of ethanol or the different three calibrator concentrations of U-47700 and *N*-desmethyl-U-47700 or tramadol and *O*-desmethyltramadol were added according to Table S1. 50 µL of the ethanolic SIL-IS solution (20 ng/50 µL) and 2 mL phosphate buffer were added to the prepared homogenates. The samples were vortexed and centrifuged at 3,200 g for 8 min. Afterwards, SPE was carried out as described below.

Solid phase extraction

Bond Elut HCX cartridges (130 mg/3 mL; Agilent, Waldbronn, Germany) were used for SPE as already mentioned in former studies (Nordmeier et al. 2021a, b). First, the columns were conditioned two times with 3 mL methanol and one time with 3 mL phosphate buffer (0.1 M, pH 6). The prepared blood specimens or tissue homogenates were subsequently loaded onto the cartridges. Afterwards, the cartridges were washed twice with 2 mL phosphate buffer and one time with 2.75 mL hydrochloric acid (0.01 M). The columns were dried with swabs and afterwards for 10 min under maximum vacuum (10 inHg). The columns were dried again for 3 min under maximum vacuum following a carefully treatment with 2 mL of methanol. The analytes were eluted with 1.75 mL of dichloromethane-methanol-ammonia solution (25%) (30:15:1.25, v/v). Subsequently, the eluates were evaporated under a gentle stream of nitrogen at 60 °C and reconstituted in 100 µL of mobile phase A (50 mM aqueous ammoniumformiate, pH 3.5). Then, the extracts were shaken for 15 min and 20 µL were injected onto the liquid-chromatography tandem mass spectrometry (LC-MS/MS) system.

LC-MS/MS conditions

As described previously (Nordmeier et al. 2021a, b), an AB SCIEX (Darmstadt, Germany) API 3200 QTrap tandem mass spectrometer with electrospray ionization (ESI) was used for

detection. The MS was linked to a Shimadzu Prominance HPLC equipped with two solvent delivery units (LC-20AD), communication bus modul (CBM-20A), autosampler (SIL-20AC), degasser (DGU-20), and column oven (CTO-10AC).

A Waters (Wexford, Ireland) Sunfire C_{18} column (150 x 2.1 mm, 3.5 µm) with a gradient elution was applied using mobile phase A (50 mM aqueous ammoniumformiate, pH 3.5) and B (0.1 % formic acid in acetonitrile). The runtime was about 16 min. The gradient started with 25 % eluent B, ramped to 36 % eluent B from 1.5 to 10 min, ramped to 95 % eluent B from 10 to 11 min, hold 95 % eluent B for 1 min, reducing to 25 % eluent B from 12 to 12.5 min, and held 25 % eluent B from 12.5 to 16 min. A flow rate of 0.3 mL/min was adjusted. The oven temperature was set at 30 °C and the injection volume amounted to 20 µL.

Ionization was performed with the ESI source in positive mode. Multiple-reaction monitoring (MRM) was carried out under the usage of a dwell time of 100 ms. Three transitions per precursor ion for U-47700 and *N*-demethyl-U-47700, and two for tramadol and *O*-demethyltramadol were settled for the detection of the compounds (Table S2). The source and gas settings were as follows: curtain gas (N_2) – 35 psi, collision gas (N_2) – medium, temperature – 500 °C, ion source gas 1 (N_2) – 50 psi, ion source gas 2 (N_2) – 80 psi, ion spray voltage – 5500 V. Quantification was performed with the Analyst software Version 1.6.

Table S1 Calibrator concentrations, addition per mL homogenized tissue of the analytes used for the standard addition approach in the different specimens.

Analyte	Specimen	Calibrator Conc. [ng/mL homogenized tissue]		
		1	**2**	**3**
U-47700 ***N*-desmethyl-U-47700**	Muscle tissue/Brain	5	10	15
	Kidney/Bile Fluid	10	20	30
	Lung/Liver/Adipose tissue	20	40	60
	Duodenum Content	40	80	120
Tramadol ***O*-desmethyltramadol**	Liver/Muscle tissue	10	20	30
	Brain/Duodenum content/Adipose tissue	20	40	60
	Kidney/Lung/Bile Fluid	40	80	120

Table S2 MRM transitions and MS conditions for all analytes and the stable-isotope-labeled internal standard with collision energy (CE), declustering potential (DP), entrance Potential (EP), and collision cell exit potential (CXP).

Analyte	RT (min)	Precursor Ion (Q1, m/z)	Product Ion (Q3, m/z)	DP (V)	EP (V)	CE (V)	CXP (V)
U-47700	7.99	329.016	173.000	41	6.5	39	6
		329.016	284.200	41	6.5	19	16
		329.016	204.100	41	6.5	33	6
***N*-desmethyl-U-47700**	7.42	314.946	284.00	41	7	21	12
		314.946	173.100	41	7	35	6
		314.946	204.100	41	7	35	8
Tramadol	2.88	264.269	58.200	21	6.5	37	4
		264.269	57.400	21	6.5	37	58
***O*-desmethyltramadol**	2.33	250.223	57.900	21	10	39	8
		250.223	57.100	21	10	77	4
***N*-desmethyl-U-47700-d_3**	7.36	318.083	287.200	41	9	21	10
		318.083	176.100	41	9	39	6
		318.083	148.100	41	9	65	4
Tramadol-C_{13}-d_3	2.84	268.231	58.00	31	4	37	8
		268.231	57.100	31	4	89	56
***O*-desmethyltramadol-d_6**	2.32	256.151	64.100	36	3	29	4
		256.151	77.000	36	3	79	4

References

Nordmeier F, Doerr A, Laschke MW, et al (2020) Are pigs a suitable animal model for in vivo metabolism studies of new psychoactive substances? A comparison study using different in vitro/in vivo tools and U-47700 as model drug. Toxicol Lett 329:12-19. https://doi.org/https://doi.org/10.1016/j.toxlet.2020.04.001

Nordmeier F, Doerr AA, Potente S, et al (2021a) Perimortem distribution of U-47700, tramadol and their main metabolites in pigs following intravenous administration. J Anal Toxicol. https://doi.org/10.1093/jat/bkab044

Nordmeier F, Sihinevich I, Doerr A, et al (2021b) Toxicokinetics of U-47700, tramadol, and their main metabolites in pigs following intravenous administration – Is a multiple species allometric scaling approach useful for the extrapolation of toxicokinetic parameters to humans? . Arch Toxicol *submitted*

4. DISCUSSION AND CONCLUSION

TK data are profitably for the interpretation of analytical results in clinical and forensic toxicology since they are necessary for a superior explanation in such cases. In this context, TK data could be used e.g., for an appraisal of the time of a consumption based on the results of an analytical approach. Furthermore, the understanding of the metabolic behavior of a substance is important. Especially in terms of extensive metabolism of a substance, parent compounds may not be the proper analytical targets in urinary analytical approaches. Furthermore, in forensic cases with a long period of time between consumption and sampling, parent compounds might not be detectable anymore, as well. Such cases bear the challenge of the discovery of a possible intoxication and sometimes could only be revealed through the detection of metabolites. Because of an increasing consumption of NPS, this class of drugs is gaining an increasing relevance in clinical and forensic toxicology, e.g., in DUID cases. Due to their high potency, NSO-induced intoxications and fatalities rose worldwide in a dramatic way during the last years. Whereas new releases of some NPS subclasses decreased during the last years, new appearances of NSO still increased or stagnated. Therefore, an enhancement of the knowledge concerning the TK of NPS and particularly of NSO is imperative. In this way, the presented studies clearly expanded the knowledge on TK data of NSO in terms of the metabolic fate of three different model NSO covering fentanyl derived and non-fentanyl derived substances with MOR or KOR affinity. Furthermore, several TK parameters of one of the most famous NSO, namely U-47700, were elucidated using a comprehensive controlled pig study following i.v. administration.

In a first step, the metabolic excretion profiles of U-51754, U-47931E, and methoxyacetylfentanyl were elucidated in rat urine and subsequently compared to the metabolic pattern generated in an in vitro metabolism approach using phS9 fractions. Regarding the non-fentanyl derived NSO U-51754 and U-47931E, the most intensive metabolites in rat urine were formed by *N*-demethylation of the amine part, hydroxylation of the hexyl ring and combinations thereof. Main metabolites of methoxyacetylfentanyl were formed by *N*-dealkylation, *O*-demethylation, and hydroxylation at the alkyl moiety. Phase II metabolites were formed by glucuronidation or in terms of U-51754 additionally by sulfation but only played a minor role in the urinary excretion profile. Thus, they are not useful as targets for routine analysis and a possible conjugation cleavage prior to analysis might not be necessary in such approaches. Interestingly, U-51754 showed a pronounced metabolism in contrast to U-47931E. Whilst for U-47931E only few metabolites were formed in vitro, many metabolites of U-51754 were found in phS9 fractions. Furthermore, phase II metabolites of U-51754 were extensively formed in rat urine while the formation of phase II metabolites of U-47931E was less presented. The fact, that U-47931E was highly detectable in rat urine whereas the unaltered parent compound of U-51754 was only found to a minor extent leads to the conclusion that U-47931E might be less metabolized and could be excreted in its unchanged form. Reported by Gampfer et *al.* (56), who studied the metabolism of U-48800, only trace amounts of the unchanged parent compound were found in rat urine, as well. This might tempt to

the suggestion that the chemical differences in the structure of the different U-substances are crucial for the higher metabolism rate of U-51754 and U-48800, which both contain two chlorine atoms, while U-47931E contains only one bromine atom instead of chlorine. The different chemico-physical properties of both halogenic atoms may influence the fitting to the metabolizing CYP enzymes. Next to this, the methylene spacer between the aromatic ring system and the carbonyl part of the molecule (inserted in U-51754 and U-48800) may have an impact on the metabolism rate due to different possible spatial orientations. However, the fact that U-47700 contains no methylene spacer and was only low abundant in rat urine samples either, contradicts this hypothesis (104). Overall, metabolite formation in rat and in phS9 fractions was comparable concerning the main metabolites, but in general, fewer metabolites, especially phase II metabolites or those formed by multiple reaction steps, were found in vitro. Furthermore, attached processes following the actual metabolism, such as enterohepatic circulation, reabsorption, and overall renal elimination are not covered by in vitro approaches and limit them. Equal results for the comparison of phS9 or other in vitro metabolism approaches with rat urinary excretion profiles have already been found in other studies as well (54, 106, 107). This fact indicates that in vitro approaches display a good alternative to in vivo metabolism approaches, but not necessarily reflect the authentic urinary excretion profile. Hence, in vitro results should be verified by in vivo approaches. Firstly, main metabolites might not be formed in vitro if they are related to multiple reaction steps or phase II metabolites. Secondly, no estimations of metabolite quantity are possible with in vitro approaches. Furthermore, metabolites of the U-compounds were found in rat urine with hydroxylation predominantly occurring at the hexyl ring as observed in phS9, but also at the phenyl ring. However, it was not possible to differentiate if this finding was ascribed to differences between in vitro and in vivo models or to differences between rat and human metabolism. Nevertheless, the results found in this study were in good agreement to those obtained in former studies presented in the literature (70, 108). In general, parent compounds were only present in trace quantities in rat urine except for U-47931E. Therefore, metabolites might be essential urinary targets for the analysis of NSO in real case samples, especially if the consumption of such substances took place a long time ago.

In a next step, different TK data of the model NSO U-47700 in comparison to tramadol were obtained in a systematic study using pigs as an in vivo model following i.v. administration. In pig urine samples, Concerning the metabolism, 7 phase I and 2 phase II metabolites of U-47700 were found in pig urine samples. Major phase I reactions were *N*-demethylation, hydroxylation, and combination of thereof leading to the main metabolites *N*-desmethyl-U-47700 and *N*,*N*-bisdesmethyl-hydroxy-U-47700. Both were detectable 2-3 h following administration until the end of the experiment (8 h). Metabolites which are more polar, such as the hydroxy metabolite or the *N*-oxide metabolite, were only detectable in the first period of the experiment. Phase II metabolites were formed by further glucuronidation of the phase I metabolites but only to a limited extent and thus play a minor role as targets in routine toxicological analysis. Comparable metabolites were identified in rat and human urine as well as in different in vitro metabolism approaches (pig liver microsomes (PLM), pHLM and phS9). Thereby, the production of

PLM allowed for the evaluation of the intraspecies correlation between in vivo and in vitro metabolism not only in human, but also in pig. Overall, 12 phase I and 8 phase II metabolites were tentatively identified. The human in vitro initial formation of phase I metabolites was predominantly catalyzed by CYP2B6, CYP2C19, CYP3A4, and CYP3A5. The flavin-containing monooxygenase 3 catalyzed the *N*-oxidation. In the different in vivo models, the same urinary main metabolites (*N*-desmethyl-, *N*,*N*-bisdesmethyl-, *N*-desmethyl-hydroxy-, *N*,*N*-bisdesmethyl-hydroxy-U-47700) were identified. They are, next to the parent compound, appropriate urinary targets for the proof of an U-47700 consumption. Nevertheless, minor differences were observed between those three species. Metabolites formed by hydroxylation at the phenyl ring were solely formed by rats, whereas the *N*-oxide metabolite was only found in pig urine samples indicating a different involvement of several CYP enzymes or other metabolizing enzymes in various species. All in vitro formed metabolites were in good agreement in every chosen model. Furthermore, the main metabolites formed in vitro were similar to those formed in the different in vivo models. However, phase II metabolites and metabolites formed by more than one or two reaction steps were not covered by the different in vitro models or only to a limited extent. Thus, this study additionally showed that in vitro metabolism approaches are a suitable tool for metabolite investigations, but especially concerning phase II metabolites, in vivo models are necessary for metabolite investigations. Apart from some minor disagreements, the results of our pig study were comparable to those acquired from human specimens. This leads to the suggestion that pigs are an appropriate model for the examination of (human) NSO metabolism. Based on the comparable metabolism between humans and pigs, the following implementation of a comprehensive TK study in pigs including the investigation of TK parameters and tissue distribution appeared to be promising. Furthermore, an extrapolation of the pig TK parameters to humans seemed to be possible.

Therefore, subsequently, an LC-MS/MS method for the concomitant quantification of U-47700, tramadol, and their main metabolites in pig serum and whole blood was developed and fully validated according to national and international guidelines. This method was used for the assessment of concentration-time profiles of both substances by analyzing samples of both matrices following the i.v. administration to pigs. Afterwards, a popTK model was successfully developed for the description of the concentration-time profiles of U-47700 and tramadol in serum. The TK data of those opioids were best recovered by a three-compartment model. Via allometric scaling techniques, the final popTK model parameters for pigs were upscaled to predict human exposure of tramadol. In this context, single and multiple species scaling were evaluated. Although this empirical approach using multiple species scaling is widespread used in drug development, especially with small mammals (109, 110), it was a challenging task in our animal study, probably due to the very large interspecies variability between the considered species. Since tramadol is primarily eliminated through metabolism by CYP enzymes in the liver (5), differences in expression of CYPs in different species may have a considerable impact on the output of scaling approaches (77). Despite the utilization of additional correction factors to address this issue, the prediction of tramadol could not be improved. However, single species scaling approaches are

commonly used for the extrapolation from animal experiments to humans (110, 111). In our study, a single species scaling from pig to human revealed best results for the prediction of human tramadol exposure. Although the concentration-time profiles of tramadol and *O*-desmethyltramadol suggested a faster metabolism of tramadol in pig, the single species scaling was reasonably applicable for the prediction of human tramadol data by the incorporation of the liver blood flow. Overall, the TK parameters determined for tramadol and U-47700 showed many similarities indicating that the usage of tramadol as a well-studied reference compound was a good choice. The correlation of our U-47700 TK data with case reports from the literature allowed the conclusion of a faster metabolism of this substance in pig compared to human as well. Hence, the same scaling method was successfully applied to simulate a potential concentration-time curve of U-47700 for human. Indeed, a limitation is the lack of human TK data of U-47700 for the final evaluation of this model. Nevertheless, due to the great similarities of the TK data of tramadol and U-47700 determined in this study, one can conclude that this pig model in combination with corresponding TK modeling approaches might be a powerful instrument for the prediction of human NSO data. Especially since NSO are marketed without previous pre-clinical safety investigations and in general, few to nothing is known about TK data, this approach may offer interesting and useful TK facts, which could be helpful in the interpretation of clinical and forensic cases.

In a next step, various specimens involving relevant organs, tissues and body fluids were sampled for the investigation of the perimortem distribution pattern of the drugs of interest. U-47700, tramadol and their main metabolites were found in all analyzed specimens except for *O*-desmethyltramadol, which was not observed in adipose tissue. Both parent compounds displayed highest concentrations in bile and duodenum content besides routinely analyzed samples for PM toxicology such as lung, liver, and kidney. Insofar, these specimens are suitable samples for PM toxicological analysis. A storage in lung was noticeable for tramadol. Furthermore, both parent compounds accumulated in adipose tissue, implying this matrix to be appropriate as an alternative, especially if other specimens are not available anymore. At the time of death, the drugs were also detectable in muscle tissue and brain. Regarding the metabolites, *N*-desmethyl-U-47700 and *O*-desmethyltramadol revealed highest concentrations in organs involved in metabolism and excretion. *N*-desmethyl-U-47700 displayed elevated concentrations in routinely analyzed body fluids, organs, and tissues compared to U-47700. Therefore, next to the parent compound, this metabolite might be a helpful target in PM toxicological analysis particularly in intoxication cases with long term PMI. Blood concentrations of all substances were very low in comparison to concentrations in organ and tissue specimens. Despite higher consumed doses, detection in blood specimens might be difficult especially in intoxication cases with long term PMI. Therefore, toxicological investigations of the recommended specimens would be a powerful tool for the detection of NSO and tramadol in PM toxicology. This part of the study shows that rarely analyzed matrices like duodenum content and adipose tissue might also be helpful in the enlightenment of forensic cases if no or only low concentrations could be found in others. Hence, the sampling of an extensive spectrum of different matrices during the autopsy might be helpful regarding unexplained cases with the suspicion

of an intoxication. In these cases, a possible fall back on these additional biopsies and a further screening next to routine samples might yield the decisive hint.

In a last step of this work, the PM distribution as well as time-dependent concentration changes at room temperature during three different PMI (24 h, 48 h, 72 h) were assessed in the already perimortem analyzed organs and body fluids for the examined drugs. The results of this study revealed that the PM distribution of all substances was comparable to the perimortem one with only minor exceptions. Thus, the routinely analyzed PM specimens (lung, liver, kidney) are suitable matrices for a qualitative PM analysis of U-47700 and tramadol. Duodenum content and bile are also viable matrices. Since both parent compounds seem to be stored in adipose tissue, these specimens could serve as alternative matrices. *N*-desmethyl-U-47700 was found in all analyzed tissues, organs, and body fluids, whereas *O*-desmethyltramadol was not detectable in dorsal and subcutaneous adipose tissue excluding these specimens as alternative matrices for the analysis of this metabolite. As already observed in perimortem samples, concentrations of *N*-desmethyl-U-47700 were higher in most of the analyzed PM specimens compared to its parent compound as well. In general, only low to moderate time-dependent concentration changes of all compounds were detected in the analyzed specimens during the storage at room temperature. However, regarding tramadol, a remarkable concentration increase in lung and a distinctive concentration decrease in duodenum content and bile were observed. The decrease of the concentration in duodenum content and bile was noticed for the metabolite *O*-desmethyltramadol as well. Hence, a PM quantification in those specimens should be avoided, but the specimens are still suitable for qualitative analysis. No clear trend for concentration changes were observed in peripheral blood, whereas all analytes showed more or less stable concentrations in central blood during the examined PMI. Insofar, the matrix of first choice for the quantification of U-47700 and tramadol is central blood. Since no remarkable PMR was observed, muscle tissue and brain could serve as alternative matrices for quantification, especially if no blood is available. In conclusion, U-47700, tramadol, and their main metabolites are only slightly to moderately prone to PMR but the distinct concentration decrease of tramadol in duodenum content clarified that the examination of a possible PMR was necessary.

The basic principle of this experimental approach using pigs as animal models for the investigation of TK parameters was already established for synthetic cannabinoids with Δ9-tetrahydrocannabinol (THC) as reference compound. Based on this model and in combination with popTK modeling, human THC exposure was successfully predicted after i.v. (36), as well as after pulmonary administration reflecting typical user habits (35). With this study, it has already been possible to determine TK data and predict human data for the second class of NPS indicating that pigs in combination with popTK modeling are a powerful tool in TK. Pigs are more and more used in the medicinal and pharmaceutical research and often replace studies for example in dogs (83). Although the number of animal studies dropped down over the last years and especially in first phase trials, animals still play a central role in pharmaceutical drug development processes, biomedical research, and toxicity testing (112, 113). Whereas in early

phase stages in pharmaceutical drug development (preclinical phases) mostly small animals such as (genetically modified) mice, rats, guinea pigs, and rabbits are preferred, larger animals like dogs, pigs, and primates are still commonly used in later phase trials (113). Unfortunately, especially toxicity results from rodent animal studies are often highly inconsistent for the prediction of the human toxic response (114). In comparison to rats and mice, both commonly used as experimental animals amongst others in metabolic investigations (54, 107), pigs offer the benefit of a larger sampling volume. Whereas, due to a very small blood volume, multiple rats are necessary for the determination of one concentration-time curve covering a longer time period (80), a whole TK study incorporating the establishment of a whole concentration-time profile, metabolic investigations, and multiple organ sampling is possible within one single pig. Hence, a reduction of the number of experimental animals is possible by the utilization of larger animals, keeping in mind that a moderate to high population/sample size is essential for the improvement of the predictive performance of a model as well as for representative results. If large animals such as pigs are used, an ethically justifiable number of experimental animals is sufficient for a comprehensive TK study. The main advantage of pigs is the great similarity to the human species regarding anatomical and metabolic properties making this species the best fit and promise the best and especially reliable results of a TK study with subsequently extrapolation to humans (83). Although this study indicated a higher metabolism rate in pigs as compared to humans in terms of tramadol and U-47700, a successful prediction of the human tramadol exposure was possible due to the usage of popTK modeling in combination with comprehensive allometric scaling techniques. The usage of single allometric scaling with incorporation of covariables considering the differences in size and metabolism revealed the best results and was also necessary, because interspecies differences had a big impact on TK parameters. In contrast, the failure of the multiple allometric scaling approach evaluated in this study clarifies that the transferability of TK data is the more challenging, the greater the anatomical/physiological differences are between different species. Overall, this study showed that a complex TK modeling is mandatory if the determined parameters investigated in an animal study should be used for the interpretation of clinic or forensic toxicological results of human cases. In general, one can ethically question the necessity of animal studies for the investigations of TK parameters. With respect to the lack of preclinical data and thus of TK data of NPS, no adequate in vivo alternatives exist to get precise information on TK parameters. Of course, one can deduce different TK parameters from authentic human intoxication cases, but these parameters are mostly afflicted by several unknown factors. Crucial issues for the calculation of TK parameters such as dosage, route of administration, or repetitive and controlled sampling over a certain period are mostly unknown or not possible (29, 34). Thus, lacking information result in flawed TK parameters, that could only be used for very rough estimations. Another possibility are human in vitro approaches for the estimation of TK parameters (115), but metabolic investigations showed differences between static systems and organisms in their output (54). In spite of some limitations, in vitro approaches represent a suitable alternative to in vivo models in metabolic investigation (55). However, other TK parameters might be deviate in a stronger

manner if they are investigated in static enzyme approaches or cell culture in contrast to whole organisms. A quite new model organism and increasingly used for pharmacological and toxicological research are zebrafish larvae (71, 116). This vertebrate model organism offers advantages such as moderate to high genetic homology to humans, the possibility of high-throughput experiments and no need of a request for animal studies (116). Zebrafish larvae propose a high potential especially in metabolism studies and in toxicity studies (55, 117). However, quantifications in blood or organs for distribution studies are limited due to the very small sample size and a total blood volume of a few hundred nanoliters (118). Hence, animal studies may promise the finest results of TK parameters, which could be used for the interpretation of human cases. Of course, one can question if especially the determination of TK parameters concerning NPS is meaningful considering the highly fluctuating market. Particularly the implementation of comprehensive animal studies requires a long time incorporating the request of an animal study as well as the application of the study itself. Since the NPS market is highly fluctuating, the time-consuming preparation before conducting the study might lead to the examination of a less relevant drug, even though it was up-to-date when organizing the study. On the other side, multiple NPS and especially NSO are structurally very close to each other and partially showing similar behavior in e.g. metabolism (23). Interestingly, our pig study revealed plenty of similarities between tramadol and U-47700 popTK in pigs although the chemical structure is not very close and human metabolism differs in the involvement of CYP enzymes. Nevertheless, both substances showed a similar behavior in their TK parameters, and one may speculate, if this offers a potential transferability of TK parameters investigated in this study to other NSO structurally related to U-47700 and close in their metabolic behavior. Of course, such parameters could only be used for rough estimations while interpreting appropriate forensic cases, but especially in terms of other U-components these results might be helpful. Therefore, many results could be gained within this one single study. In contrast, regarding e.g., fentanyl-derived substances with a different chemical structure, a remarkable difference in metabolism, and a higher lipophilicity (25), a transferability of our results should not be assumed.

Overall, for NSO, many results including metabolism, TK properties, tissue distribution, and redistribution were determined within this work. With this one pig study, crucial and broad outcomes were assembled. The presented results of this study indicate that in vitro metabolism approaches serve as helpful tools for the assessment of possible urinary targets of NSO. Since NSO are extensively metabolized, the additional identification of metabolites next to parent compounds might often be necessary in clinical or forensic intoxication cases. In vitro approaches as time-saving and cheap assays provide comparable results to in vivo approaches but should be verified with authentic human samples, if possible, particularly regarding phase II metabolites or metabolites formed by multiple reaction steps. Furthermore, the used pig model is a suitable and helpful tool for the elucidation of TK properties of NSO. Together with a TK modeling approach, this systematic study provides comprehensive TK data to deepen the important knowledge of this hazardous subclass of NPS. Moreover, after a previous pig

study concerning the TK of different synthetic cannabinoids, this study approach already yields successful results for the second drug class. This implies that further knowledge on the TK of new emerging NPS of other drug classes might be gained using the presented model as well. The understanding of the TK is essential to enhance the interpretation of analytical results obtained from poisoning or fatal cases after the consumption of NPS/DOA and finally provide a well-founded opinion in different clinical or forensic cases based on scientific outcomes of systematic experimental studies.

5. REFERENCES

1. Faria J, Barbosa J, Moreira R, Queirós O, Carvalho F and Dinis-Oliveira RJ (2018) Comparative pharmacology and toxicology of tramadol and tapentadol. *European Journal of Pain*, 22(5), 827-844. https://doi.org/10.1002/ejp.1196.

2. Bethesda (MD): National Institute of Diabetes and Digestive and Kidney Diseases (2012) LiverTox: Clinical and research information on drug-induced liver injury. Opioids. https://www.ncbi.nlm.nih.gov/books/NBK547864/.

3. Trescot AM, Datta S, Lee M and Hansen H (2008) Opioid pharmacology. *Pain Physician*, 11(2Supple), 133–153.

4. Kullak-Ublick GA, Siepmann T and Kirch W (2012) Arzneimitteltherapie, Wirksamkeit - Sicherheit - Praktische Anwendung. Thieme Verlagsgruppe, Stuttgart.

5. Miotto K, Cho AK, Khalil MA, Blanco K, Sasaki JD and Rawson R (2017) Trends in tramadol: Pharmacology, metabolism, and misuse. *Anesthesia and Analgesia*, 124(1), 44-51. https://doi.org/10.1213/ANE.0000000000001683.

6. UNODC. United Nations Office on Drug and Crime (2020) World drug report. *United Nations Publication*, Sales No E.20:XI.6. https://wdr.unodc.org/wdr2020/index.html. (accessed July 2021)

7. UN. United Nations (1961) Single convention on narcotic drugs. https://www.unodc.org/documents/commissions/CND/Int_Drug_Control_Conventions/Ebook/The_International_Drug_Control_Conventions_E.pdf. (accessed July 2021)

8. Van Hout MC and Hearne E (2017) New psychoactive substances (NPS) on cryptomarket fora: An exploratory study of characteristics of forum activity between NPS buyers and vendors. *International Journal of Drug Policy*, 40, 102-110. https://doi.org/10.1016/j.drugpo.2016.11.007.

9. Brandt SD, King LA and Evans-Brown M (2014) The new drug phenomenon. *Drug Testing and Analysis*, 6(7-8), 587–597. https://doi.org/10.1002/dta.1686.

10. Zawilska JB (2017) An expanding world of novel psychoactive substances: Opioids. *Frontiers in Psychiatry*, 8, 110. https://doi.org/10.3389/fpsyt.2017.00110.

11. EMCDDA: European Monitoring Center of Drugs and Drug Addiction (2020) European drug report: Trends and developments. https://doi.org/10.2810/420678. (accessed July 2021)

12. Zamengo L, Frison G, Bettin C and Sciarrone R (2014) Understanding the risks associated with the use of new psychoactive substances (NPS): High variability of active ingredients concentration, mislabelled preparations, multiple psychoactive substances in single products.

Toxicology Letters, 229(1), 220–228. https://doi.org/10.1016/j.toxlet.2014.06.012.

13. Meyer MR (2016) New psychoactive substances: an overview on recent publications on their toxicodynamics and toxicokinetics. *Archives of Toxicology*, 90(10), 2421–2444. https://doi.org/10.1007/s00204-016-1812-x.

14. UNODC. United Nations Office on Drug and Crime (2020) Current NPS threats volume III. https://www.unodc.org/documents/scientific/Current_NPS_Threats_Vol.3.pdf. (accessed July 2021)

15. Ruan X, Chiravuri S and Kaye AD (2016) Comparing fatal cases involving U-47700. *Forensic Science, Medicine, and Pathology*, 12(3), 369-371. https://doi.org/10.1007/s12024-016-9795-8.

16. O'Donnell JK, Halpin J, Mattson CL, Goldberger BA and Gladden RM (2017) Deaths involving fentanyl, fentanyl analogs, and U-47700 — 10 states, July–December 2016. *MMWR Morbidity and Mortality Weekly Report*, 66(43), 1197-1202. https://doi.org/10.15585/mmwr.mm6643e1.

17. Lucyk SN and Nelson LS (2017) Novel synthetic opioids: An opioid epidemic within an opioid epidemic. *Annals of Emergency Medicine*, 69(1), 91-93. https://doi.org/10.1016/j.annemergmed.2016.08.445.

18. Židková M, Horsley R, Hloch O and Hložek T (2019) Near-fatal intoxication with the "new" synthetic opioid U-47700: The first reported case in the czech republic. *Journal of Forensic Sciences*, 64(2), 647–650. https://doi.org/10.1111/1556-4029.13903.

19. Prekupec MP, Mansky PA and Baumann MH (2017) Misuse of novel synthetic opioids: A deadly new trend. *Journal of Addiction Medicine*, 11(4), 256-265. https://doi.org/10.1097/ADM.0000000000000324.

20. Vogliardi S, Stocchero G, Maietti S, Tucci M, Nalesso A, Snenghi R, et al. (2018) Non-fatal overdose with U-47700: Identification in biological matrices. *Current Pharmaceutical Biotechnology*, 19(2), 180–187. https://doi.org/10.2174/1389201019666180509164240.

21. Baumann MH, Majumdar S, Le Rouzic V, Hunkele A, Uprety R, Huang XP, et al. (2018) Pharmacological characterization of novel synthetic opioids (NSO) found in the recreational drug marketplace. *Neuropharmacology*, 134(Pt A), 101–107. https://doi.org/10.1016/j.neuropharm.2017.08.016.

22. Logan BK, Mohr ALA, Friscia M, Krotulski AJ, Papsun DM, Kacinko SL, et al. (2017) Reports of adverse events associated with use of novel psychoactive substances, 2013-2016: A review. *Journal of Analytical Toxicology*, 41(7), 573-6410. https://doi.org/10.1093/jat/bkx031.

23. Baumann MH, Tocco G, Papsun DM, Mohr AL, Fogarty MF and Krotulski AJ (2020) U-47700 and its analogs: Non-fentanyl synthetic opioids impacting the recreational drug market. *Brain*

sciences, 10(11), 895. https://doi.org/10.3390/brainsci10110895.

24. Kyei-Baffour K and Lindsley CW (2020) DARK classics in chemical neuroscience: U-47700. *ACS Chemical Neuroscience*, 11(23), 3928–3936. https://doi.org/10.1021/acschemneuro.0c00330.

25. Watanabe S, Vikingsson S, Roman M, Green H, Kronstrand R and Wohlfarth A (2017) In vitro and in vivo metabolite identification studies for the new synthetic opioids acetylfentanyl, acrylfentanyl, furanylfentanyl, and 4-fluoro-isobutyrylfentanyl. *The AAPS Journal*, 19(4), 1102-1122. https://doi.org/10.1208/s12248-017-0070-z.

26. Concheiro M, Chesser R, Pardi J and Cooper G (2018) Postmortem toxicology of new synthetic opioids. *Frontiers in Pharmacology*, 9, 1210. https://doi.ord/10.3389/fphar.2018.01210.

27. Solimini R, Pichini S, Pacifici R, Busardò FP and Giorgetti R (2018) Pharmacotoxicology of non-fentanyl derived new synthetic opioids. *Frontiers in Pharmacology*, 9, 654. https://doi.ord/10.3389/fphar.2018.00654.

28. Rambaran KA, Fleming SW, An J, Burkhart S, Furmaga J, Kleinschmidt KC, et al. (2017) U-47700: A clinical review of the literature. *The Journal of Emergency Medicine*, 53(4), 509–519. https://doi.org/10.1016/j.jemermed.2017.05.034.

29. Koch K, Auwärter V, Hermanns-Clausen M, Wilde M and Neukamm MA (2018) Mixed intoxication by the synthetic opioid U-47700 and the benzodiazepine flubromazepam with lethal outcome: Pharmacokinetic data. *Drug Testing and Analysis*, 10(8), 1336-1341 https://doi.org/10.1002/dta.2391.

30. Dziadosz M, Klintschar M and Teske J (2017) Postmortem concentration distribution in fatal cases involving the synthetic opioid U-47700. *International Journal of Legal Medicine*, 131, 1555–1556. https://doi.org/10.1007/s00414-017-1593-7.

31. Elliott SP, Brandt SD and Smith C (2016) The first reported fatality associated with the synthetic opioid 3,4-dichloro-N-[2-(dimethylamino)cyclohexyl]-N-methylbenzamide (U-47700) and implications for forensic analysis. *Drug Testing and Analysis*, 8(8), 875-879. https://doi.org/10.1002/dta.1984.

32. Coopman V, Blanckaert P, Van Parys G, Van Calenbergh S and Cordonnier J (2016) A case of acute intoxication due to combined use of fentanyl and 3,4-dichloro-N-[2-(dimethylamino)cyclohexyl]-N-methylbenzamide (U-47700). *Forensic Science International*, 266, 68–72. https://doi.org/10.1016/j.forsciint.2016.05.001.

33. Schaefer N, Kettner M, Laschke MW, Schlote J, Ewald AH, Menger MD, et al. (2017) Distribution of synthetic cannabinoids JWH-210, RCS-4 and Δ 9-tetrahydrocannabinol after intravenous administration to pigs. *Current Neuropharmacology*, 15(5), 713–723.

https://doi.org/10.2174/1570159X15666161111114214.

34. Schaefer N., Kroell A-K, Koerbel C, Laschke MW, Menger MD, Maurer HH, et al. (2019) Distribution of the (synthetic) cannabinoids JWH-210, RCS-4, as well as Δ9-tetrahydrocannabinol following pulmonary administration to pigs. *Archives of Toxicology*, 93, 2211–2218. https://doi.org/10.1007/s00204-019-02493-8.

35. Schaefer N, Wojtyniak J-G, Kroell A-K, Koerbel C, Laschke MW, Lehr T, et al. (2018) Can toxicokinetics of (synthetic) cannabinoids in pigs after pulmonary administration be upscaled to humans by allometric techniques? *Biochemical Pharmacology*, 155, 403–418. https://doi.org/10.1016/j.bcp.2018.07.029.

36. Schaefer N, Wojtyniak, J-G, Kettner M, Schlote J, Laschke MW, Ewald AH, et al. (2016) Pharmacokinetics of (synthetic) cannabinoids in pigs and their relevance for clinical and forensic toxicology. *Toxicology Letters*, 253, 7–16. https://doi.org/10.1016/j.toxlet.2016.04.021.

37. Schaefer N, Kroell A-K, Koerbel C, Laschke MW, Menger MD, Maurer HH, et al. (2020) Time- and temperature-dependent postmortem concentration changes of the (synthetic) cannabinoids JWH-210, RCS-4, as well as Δ9-tetrahydrocannabinol following pulmonary administration to pigs. *Archives of Toxicology*, 94, 1585-1599. https://doi.org/10.1007/s00204-020-02707-4.

38. Marchei E, Pacifici R, Mannocchi G, Marinelli E, Busardò FP and Pichini S (2018) New synthetic opioids in biological and non-biological matrices: A review of current analytical methods. *TrAC - Trends in Analytical Chemistry*, 102, 1-15. https://doi.org/10.1016/j.trac.2018.01.007.

39. Noble C, Dalsgaard PW, Johansen SS and Linnet K (2017) Application of a screening method for fentanyl and its analogues using UHPLC-QTOF-MS with data-independent acquisition (DIA) in MS ^{E} mode and retrospective analysis of authentic forensic blood samples. *Drug Testing and Analysis*, 10(4), 651-662. https://doi.org/10.1002/dta.2263.

40. Seither J and Reidy L (2017) Confirmation of carfentanil, U-47700 and other synthetic opioids in a human performance case by LC-MS-MS. *Journal of Analytical Toxicology*, 41(6), 493-497. https://doi.org/10.1093/jat/bkx049.

41. Strayer KE, Antonides HM, Juhascik MP, Daniulaityte R and Sizemore IE (2018) LC-MS/MS-based method for the multiplex detection of 24 fentanyl analogues and metabolites in whole blood at sub ng mL $^{-1}$ concentrations. *ACS Omega*, 3(1), 514-523. https://doi.org/10.1021/acsomega.7b01536.

42. Fogarty MF, Papsun DM and Logan BK (2018) Analysis of fentanyl and 18 novel fentanyl analogs and metabolites by LC–MS-MS, and report of fatalities associated with methoxyacetylfentanyl and cyclopropylfentanyl. *Journal of Analytical Toxicology*, 42(9), 592-604. https://doi.org/10.1093/jat/bky035.

43. Shoff EN, Zaney ME, Kahl JH, Hime GW and Boland DM (2017) Qualitative identification of fentanyl analogs and other opioids in postmortem cases by UHPLC-Ion Trap-MSn. *Journal of Analytical Toxicology*, 41(6), 484-492. https://doi.org/10.1093/jat/bkx041.

44. Moody MT, Diaz S, Shah P, Papsun D and Logan BK (2018) Analysis of fentanyl analogs and novel synthetic opioids in blood, serum/plasma, and urine in forensic casework. *Drug Testing and Analysis*, 10(9), 1358-1367. https://doi.org/10.1002/dta.2393.

45. Mohr ALA, Friscia M, Papsun D, Kacinko SL, Buzby D and Logan BK (2016) Analysis of novel synthetic opioids U-47700, U-50488 and furanyl fentanyl by LC-MS/MS in postmortem casework. *Journal of Analytical Toxicology*, 40(9), 709-717. https://doi.org/10.1093/jat/bkw086.

46. Coopman V, Blanckaert P, Van Parys G, Van Calenbergh S and Cordonnier J (2016) A case of acute intoxication due to combined use of fentanyl and 3,4-dichloro-N-[2-(dimethylamino)cyclohexyl]-N-methylbenzamide (U-47700). *Forensic Science International*, 266, 68–72. https://doi.org/10.1016/j.forsciint.2016.05.001.

47. Ellefsen KN, Taylor EA, Simmons P, Willoughby V and Hall BJ (2017) Multiple drug-toxicity involving novel psychoactive substances, 3-fluorophenmetrazine and U-47700. *Journal of Analytical Toxicology*, 41(9), 765-770. https://doi.org/10.1093/jat/bkx060.

48. Maurer HH and Meyer MR (2016) High-resolution mass spectrometry in toxicology: current status and future perspectives. *Archives of Toxicology*, 90(9), 2161-2172. https://doi.org/10.1007/s00204-016-1764-1.

49. Xian F, Hendrickson CL and Marshall AG (2012) High resolution mass spectrometry. *Analytical Chemistry*, 84(2), 708–719. https://doi.org/10.1021/ac203191t.

50. Meyer MR and Maurer HH (2016) Review: LC coupled to low- and high-resolution mass spectrometry for new psychoactive substance screening in biological matrices – Where do we stand today? *Analytica Chimica Acta*, 927, 13–20. https://doi.org/10.1016/j.aca.2016.04.046.

51. Meyer MR and Maurer HH (2012) Current applications of high-resolution mass spectrometry in drug metabolism studies. *Analytical and Bioanalytical Chemistry*, 403(5), 1221–1231. https://doi.org/10.1007/s00216-012-5807-z.

52. Meyer MR, Helfer AG and Maurer HH (2014) Current position of high-resolution MS for drug quantification in clinical & forensic toxicology. *Bioanalysis*, 6(17), 2275–2284. https://doi.org/10.4155/bio.14.164.

53. Helfer AG, Michely JA, Weber AA, Meyer MR and Maurer HH (2015) Orbitrap technology for comprehensive metabolite-based liquid chromatographic–high resolution-tandem mass spectrometric urine drug screening – Exemplified for cardiovascular drugs. *Analytica Chimica*

Acta, 891, 221–233. http://doi.org/10.1016/j.aca.2015.08.018.

54. Caspar AT, Helfer AG, Michely JA, Auwärter V, Brandt SD, Meyer MR, et al. (2015) Studies on the metabolism and toxicological detection of the new psychoactive designer drug 2-(4-iodo-2,5-dimethoxyphenyl)-N-[(2-methoxyphenyl)methyl]ethanamine (25I-NBOMe) in human and rat urine using GC-MS, LC-MSn, and LC-HR-MS/MS. *Analytical and Bioanalytical Chemistry*, 407, 6697–6719. https://doi.org/10.1007/s00216-015-8828-6.

55. Richter LHJ, Herrmann J, Andreas A, Park Y., Wagmann L, Flockerzi V, et al. (2019) Tools for studying the metabolism of new psychoactive substances for toxicological screening purposes – A comparative study using pooled human liver S9, HepaRG cells, and zebrafish larvae. *Toxicology Letters*, 305(Suppl 1), 73–80. http://doi.org/10.1016/j.toxlet.2019.01.010.

56. Gampfer TM, Richter LHJ, Schäper J, Wagmann L and Meyer MR (2019) Toxicokinetics and analytical toxicology of the abused opioid U-48800 — in vitro metabolism, metabolic stability, isozyme mapping, and plasma protein binding. *Drug Testing and Analysis*, 11(10), 1572–1580. https://doi.org/10.1002/dta.2683.

57. Wagmann L, Manier SK, Felske C, Gampfer TM, Richter MJ, Eckstein N, et al. (2020) Flubromazolam-Derived Designer Benzodiazepines: Toxicokinetics and Analytical Toxicology of Clobromazolam and Bromazolam. *Journal of Analytical Toxicology*. https://doi.org/10.1093/jat/bkaa161.

58. Schaefer N, Helfer AG, Kettner M, Laschke MW, Schlote J, Ewald AH, et al. (2017) Metabolic patterns of JWH-210, RCS-4, and THC in pig urine elucidated using LC-HR-MS/MS: Do they reflect patterns in humans? *Drug Testing and Analysis*, 9(4), 613–625. https://doi.org/10.1002/dta.1995.

59. Skopp G (2010) Postmortem toxicology. *Forensic Science, Medicine, and Pathology*, 6, 314–325. https://doi.org/10.1007/s12024-010-9150-4.

60. Saghir SA and Ansari RA (2018) Pharmacokinetics. *Reference Module in Biomedical Sciences*. Elsevier. https://doi.org/10.1016/B978-0-12-801238-3.62154-2.

61. OECD Guideline for the testing of chemicals, Section 4. Test No 417: Toxicokinetics (2010). https://doi.org/10.1787/9789264070882-en.

62. Cone EJ, Tsadik A, Oyler J and Darwin WD (1998) Cocaine metabolism and urinary excretion after different routes of administration. *Therapeutic Drug Monitoring*, 20(5), 556-560. https://doi.org/10.1097/00007691-199810000-00019.

63. Hadland SE and Levy S (2016) Objective testing: urine and other drug tests. *Child and Adolescent Psychiatric Clinics of North America*, 25(3), 549–565. https://doi.org/10.1016/j.chc.2016.02.005.

64. Singh Z (2017) Forensic toxicology: Biological sampling and use of different analytical techniques. *Foresic Research and Criminology International Journal*, 4(4), 117-120. https://doi.org/10.15406/frcij.2017.04.00120

65. Elbe A-M, Jensen SN, Elsborg P, Wetzke M, Woldemariam GA, Huppertz B, et al. (2016) The urine marker test: An alternative approach to supervised urine collection for doping control. *Sports Medicine*, 46, 15–22. https://doi.org/10.1007/s40279-015-0388-6.

66. Vignali C, Stramesi C, Morini L, San Bartolomeo P and Groppi A (2015) Workplace drug testing in Italy: Findings about second-stage testing. *Drug Testing and Analysis*, 7(3), 173–177. https://doi.org/10.1002/dta.1640.

67. Garza AZ, Park SB and Kocz R (2020) Drug elimination. StatPearls Publishing LLC. https://www.ncbi.nlm.nih.gov/books/NBK547662/. (accessed July 2021).

68. Guengerich FP (2001) Common and uncommon cytochrome P450 reactions related to metabolism and chemical toxicity. *Chemical Research in Toxicology*, 14(6), 611–650. https://doi.org/10.1021/tx0002583.

69. Liston HL, Markowitz JS and DeVane CL (2001) Drug glucuronidation in clinical psychopharmacology. *Journal of Clinical Psychopharmacology*, 21(5), 500-515. https://doi.org/10.1097/00004714-200110000-00008.

70. Krotulski AJ, Mohr ALA., Papsun DM and Logan BK (2017) Metabolism of novel opioid agonists U-47700 and U-49900 using human liver microsomes with confirmation in authentic urine specimens from drug users. *Durg Testing and Analysis*, 10(1), 127-136. https://doi.org/10.1002/dta.2228.

71. Gampfer TM, Wagmann L, Park YM, Cannaert A, Herrmann J, Fischmann S, et al. (2020) Toxicokinetics and toxicodynamics of the fentanyl homologs cyclopropanoyl-1-benzyl-4´-fluoro-4-anilinopiperidine and furanoyl-1-benzyl-4-anilinopiperidine. *Archives of Toxicology*, 94, 2009–2025. https://doi.org/10.1007/s00204-020-02726-1.

72. Åstrand A, Töreskog A, Watanabe S, Kronstrand R, Gréen H and Vikingsson S (2019) Correlations between metabolism and structural elements of the alicyclic fentanyl analogs cyclopropyl fentanyl, cyclobutyl fentanyl, cyclopentyl fentanyl, cyclohexyl fentanyl and 2,2,3,3-tetramethylcyclopropyl fentanyl studied by human hepatocytes and LC-QTOF-MS. *Archives of Toxicology*, 93, 95–106. https://doi.org/10.1007/s00204-018-2330-9.

73. Wilde, M., Pichini, S., Pacifici, R., Tagliabracci, A., Busardò, F.P., Auwärter, V., et al. (2019) Metabolic Pathways and Potencies of New Fentanyl Analogs. *Frontiers in Pharmacology*, 10, 238. https://doi.org/10.3389/fphar.2019.00238.

74. Richter LH., Maurer HH and Meyer MR (2017) New psychoactive substances: Studies on the metabolism of XLR-11, AB-PINACA, FUB-PB-22, 4-methoxy-α-PVP, 25-I-NBOMe, and meclonazepam using human liver preparations in comparison to primary human hepatocytes, and human urine. *Toxicology Letters*, 280, 142–150. https://doi.org/10.1016/j.toxlet.2017.07.901.

75. Peters FT and Meyer MR (2011) In vitro approaches to studying the metabolism of new psychoactive compounds. *Drug Testing and Analysis*, 3(7-8), 483–495. https://doi.org/10.1002/dta.295.

76. Peters FT (2014) Recent developments in urinalysis of metabolites of new psychoactive substances using LC–MS. *Bioanalysis*, 6(15), 2083–2107. https://doi.org/10.4155/bio.14.168.

77. Martignoni M, Groothuis GMM and de Kanter R. (2006) Species differences between mouse, rat, dog, monkey and human CYP-mediated drug metabolism, inhibition and induction. *Expert Opinion on Drug Metabolism and Toxicology*, 2(6), 875–894. https://doi.org/10.1517/17425255.2.6.875.

78. Taneja I, Karsauliya K, Rashid M, Sonkar AK, Rama Raju KS, Singh SK, et al. (2018) Species differences between rat and human in vitro metabolite profile, in vivo predicted clearance, CYP450 inhibition and CYP450 isoforms that metabolize benzanthrone: Implications in risk assessment. *Food and Chemical Toxicology*, 111, 94–101. https://doi.org/10.1016/j.fct.2017.11.009.

79. Hsin-Hung Chen M, Dip A, Ahmed M, Tan ML, Walterscheid JP, Sun H, et al. (2016) Detection and characterization of the effect of AB-FUBINACA and its metabolites in a rat model. *Journal of Cellular Biochemistry*, 117(4), 1033–1043. https://doi.org/10.1002/jcb.25421.

80. Truver MT, Smith CR, Garibay N, Kopajtic TA, Swortwood MJ and Baumann MH (2020) Pharmacodynamics and pharmacokinetics of the novel synthetic opioid, U-47700, in male rats. *Neuropharmacology*, 177, 108195. https://doi.org/10.1016/j.neuropharm.2020.108195.

81. Brunet B, Doucet C, Venisse N, Hauet T, Hébrard W, Papet Y, et al. (2006) Validation of large white pig as an animal model for the study of cannabinoids metabolism: Application to the study of THC distribution in tissues. *Forensic Science International*, 161(2-3), 169–174. http://doi.org/10.1016/j.forsciint.2006.04.018.

82. Anzenbacher P, Soucek P, Anzenbacherova E, Gut I, Hrubý K, Svoboda Z, et al. (1998) Presence and activity of cytochrome P450 isoforms in minipig liver microsomes - Comparison with human liver samples. *Drug Metabolism and Disposition*, 26(1), 56–59.

83. Swindle MM, Makin ., Herron AJ, Clubb FJ and Frazier KS (2011) Swine as Models in Biomedical Research and Toxicology Testing. *Veterinary Pathology*, 49(2), 344–356. https://doi.org/10.1177/0300985811402846.

84. Derendorf H, Gramatté T, Schaefer HG and Staab A (2011) Pharmakokinetik kompakt. Grundlagen und Praxisrelevanz. Wissenschalftliche Verlagsgesellschaft Stuttgard, Stuttgard.

85. Benet LZ and Zia-Amirhosseini P (1995) Basic principles of pharmacokinetics. *Toxicologic Pathology*, 23(2), 115–123. https://doi.org/10.1177/019262339502300203.

86. Foster DM (2007) Chapter 8 - Noncompartmental versus compartmental approaches to pharmacokinetic analysis. *Principles of Clinical Pharmacology (Second Edition)*, 89-105. Academic Press, Burlington. https://doi.org/10.1016/B978-012369417-1/50048-1

87. Fleishaker JC and Smith RB (1987) Compartmental model analysis in pharmacokinetics. *The Journal of Clinical Pharmacology*, 27(12), 922–926. https://doi.org/10.1002/j.1552-4604.1987.tb05591.x.

88. Ahmed TA (2015) Chapter 3: Pharmacokinetics of drugs following iv bolus, iv infusion, and oral administration. *Basic Pharmacokinetic Concepts and Some Clinical Applications*. IntechOpen, London, United Kingdom. https://doi.org/10.5772/61573

89. Banks G (2018) What is population pharmacokinetic (popPK) analysis? https://www.nuventra.com/resources/blog/what-is-population-pk-poppk/. (accessed July 2021)

90. Mould DR and Upton RN (2013) Basic concepts in population modeling, simulation, and model-based drug development-part 2: introduction to pharmacokinetic modeling methods. *CPT: Pharmacometrics and Systems Pharmacology*, 2(4), e38. https://doi.org/10.1038/psp.2013.14.

91. Knibbe CAJ, Zuideveld KP, Aarts LPHJ, Kuks PFM and Danhof M. (2005) Allometric relationships between the pharmacokinetics of propofol in rats, children and adults. *British Journal of Clinical Pharmacology*, 59(6), 705–711. https://doi.org/10.1111/j.1365-2125.2005.02239.x.

92. Grond S and Sablotzki A (2004) Clinical pharmacology of tramadol. *Clinical Pharmacokinetics*, 43(13), 879–923. https://doi.org/10.2165/00003088-200443130-00004.

93. Vullo C, Kim TW, Meligrana M, Marini C and Giorgi M.(2014) Pharmacokinetics of tramadol and its major metabolite after intramuscular administration in piglets. *Journal of Veterinary Pharmacology and Therapeutics*, 37(6), 603-606. https://doi.org/10.1111/jvp.12133.

94. Bortolami E, Della Rocca G, Di Salvo A, Giorgi M, Kim TW, Isola M, et al. (2015) Pharmacokinetics and antinociceptive effects of tramadol and its metabolite O-desmethyltramadol following intravenous administration in sheep. *The Veterinary Journal*, 205(3), 404-409. https://doi.org/10.1016/j.tvjl.2015.04.011.

95. Sheikholeslami B, Gholami M, Lavasani H and Rouini M (2016) Evaluation of the route dependency of the pharmacokinetics and neuro-pharmacokinetics of tramadol and its main

metabolites in rats. *European Journal of Pharmaceutical Sciences*, 92, 55-63. https://doi.org/10.1016/j.ejps.2016.06.021

96. Murthy B, Pandya K, Booker P, Murray A, Lintz W and Terlinden R (2000) Pharmacokinetics of tramadol in children after IV or caudal epidural administration. *British Journal of Anaesthesia*, 84(3), 346–349. https://doi.org/10.1093/oxfordjournals.bja.a013437.

97. Pélissier-Alicot A-L, Gaulier J-M, Champsaur P and Marquet P (2003) Mechanisms underlying postmortem redistribution of drugs: A Review. *Journal of Analytical Toxicology*, 27(8), 533–544. https://doi.org/10.1093/jat/27.8.533.

98. Leikin JB and Watson WA (2003) Post-mortem toxicology: What the dead can and cannot tell us. *Journal of Toxicology: Clinical Toxicology*, 41(1), 47–56. https://doi.org/10.1081/CLT-120018270.

99. Yarema MC and Becker CE (2005) Key concepts in postmortem drug redistribution. *Clinical Toxicology*, 43(4), 235–241. https://doi.org/10.1081/CLT-58950.

100. Kennedy MC (2010) Post-mortem drug concentrations. *Internal Medicine Journal*, 40(3), 183–187. https://doi.org/10.1111/j.1445-5994.2009.02111.x.

101. Han E, Kim E, Hong H, Jeong S, Kim J, In S, et al. (2012) Evaluation of postmortem redistribution phenomena for commonly encountered drugs. *Forensic Science International*, 219(1-3), 265–271. http://doi.org/10.1016/j.forsciint.2012.01.016.

102. McIntyre IM (2014) Liver and peripheral blood concentration ratio (L/P) as a marker of postmortem drug redistribution: a literature review. *Forensic Science, Medicine, and Pathology*, 10(1), 91–96. https://doi.org/10.1007/s12024-013-9503-x.

103. Nordmeier F, Richter LHJ, Schmidt PH, Schaefer N and Meyer MR (2019) Studies on the in vitro and in vivo metabolism of the synthetic opioids U-51754, U-47931E, and methoxyacetylfentanyl using hyphenated high-resolution mass spectrometry. *Scientific reports*, 9(1), 1-17. https://doi.org/10.1038/s41598-019-50196-y.

104. Nordmeier F, Doerr A, Laschke MW, Menger MD, Schmidt PH, Schaefer N, et al. (2020) Are pigs a suitable animal model for in vivo metabolism studies of new psychoactive substances? A comparison study using different in vitro/in vivo tools and U-47700 as model drug. *Toxicology Letters*, 329, 12-19. https://doi.org/10.1016/j.toxlet.2020.04.001.

105. Nordmeier F, Doerr AA, Potente S, Walle N, Laschke MW, Menger MD et al. (2021) Perimortem distribution of U-47700, tramadol and their main metabolites in pigs following intravenous administration. *Journal of Analytical Toxicology*. https://doi.org/10.1093/jat/bkab044.

106. Richter LHJ, Kaminski YR, Noor F, Meyer MR and Maurer HH (2016) Metabolic fate of desomorphine elucidated using rat urine, pooled human liver preparations, and human hepatocyte cultures as well as its detectability using standard urine screening approaches. *Analytical and Bioanalytical Chemistry*, 408(23), 6283–6294. https://doi.org/10.1007/s00216-016-9740-4.

107. Richter LHJ, Maurer HH and Meyer MR (2019) Metabolic fate of the new synthetic cannabinoid 7'N-5F-ADB in rat, human, and pooled human S9 studied by means of hyphenated high-resolution mass spectrometry. *Drug Testing and Analysis*, 11(2), 305–317. https://doi.org/10.1002/dta.2493.

108. Mardal M, Johansen SS, Davidsen AB, Telving R, Jornil JR, Dalsgaard PW, et al. (2018) Postmortem analysis of three methoxyacetylfentanyl-related deaths in Denmark and in vitro metabolite profiling in pooled human hepatocytes. *Forensic Science International*, 290, 310–317. https://doi.org/10.1016/j.forsciint.2018.07.020.

109. Hunter, R. (2010) Comperative and veterinary pharmacology - Interspecies allometric scaling. *Handbook of Experimental Pharmacology* 199, 139–157. https://doi.org/10.1007/978-3-642-10324-7_6.

110. Patel D and Dierks E (2018) Single-species allometric scaling: A strategic approach to support drug discovery. *Journal of Pharmaceutical Research International*, 22(3), 1–7. http://doi.org/10.9734/JPRI/2018/41693.

111. Huh Y, Smith DE and Rose Feng M (2011) Interspecies scaling and prediction of human clearance: comparison of small- and macro-molecule drugs. *Xenobiotica*, 41(11), 972–987. https://doi.org/10.3109/00498254.2011.598582.

112. Bailey J, Thew M and Balls M (2014) An analysis of the use of animal models in predicting human toxicology and drug safety. *Alternatives to Laboratory Animals*, 42(3), 181–199. https://doi.org/10.1177/026119291404200306.

113. Nuffield Council on Bioethics (2005) The ethics of research involving animals. London, United Kingdom. https://www.nuffieldbioethics.org/wp-content/uploads/The-ethics-of-research-involving-animals-full-report.pdf. (accessed July 2021)

114. Van Norman GA (2019) Limitations of animal studies for predicting toxicity in clinical trials: Is it time to rethink our current approach? *JACC: Basic to Translational Science*, 4 (7), 845–854. https://doi.org/10.1016/j.jacbts.2019.10.008

115. MacGowan A and Bowker K (2002) Developments in PK/PD: optimising efficacy and prevention of resistance. A critical review of PK/PD in in vitro models. *International Journal of Antimicrobial Agents*, 19(4), 291–298. https://www.doi.org/10.1016/s0924-8579(02)00027-4.

116. Van Wijk RC, Krekels EHJ, Kantae V, Ordas A, Kreling T, Harms AC, et al. (2019) Mechanistic and quantitative understanding of pharmacokinetics in zebrafish larvae through nanoscale blood sampling and metabolite modeling of paracetamol. *Journal of Pharmacology and Experimental Therapeutics*, 371(1), 15. https://doi.org/10.1124/jpet.119.260299

117. Kolesnikova TO, Shevyrin VA, Eltsov OS, Khatsko SL, Demin KA, Galstyan DS, et al. (2021) Psychopharmacological characterization of an emerging drug of abuse, a synthetic opioid U-47700, in adult zebrafish. *Brain Research Bulletin*, 167, 48–55. https://doi.org/10.1016/j.brainresbull.2020.11.017.

118. Craig MP, Gilday SD, Dabiri D and Hove JR (2012) An optimized method for delivering flow tracer particles to intravital fluid environments in the developing zebrafish. *Zebrafish*, 9(3), 108–119. https://doi.org/10.1089/zeb.2012.0740.

6. ABBREVIATIONS

AUC	area under the curve
Cl	clearance
CYP	cytochrome P450 monooxygenase
DOA	drugs of abuse
DUID	driving under the influence of drugs
EMCDDA	European Monitoring Center for Drugs and Drug Addiction
ESI	electrospray ionization
EU	European
EWS	Early Warning System
HR	high resolution
i.v.	intravenous
KOR	κ opioid receptor
LC	liquid chromatography
MOR	μ opioid receptor
MRM	multi-reaction monitoring
MS/MS	tandem mass spectrometry
m/z	mass-to-charge
NPS	new psychoactive substances
NSO	new synthetic opioids
OR	opioid receptor
pHLM	pooled human liver microsomes
phS9	pooled human liver S9 fraction
PK	pharmacokinetic
PLM	pig liver microsomes
PM	postmortem
PMI	postmortem interval
PMR	postmortem redistribution
popTK	Population toxicokinetic
$t_{1/2}$	elimination half-life time
THC	Δ9-tetrahydrocannabinol
TK	toxicokinetic
V_d	volume of distribution